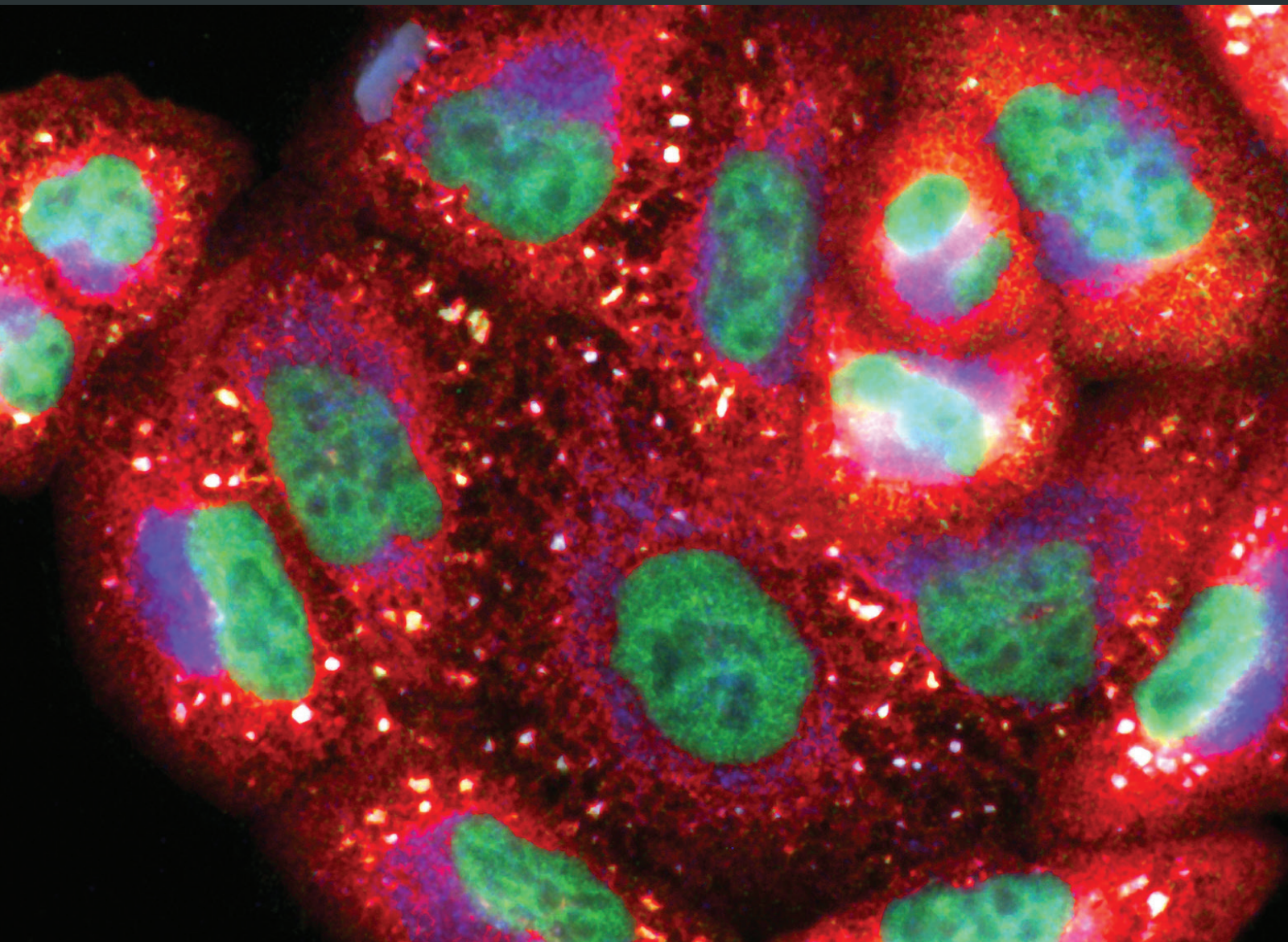



Oxidative Medicine and Cellular Longevity

Oxidative Molecular Mechanisms Underlying Liver Diseases: From Systems Biology to the Personalized Medicine

Lead Guest Editor: Anna M. Giudetti

Guest Editors: Daniele Vergara and Andrea C. Gardini





**Oxidative Molecular Mechanisms Underlying
Liver Diseases: From Systems Biology to
the Personalized Medicine**

Oxidative Medicine and Cellular Longevity

**Oxidative Molecular Mechanisms Underlying
Liver Diseases: From Systems Biology to
the Personalized Medicine**

Lead Guest Editor: Anna M. Giudetti

Guest Editors: Daniele Vergara and Andrea C. Gardini




Copyright © 2019 Hindawi. All rights reserved.

This is a special issue published in "Oxidative Medicine and Cellular Longevity." All articles are open access articles distributed under the Creative Commons Attribution License, which permits unrestricted use, distribution, and reproduction in any medium, provided the original work is properly cited.

Editorial Board

- Fabio Altieri, Italy
Fernanda Amicarelli, Italy
José P. Andrade, Portugal
Cristina Angeloni, Italy
Antonio Ayala, Spain
Elena Azzini, Italy
Peter Backx, Canada
Damian Bailey, UK
Sander Bekeschus, Germany
Ji C. Bihl, USA
Consuelo Borrás, Spain
Nady Braidy, Australia
Ralf Braun, Germany
Laura Bravo, Spain
Amadou Camara, USA
Gianluca Carnevale, Italy
Roberto Carnevale, Italy
Angel Catalá, Argentina
Giulio Ceolotto, Italy
Shao-Yu Chen, USA
Ferdinando Chiaradonna, Italy
Zhao Zhong Chong, USA
Alin Ciobica, Romania
Ana Cipak Gasparovic, Croatia
Giuseppe Cirillo, Italy
Maria R. Ciriolo, Italy
Massimo Collino, Italy
Graziamaria Corbi, Italy
Manuela Corte-Real, Portugal
Mark Crabtree, UK
Manuela Curcio, Italy
Andreas Daiber, Germany
Felipe Dal Pizzol, Brazil
Francesca Danesi, Italy
Domenico D'Arca, Italy
Sergio Davinelli, USA
Claudio De Lucia, Italy
Yolanda de Pablo, Sweden
Sonia de Pascual-Teresa, Spain
Cinzia Domenicotti, Italy
Joël R. Drevet, France
Grégory Durand, France
Javier Egea, Spain
Ersin Fadillioglu, Turkey
- Ioannis G. Fatouros, Greece
Qingping Feng, Canada
Gianna Ferretti, Italy
Giuseppe Filomeni, Italy
Swaran J. S. Flora, India
Teresa I. Fortoul, Mexico
Jeferson L. Franco, Brazil
Rodrigo Franco, USA
Joaquin Gadea, Spain
Juan Gambini, Spain
José Luís García-Giménez, Spain
Gerardo García-Rivas, Mexico
Janusz Gebicki, Australia
Alexandros Georgakilas, Greece
Husam Ghanim, USA
Rajeshwary Ghosh, USA
Eloisa Gitto, Italy
Daniela Giustarini, Italy
Saeid Golbidi, Canada
Aldrin V. Gomes, USA
Tilman Grune, Germany
Nicoletta Guaragnella, Italy
Solomon Habtemariam, UK
E.- M. Hanschmann, Germany
Tim Hofer, Norway
John D. Horowitz, Australia
Silvana Hrelia, Italy
Stephan Immenschuh, Germany
Maria Isagulians, Latvia
Luigi Iuliano, Italy
Vladimir Jakovljevic, Serbia
Marianna Jung, USA
Peeter Karihtala, Finland
Eric E. Kelley, USA
Kum Kum Khanna, Australia
Neelam Khaper, Canada
Thomas Kietzmann, Finland
Demetrios Kouretas, Greece
Andrey V. Kozlov, Austria
Jean-Claude Lavoie, Canada
Simon Lees, Canada
Ch. Horst Lillig, Germany
Paloma B. Liton, USA
Ana Lloret, Spain
- Lorenzo Loffredo, Italy
Daniel Lopez-Malo, Spain
Antonello Lorenzini, Italy
Nageswara Madamanchi, USA
Kenneth Maiese, USA
Marco Malaguti, Italy
Tullia Maraldi, Italy
Reiko Matsui, USA
Juan C. Mayo, Spain
Steven McAnulty, USA
Antonio Desmond McCarthy, Argentina
Bruno Meloni, Australia
Pedro Mena, Italy
Víctor M. Mendoza-Núñez, Mexico
Maria U. Moreno, Spain
Trevor A. Mori, Australia
Ryuichi Morishita, Japan
Fabiana Morroni, Italy
Luciana Mosca, Italy
Ange Mouithys-Mickalad, Belgium
Iordanis Mourouzis, Greece
Danina Muntean, Romania
Colin Murdoch, UK
Pablo Muriel, Mexico
Ryoji Nagai, Japan
David Nieman, USA
Hassan Obied, Australia
Julio J. Ochoa, Spain
Pál Pacher, USA
Pasquale Pagliaro, Italy
Valentina Pallottini, Italy
Rosalba Parenti, Italy
Vassilis Paschalis, Greece
Visweswara Rao Pasupuleti, Malaysia
Daniela Pellegrino, Italy
Ilaria Peluso, Italy
Claudia Penna, Italy
Serafina Perrone, Italy
Tiziana Persichini, Italy
Shazib Pervaiz, Singapore
Vincent PIALoux, France
Ada Popolo, Italy
José L. Quiles, Spain
Walid Rachidi, France



Zsolt Radak, Hungary	Sebastiano Sciarretta, Italy	Jeannette Vasquez-Vivar, USA
N. Soorappan Rajasekaran, USA	Ratanesh K. Seth, USA	Daniele Vergara, Italy
Kota V. Ramana, USA	Honglian Shi, USA	Victor M. Victor, Spain
Sid D. Ray, USA	Cinzia Signorini, Italy	László Virág, Hungary
Hamid Reza Rezvani, France	Mithun Sinha, USA	Natalie Ward, Australia
Alessandra Ricelli, Italy	Carla Tatone, Italy	Philip Wenzel, Germany
Paola Rizzo, Italy	Frank Thévenod, Germany	Anthony R. White, Australia
Francisco J. Romero, Spain	Shane Thomas, Australia	Georg T. Wondrak, USA
Joan Roselló-Catafau, Spain	Carlo G. Tocchetti, Italy	Michal Wozniak, Poland
H. P. Vasantha Rupasinghe, Canada	Angela Trovato Salinaro, Jamaica	Sho-ichi Yamagishi, Japan
Gabriele Saretzki, UK	Paolo Tucci, Italy	Liang-Jun Yan, USA
Luciano Saso, Italy	Rosa Tundis, Italy	Guillermo Zalba, Spain
Nadja Schroder, Brazil	Giuseppe Valacchi, Italy	Mario Zoratti, Italy

Contents

Oxidative Molecular Mechanisms Underlying Liver Diseases: From Systems Biology to the Personalized Medicine

Daniele Vergara , Andrea Casadei-Gardini , and Anna M. Giudetti 

Editorial (2 pages), Article ID 7864316, Volume 2019 (2019)

TNF α -Mediated Necroptosis Aggravates Ischemia-Reperfusion Injury in the Fatty Liver by Regulating the Inflammatory Response

Faji Yang, Longcheng Shang, Shuai Wang, Yang Liu , Haozhen Ren , Wei Zhu , and Xiaolei Shi 

Research Article (14 pages), Article ID 2301903, Volume 2019 (2019)

Fasting Whole-Body Energy Homeostasis and Hepatic Energy Metabolism in Nondiabetic Humans with Fatty Liver

Guido Lattuada, Maria Grazia Radaelli, Francesco De Cobelli, Antonio Esposito, Giuseppina Manzoni,

Silvia Perra, Alessandro Del Maschio , Giovanna Castoldi , and Gianluca Perseghin 

Research Article (7 pages), Article ID 9796175, Volume 2019 (2019)


Reduced Liver Lipid Peroxidation in Subcellular Fractions Is Associated with a Hypometabolic State in Rats with Portacaval Anastomosis

Olivia Vázquez-Martínez , Héctor Valente-Godínez, Andrés Quintanar-Stephano, Deisy Gasca-Martínez, Mayra L. López-Cervantes, Lourdes Palma-Tirado, María de Jesús Guerrero-Carrillo, Mariela Pérez-Solís,

and Mauricio Díaz-Muñoz 

Research Article (13 pages), Article ID 4565238, Volume 2019 (2019)

Antifibrotic Effect of Marine Ovothiol in an *In Vivo* Model of Liver Fibrosis

Mariarita Brancaccio, Giuseppe D'Argenio, Vincenzo Lembo , Anna Palumbo ,

and Immacolata Castellano 



Research Article (10 pages), Article ID 5045734, Volume 2018 (2019)

Protective Effects of Aqueous Extracts of *Flos Ionicæ Japonicæ* against Hydroquinone-Induced Toxicity in Hepatic L02 Cells

Yanfang Gao, Huanwen Tang, Liang Xiong, Lijun Zou, Wenjuan Dai, Hailong Liu, and Gonghua Hu 

Research Article (10 pages), Article ID 4528581, Volume 2018 (2019)




Aberrant Metabolism in Hepatocellular Carcinoma Provides Diagnostic and Therapeutic Opportunities

Serena De Matteis, Andrea Ragusa , Giorgia Marisi, Stefania De Domenico, Andrea Casadei Gardini ,

Massimiliano Bonafè, and Anna Maria Giudetti 

Review Article (13 pages), Article ID 7512159, Volume 2018 (2019)

Heme Oxygenase-1 May Affect Cell Signalling via Modulation of Ganglioside Composition

Václav Šmíd , Jakub Šuk , Neli Kachamakova-Trojanowska, Jana Jašprová, Petra Valášková ,

Alicja Józkowicz , Józef Dulak, František Šmíd, Libor Vítek , and Lucie Muchová 

Research Article (12 pages), Article ID 3845027, Volume 2018 (2019)

Role of Oxidative Stress in Pathophysiology of Nonalcoholic Fatty Liver Disease

Mario Masarone , Valerio Rosato, Marcello Dallio, Antonietta Gerarda Gravina , Andrea Aglitti ,

Carmelina Loguercio, Alessandro Federico , and Marcello Persico 

Review Article (14 pages), Article ID 9547613, Volume 2018 (2019)

Hypoxic Signaling and Cholesterol Lipotoxicity in Fatty Liver Disease Progression

Oren Tirosh 

Review Article (15 pages), Article ID 2548154, Volume 2018 (2019)

Editorial

Oxidative Molecular Mechanisms Underlying Liver Diseases: From Systems Biology to the Personalized Medicine

Daniele Vergara ¹, **Andrea Casadei-Gardini** ², and **Anna M. Giudetti** ¹

¹Department of Biological and Environmental Sciences and Technologies, University of Salento, Lecce, Italy

²Division of Medical Oncology, Department of Medical and Surgical Sciences for Children and Adults, University Hospital of Modena, Italy

Correspondence should be addressed to Anna M. Giudetti; anna.giudetti@unisalento.it

Received 28 April 2019; Accepted 30 April 2019; Published 2 June 2019

Copyright © 2019 Daniele Vergara et al. This is an open access article distributed under the Creative Commons Attribution License, which permits unrestricted use, distribution, and reproduction in any medium, provided the original work is properly cited.

The liver is the second largest organ in the body with a major contribution to the regulation of systemic metabolism. This places the liver at the centre of an extraordinary biomedical interest due to the increased prevalence worldwide of liver-associated diseases and due to the complex molecular background behind these conditions. Moreover, the liver plays a key role in the control of whole-body energy through the physiological regulation of different metabolisms including that of sugars, lipids, and amino acids. The alteration of liver metabolic homeostasis is critical for the development and progression of different diseases including nonalcoholic fatty liver disease (NAFLD), nonalcoholic steatohepatitis (NASH), and hepatocellular carcinoma (HCC). These circumstances generate a fertile ground for the definition of altered cellular and molecular functions at the basis of these conditions. To further increase our understanding of this complexity, this special issue provides an overview of these processes with potential advances in the development of diagnostic and clinical applications.

Fatty liver is considered a consequence of a higher flux of nonesterified fatty acids derived from adipose tissue and/or an alteration in the hepatic energy metabolism that facilitate intrahepatic fat accumulation. The study conducted by G. Lattuada and collaborators focuses on this clinical aspect. They evaluated the whole-body energy metabolism and hepatic high-energy phosphates in nondiabetic individuals with fatty liver with respect to control individuals matched for anthropometric features. The study analysed the intrahepatic fat content by ¹H-Magnetic

Resonance Spectroscopy, the relative content of hepatic high-energy phosphates (phosphomonoesters, phosphodiester, inorganic phosphorus, and ATP) by ³¹P-Magnetic Resonance Spectroscopy, and the whole-body resting energy expenditure and substrate oxidation by indirect calorimetry. The authors demonstrated that fasting whole-body energy metabolism and the relative content of hepatic high-energy phosphates in nondiabetic patients with fatty liver are not different than in controls when the two groups of patients are matched for anthropometric features.

F. Yang and collaborators investigated the role of necroptosis during ischemia and reperfusion injury (IRI) in fatty liver. They demonstrated that this cellular process is activated during IRI and that targeting necroptosis can have effects on IRI and ROS production with potential clinical implications.

Experimental data support a role for oxidative stress in the progression of NAFLD toward NASH. These works are well reviewed by M. Masarone and colleagues, who presented the main evidence on the strict pathophysiologic linkage between oxidative stress and NAFLD. Oxidative stress may also affect the synthesis and distribution of gangliosides as reported by V. Šmíd and collaborators. As gangliosides are involved in cell recognition, signalling, and membrane stabilization, the alteration in their expression is often at the basis of many pathological and physiological conditions including cell death, proliferation, and differentiation. Using *in vitro* and *in vivo* models, the authors evaluated the functional consequences of Heme oxygenase 1 deficiency on ganglioside

metabolism providing evidence of a tissue-specific increase in the main gangliosides together with changes in the mRNA expression of key enzymes of ganglioside synthesis.

O. Tirosh reviews key mechanisms responsible for the occurrence of NAFLD in lean subjects with a healthy metabolism. In these subjects, the activation of several redox and oxidant signalling pathways involving cholesterol plays a role in fatty liver disease thus indicating that direct lipotoxic effects, more than metabolic alterations, are crucial for the disease progression. Main mechanisms responsible for the cholesterol-induced NAFLD include impairment of the mitochondrial and lysosomal function due to cholesterol loading of the inner cell membrane and the activation of specific signalling and inflammatory pathways. This result has clinical consequences for the development of personal drug and dietary treatment strategies.

Chronic hepatic injury is often related to fibrosis, thus leading to an excessive increase in extracellular matrix protein accumulation and fibrogenesis. Without proper clinical management, liver damage may progress to cirrhosis and ultimately to liver failure or cancer. M. Brancaccio and collaborators put the spotlight on the effect of a marine compound, isolated from sea urchin eggs, as a potential therapeutic molecule for the treatment of liver fibrosis. In particular, they report the effect of ovothiol A, π -methyl-5-thiohistidine, on an *in vivo* murine model of liver fibrosis. Interestingly, ovothiol A showed an antifibrotic effect associated with the decrease of fibrogenic markers involved in liver fibrosis progression, such as the transforming growth factor- β (TGF- β), the α -smooth muscle actin (α -SMA), and the tissue metalloproteinase inhibitor (TIMP-1). Similarly, in the work of Y. Gao and colleagues, the protective effects of aqueous extracts of *Flos lonicerae Japonicae*, a traditional Chinese medicine, against hydroquinone-induced toxicity were demonstrated using hepatic L02 cells. Aqueous extracts interfere with the production of ROS mediated by hydroquinone, protecting cells from DNA damage and apoptosis.

O. Vázquez-Martínez and collaborators used rat models to evaluate the effect of portacaval anastomosis (PCA) on liver metabolic parameters. Overall, data from their study demonstrated significant liver metabolic and structural adaptations indicating a vascularization process and a reduction of mitochondrial content as consequences of PCA.

Altered cellular metabolism is at the foundation of different liver diseases including HCC. Metabolic pathways that support tumor pathophysiology were summarised by S. De Matteis and collaborators in a comprehensive review article. They discussed how metabolic pathways reprogram liver metabolism to support a specific metabolic demand and how this can be translated into a specific metabolic signature clinically useful for the diagnosis and prognosis of HCC.

Although detailed mechanisms remain to be fully elucidated, several common observations emerge from this special issue pointing to the role that oxidative stress and metabolic pathways may play in liver-associated disorders. Indeed, clinical and biological data clearly show significant differences between normal and pathological conditions. As we are moving toward a systemic classification of human diseases, these

metabolic alterations have some practical perspectives in the diagnostic and prognostic clinical field that should be taken into account.

Conflicts of Interest

The authors declare that there is no conflict of interest regarding the publication of this paper.

Daniele Vergara
Andrea Casadei-Gardini
Anna M. Giudetti

Research Article

TNF α -Mediated Necroptosis Aggravates Ischemia-Reperfusion Injury in the Fatty Liver by Regulating the Inflammatory Response

Faji Yang,¹ Longcheng Shang,¹ Shuai Wang,¹ Yang Liu ,¹ Haozhen Ren ,¹ Wei Zhu ,² and Xiaolei Shi ¹

¹Department of Hepatobiliary Surgery, Affiliated Drum Tower Hospital of Nanjing University Medical School, 321 Zhongshan Road, Nanjing, 210008 Jiangsu Province, China

²Department of Anesthesiology, Affiliated Drum Tower Hospital of Nanjing University Medical School, 321 Zhongshan Road, Nanjing, 210008 Jiangsu Province, China

Correspondence should be addressed to Wei Zhu; chzhuwei118@qq.com and Xiaolei Shi; njsxl2000@163.com

Received 26 September 2018; Revised 19 December 2018; Accepted 3 April 2019; Published 12 May 2019

Guest Editor: Anna M. Giudetti

Copyright © 2019 Faji Yang et al. This is an open access article distributed under the Creative Commons Attribution License, which permits unrestricted use, distribution, and reproduction in any medium, provided the original work is properly cited.

Nonalcoholic fatty liver disease (NAFLD) is more sensitive to ischemia and reperfusion injury (IRI), while there are no effective methods to alleviate IRI. Necroptosis, also known as “programmed necrosis,” incorporates features of necrosis and apoptosis. However, the role of necroptosis in IRI of the fatty liver remains largely unexplored. In the present study, we aimed to assess whether necroptosis was activated in the fatty liver and whether such activation accelerated IRI in the fatty liver. In this study, we found that the liver IRI was enhanced in HFD-fed mice with more release of TNF α . TNF α and supernatant of macrophages could induce necroptosis of hepatocytes *in vitro*. Necroptosis was activated in NAFLD, leading to more severe IRI, and such necroptosis could be inhibited by TN3-19.12, the neutralizing monoclonal antibody against TNF α . Pretreatment with Nec-1 and GSK'872, two inhibitors of necroptosis, significantly reduced the liver IRI and ROS production in HFD-fed mice. Moreover, the inhibition of necroptosis could decrease ROS production of hepatocytes *in vitro*. Inflammatory response was activated during IRI, and necroptosis inhibitors could suppress signaling pathways of inflammation and the sojourn of inflammation cells. In conclusion, TNF α -induced necroptosis played an important role during IRI in the fatty liver. Our findings demonstrated that necroptosis might be a potential target to reduce the fatty liver-associated IRI.

1. Introduction

Hepatic ischemia-reperfusion injury (IRI) occurs under a variety of clinical conditions, such as liver transplantation and resection, as well as hemorrhagic shock [1, 2]. IRI emerges due to not only the depletion of oxygen and ATP during hypoxia but also an excessive inflammatory response after reperfusion, leading to cell death, including apoptosis, necrosis, and ultimately organ dysfunction [3]. Although the nature of hepatic IRI has been widely studied, the molecular mechanism underlying the hepatocyte death remains largely unexplored. Nonalcoholic fatty liver disease (NAFLD) is the most common cause of chronic liver disease in Western countries, and it is predicted to become also the most frequent indication for liver transplantation by 2030 [4]. Both clinical studies and animal experiments have found that the

steatotic liver is particularly susceptible to IRI [5, 6]. Currently, as the main source of marginal donors, livers with greater than 30% of macrovesicular fat are considered unsuitable for transplantation due to their increased susceptibility to IRI and greater risk of early graft dysfunction [7]. The productions of proinflammatory cytokines, TNF α and IL1 β , are increased during IRI, which are two critical mediators in the fatty liver [8]. TNF α plays a crucial role in almost all the pathogenic nodes of NAFLD, such as development of hepatic steatosis [9], hepatocyte death [10], and fibrosis [11]. However, whether proinflammatory cytokines, such as TNF α , are involved in regulating IRI in the fatty livers remains unknown.

Necroptosis is a novel mode of cell death, known as “programmed necrosis,” which incorporates features of necrosis and apoptosis, and such type of cell death is controlled by

two kinase receptor-interacting proteins (RIP1 and RIP3) [12]. At the functional level, the auto- and transphosphorylations of RIP1 and RIP3 are required for necrosome assembly and activation of necroptotic signaling [13]. RIP3 recruits and phosphorylates the mixed lineage kinase domain-like protein (MLKL), which in turn oligomerizes and causes irreversible cellular membrane damage, resulting in necrotic cell death [14]. It has been suggested that MLKL increases the production of mitochondrial reactive oxygen species (ROS) through mitochondrial targets. Accumulating evidence indicates that necroptosis plays a crucial role in the pathogenesis of inflammatory diseases, including NAFLD [15, 16]. A study has found that necroptosis is best characterized in the setting of TNF α -induced cell death, which has high relevance for many types of liver diseases, but it may also occur under other conditions, including IRI [17]. It has already been shown that the inhibition of necroptosis attenuates necrotic cell death in cardiac, renal, and brain IRI as well as in the liver [18–21]. However, it remains unknown whether necroptosis can be activated by TNF α , and the role of necroptosis during IRI in the fatty liver is also unclear.

In the present study, we found that IRI and ROS production were more serious in the fatty liver compared with the normal liver. Macrophages stimulated with fatty acid expressed and released more TNF α during IRI both *in vivo* and *in vitro*. Moreover, necroptosis was activated in hepatocytes stimulated with TNF α or supernatant from palmitic acid- (PA-) treated macrophages followed by hypoxia-reoxygenation (H/R) injury. Necroptosis inhibitors necrostatin-1 (Nec-1) and GSK'872 could protect livers from IRI in both CD- and HFD-fed mice. In addition, Nec-1 and GSK'872 reduced the ROS level induced by IRI. Furthermore, the inhibition of necroptosis could alleviate inflammatory reaction. Collectively, we, for the first time, investigated the roles of necroptosis during IRI in the fatty liver and provided a potential target to alleviate the fatty liver-associated IRI in liver surgery.

2. Materials and Methods

2.1. Animals. Experiments were conducted using male C57BL/6J mice, which were purchased from the Animal Center of the Affiliated Drum Tower Hospital of Nanjing University Medical School and housed under specific pathogen-free conditions. The animal protocols were approved by the Institutional Animal Care and Use Committee of Nanjing University, China, based on the NIH *Guide for the Care and Use of Laboratory Animals*. All efforts were made to minimize suffering of animals.

Male C57BL/6 mice (3–4 weeks old) were fed with a high-fat diet (HFD: 60% fat, 20% protein, and 20% carbohydrates; 520 kcal/100 g; D12492; Research Diets, New Brunswick, NJ, USA) for 14 weeks to induce steatosis.

2.2. Mouse Hepatic IR Injury. Briefly, 70% hepatic warm ischemia of mice was induced as previously described [22]. After anesthesia, the hepatic artery, portal vein, and bile duct branches to the left and median liver lobes were clamped for 60 min. Mice were sacrificed after 6 h, and liver and serum

samples were collected. Blood samples were analyzed immediately using an automatic analyzer (Fuji, Tokyo, Japan) for alanine aminotransferase (ALT) and aspartate aminotransferase (AST). The livers were cut into pieces and preserved in 4% formalin or snap frozen in liquid nitrogen.

2.3. Cell Culture. Kupffer cells (KCs) were isolated as previously described [22]. Briefly, livers were perfused *in situ* via the portal vein with CMF-HBSS, followed by 0.02% type IV collagenase in HBSS. Then, the liver was dissociated in 0.02% type IV collagenase and filtered through sterile nylon gauze to remove undigested tissue and connective tissue, followed by centrifugation at 35g for 3 min for two times to separate nonparenchymal cells (NPCs). NPCs were then suspended in HBSS and layered onto a 50/25% two-step Percoll gradient (Sigma-Aldrich, USA) in a 50 mL conical centrifuge tube and centrifuged at 1,800g for 15 min at 4°C. KCs in the middle layer were collected and allowed attaching onto cell culture plates in RPMI 1640 medium containing 1% penicillin/streptomycin and 10% fetal bovine serum (FBS).

For primary mouse hepatocytes, cell suspension was washed in William's medium supplemented with 100 nM dexamethasone, 2 mM L-glutamine, 1 μ M insulin, 10% FBS, and 1% penicillin/streptomycin (attachment medium) twice. The hepatocyte suspension was plated on rat tail collagen I-coated six-well plates in the attachment medium. The cells were incubated for 4 h, and then they were washed and further incubated in William's medium supplemented with 2 mM L-glutamine, 10% FBS, and 1% penicillin/streptomycin. Primary hepatocytes were used for experiments within 2–3 days after isolation.

For evaluation of H/R injury *in vitro*, cells were treated with PA (Sigma-Aldrich, USA) for 16 h, followed by fluxing with 95% N₂/5% CO₂ in the absence of FBS and incubation at 37°C for 16 h. For reoxygenation, cells were transferred to a 95% air/5% CO₂ gas mixture and 10% FBS was added.

2.4. Western Blotting Analysis. Proteins were subjected by SDS/PAGE (12% or 10% gel), and the blots were incubated overnight with primary antibodies. The following primary antibodies were used: anti-RIP1 (Cell Signaling Technology, #3493), anti-RIP3 (Santa Cruz Biotechnology, sc-374639), anti-MLKL (phospho S345) (Abcam, ab196436), anti-MLKL (Cell Signaling Technology, #37705), anti-JNK1+JNK2+JNK3 (Abcam, ab208035), anti-JNK1+JNK2+JNK3 (phospho T183+T183+T221) (Abcam, ab124956), anti-c-Jun (Abcam, ab32137), anti-c-Jun (phospho S73) (Abcam, ab30620), anti-ERK1+ERK2 (Abcam, ab17942), anti-ERK1 (pT202/pY204)+ERK2 (pT185/pY187) (Abcam, ab50011), anti-p38 (Abcam, 170099), anti-p38 (phospho Y182) (Abcam, ab47363), anti-NF- κ B (Abcam, ab16502), anti-NF- κ B (phospho S536) (Abcam, ab86299), anti-IK β (Abcam, ab32518), anti-IK β (phospho S36) (Abcam, ab133462), and anti-GAPDH (Abcam, ab181603).

2.5. Quantitative Real-Time Polymerase Chain Reaction (qRT-PCR). Hepatocyte RNA was extracted from snap-frozen liver tissues with TRIzol™ reagent (Life Technologies, USA) according to the manufacturer's instructions. Reverse

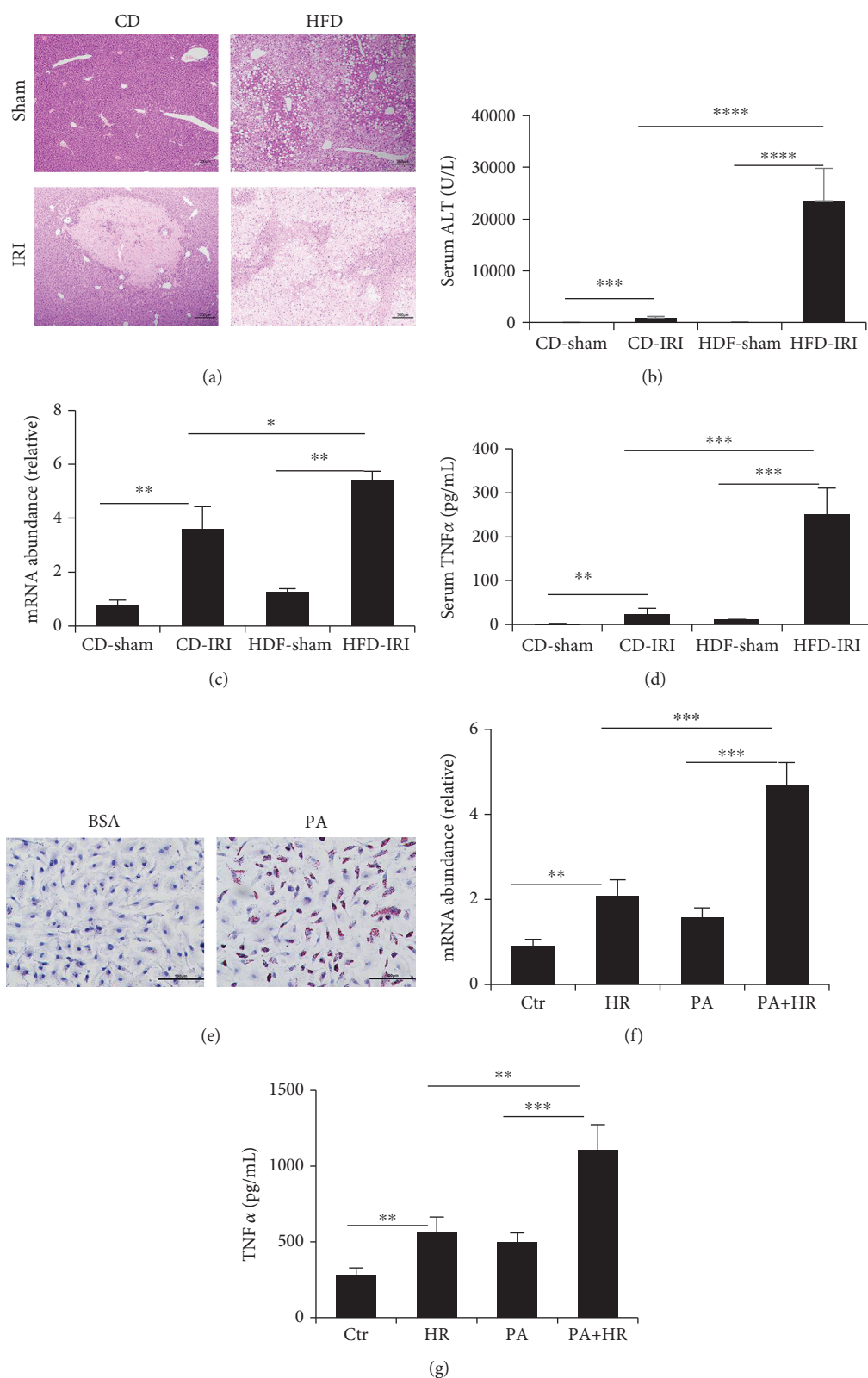


FIGURE 1: Expression and secretion of TNF α are increased in the fatty liver after IRI. (a) Representative H&E staining of liver sections of CD- and HFD-fed mice after IR. Scale bars, 200 μm . (b) Serum ALT of CD- and HFD-fed mice after IR were measured ($n = 6 - 8$). (c) qPCR analysis of TNF α of CD- and HFD-fed mice after IR ($n = 4 - 5$ per group). (d) Serum TNF α was measured after IR in CD- and HFD-fed mice ($n = 5 - 6$ per group). (e) Representative Oil Red O staining of KCs treated with PA (500 μM , Sigma-Aldrich, USA) or PBS for 24 h. Scale bars, 100 μm . (f) TNF α in cell supernatant were measured ($n = 6$ per group). (g) qPCR analysis of TNF α in KCs treated with PA followed by H/R. Data are mean \pm SEM; * $P < 0.05$, ** $P < 0.01$, *** $P < 0.001$, and **** $P < 0.0001$ by unpaired Student's t -test.

transcription was performed with PrimeScript™ RT Master Mix (Takara, Japan) according to the manufacturer's instructions. qRT-PCR was performed using TB Green™ *Premix Ex Taq*™ (Takara, Japan) and ABI Prism 7500 real-time PCR System (Applied Biosystems, USA). Primers used for qPCR are as follows: β -actin forward: 5'-AGTGTGACGTTGACA TCCGTA-3', reverse: 5'-GCCAGAGCAGTAATCTCCT TCT-3' and TNF α forward: 5'-GACGTGGAAGTGGCAG AAGAG-3', reverse: 5'-ACCGCCTGGAGTTCTGGAA-3'.

2.6. Enzyme-Linked Immunosorbent Assay (ELISA). The levels of TNF α (eBioscience, USA) in mouse serum and cell culture supernatants were measured using commercially available ELISA kits according to the manufacturer's instructions.

2.7. Histological and Immunohistochemical Analysis. Paraffin liver sections (5 μ m) were stained with hematoxylin and eosin (HE) for histological evaluation of IRI based on standard pathology methods and visualized using a light microscope. Liver damage was evaluated using Suzuki's score by two independent pathologists. To identify macrophages and neutrophils, paraffin-embedded liver sections (5 μ m) were stained with F4-80 (Abcam, USA) and myeloperoxidase (MPO, Abcam, USA) as previously described [22].

2.8. PI Staining. Cells and frozen liver sections (4 μ m) were fixed with 4% paraformaldehyde for 30 min and washed twice with PBS. After treatment with 10 mg/mL DNase-free RNase at 37°C for 30 min, cell nuclei were stained with 10 mg/mL propidium iodide (PI, KeyGEN BioTECH, China) at room temperature for 5 min in the dark, then counterstained with DAPI, and observed under a fluorescence microscope.

2.9. Determination of ROS. For liver tissues, the ROS level was measured with the dihydroethidium (DHE, KeyGEN BioTECH, China) following the manufacturer's instructions. Briefly, frozen liver sections (4 μ m) were incubated with 20 μ M DHE in the dark at 37°C for 30 min and then counterstained with DAPI. After washing, slides were mounted and observed under an immunofluorescence microscope.

For cells, cells were incubated in the dark with 10 μ mol/L DCFH-DA (Beyotime Institute of Biotechnology, China) at 37°C for 20 min and then washed with PBS three times to remove residual probes. DCFH-DA was intracellularly by nonspecific esterase and oxidized by oxidant species to form the fluorescent compound 2',7'-dichloro-fluorescein (DCF). The fluorescent signal intensity of DCF was detected under an immunofluorescence microscope.

2.10. Oil Red O Stain Assay. To detect lipid accumulation in macrophages, Oil Red O Stain Kit (Jiancheng Bioengineering Institute, China) was used according to the manufacturer's instructions and visualized using a light microscope.

2.11. Immunocytofluorescence (ICF) Analysis. Immunofluorescence analysis was performed according to the previously described protocols. Briefly, frozen liver sections (4 μ m) fixed with acetone were penetrated with 0.3% Triton for 15 min. Then, the slides were blocked with 10% fetal sheep serum,

TABLE 1: The mice fed with a HFD exhibited significantly increased Suzuki's score of IRI in HFD-fed mice.

Group	Suzuki's score
CD-sham	0.46 \pm 0.23
CD-IRI	4.01 \pm 0.26 ^a
HFD-sham	2.97 \pm 0.45 ^b
HFD-IRI	7.13 \pm 0.83 ^{c,d}

The results are presented as the mean \pm SEM of 6 to 8 animals per group. ^aSignificant difference ($P < 0.001$) versus the CD-sham group. ^bSignificant difference ($P < 0.01$) versus the CD-sham group. ^cSignificant difference ($P < 0.01$) versus the CD-IRI group. ^dSignificant difference ($P < 0.01$) versus the HFD-sham group.

followed by incubation with primary antibodies overnight at 4°C. After washing, slides were incubated with the corresponding secondary antibodies, followed by incubation with DAPI. Representative images were observed under an immunofluorescence microscope. The following antibodies were used: anti-RIP3 (Santa Cruz Biotechnology, sc-374639) and goat anti-mouse IgG H&L (Alexa Fluor® 488) (Abcam, ab150117).

2.12. Statistical Analysis. Statistical analysis was performed using the GraphPad Prism software version 6.0. All data were expressed as mean \pm standard error of the mean (SEM). Normally distributed data were tested by Student's *t*-test. *P* value less than 0.05 was considered statistically significant.

3. Results

3.1. Expression and Secretion of TNF α Are Increased in the Fatty Liver after IRI. Compared with the control group (fed with a control diet, CD), the mice fed with a HFD exhibited significantly worse IRI, evidenced by higher serum ALT and increased Suzuki's score in HFD-fed mice (Figures 1(a) and 1(b) and Table 1). From the pathological liver sections, there were more edema, sinusoidal congestion, and necrosis in HFD-fed mice (Figure 1(a)). The expression of TNF α at both the liver tissue and serum levels was higher in HFD-fed mice compared with those fed with a CD (Figures 1(c) and 1(d)). Macrophages are the major source of inflammatory factors, including TNF α . Therefore, we extracted KCs and treated with PA (50 μ m) to simulate macrophages in the fatty liver. After 24 h of stimulation, lipid accumulation was found in the cytoplasm (Figure 1(e)). Then, we investigated the effect of IRI on KCs with steatosis using an *in vitro* model of IRI. After H/R stimulation, the expression of TNF α at the mRNA level in KCs and cellular supernatant was increased. Moreover, PA treatment enhanced the expression of TNF α (Figures 1(f) and 1(g)). In conclusion, macrophages in the fatty liver expressed and released more TNF α compared with the normal liver after IRI.

3.2. TNF α Induces Necroptosis In Vitro. Studies have shown that necroptosis is best characterized in the setting of TNF α -induced cell death. To further verify whether

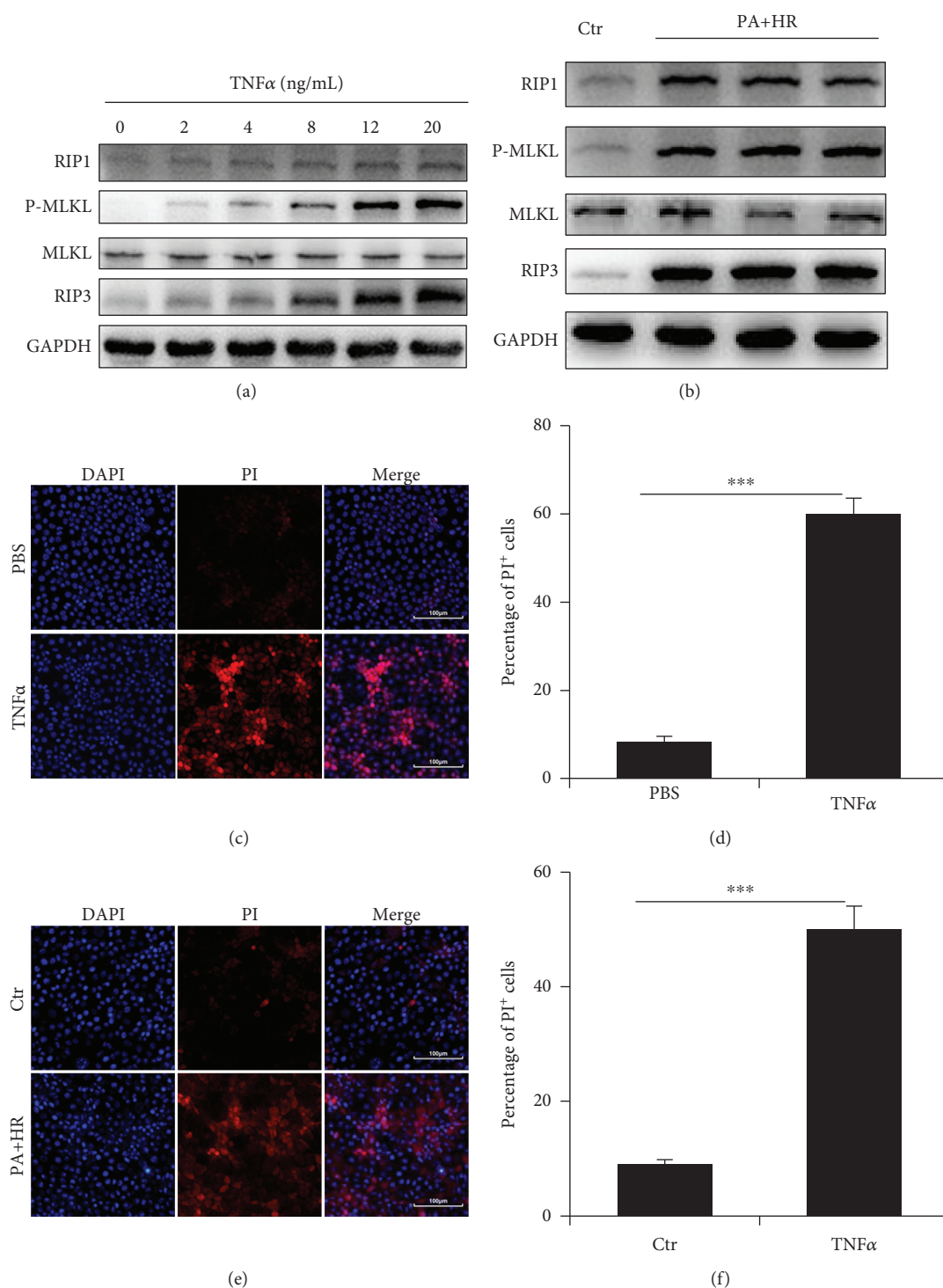


FIGURE 2: TNF α induces necroptosis *in vitro*. Hepatocytes were cultured with TNF α (PeproTech, USA) or cell supernatant of KCs treated with PA followed by H/R for 24 h. (a) Immunoblot analysis of RIP1, RIP3, and MLKL of hepatocytes treated with different concentrations of TNF α . (b) Immunoblot analysis of RIP1, RIP3, and MLKL of hepatocytes treated with cell supernatant of KCs for 24 h. (c, d) Representative immunofluorescence staining of propidium iodide (PI) staining of hepatocytes treated with TNF α (20 ng/mL) for 24 h. Scale bars, 100 μ m. (e, f) Representative immunofluorescence staining of PI of hepatocytes treated with cell supernatant of KCs for 24 h. Scale bars, 100 μ m. Data are mean \pm SEM; * P < 0.05, ** P < 0.01, and *** P < 0.001 by unpaired Student's t -test.

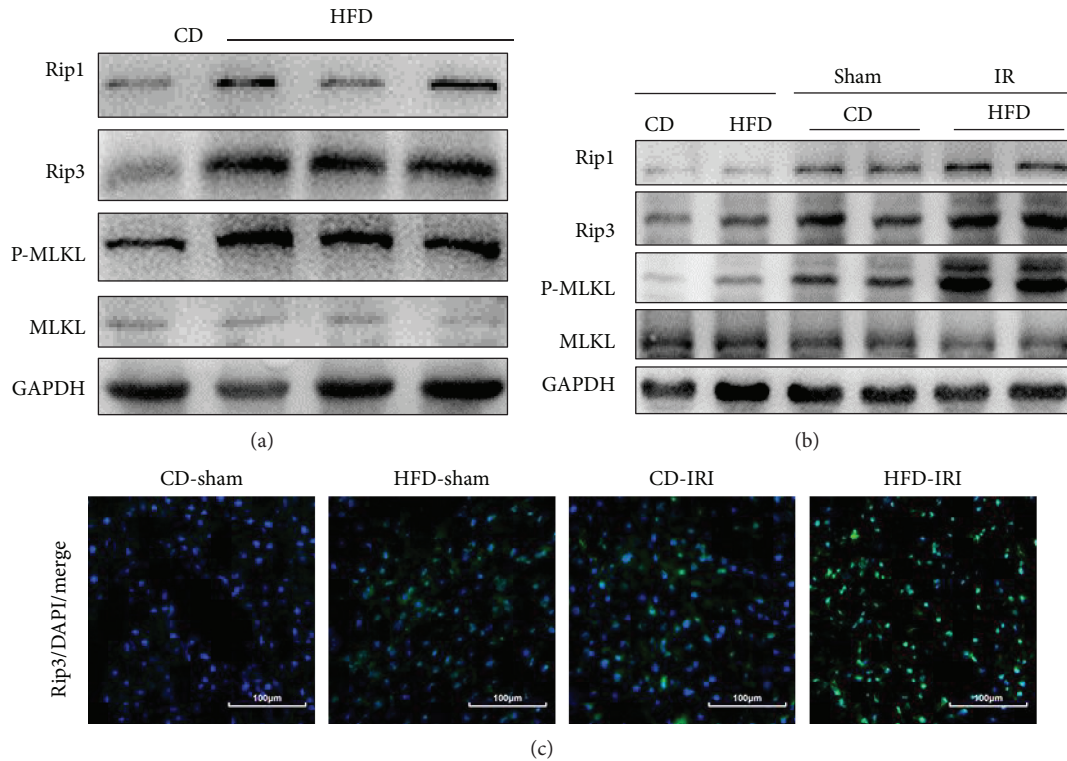


FIGURE 3: Necroptosis is found in NAFLD after IRI. (a) Immunoblot analysis of necroptosis markers RIP1, RIP3, and MLKL of mice fed with a CD or a HFD. (b) Immunoblot analysis of RIP1, RIP3, and MLKL of CD- and HFD-fed mice after 60 min of ischemia and 6 h of reperfusion. (c) Representative immunofluorescence staining of RIP3 was performed in CD- and HFD-fed mice with or without 60 min of ischemia and 6 h of reperfusion. Scale bars, 100 μ m.

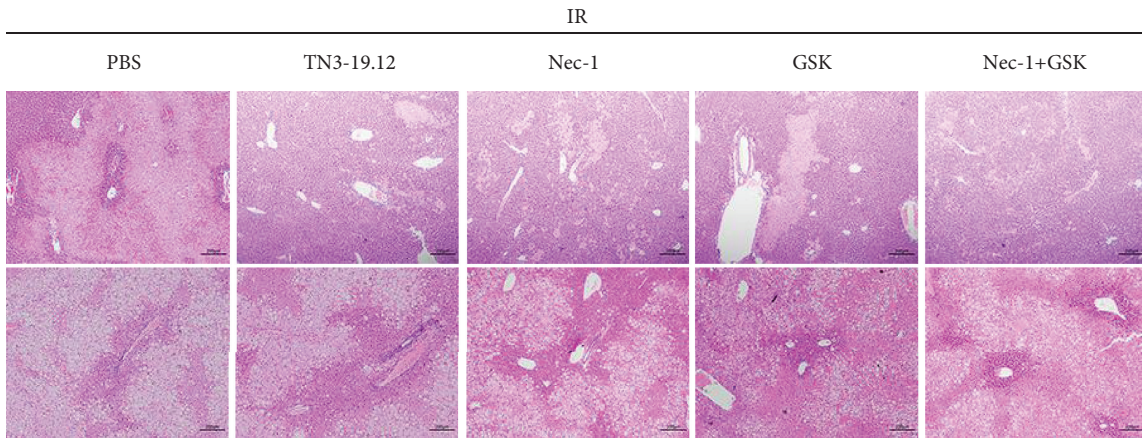
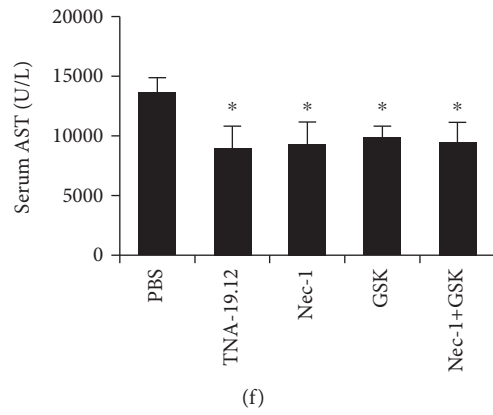
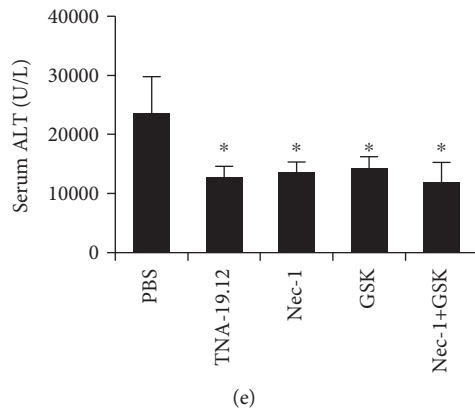
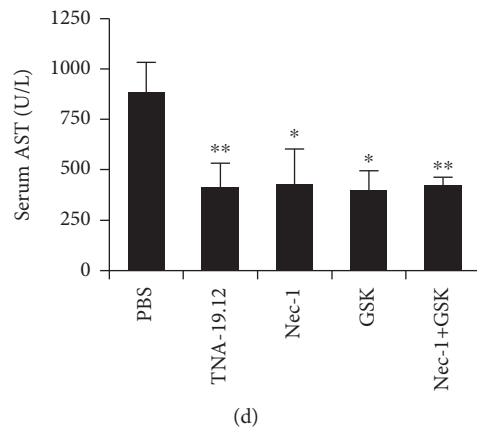
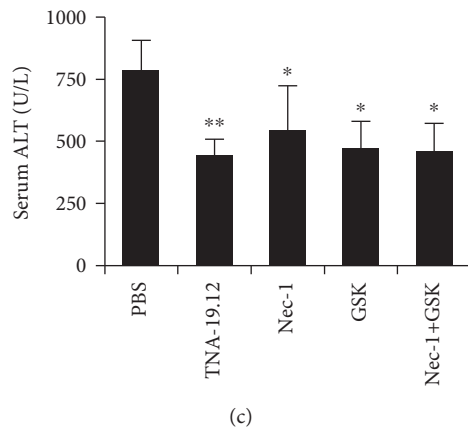
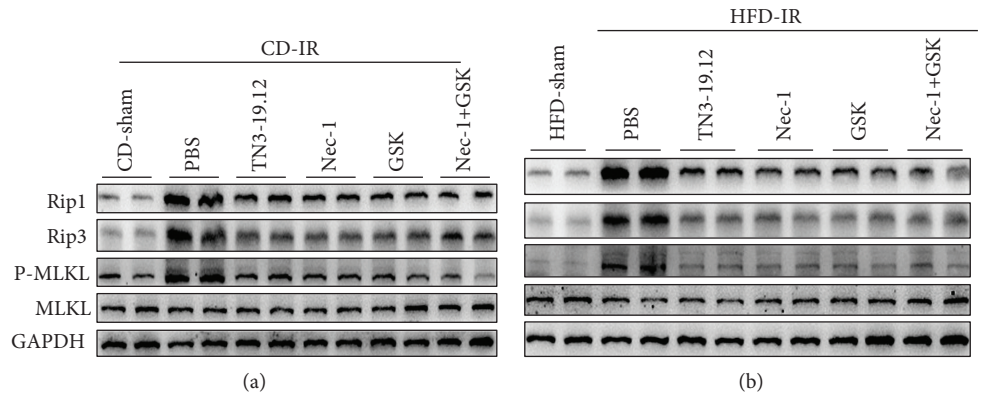
necroptosis was associated with TNF α , primary mouse hepatocytes were treated with TNF α for 24 h. Figure 2(a) shows that the expressions of RIP1, RIP3, and MLKL were significantly increased upon stimulation of TNF α and necroptosis was induced by TNF α in a concentration-dependent manner. Cellular supernatant of KCs treated with PA and H/R could also activate necroptosis of hepatocytes (Figure 2(b)). The viability of hepatocytes was assessed by dual staining of DAPI and PI. A high proportion of PI⁺ cells was found after TNF α treatment (Figures 2(c) and 2(d)). The number of PI⁺ cells was also markedly increased when stimulated with supernatant of KCs treated with PA and H/R (Figures 2(e) and 2(f)). Therefore, these results showed that TNF α could induce necroptosis *in vitro*.

3.3. Necroptosis Is Found in NAFLD after IRI. We showed TNF α -induced necroptosis *in vitro*, and then we detected necroptosis in the fatty liver following IRI. Figure 3(a) reveals that necroptosis was activated in livers of HFD-fed mice. After IRI, necroptosis was further activated, exhibiting the upregulation of necroptotic markers (RIP1, RIP3, and MLKL). This finding suggested that necroptosis was further activated by IRI (Figure 3(b)). Moreover, immunofluorescence staining of RIP3 further indicated that necroptosis was activated in NAFLD with or without IRI (Figure 3(c)). Taken together, necroptosis was activated in the fatty liver

and further enhanced after IRI, which might contribute to the enhanced IRI in HFD-fed mice.

3.4. Inhibition of Necroptosis Reduces IRI in NAFLD. Necroptosis was activated during IRI, and the fatty liver further aggravated the activation. Therefore, we speculated whether the inhibition of necroptosis could attenuate IRI in the fatty liver. Nec-1 and GSK'872, two necroptosis inhibitors, were administered by intraperitoneal injection 1 h before IRI. TN3-19.12, the neutralizing monoclonal antibody against TNF α [23], was also used to confirm whether TNF α was an effective trigger of necroptosis during liver IRI by intraperitoneal injection. We found that TN3-19.12, Nec-1, and GSK'872 could significantly inhibit necroptosis in both CD- and HFD-fed mice, showing increased expressions of RIP1, RIP3, and MLKL (Figures 4(a) and 4(b)). Consistent with our conjecture, Nec-1 and GSK'872 as well as TN3-19.12 reduced levels of ALT and AST in CD- and HFD-fed mice (Figures 4(c)–4(f)). HE staining and decreased Suzuki's scores revealed that liver injury was also reduced (Figure 4(g) and Tables 2 and 3). PI staining exhibited that hepatocyte necrosis, the direct result of IRI damage, was also alleviated after IRI (Figure 4(h)).

We also studied the above-mentioned conjecture *in vitro*. Primary hepatocytes were stimulated with TNF α to induce IRI. Nec-1 and GSK'872 could also reduce the expressions of RIP1, RIP3, and MLKL in TNF α -treated hepatocytes



(g)

FIGURE 4: Continued.

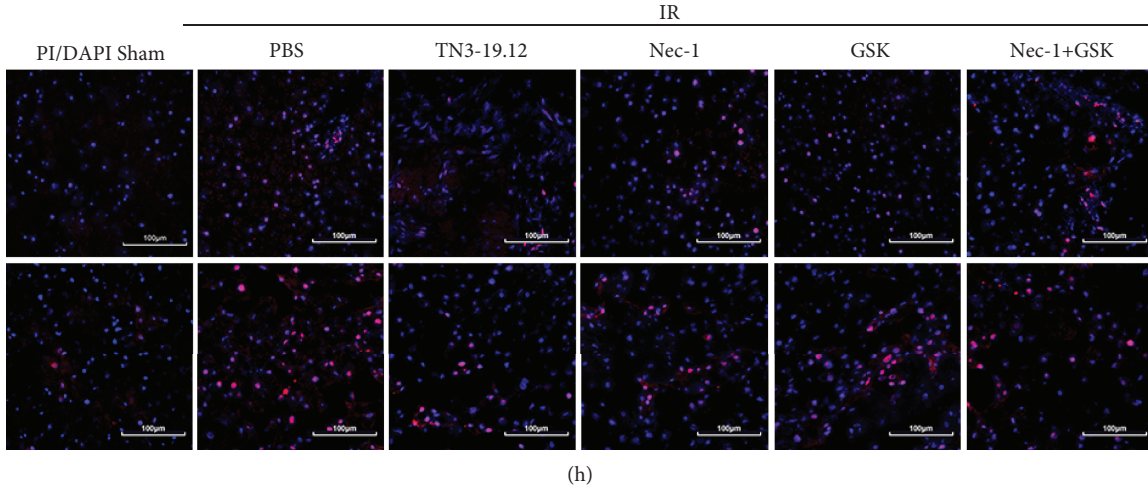


FIGURE 4: Inhibition of necroptosis reduces ischemia-reperfusion injury of NAFLD. (a) Immunoblot analysis of necroptosis markers RIP1, RIP3, and MLKL of mice fed with a CD after IRI pretreated with Nec-1 (1.65 mg/kg, Selleck, USA), GSK'872 (1.9 mM/kg, Selleck, USA), and TN3-19.12 (250 μ g/mouse, Sigma-Aldrich, USA). (b) Immunoblot analysis of necroptosis markers RIP1, RIP3, and MLKL of mice fed with HFD after IRI pretreated with TN3-19.12, Nec-1, and GSK'872. (c, d) Serum ALT and AST of mice fed with a CD after IRI ($n = 6 - 8$ per group). (e, f) Serum ALT and AST of mice fed with a HFD after IRI ($n = 6 - 8$ per group). (g) Representative H&E staining of liver sections. Scale bars, 200 μ m. (h) Representative immunofluorescence staining of PI. Scale bars, 100 μ m. Data are mean \pm SEM; * $P < 0.05$ by unpaired Student's t -test.

TABLE 2: Inhibition of necroptosis reduces Suzuki's score of IRI in CD-fed mice.

Group	Suzuki's score
PBS-IRI	3.98 ± 0.26
TN3-19.12-IRI	1.51 ± 0.36^a
Nec-1-IRI	1.77 ± 0.21^a
GSK-IRI	2.11 ± 0.29^b
Nec-1+GSK-IRI	1.62 ± 0.29^a

The results are presented as the mean \pm SEM of 6 to 8 animals per group. ^aSignificant difference ($P < 0.01$) versus the PBS-IRI group. ^bSignificant difference ($P < 0.05$) versus the PBS-IRI group.

TABLE 3: Inhibition of necroptosis reduces Suzuki's score of IRI in HFD-fed mice.

Group	Suzuki's score
PBS-IRI	7.03 ± 0.83
TN3-19.12-IRI	4.51 ± 0.57^a
Nec-1-IRI	5.57 ± 0.48^b
GSK-IRI	4.77 ± 0.56^a
Nec-1+GSK-IRI	4.73 ± 0.79^b

The results are presented as the mean \pm SEM of 6 to 8 animals per group. ^aSignificant difference ($P < 0.01$) versus the PBS-IRI group. ^bSignificant difference ($P < 0.05$) versus the PBS-IRI group.

(Figure 5(a)). Furthermore, Nec-1 and GSK'872 also decreased the proportion of PI⁺ hepatocytes (Figure 5(b)). Taken together, the inhibition of necroptosis could reduce cell injury induced by TNF α during IRI in NAFLD.

3.5. Inhibition of Necroptosis Reduces ROS Production after IRI in NAFLD Both In Vivo and In Vitro. The pathophysiology of hepatic IRI generally includes ROS production. In terms of entity of oxidative stress, the most relevant event is ROS production by activated inflammatory cells, while liver cells can also produce ROS by the uncoupled mitochondria due to oxygen readmission [24]. Moreover, it has been suggested that MLKL increases mitochondrial ROS production through mitochondrial targets [25]. Therefore, we detected whether Nec-1 and GSK'872 could reduce the ROS production. Figure 6(a) reveals that ROS production was increased during IRI, and it was further enhanced in the fatty liver. Pretreatment with Nec-1 and GSK'872 could significantly decrease the ROS level. The same results were also found by *in vitro* experiments (Figure 6(b)). Therefore, the inhibition of necroptosis could reduce the ROS level after IRI in NAFLD, and this might be another mechanism of alleviating IRI in the fatty liver.

3.6. Inhibition of Necroptosis Reduces the Inflammatory Response after IRI in NAFLD. Danger-associated molecular patterns (DAMPs) are either passively released by necrotic cells and the damaged extracellular matrix or are actively secreted by stressed and injured cells [26]. Various types of DAMPs are released during liver IRI, and these DAMPs can interact with and activate toll-like receptor (TLRs). The TLRs are one of the components by which the innate immune system senses the invasion of pathogenic microorganisms or tissue damage by recognizing DAMPs [27]. Transcription factors have been shown to mediate TLR activation in liver IRI, including NF- κ B, JNK, ERK, p38, and IKB α [28]. Therefore, we assessed the expressions of these transcription factors in the fatty livers. Figure 7(a) shows that compared

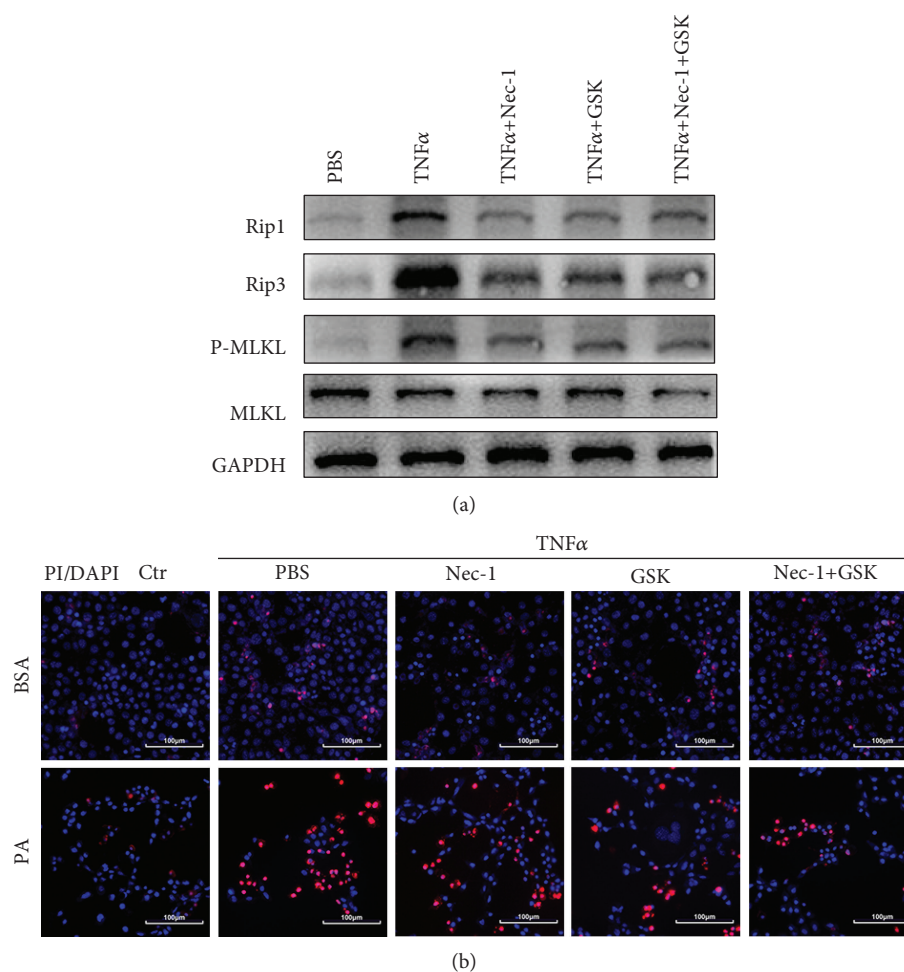


FIGURE 5: Inhibition of necroptosis reduces hepatocyte death induced by TNF α *in vitro*. (a) Hepatocytes were cultured with TNF α (20 ng/mL) for 24 h. Immunoblot analysis of necroptosis markers RIP1, RIP3, and MLKL of hepatocytes pretreated with Nec-1 (100 μ M) and GSK'872 (5 μ M). (b) Representative immunofluorescence staining of PI. Scale bars, 100 μ m.

with CD-fed mice, all the transcription factors were activated in HFD-fed mice and IRI increased the expressions of NF- κ B, JNK, ERK, p38, and IKB α . Moreover, we found that the liver inflammatory response after IRI was inhibited by Nec-1 and GSK'872 in both CD- and HFD-fed mice (Figures 7(b) and 7(c)). In addition, the same findings were achieved by *in vitro* experiments (Figure 7(d)). There was also more infiltration of MPO- and F4-80-positive cells in HFD-fed mice after IRI. Inhibition of necroptosis could also decrease the soakage of inflammation cells (Figures 7(e) and 7(f)). In summary, the inhibition of necroptosis by Nec-1 and GSK'872 could reduce the inflammatory response after IRI in NAFLD, which might be another mechanism protecting the fatty liver from IRI.

4. Discussion

IRI results from a prolonged ischemic insult, followed by the restoration of blood perfusion. Hepatic IRI can lead to severe liver injury, and it is a major cause for the failure of liver

transplantation. However, the fatty liver is more sensitive to IRI, leading to more severe outcomes of patients. Moreover, in the past two decades, urbanization has led to sedentary lifestyle and overnutrition, setting the stage for the epidemic of obesity and NAFLD, which is currently estimated to be 24% worldwide [29, 30]. Therefore, it is urgently necessary to prevent and attenuate IRI [22, 31]. However, there are no available effective and simple methods available to reduce IRI in the fatty liver. In the present study, we also found that IRI in the fatty liver was more severe compared with the normal liver and the TNF α level was increased in serum and liver of NASH animals, which was in agreement with the previous report [11].

As a newly defined type of programmed cell death, necroptosis is tightly controlled by the multiprotein complex of RIP1 and RIP3, known as the necrosome. Accumulating evidence indicates that MLKL and the protein kinases (RIPK1 and RIPK3) contribute to inflammatory processes through both the induction of necroptotic cell death and other cellular changes [32, 33]. Necroptosis has been shown to be involved in various ischemic, inflammatory, and

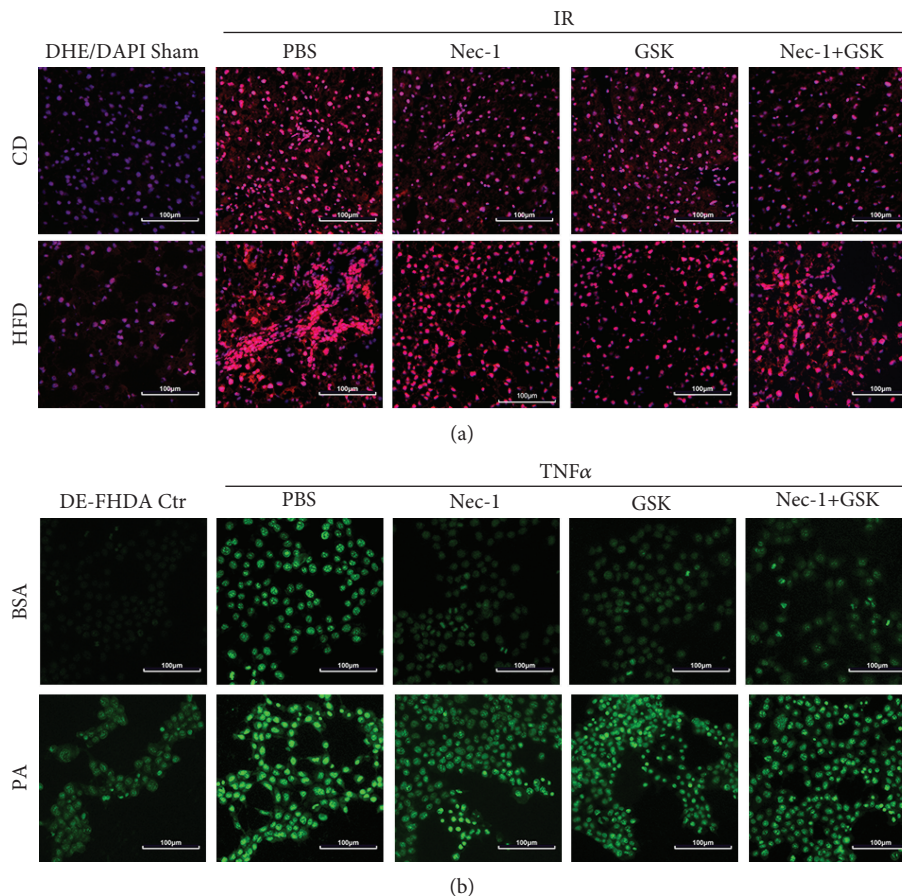


FIGURE 6: Inhibition of necroptosis reduces ROS after IRI of NAFLD both *in vivo* and *in vitro*. (a) Representative images of DHE staining of liver sections in CD- and HFD-fed mice with Nec-1 and GSK'872 pretreatment. Scale bars, 100 μm. (b) Representative images of DE-FHDA staining of hepatocytes with Nec-1 and GSK'872 pretreatment followed by TNF α stimulation. Scale bars, 100 μm.

neurodegenerative human disorders [34]. Necroptosis has been identified as a mechanism of cell death in renal, cardiac, and retinal IRI [18, 35, 36]. A recent study has found that necroptosis contributes to hepatic damage during IR, which induces autophagy via ERK activation [21]. However, another study has found that necroptotic molecules are not increased in the necrosis-dominant hepatic IRI model, and antinecroptosis does not have an overall protective effect on necrosis-dominant hepatic IRI [37]. Therefore, the role of necroptosis or even whether necroptosis is activated in liver IRI remains largely unexplored. In the present study, we found that TNF α was upregulated in the fatty liver and its level was further increased after IRI. Early studies have found that TNF α is the best characterized activator to induce necroptosis. Therefore, we stimulated hepatocytes with TNF α . As expected, necroptosis was significantly activated by TNF α as well as supernatant of KCs treated with PA and H/R. Moreover, we tested the expressions of RIP1, RIP3, and MLKL in liver tissues suffering IRI, and all three markers of necroptosis were upregulated. In addition, the activation of necroptosis was much more intensive in the fatty liver, which was consistent with the level of TNF α . Furthermore, Nec-1 and GSK'872 could significantly reduce necroptosis and protect the liver from IRI in both CD- and

HFD-fed mice (Figure 8). To the best of our knowledge, we, for the first time, demonstrated that necroptosis was activated during IRI in the fatty liver, and inhibition of necroptosis could reduce IRI in NAFLD.

Immune cells, such as macrophages, are activated during the ischemic phase and even more during reperfusion. Once activated, they produce proinflammatory cytokines, including TNF α [38]. Cytokines play critical roles by stimulating hepatocytes to produce ROS, greatly contributing to their damage [39]. In the present study, we also found that ROS production was increased in hepatocytes of the fatty liver after IRI as well as hepatocytes stimulated with TNF α . Inhibition of necroptosis could reduce the level of ROS. Therefore, necroptosis contributed to the ROS production, which might aggravate the IRI in the fatty liver. DAMPs released during liver IRI bind to a group of receptors termed pattern recognition receptors (PRRs) to induce the inflammatory response [40]. Transcription factors, including NF- κ B, JNK, ERK, p38, and IKB α , participate in the activation of the inflammatory response. In this study, we found that transcription factors, as well as the sojourn of inflammation cells, were all significantly upregulated during IRI in the fatty liver, while the inhibition of necroptosis could reduce the inflammatory response (Figure 8).

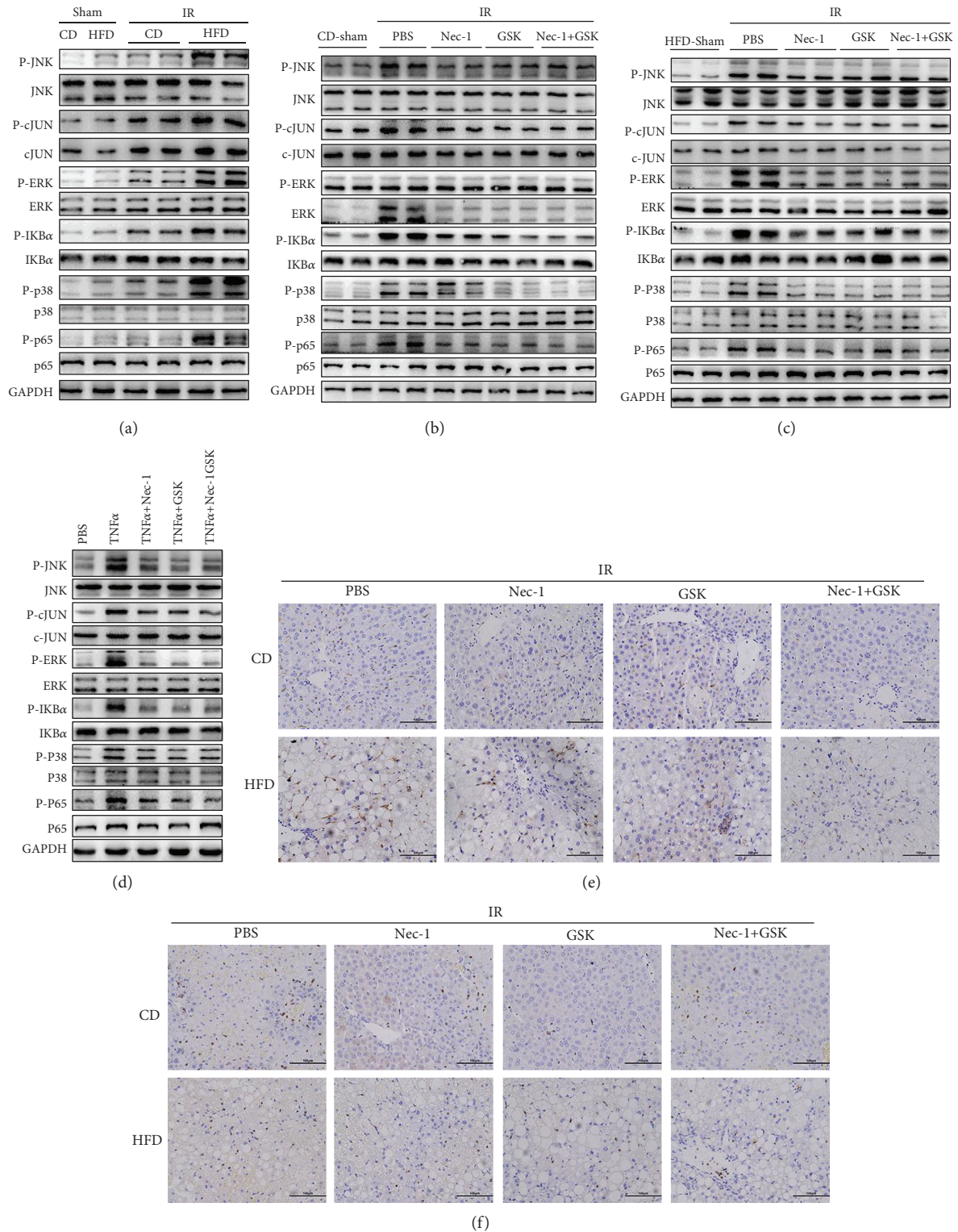


FIGURE 7: Inhibition of necroptosis reduces the inflammatory response after IRI of NAFLD. (a) Immunoblot analysis of JNK, cJUN, ERK, IKB α , p38, and p65 of CD- and HFD-fed mice with or without IRI. (b) Immunoblot analysis of JNK, cJUN, ERK, IKB α , p38, and p65 of CD-fed mice after IRI with Nec-1 and GSK'872 pretreatment. (c) Immunoblot analysis of JNK, cJUN, ERK, IKB α , p38, and p65 of CD-fed mice after IRI with Nec-1 and GSK'872 pretreatment. (d) Immunoblot analysis of JNK, cJUN, ERK, IKB α , p38, and p65 of hepatocytes with Nec-1 and GSK'872 pretreatment. (e) Representative F4-80 immunohistochemistry of liver sections with IRI in CD- and HFD-fed mice. Scale bars, 100 μ m. (f) Representative MPO immunohistochemistry of liver sections with IRI in CD- and HFD-fed mice. Scale bars, 100 μ m.

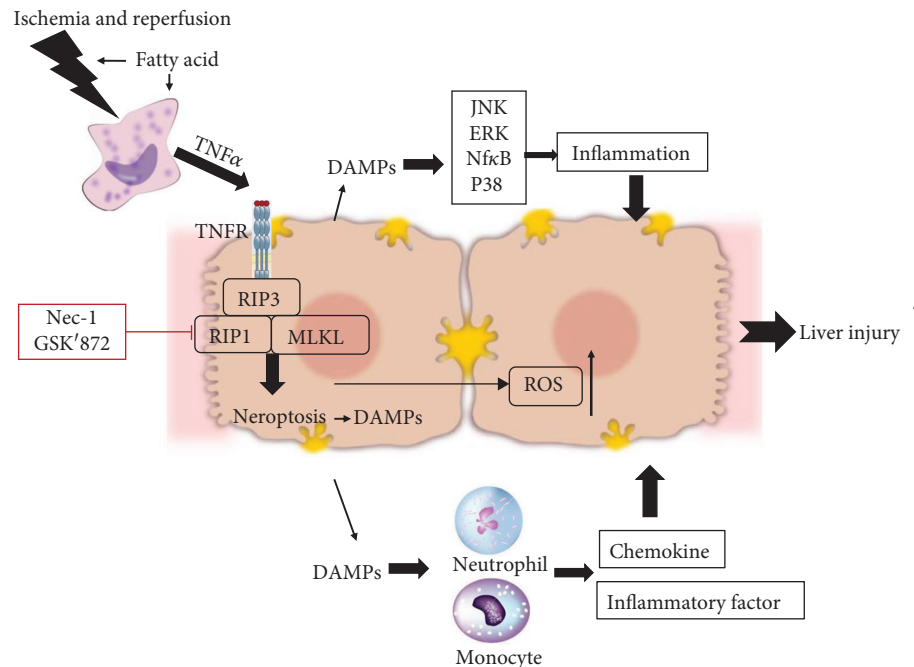


FIGURE 8: TNF α -mediated necroptosis aggravates IRI in the fatty liver by regulating the inflammatory response. Macrophages were activated during IRI, which secreted more TNF α in the fatty liver compared with the normal liver. Necroptosis induced by TNF α was activated in NAFLD, leading to more severe IRI. Necroptosis promoted the production of DAMPs, which increased signaling pathways of inflammation and the sojourn of inflammation cells to aggravate IRI. Inhibition of necroptosis with Nec-1 and GSK'872 could decrease the signaling pathway of inflammation and ROS production to protect the liver from IRI.

5. Conclusions

In the present study, we found a new mechanism, which could explain why the fatty liver was more susceptible to IRI, and demonstrated the mechanism underlying the necroptosis of the fatty liver. Our findings provided a potential target to reduce the fatty liver-associated IRI in liver transplantation.

Abbreviations

NAFLD: Nonalcoholic fatty liver disease
 IRI: Ischemia and reperfusion injury
 ALT: Alanine aminotransferase
 AST: Aspartate aminotransferase
 KCs: Kupffer cells
 TNF α : Tumor necrosis factor α
 HFD: High-fat diet
 CD: Control diet
 PA: Palmitic acid
 ROS: Reactive oxygen species
 RIP1: Receptor-interacting protein 1
 RIP3: Receptor-interacting protein 3
 MLKL: Mixed lineage kinase domain-like protein
 JNK: c-Jun NH2-terminal kinase
 p38: Mitogen-activated protein kinase 14
 NF κ B: Nuclear factor kappa B
 ERK: Extracellular-regulated MAP kinase
 I κ B α : NF κ B inhibitor alpha
 DAMPs: Danger-associated molecular patterns

Nec-1: Necrostatin-1

PRRs: Pattern recognition receptors.

Data Availability

The data used to support the findings of this study are available from the corresponding authors upon request.

Conflicts of Interest

The authors declare that they have no conflict of interest.

Authors' Contributions

Faji Yang, Longcheng Shang, and Shuai Wang contributed equally to this work.

Acknowledgments

This project was supported by grants from the National Natural Science Foundation of China (NSFC) (Grant Nos. 81670566 and 81872359) and the Key Project Supported by Medical Science and Technology Development Foundation, Nanjing Department of Health (Grant No. ZKX14025).

References

- [1] Y. Zhai, H. Petrowsky, J. C. Hong, R. W. Busuttil, and J. W. Kupiec-Weglinski, "Ischaemia-reperfusion injury in liver transplantation—from bench to bedside," *Nature Reviews. Gastroenterology & Hepatology*, vol. 10, no. 2, pp. 79–89, 2013.

- [2] B. Vollmar and M. D. Menger, "The hepatic microcirculation: mechanistic contributions and therapeutic targets in liver injury and repair," *Physiological Reviews*, vol. 89, no. 4, pp. 1269–1339, 2009.
- [3] R. F. van Golen, M. J. Reiniers, P. B. Olthof, T. M. van Gulik, and M. Heger, "Sterile inflammation in hepatic ischemia/reperfusion injury: present concepts and potential therapeutics," *Journal of Gastroenterology and Hepatology*, vol. 28, no. 3, pp. 394–400, 2013.
- [4] C. D. Byrne and G. Targher, "NAFLD: a multisystem disease," *Journal of Hepatology*, vol. 62, no. 1, pp. S47–S64, 2015.
- [5] M. B. Jiménez-Castro, N. Meroño, M. Mendes-Braz et al., "The effect of brain death in rat steatotic and non-steatotic liver transplantation with previous ischemic preconditioning," *Journal of Hepatology*, vol. 62, no. 1, pp. 83–91, 2015.
- [6] M. Elias-Miró, M. Mendes-Braz, R. Cereijo et al., "Resistin and visfatin in steatotic and non-steatotic livers in the setting of partial hepatectomy under ischemia-reperfusion," *Journal of Hepatology*, vol. 60, no. 1, pp. 87–95, 2014.
- [7] R. W. Busuttill and K. Tanaka, "The utility of marginal donors in liver transplantation," *Liver Transplantation*, vol. 9, no. 7, pp. 651–663, 2003.
- [8] P. Kubes and W. Z. Mehal, "Sterile inflammation in the liver," *Gastroenterology*, vol. 143, no. 5, pp. 1158–1172, 2012.
- [9] J. M. Hui, A. Hodge, G. C. Farrell, J. G. Kench, A. Kriketos, and J. George, "Beyond insulin resistance in NASH: TNF-alpha or adiponectin?," *Hepatology*, vol. 40, no. 1, pp. 46–54, 2004.
- [10] P. S. Ribeiro, H. Cortez-Pinto, S. Solá et al., "Hepatocyte apoptosis, expression of death receptors, and activation of NF- κ B in the liver of nonalcoholic and alcoholic steatohepatitis patients," *The American Journal of Gastroenterology*, vol. 99, no. 9, pp. 1708–1717, 2004.
- [11] K. Tomita, G. Tamiya, S. Ando et al., "Tumour necrosis factor alpha signalling through activation of Kupffer cells plays an essential role in liver fibrosis of non-alcoholic steatohepatitis in mice," *Gut*, vol. 55, no. 3, pp. 415–424, 2006.
- [12] S. He, L. Wang, L. Miao et al., "Receptor interacting protein kinase-3 determines cellular necrotic response to TNF-alpha," *Cell*, vol. 137, no. 6, pp. 1100–1111, 2009.
- [13] J. Li, T. McQuade, A. B. Siemer et al., "The RIP1/RIP3 necrosome forms a functional amyloid signaling complex required for programmed necrosis," *Cell*, vol. 150, no. 2, pp. 339–350, 2012.
- [14] H. Wang, L. Sun, L. Su et al., "Mixed lineage kinase domain-like protein MLKL causes necrotic membrane disruption upon phosphorylation by RIP3," *Molecular Cell*, vol. 54, no. 1, pp. 133–146, 2014.
- [15] T. Luedde, N. Kaplowitz, and R. F. Schwabe, "Cell death and cell death responses in liver disease: mechanisms and clinical relevance," *Gastroenterology*, vol. 147, no. 4, pp. 765–783.e4, 2014.
- [16] M. B. Afonso, P. M. Rodrigues, T. Carvalho et al., "Necroptosis is a key pathogenic event in human and experimental murine models of non-alcoholic steatohepatitis," *Clinical Science (London, England)*, vol. 129, no. 8, pp. 721–739, 2015.
- [17] N. N. Danial and S. J. Korsmeyer, "Cell death: critical control points," *Cell*, vol. 116, no. 2, pp. 205–219, 2004.
- [18] A. Linkermann, J. H. Bräsen, N. Himmerkus et al., "Rip1 (receptor-interacting protein kinase 1) mediates necroptosis and contributes to renal ischemia/reperfusion injury," *Kidney International*, vol. 81, no. 8, pp. 751–761, 2012.
- [19] R. Chavez-Valdez, L. J. Martin, D. L. Flock, and F. J. Northington, "Necrostatin-1 attenuates mitochondrial dysfunction in neurons and astrocytes following neonatal hypoxia-ischemia," *Neuroscience*, vol. 219, pp. 192–203, 2012.
- [20] M. I. F. J. Oerlemans, J. Liu, F. Arslan et al., "Inhibition of RIP1-dependent necrosis prevents adverse cardiac remodeling after myocardial ischemia-reperfusion in vivo," *Basic Research in Cardiology*, vol. 107, no. 4, p. 270, 2012.
- [21] J. M. Hong, S. J. Kim, and S. M. Lee, "Role of necroptosis in autophagy signaling during hepatic ischemia and reperfusion," *Toxicology and Applied Pharmacology*, vol. 308, pp. 1–10, 2016.
- [22] F. Yang, S. Wang, Y. Liu et al., "IRE1 α aggravates ischemia reperfusion injury of fatty liver by regulating phenotypic transformation of kupffer cells," *Free Radic Biol Med*, vol. 124, pp. 395–407, 2018.
- [23] R. B. Zinyama, G. J. Bancroft, and L. B. Sigola, "Adrenaline suppression of the macrophage nitric oxide response to lipopolysaccharide is associated with differential regulation of tumour necrosis factor-alpha and interleukin-10," *Immunology*, vol. 104, no. 4, pp. 439–446, 2001.
- [24] P. Mukhopadhyay, B. Horváth, Z. Zsengeller et al., "Mitochondrial reactive oxygen species generation triggers inflammatory response and tissue injury associated with hepatic ischemia-reperfusion: therapeutic potential of mitochondrially targeted antioxidants," *Free Radical Biology and Medicine*, vol. 53, no. 5, pp. 1123–1138, 2012.
- [25] Z. Cai, S. Jitkaew, J. Zhao et al., "Plasma membrane translocation of trimerized MLKL protein is required for TNF-induced necroptosis," *Nature Cell Biology*, vol. 16, no. 1, pp. 55–65, 2014.
- [26] M. Abu-Amara, S. Y. Yang, N. Tapuria, B. Fuller, B. Davidson, and A. Seifalian, "Liver ischemia/reperfusion injury: processes in inflammatory networks—a review," *Liver Transplantation*, vol. 16, no. 9, pp. 1016–1032, 2010.
- [27] S. Akira and K. Takeda, "Toll-like receptor signalling," *Nature Reviews Immunology*, vol. 4, no. 7, pp. 499–511, 2004.
- [28] A. Tsung, R. A. Hoffman, K. Izuishi et al., "Hepatic ischemia/reperfusion injury involves functional TLR4 signaling in non-parenchymal cells," *Journal of Immunology*, vol. 175, no. 11, pp. 7661–7668, 2005.
- [29] J.-G. Fan, S.-U. Kim, and V. W.-S. Wong, "New trends on obesity and NAFLD in Asia," *Journal of Hepatology*, vol. 67, no. 4, pp. 862–873, 2017.
- [30] Z. Younossi, Q. M. Anstee, M. Marietti et al., "Global burden of NAFLD and NASH: trends, predictions, risk factors and prevention," *Nature Reviews Gastroenterology & Hepatology*, vol. 15, no. 1, pp. 11–20, 2017.
- [31] F. Robertson, B. Fuller, and B. Davidson, "An evaluation of ischaemic preconditioning as a method of reducing ischaemia reperfusion injury in liver surgery and transplantation," *Journal of Clinical Medicine*, vol. 6, no. 7, 2017.
- [32] D. Ofengeim and J. Yuan, "Regulation of RIP1 kinase signaling at the crossroads of inflammation and cell death," *Nature Reviews Molecular Cell Biology*, vol. 14, no. 11, pp. 727–736, 2013.
- [33] F. K.-M. Chan, N. F. Luz, and K. Moriwaki, "Programmed necrosis in the cross talk of cell death and inflammation," *Annual Review of Immunology*, vol. 33, no. 1, pp. 79–106, 2015.
- [34] L. Galluzzi, O. Kepp, F. K.-M. Chan, and G. Kroemer, "Necroptosis: mechanisms and relevance to disease," *Annu Rev Pathol*, vol. 12, no. 1, pp. 103–130, 2017.

- [35] A. Linkermann, F. De Zen, J. Weinberg, U. Kunzendorf, and S. Krautwald, "Programmed necrosis in acute kidney injury," *Nephrology, Dialysis, Transplantation*, vol. 27, no. 9, pp. 3412–3419, 2012.
- [36] M. I. F. J. Oerlemans, S. Koudstaal, S. A. Chamuleau, D. P. de Kleijn, P. A. Doevendans, and J. P. G. Sluijter, "Targeting cell death in the reperfused heart: pharmacological approaches for cardioprotection," *International Journal of Cardiology*, vol. 165, no. 3, pp. 410–422, 2013.
- [37] W. K. Saeed, D. W. Jun, K. Jang, Y. J. Chae, J. S. Lee, and H. T. Kang, "Does necroptosis have a crucial role in hepatic ischemia-reperfusion injury?," *PLoS One*, vol. 12, no. 9, article e0184752, 2017.
- [38] L. Llacuna, M. Marí, J. M. Lluís, C. García-Ruiz, J. C. Fernández-Checa, and A. Morales, "Reactive oxygen species mediate liver injury through parenchymal nuclear factor- κ B inactivation in prolonged ischemia/reperfusion," *The American Journal of Pathology*, vol. 174, no. 5, pp. 1776–1785, 2009.
- [39] H. Taniai, I. N. Hines, S. Bharwani et al., "Susceptibility of murine periportal hepatocytes to hypoxia-reoxygenation: role for NO and Kupffer cell-derived oxidants," *Hepatology*, vol. 39, no. 6, pp. 1544–1552, 2004.
- [40] A. Katsargyris, C. Klonaris, A. Alexandrou, A. E. Giakoustidis, I. Vasileiou, and S. Theocharis, "Toll-like receptors in liver ischemia reperfusion injury: a novel target for therapeutic modulation?," *Expert Opinion on Therapeutic Targets*, vol. 13, no. 4, pp. 427–442, 2009.

Research Article

Fasting Whole-Body Energy Homeostasis and Hepatic Energy Metabolism in Nondiabetic Humans with Fatty Liver

Guido Lattuada,¹ Maria Grazia Radaelli,¹ Francesco De Cobelli,² Antonio Esposito,² Giuseppina Manzoni,¹ Silvia Perra,¹ Alessandro Del Maschio ,^{2,3} Giovanna Castoldi ,⁴ and Gianluca Perseghin ^{1,4}

¹Department of Medicine and Rehabilitation, Policlinico di Monza, Italy

²Diagnostic Radiology San Raffaele Scientific Institute, Milan, Italy

³Università San Raffaele Vita e Salute, Milan, Italy

⁴Department of Medicine and Surgery, Università degli Studi di Milano-Bicocca, Monza, Italy

Correspondence should be addressed to Gianluca Perseghin; gianluca.perseghin@policlinicodimonza.it

Received 4 July 2018; Revised 27 August 2018; Accepted 18 March 2019; Published 11 April 2019

Academic Editor: Andrea C. Gardini

Copyright © 2019 Guido Lattuada et al. This is an open access article distributed under the Creative Commons Attribution License, which permits unrestricted use, distribution, and reproduction in any medium, provided the original work is properly cited.

Background. Fatty liver is believed to be sustained by a higher than normal adipose-derived NEFA flux to the liver. Also, hepatic energy metabolism may be a rate-limiting step of intrahepatic fat (IHF) accumulation. **Aims.** To assess whole-body energy metabolism and hepatic high-energy phosphates (HEPs) in individuals with fatty liver. **Methods.** We studied 22 individuals with fatty liver and 22 control individuals matched for anthropometric features by means of (1) hepatic ¹H-magnetic resonance spectroscopy (MRS) to measure the IHF content, (2) hepatic ³¹P-MRS to assess the relative content of HEPs (phosphomonoesters, phosphodiester, inorganic phosphorus, and ATP), and (3) indirect calorimetry to assess whole-body resting energy expenditure and substrate oxidation. **Results.** Patients with newly diagnosed fatty liver and controls were not different for anthropometric parameters. Based on HOMA2%-S, individuals with fatty liver were more insulin resistant than controls. Resting energy expenditure and the pattern of substrate oxidation were not different between groups. Relative content of HEPs was not different between groups; in particular, the Pi/γ-ATP ratio, the most important signals in terms of monitoring energy homeostasis, was not different even if it was associated with indirect calorimetry-derived parameters of oxidative substrate disposal. **Conclusions.** These data demonstrate that fasting whole-body energy metabolism and the relative content of HEPs in nondiabetic patients with fatty liver are not different than those in controls when they are matched for anthropometric features.

1. Introduction

Fatty liver is the body composition manifestation of visceral obesity in insulin-resistant subjects [1, 2]. Intrahepatic fat accumulation is thought to be due to increased adipose-derived NEFA flux to the liver [3] as reported in the fasting state [4], during euglycemic-hyperinsulinemic clamps [4, 5] and during OGTT [6]. Insulin resistance with respect to lipolysis, therefore, plays a relevant role in patients with fatty liver. Using tracer methodologies, it was found that in patients with NAFLD 60% of liver triglycerides arises from NEFA in the fasting state [7]. In the same conditions, 26% of liver triglycerides arose from

de novo lipogenesis [8], and an apparent increased contribution of de novo lipogenesis vs. NEFA reesterification was reported in patients with NAFLD [7, 8]. Based on this evidence, efforts to treat hepatic steatosis by reducing fatty acids flux through dietary and pharmacological therapy (thiazolidinediones) received strong emphasis [9, 10]. Fatty liver is associated not only with hepatic but also with whole-body insulin resistance which frequently associates with higher intramyocellular lipid contents (IMCL) [11]. IMCL accumulation is associated with impaired muscle energy metabolism [12], and also, the heart of insulin-resistant subjects with fatty liver showed impaired energy metabolism [13].

Little data on the association between fatty liver and hepatic energy metabolism are currently available; Sharma et al. [14] reported that using hepatic ^{31}P -MR spectroscopy, the fasting relative content of high-energy phosphates (HEPs) was altered in obese individuals with NAFLD than in controls. In the present study, we performed hepatic ^{31}P -MRS to assess the liver content of HEPs and indirect calorimetry to assess whole-body resting energy expenditure and substrate oxidation to look for alterations reflecting potential abnormalities of energy metabolism in individuals with newly found fatty liver, when compared to age and BMI-matched individuals used to rule out the effect of overweight and obesity.

2. Materials and Methods

2.1. Subjects. Study subjects were selected among a large group of otherwise healthy employees of the San Raffaele Scientific Institute previously studied to assess the relationship between habitual physical activity and hepatic triglyceride content using hepatic ^1H -MRS [15]. Within that original population, twenty-two individuals known to have excessive IHF content and twenty-two control individuals known to have normal IHF content and selected to be comparable for the anthropometric features to those with fatty liver (in order to minimize the confounding effect of obesity on the parameters of interest) performed hepatic ^{31}P -MRS to assess HEP content and indirect calorimetry to assess whole-body energy metabolism. The 1:1 procedure of matching was based using the criteria of age within 3 years and BMI within 1 unit. This strategy has been similarly used in the past to assess whether a difference in cardiac HEP metabolism could be associated with the excessive IHF content [13], and thirteen patients out of the twenty-two with fatty liver and ten control subjects out of the twenty-two who participated to the cardiac protocol [13] performed this additional measurement of HEP content also at the level of the liver. According to the American Association for the Study of Liver Diseases (AASLD), normal or higher than normal IHF content was set at 5% ww [16]. Outpatients admitted to the Center of Nutrition/Metabolism of the San Raffaele Scientific Institute were studied. In order to be recruited, body weight had to be stable for at least six months. Patients with history of hepatic disease, substance abuse, or daily consumption of more than one alcohol drink daily (<20 g/day) or the equivalent in beer and wine were excluded from the study. Table 1 summarized the anthropometric characteristic of the recruited subjects, which, based on the medical history, physical examination, blood and urinary tests, were in good health. An informed written consent was collected for each subject who participated in the study. Recruited subjects gave their informed written consent after the explanation of purposes, nature, and potential risks of the study. The Ethical Committee of the Istituto Scientifico H San Raffaele approved the studies.

2.2. Experimental Protocol. In three days before the study, the recruited subjects were asked to consume isocaloric diet and to abstain from exercise activity. They were studied after an 8-10-hour overnight fast by means of ^{31}P -MRS and

^1H -MRS for the assessment of the hepatic relative high-energy phosphates and the IHF content, respectively. Assessment of whole-body energy metabolism by means of indirect calorimetry and blood drawing to measure serum insulin, C-peptide, plasma glucose, NEFA, lipid profile, and biochemical parameters was performed the same morning or a few days apart.

2.2.1. ^{31}P -MR Spectroscopy. Hepatic ^{31}P -MRS was performed with volunteers in the supine position within a 1.5 T whole-body scanner (Gyrosan Intera Master 1.5 MR System; Philips Medical Systems, Best, the Netherlands). ^{31}P spectra were obtained by means of a 10 cm diameter surface coil used for the transmission and detection of radio frequency signals at the resonance frequency of ^{31}P (at 1.5 T, 25.85 MHz). A small sample container built in the coil center, containing an aqueous solution of methyl-phosphonate, served as geometrical reference. The surface coil was secured in place with a Velcro band around the abdomen and chest, helping to minimize breathing artifacts. MR imaging was performed to acquire scout images, to establish the exact position of the ^{31}P surface coil, and eventually to reposition it. Localized homogeneity adjustment was performed using the body coil by optimizing the ^1H -MR spectroscopy water signal. Shim volumes were planned on the transverse and sagittal scout images. The transmitter-receiver was then switched without time delay to the ^{31}P frequency. Manual tuning and matching of the ^{31}P surface coil was performed to adjust for different coil loading. The radio frequency level was adjusted to obtain a 180° pulse of 40 ms for the reference sample at the center of the ^{31}P -surface coil. The acquisition of ^{31}P -MR spectra was performed with a recycle time of 3.6 s. ISIS volume selection in three dimensions (3D-ISIS) was employed. It was based on 192 averaged free induction decays. The Volume of Interest (VOI) was oriented perpendicular to the abdomen wall, avoiding inclusion of abdominal wall muscle and diaphragm muscle. The volume size was approximately 3 (caudocranial) $\times 4 \times 4$ cm^3 . The acquisition time was 11 min. Adiabatic frequency-modulated hyperbolic secant pulses and adiabatic half-passage detection pulses were used to achieve inversion and excitation over the entire VOI. The examination time was 40-45 min. 3D-ISIS was employed after testing that uses higher spatial resolution (2D-ISIS+1D SI using a one-dimensional phase encoding bar with 32 rows of 1 cm thickness each angulated perpendicular to the abdominal wall for the anterior-posterior direction and lateral and craniocaudal dimensions dependent on the patients' liver size); the Pi/ γ -ATP ratios were in agreement and showed absence of muscle PCr signal.

2.2.2. ^1H -MR Spectroscopy. Hepatic ^1H -MR spectroscopy was performed in all volunteers with the same MR system as previously described [15].

2.2.3. Indirect Calorimetry. After lying quietly for 30 min, REE was measured by continuous indirect calorimetry with a ventilated hood system (SensorMedics 2900, Metabolic Measurement Cart) performed for 45 min as previously described [17]. The mean coefficient of variation (CV) within

TABLE 1: Biochemistry and clinical features of individuals with newly diagnosed fatty liver and controls.

	Fatty liver	Controls	<i>P</i> value
Number and sex (F/M)	22 (2/20)	22 (2/20)	
Age (years)	34 ± 7	35 ± 8	
BMI (kg/m ²)	27.9 ± 2.9	27.7 ± 1.8	
Total cholesterol (mg/dl)	195 ± 39	185 ± 32	0.37
HDL cholesterol (mg/dl)	45 ± 12	52 ± 13	0.07
Triglycerides (mg/dl)	169 ± 85	91 ± 42	0.01
NEFA (mg/dl)	0.61 ± 0.18	0.60 ± 0.29	0.91
Creatinine (mg/dl)	0.85 ± 0.22	0.94 ± 0.14	0.29
Plasma glucose (mg/dl)	91 ± 9	89 ± 11	0.62
Plasma insulin (μU/ml)	17 ± 6	11 ± 4	0.06
Plasma C-peptide (ng/ml)	3.20 ± 1.21	2.29 ± 0.82	0.01
HOMA2-B (%)	160 ± 39	149 ± 53	0.46
HOMA2-S (%)	51 ± 14	72 ± 51	0.05
IHF content (% wet weight)	13.93 ± 8.25 Range: 5.40–39.25	2.43 ± 0.99 Range: 0.84–4.28	0.0001

Mean ± SD; independent-samples *t*-test (2-tailed). HOMA: HOMA2: homeostatic model assessment; HOMA2-S: insulin sensitivity; HOMA2-B: β-cell sensitivity.

the session for both O₂ (2.1 ± 0.2%) and CO₂ (2.3 ± 0.3%) measurements was below 5%.

2.3. Analytical Determinations. Glucose (Beckman Coulter Inc., Fullerton, CA), FFA, triglycerides, total cholesterol, and HDL cholesterol were measured as previously described [15]. Plasma levels of insulin (sensitivity 2 μU/ml; intra- and inter-assay CV <3.1% and 6%, respectively) were measured with RIA (Linco Research, Missouri, USA). Plasma C-peptide was measured (CVs: intra – assay = 2.3%, interassay = 4.1%) using a double-antibody RIA kit (Diagnostic Product Corporation, Los Angeles, CA).

2.4. Calculations. Fasting-based indices of insulin sensitivity (HOMA2-%S) and β-cell responsivity (HOMA2-%B) were determined by the updated HOMA2 method [18] available from <http://www.OCDEM.ox.ac.uk>. ³¹P-MR spectra were transferred to a remote SUN-SPARC workstation for analysis. The spectra were quantified automatically by model function analysis in the time domain. The spectral fitting routine was based on a nonlinear least-squares Gauss-Newton implementation for exponential damping as previously performed for the postprocessing of spectra obtained from transplanted kidney [19]. A typical ³¹P spectrum is depicted in Figure 1 with description of the signals in the legend. γ-ATP and Pi are considered the most important signals in terms of monitoring energy homeostasis because the γ-ATP phosphorous is the one which is released as Pi in the reaction of ATP hydrolysis to ADP. For this reason, in the present work, we have chosen the Pi/γ-ATP and the Pi/ATP (mean of the three phosphorous signals) ratios as markers of intrahepatic ATP metabolism. We also calculated the PME/Pi, PME/γ-ATP, and PME/ATP ratios as comparison with previously published data in hepatic diseases. The percent IHF was

calculated as previously described [14]. REE was calculated by Weir's standard equation [20] from the O₂ consumption rate and the CO₂ production rates measured by means of indirect calorimetry (excluding the first 10 min of data acquisition) and from the urinary nitrogen excretion. Predicted REE was calculated using the Harris-Benedict equations [21]. Glucose, lipid, and protein oxidation was estimated as previously described [22].

2.5. Statistical Analysis. Data in text tables are means ± SD. Analyses were performed using the SPSS software (ver. 13.0; SPSS Inc., Chicago). Comparison between groups was performed using the 2-tailed independent-samples *t*-test, and a *P* value less than 0.05 was considered to be significant. Variables with skewed distribution assessed using the Kolmogorov-Smirnov test of normality were log-transformed before the analysis. Correlation analysis was performed using two-tailed Pearson's correlation.

Sample size calculation was based on preliminary acquisitions in a small (*n* = 12) group of normal-weight subjects. 11 individuals for each group provided a power of 85% using a *t*-test at a one-side α of 0.05 when assuming a 20% difference between groups in the Pi/γ-ATP ratio with a standard deviation of 0.50.

3. Results

3.1. Anthropometric and Laboratory Characteristics of Study Subjects. Individuals with or without fatty liver (mean ± standard deviation and ranges of the IHF content are summarized in Table 1) were not different with respect to age and BMI (Table 1). Subjects with excessive IHF content had higher serum triglycerides and plasma C-peptide concentrations. HOMA2-S, as a surrogate index of insulin

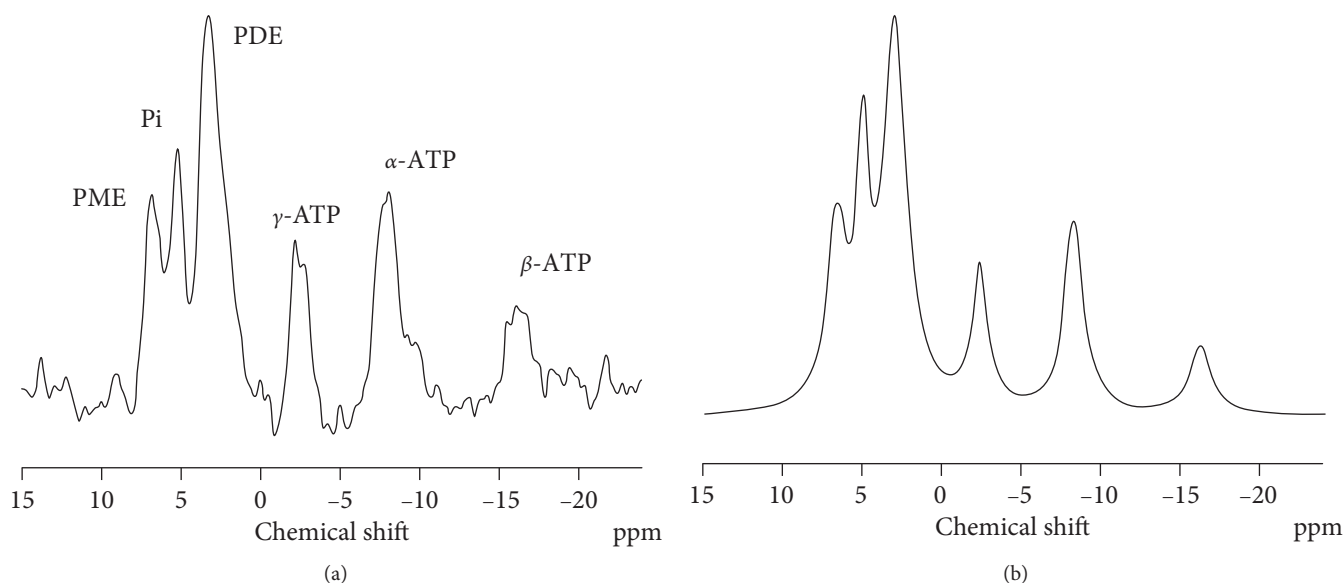


FIGURE 1: A typical ^{31}P spectrum of a normal subject is depicted in (a). In (b), the spectrum after line-fitting procedures is shown. The signals that can be detected are the signals of the three phosphorous atoms of adenosine triphosphates (γ , α , and β). Phosphomonoesters (PME), inorganic phosphorous (Pi), and phosphodiester (PDE) are detectable at ppm on the left side of the spectrum. PMEs (phosphocholine, phosphoethanolamine, adenosine monophosphate, and glycolytic intermediates including glucose-6-phosphate) and PDEs (glycerolphosphorylcholine and glycerolphosphorylethanolamine) represent a heterogeneous mix of compounds that share only a similar chemical feature but otherwise have diverse chemical structures and functions. Pi signal corresponds to free inorganic phosphorous. In contrast with the skeletal muscle and the heart, very little, if any, phosphocreatine is detectable in the liver (chemical shift at 0 ppm); its presence in the spectrum is likely a marker of extrahepatic muscle contamination from malpositioning of the spectroscopic voxel.

sensitivity, was lower in subjects with fatty liver than in normals.

3.2. Parameters of Whole-Body Energy Metabolism. Resting energy expenditure (REE) and the percent of predicted REE were not different between groups. Also, whole-body glucose and lipid oxidation was not different between groups as reflected by the similar respiratory quotient (Table 2).

3.3. Intrahepatic High-Energy Phosphates. The intrahepatic high-energy phosphate content is summarized in Table 2. The peak area of each metabolite (PME, Pi, PDE, γ -ATP, α -ATP, and β -ATP) was expressed as a percentage of the total ^{31}P -MR signal (the sum of all the resonances). No difference was detected for each of the metabolites between the two groups of study. Also, the Pi/ γ -ATP, Pi/ATP, PME/Pi, PME/ γ -ATP, and PME/ATP ratios were not different between groups.

3.4. Correlation Analysis with Parameters of Hepatic High-Energy Phosphates. The Pi/ γ -ATP ratio was not associated with anthropometric features or with the features of the metabolic syndrome. It was not associated with the IHF content ($r = -0.001$; $P = 0.96$). It was not associated with parameters of lipid metabolism and fasting plasma NEFA or with fasting plasma glucose, insulin, and HOMA indices. Interestingly, it was associated with indirect calorimetry-derived parameters of oxidative substrate disposal; in fact, it correlated with the respiratory quotient ($r = -0.52$; $P = 0.001$), the fasting whole-body glucose oxidation ($r = -0.57$; $P = 0.001$),

and the fasting lipid oxidation ($r = 0.45$; $P = 0.005$). This association with the respiratory quotient was detectable in a more robust fashion in individuals with fatty liver ($r = -0.75$; $P = 0.0001$) than in the control individuals ($r = -0.34$; $P = 0.03$). A similar pattern of correlation was found when the Pi/ATP ratio was used. The PME/Pi and PME/ATP ratios were not correlated with any of the metabolic parameters summarized in Table 1.

4. Discussion

The present study demonstrates that in nondiabetic individuals with newly found fatty liver, the fasting whole-body energy metabolism and the relative amount of hepatic HEPs are not different than in age- and BMI-matched nondiabetic individuals without fatty liver.

Little data about whole-body energy metabolism were available in patients with fatty liver. Bugianesi et al. [23] reported that during hyperinsulinemic conditions, whole-body lipid oxidation rate was higher in a small group of individuals with biopsy proven NAFLD ($n = 12$) when compared to 6 control subjects. As discussed in the introduction section, this finding may be secondary to the higher plasma NEFA characterizing these patients [4–6]. In our study, we did not assess insulin sensitivity with the clamp procedure, but based on the higher insulin resistance estimated using the fasting-derived index (HOMA2-S in Table 1), it is likely that also our cohort of subjects in the same insulin-stimulated condition could be characterized by higher lipid oxidation rate. The other facet of energy metabolism is the

TABLE 2: Whole-body energy metabolism as assessed by indirect calorimetry and high-energy phosphate hepatic relative content as assessed by ^{31}P MRS.

	Fatty liver	Controls	<i>P</i> value
Indirect calorimetry			
REE (Kcal/die)	1935 ± 368	1886 ± 261	0.64
% of predicted REE (%)	107 ± 12	103 ± 12	0.25
Respiratory quotient	0.81 ± 0.05	0.81 ± 0.05	0.93
Glucose oxidation (mg/(kg min))	1.30 ± 0.74	1.25 ± 0.75	0.83
Lipid oxidation (mg/(kg min))	0.93 ± 0.36	0.87 ± 0.35	0.58
Hepatic ^{31}P -MRS			
% PME	12 ± 5	11 ± 5	0.48
% Pi	11 ± 4	11 ± 4	0.94
% PDE	42 ± 6	41 ± 6	0.72
% γ -ATP	10 ± 2	10 ± 2	0.50
% α -ATP	17 ± 3	19 ± 3	0.10
% β -ATP	7 ± 3	8 ± 2	0.47
% ATP	11 ± 2	12 ± 2	0.49
Pi/ γ -ATP ratio	1.17 ± 0.55	1.19 ± 0.34	0.83
Pi/ATP ratio	1.00 ± 0.46	0.95 ± 0.27	0.63
PME/Pi ratio	1.14 ± 0.50	1.04 ± 0.57	0.56
PME/ γ -ATP ratio	1.30 ± 0.72	1.24 ± 0.79	0.79
PME/ATP ratio	1.14 ± 0.67	0.96 ± 0.55	0.36

The peak area of each metabolite (PME, Pi, PDE, γ -ATP, α -ATP, and β -ATP) was expressed as a percentage of the total ^{31}P -MR signal (the sum of all the resonances). Mean ± SD; independent-samples *t*-test (2-tailed). REE: resting energy expenditure.

postabsorptive and resting state. In our cohort of individuals with newly diagnosed fatty liver, postabsorptive whole-body energy metabolism was not different than that of controls in absolute terms and when normalized to the predicted values based on sex, age, race, body weight, and height. In addition, substrate oxidative disposal was remarkably similar to that of controls based on semiquantitative parameters such as the respiratory quotient and also based on the oxidative fluxes (Table 2). This may be substantially in agreement with the report of Bugianesi et al. showing only a trend ($P = 0.09$) for higher fasting lipid oxidation rate in their 12 patients when compared to 6 controls. It is possible that a more severe hepatic disease in Bugianesi's cohort may explain this little discrepancy. In fact, we have also observed that in more serious hepatic diseases, such as in individuals with cirrhosis and hepatocarcinoma, a hypercatabolic state sustained by higher fasting lipid oxidation rate could be detected and that liver transplantation in the long-term normalized this abnormality [17].

We may conclude that in individuals with newly diagnosed fatty liver, whole-body energy metabolism is not different than in age- and BMI-matched individuals during the postabsorptive and resting state.

With respect to the local hepatic energy metabolism as assessed by means of ^{31}P -MRS, Sharma et al. [14] reported higher PME/Pi, PME/ γ -ATP, PME/ β -ATP, and PME/ATP in overweight/obese Asian Indians with NAFLD when compared with normal weight individuals, either with or without NAFLD. We believe that the different HEP contents were not due to the fatty liver per se but rather to the different degrees of obesity. Several observations may support our thinking. In our study, when we compared the overweight subjects with fatty liver with a group of similarly overweight subjects without fatty liver, a difference was not detectable (Table 2). Taking a careful look to the data by Sharma et al. [14], it may be observed that when anthropometric parameters were matched between individuals with and without NAFLD (in their study the comparison may be performed at a normal range of BMI: 22 kg/m²), the difference was not significant also in their own set of data. In support of this hypothesis, a pilot study using ^{31}P -MRS of the liver suggested that in 8 obese individuals with NASH, ATP recovery within the liver after the administration of fructose e.v. was severely blunted, but the authors reported that the recovery became progressively less efficient as BMI increased also in the group of healthy controls [24]. This study would also confirm that this impairment is present in association with obesity per se, and this suggestion is also given by another study in which ATP was monitored in normal weight and obese individuals in the fasting state and after fructose administration [25].

An alternative potential explanation for this controversial finding is related to a limitation of our and Sharma's works. In both studies, there was a lack of histological characterization of the hepatic disease; therefore, no information about the inflammatory status, necrosis, and fibrosis was available. It may not be excluded that different histological features of the disease may be able to explain the reported differences in HEP relative content. In fact, increased PME ratios have been repeatedly found in patients with more severe liver diseases including chronic hepatitis C [26], liver cirrhosis [27], or tumors [28], all conditions in which extensive membrane remodeling may have an effect on the membrane phosphocholine and phosphoethanolamine kinetics and ultimately in PME content.

Based on our own data, we therefore would like to conclude that the relative content of hepatic HEPs is not different in individuals with newly found fatty liver than in controls when study groups are comparable for body mass and that the previously reported differences may be secondary to body fatness rather than fatty liver per se.

In summary, our set of data would support the hypothesis that fasting whole-body and hepatic energy metabolism is not abnormal in individuals with fatty liver when compared to matched controls in agreement with findings generated using different methodological tools [29], in contrast with the finding within the skeletal muscle [12] and the heart of insulin-resistant individuals [13].

Since in the postabsorptive and resting state the liver, along with the skeletal muscle, is the tissue contributing most to energy expenditure, we wondered whether the acquired parameters could be somehow related to each other. We noticed that a significant correlation could be detected

between the whole-body substrate oxidative disposal (expressed as respiratory quotient, glucose, and lipid oxidation) and the Pi/ γ -ATP ratio. The correlation would imply that a relatively higher hepatic content of Pi (a more catabolic condition if the hepatocellular ATP content is postulated to be comparable) is present when lipids are the preferential substrate for the oxidative processes. This correlation was not a peculiar feature of the individuals with fatty liver but was detectable also in the control individuals without fatty liver even if by a minor extent.

Even if these ^{31}P -MRS studies do not allow the assessment of the absolute hepatic HEP concentrations, which represents a methodological limitation, the expression of the signal intensities as ratios would imply that the intracellular hepatic ATP concentration is constant and not different between groups. A higher Pi/ γ -ATP ratio would therefore imply for a catabolic energetic state of the hepatocytes, in which a reduced phosphorylation status would be reflected by an increase of Pi levels relative to ATP. The lack of difference of the Pi/ γ -ATP ratio between groups we are reporting in the present work would therefore imply a normal hepatic energy metabolism, even if we cannot exclude that the absolute Pi and ATP hepatocellular content may be consensually higher and/or lower in parallel resulting in no change in the ratio. We believe that the lack of differences in the Pi/ γ -ATP ratio between the groups in the present work implies a normal hepatic metabolism because we also analyzed our data as the relative percent contribution of each single signal to the total ^{31}P detectable signals, as summarized in Table 2, and once more we found no significant difference between groups. It is important to emphasize that future studies will require the determination of the absolute substrate concentration. With this respect, Chmelík et al. [30] have validated a spectroscopic absolute quantification of ^{31}P metabolites in human livers based on the use of an external phantom with known concentrations of the substrates of interest.

In conclusion, the present work demonstrates that fasting and resting whole-body energy metabolism and the relative content of HEPs in nondiabetic patients with newly diagnosed fatty liver are not different than those in controls when they are matched for anthropometric features. Absolute quantification of these substrates remains a mandatory step to firmly establish whether alteration of hepatic energy metabolism is present in individuals with fatty liver.

Abbreviations

^{31}P -MRS:	Phosphorus-31 magnetic resonance spectroscopy
^1H -MRS:	Proton magnetic resonance spectroscopy
IHF:	Intrahepatic fat
HEPs:	High-energy phosphates
NEFA:	Nonesterified fatty acids
PME:	Phosphomonoesters
Pi:	Inorganic phosphorous
PDE:	Phosphodiester
PCr:	Phosphocreatine
OGTT:	Oral glucose tolerance test
BMI:	Body mass index

3D-ISIS:	ISIS volume selection in three dimensions
REE:	Resting energy expenditure
RQ:	Respiratory quotient
HOMA:	Homeostatic model assessment
IMCL:	Intramyocellular lipid contents
NAFLD:	Nonalcoholic fatty liver disease.

Data Availability

The data used to support the findings of this study are available from the corresponding author upon request.

Conflicts of Interest

The authors have no potential competing interests and conflicts to declare.

Authors' Contributions

G.L. and G.P. designed and conducted the research, contributed to the interpretation of the results, drafted the manuscript, and approved the final version. M.G.R., D.C.F., E.A., and D.M.A. contributed to the study design, conducted the research, performed the statistical analysis, reviewed the manuscript, and approved the final version. G.M., S.P., and G.C. contributed to the interpretation of the results, performed the statistical analysis, contributed to the manuscript writing, and approved the final version.

Acknowledgments

This study was supported by grants by (1) the Italian Ministry of Health (RF98.49, RF99.55, and RF01.1831): this grant was received in order to develop MRI/MRS techniques for the noninvasive assessment of organ and tissue metabolism in diabetes and related disorders; (2) FIRST 2007: this was a small grant from Università degli Studi di Milano for the study of the metabolic derangements in individuals with NAFLD; and (3) the European Association for the Study of Diabetes (EFSD): this grant is a given support to Gianluca Perseghin and is devoted to the study of alterations of cardiac metabolism in insulin-resistant subjects by means of the use of cardiac ^{31}P -MRS. The work was independent of it, but the cardiac ^{31}P -MRS methodology opened the possibility to apply the technique to the study of liver energy metabolism which was applied in this work.

References

- [1] G. Marchesini, M. Brizi, A. M. Morselli-Labate et al., "Association of nonalcoholic fatty liver disease with insulin resistance," *The American Journal of Medicine*, vol. 107, no. 5, pp. 450–455, 1999.
- [2] G. Marchesini, E. Bugianesi, G. Forlani et al., "Nonalcoholic fatty liver, steatohepatitis, and the metabolic syndrome," *Hepatology*, vol. 37, no. 4, pp. 917–923, 2003.
- [3] M. Roden, "Mechanisms of disease: hepatic steatosis in type 2 diabetes—pathogenesis and clinical relevance," *Nature Clinical Practice Endocrinology & Metabolism*, vol. 2, no. 6, pp. 335–348, 2006.

- [4] G. Marchesini, M. Brizi, G. Bianchi et al., "Nonalcoholic fatty liver disease: a feature of the metabolic syndrome," *Diabetes*, vol. 50, no. 8, pp. 1844–1850, 2001.
- [5] A. Gastaldelli, K. Cusi, M. Pettiti et al., "Relationship between hepatic/visceral fat and hepatic insulin resistance in nondiabetic and type 2 diabetic subjects," *Gastroenterology*, vol. 133, no. 2, pp. 496–506, 2007.
- [6] H. B. Holt, S. H. Wild, P. J. Wood et al., "Non-esterified fatty acid concentrations are independently associated with hepatic steatosis in obese subjects," *Diabetologia*, vol. 49, no. 1, pp. 141–148, 2006.
- [7] K. L. Donnelly, C. I. Smith, S. J. Schwarzenberg, J. Jessurun, M. D. Boldt, and E. J. Parks, "Sources of fatty acids stored in liver and secreted via lipoproteins in patients with nonalcoholic fatty liver disease," *The Journal of Clinical Investigation*, vol. 115, no. 5, pp. 1343–1351, 2005.
- [8] F. Diraison, P. Moulin, and M. Beylot, "Contribution of hepatic *de novo* lipogenesis and reesterification of plasma non esterified fatty acids to plasma triglyceride synthesis during non-alcoholic fatty liver disease," *Diabetes & Metabolism*, vol. 29, no. 5, pp. 478–485, 2003.
- [9] R. Belfort, S. A. Harrison, K. Brown et al., "A placebo-controlled trial of pioglitazone in subjects with nonalcoholic steatohepatitis," *The New England Journal of Medicine*, vol. 355, no. 22, pp. 2297–2307, 2006.
- [10] V. Ratziu, P. Giral, S. Jacqueminet et al., "Rosiglitazone for nonalcoholic steatohepatitis: one-year results of the randomized placebo-controlled Fatty Liver Improvement with Rosiglitazone Therapy (FLIRT) trial," *Gastroenterology*, vol. 135, no. 1, pp. 100–110, 2008.
- [11] G. Perseghin, P. Scifo, F. de Cobelli et al., "Intramyocellular triglyceride content is a determinant of in vivo insulin resistance in humans: a $1\text{H-}^{13}\text{C}$ nuclear magnetic resonance spectroscopy assessment in offspring of type 2 diabetic parents," *Diabetes*, vol. 48, no. 8, pp. 1600–1606, 1999.
- [12] K. F. Petersen, S. Dufour, and G. I. Shulman, "Decreased insulin-stimulated ATP synthesis and phosphate transport in muscle of insulin-resistant offspring of type 2 diabetic parents," *PLoS Medicine*, vol. 2, no. 9, article e233, 2005.
- [13] G. Perseghin, G. Lattuada, F. de Cobelli et al., "Increased mediastinal fat and impaired left ventricular energy metabolism in young men with newly found fatty liver," *Hepatology*, vol. 47, no. 1, pp. 51–58, 2008.
- [14] R. Sharma, S. Sinha, K. A. Danishad et al., "Investigation of hepatic gluconeogenesis pathway in non-diabetic Asian Indians with non-alcoholic fatty liver disease using in vivo (^{31}P) phosphorus magnetic resonance spectroscopy," *Atherosclerosis*, vol. 203, no. 1, pp. 291–297, 2009.
- [15] G. Perseghin, G. Lattuada, F. de Cobelli et al., "Habitual physical activity is associated with intrahepatic fat content in humans," *Diabetes Care*, vol. 30, no. 3, pp. 683–688, 2007.
- [16] B. Neuschwander-Tetri and S. H. Caldwell, "Nonalcoholic steatohepatitis: summary of an AASLD single topic conference," *Hepatology*, vol. 37, no. 5, pp. 1202–1219, 2003.
- [17] G. Perseghin, V. Mazzaferro, S. Benedini et al., "Resting energy expenditure in diabetic and nondiabetic patients with liver cirrhosis: relation with insulin sensitivity and effect of liver transplantation and immunosuppressive therapy," *The American Journal of Clinical Nutrition*, vol. 76, no. 3, pp. 541–548, 2002.
- [18] T. M. Wallace, J. C. Levy, and D. R. Matthews, "Use and abuse of HOMA modeling," *Diabetes Care*, vol. 27, no. 6, pp. 1487–1495, 2004.
- [19] P. Fiorina, G. Perseghin, F. de Cobelli et al., "Altered kidney graft high-energy phosphate metabolism in kidney-transplanted end-stage renal disease type 1 diabetic patients: a cross-sectional analysis of the effect of kidney alone and kidney-pancreas transplantation," *Diabetes Care*, vol. 30, no. 3, pp. 597–603, 2007.
- [20] J. B. V. Weir, "New methods for calculating metabolic rate with special reference to protein metabolism," *Journal of Physiology*, vol. 109, no. 1-2, pp. 1–9, 1949.
- [21] M. M. Johnson, R. Chin, and E. F. Haponik, "Nutrition, respiratory function, and disease," in *Modern Nutrition in Health and Disease*, M. E. Shils, J. A. Olson, M. Shike, and A. C. Ross, Eds., pp. 1473–1490, Williams & Wilkins, 1999.
- [22] K. N. Frayn, "Calculation of substrate oxidation rates in vivo from gaseous exchange," *Journal of Applied Physiology*, vol. 55, no. 2, pp. 628–634, 1983.
- [23] E. Bugianesi, A. Gastaldelli, E. Vanni et al., "Insulin resistance in non-diabetic patients with non-alcoholic fatty liver disease: sites and mechanisms," *Diabetologia*, vol. 48, no. 4, pp. 634–642, 2005.
- [24] H. Cortez-Pinto, J. Chatham, V. P. Chacko, C. Arnold, A. Rashid, and A. M. Diehl, "Alterations in liver ATP homeostasis in human non-alcoholic steatohepatitis. A pilot study," *JAMA*, vol. 282, no. 17, pp. 1659–1664, 1999.
- [25] S. Nair, V. P. Chacko, C. Arnold, and A. M. Diehl, "Hepatic ATP reserve and efficiency of replenishing: comparison between obese and nonobese normal individuals," *The American Journal of Gastroenterology*, vol. 98, no. 2, pp. 466–470, 2003.
- [26] A. K. P. Lim, N. Patel, G. Hamilton, J. V. Hajnal, R. D. Goldin, and S. D. Taylor-Robinson, "The relationship of in vivo ^{31}P MR spectroscopy to histology in chronic hepatitis C," *Hepatology*, vol. 37, no. 4, pp. 788–794, 2003.
- [27] R. Jalan, J. Sargentoni, G. A. Coutts et al., "Hepatic phosphorus-31 magnetic resonance spectroscopy in primary biliary cirrhosis and its relation to prognostic models," *Gut*, vol. 39, no. 1, pp. 141–146, 1996.
- [28] G. Brinkmann, U. H. Melchert, L. Emde et al., "In vivo P-31-MR-spectroscopy of focal hepatic lesions: effectiveness of tumor detection in clinical practice and experimental studies of surface coil characteristics and localization technique," *Investigative Radiology*, vol. 30, no. 1, pp. 56–63, 1995.
- [29] K. F. Petersen, D. E. Befroy, S. Dufour, D. L. Rothman, and G. I. Shulman, "Assessment of hepatic mitochondrial oxidation and pyruvate cycling in NAFLD by ^{13}C magnetic resonance spectroscopy," *Cell Metabolism*, vol. 24, no. 1, pp. 167–171, 2016.
- [30] M. Chmelik, A. I. Schmid, S. Gruber et al., "Three-dimensional high-resolution magnetic resonance spectroscopic imaging for absolute quantification of ^{31}P metabolites in human liver," *Magnetic Resonance in Medicine*, vol. 60, no. 4, pp. 796–802, 2008.

Research Article

Reduced Liver Lipid Peroxidation in Subcellular Fractions Is Associated with a Hypometabolic State in Rats with Portacaval Anastomosis

Olivia Vázquez-Martínez ¹, Héctor Valente-Godínez,¹ Andrés Quintanar-Stephano,² Deisy Gasca-Martínez,³ Mayra L. López-Cervantes,¹ Lourdes Palma-Tirado,⁴ María de Jesús Guerrero-Carrillo,¹ Mariela Pérez-Solís,¹ and Mauricio Díaz-Muñoz ¹

¹Cellular and Molecular Department, Neurobiology Institute, Campus UNAM-Juriquilla, Querétaro 76230, Mexico

²Physiology and Pharmacology Department, Basic Science Center, Autonomous University of Aguascalientes, Aguascalientes 20131, Mexico

³Behavioral Analysis Unit, Neurobiology Institute, Campus UNAM-Juriquilla, Querétaro 76230, Mexico

⁴Microscopy Unit, Neurobiology Institute, Campus UNAM-Juriquilla, Querétaro 76230, Mexico

Correspondence should be addressed to Mauricio Díaz-Muñoz; mdiaz@comunidad.unam.mx

Received 28 September 2018; Accepted 17 December 2018; Published 21 February 2019

Academic Editor: Andrea C. Gardini

Copyright © 2019 Olivia Vázquez-Martínez et al. This is an open access article distributed under the Creative Commons Attribution License, which permits unrestricted use, distribution, and reproduction in any medium, provided the original work is properly cited.

A surgical connection between portal and inferior cava veins was performed to generate an experimental model of high circulating ammonium and hepatic hypofunctioning. After 13 weeks of portacaval anastomosis (PCA), hyperammonemia and shrinkage in the liver were observed. Low glycemic levels accompanied by elevated levels of serum alanine aminotransferase were recorded. However, the activity of serum aspartate aminotransferase was reduced, without change in circulating urea. Histological and ultrastructural observations revealed ongoing vascularization and alterations in the hepatocyte nucleus (reduced diameter with indentations), fewer mitochondria, and numerous ribosomes in the endoplasmic reticulum. High activity of hepatic caspase-3 suggested apoptosis. PCA promoted a marked reduction in lipid peroxidation determined by TBARS in liver homogenate but specially in the mitochondrial and microsomal fractions. The reduced lipoperoxidative activity was also detected in assays supplemented with Fe²⁺. Only discreet changes were observed in conjugated dienes. Fluorescent probes showed significant attenuation in mitochondrial membrane potential, reactive oxygen species (ROS), and calcium content. Rats with PCA also showed reduced food intake and decreased energy expenditure through indirect calorimetry by measuring oxygen consumption with an open-flow respirometric system. We conclude that experimental PCA promotes an angiogenic state in the liver to confront the altered blood flow by reducing the prooxidant reactions associated with lower metabolic rate, along with significant reduction of mitochondrial content, but without a clear hepatic dysfunction.

1. Introduction

Portacaval anastomosis (PCA)/Eck's fistula is a surgical manoeuvre that is widely used in clinical gastroenterology to mitigate hemodynamic alterations associated with chronic liver dysfunction such as esophageal varices [1] and hepatorenal syndrome [2]. Experimentally, PCA has been utilized as

a protocol to generate hepatic encephalopathy associated with increased levels of circulating ammonium (NH₄⁺) [3]. PCA involves closing the portal vein first by disconnecting the circulation between the duodenum and the liver, then by connecting the distal section of the portal vein to an oval window on the inferior cava vein. The consequence of this surgery is the portal blood bypassing directly to the systemic

blood circulation [4]. This condition avoids the correct biochemical processing nutrients ingested by the liver and deeply alters the bioenergetic status of this organ [5].

It has been postulated that hepatic encephalopathy associated with PCA is accompanied by oxidative/nitrosative stress in cerebral components, resulting in the activation of NMDA receptors and the nitration of key enzymes in the astrocytic nitrogen-handling enzymes such as glutamine synthetase. Eventually, these alterations combined with energy disruption by manganese and ammonium participation result in neuronal circuit disruption and brain swelling [6]. In contrast, much less is known about the metabolic consequences that take place within the liver during PCA. Some reports have explored the decrease in ketogenesis [7] and the reduction in the mixed-function oxidase system [8] and lipogenic activity [9] as well as the harmful effect on the liver regenerative ability after partial hepatectomy [10].

To gain a better understanding of the effects of PCA on liver metabolic parameters, the present project was aimed at characterizing (1) the prooxidant reactions that occur in subcellular fractions by measuring the levels of conjugated dienes (CD) and thiobarbituric acid reactive substances (TBARs) as well as (2) the presence of mitochondrial ROS, the level of mitochondrial membrane potential, and mitochondrial Ca^{2+} content by using fluorescent techniques. Biochemical parameters were complemented with (3) histological and ultrastructural observations. In addition, (4) rats with PCA surgery were placed in metabolic cages to evaluate their metabolic performance by indirect calorimetric techniques (respirometry). The results showed significant metabolic and structural adaptations of the liver indicating a vascularization process and a reduction in the metabolic rate as consequences of PCA.

2. Materials and Methods

2.1. Experimental Protocol. The experiments were performed with male Wistar rats weighing approximately 280 g (~8 weeks old) at the beginning of the experiment. The animals were put in individual cages (17 × 41 × 20 cm) at room temperature (~22°C) and maintained in a 12 h light:12 h darkness cycle (light on at 08:00 h). Access to food and water was *ad libitum*. Rats were divided into 2 groups according to the surgical procedure: placebo surgery (sham) and portacaval anastomosis (PCA). All experimental procedures were approved and conducted in accordance with the institutional guide for care and use of animals under biomedical experimentation and under international ethical standards (Universidad Nacional Autónoma de México).

2.2. Surgery. Termino-lateral portacaval anastomosis was performed in rats following the procedure reported by Lee and Fisher [11]. Briefly, rats were put under anesthesia (Ketamine/Xylazine) and a laparotomy was performed to access the abdominal organs. The portal vein was dissected and occluded. The extreme of the portal vein was then connected to a window on the inferior portal vein that was previously obstructed with surgical clips. The PCA was done in less than 20 min. Sham-operated rats were subjected to the same

procedure (until the use of the surgical clips) but without cutting any blood vessel. The success of the PCA surgery was ~50% whereas all sham-operated rats survived. Rats with PCA were supplemented with 10% glucose solution the first 2 days after the surgery, and then, they were put in cages with food and water *ad libitum* until the day of their sacrifice (13 weeks later). All operated animals were used in the experimental protocols.

2.3. Liver Sampling and Subcellular Fractionation. All rats in each group were decapitated for trunk blood collection. A sample of approximately 3 g was taken from the liver and homogenized in a 10:1 proportion in 10 mM Tris-HCl (pH 7.4). Cellular fractionation was done by differential centrifugation as previously reported [12]. Briefly, the homogenate was centrifuged at 1,500 g for 15 min, and the resulting pellet was resuspended and divided into halves for further isolation of plasma membrane fractions. The supernatant was spun at 10,000 g for 15 min to sediment the mitochondrial fraction. The supernatant was ultracentrifuged at 100,000 g for 60 min, resulting in a pellet designated as the microsomal fraction and a supernatant, which was the cytosolic fraction. Both the mitochondrial and microsomal fractions were resuspended in Tris-HCl buffer. All centrifugations were performed at 4°C. The plasma membrane fraction was obtained by centrifuging the first pellet through a Percoll gradient, as described by Loten and Redshaw-Loten [13].

2.4. Blood Parameters. Glucose, urea, and triacylglycerides (TAG) were measured by quantitative commercial kits (SPINREACT, Lab-Center, Mexico). Briefly, for glucose determination, glucose oxidase catalyzed the oxidation of glucose to gluconic acid. The formed H_2O_2 was detected by the chromogenic oxygen acceptor, phenol 4-aminophenazone, in the presence of peroxidase. Urea in the sample reacted with o-phthaldialdehyde in acid medium forming a colored complex that could be measured by spectrophotometry. Sample TAG was incubated with lipoprotein-lipase, liberating glycerol, and free fatty acids. Glycerol was turned into glycerol 3-phosphate and ADP by glycerol kinase and ATP. Glycerol 3-phosphate was then converted by glycerol 3-phosphate dehydrogenase to dihydroxyacetone phosphate and H_2O_2 . In the last reaction, H_2O_2 reacted with 4-aminophenazone and p-chlorophenol in the presence of peroxidase to give it a red color. Alanine aminotransferase (ALT) and aspartate aminotransferase (AST) were measured as described by Bergmeyer and Bernt [14]. The method used dinitrophenylhydrazine in an acidic medium to develop color that was recorded at 546 nm.

2.5. Hematoxylin and Eosin Staining (H&E). Several segments of the liver (~3 cm²) were taken and fixed in formaldehyde 10% buffered at pH 7.4 with potassium phosphate (monobasic and dibasic) for 72 h. The tissue was dehydrated and embedded in paraffin. Paraffin sections were made at 6 μm and stained according to the H&E protocol. Briefly, 1 g of hematoxylin was dissolved in 95% ethyl alcohol, 20 g potassium-aluminum sulfate, and then it was boiled.

Hematoxylin is selective for nuclear material. Eosin was dissolved in 80% ethyl alcohol and 0.5 ml acetic acid. Eosin is selective for cytoplasmic material. Slides were sealed with Entellan solution and analyzed in an Olympus microscope CX30. Photographs were evaluated by a pathology expert. To quantify angiogenic activity, 500 liver acini from 5 different sham and PCA samples were inspected to detect the percentage of structures showing ongoing neovascularization.

2.6. Electron Microscopy. Liver sections ($\sim 1 \text{ mm}^3$) were cut with sharp razors and fixed in 0.1 mmol/l cacodylate buffer, pH 7.4, containing 2% OsO_4 and 2.5% glutaraldehyde for 2 h. Dehydration was achieved with ethanol in increasing concentrations: 30%, 50%, 70%, 90%, and 100%. After dehydration, the samples were put into 100% acetone for 30 min and impregnated in a mixture of acetone and Durcupan resin (1:1) with gentle rotation overnight. The resin was polymerized by placing the samples in an oven at 60°C for 30 min. The samples were sectioned into 60–80 nm slices in an ultramicrotome and prepared for electron microscopy (JOEL, model 1010). Observations from 6 individual subjects were evaluated for sham and PCA livers. Quantification of the surface cover with mitochondrial corpuscles was done in 12–15 ultrastructural images from sham and PCA samples displaying entire hepatocytes by using ImageJ software (NIH-USA).

2.7. Lipid Peroxidation and Conjugated Dienes. Lipid peroxidation (LP) measured *in vitro* was quantified by the 2-thiobarbituric acid method [15] using liver homogenate and subcellular fractions as prooxidative sources. Some modifications to the original method were introduced [16]. Briefly, a sample of the homogenate ($\sim 3 \text{ mg}$ protein) was incubated for 30 min at 37°C in 1 ml of 0.15 M Tris, pH 7.4; incubation was ended by adding 1.5 ml of 20% acetic acid (adjusted to pH 2.5 with KOH) and 1.5 ml of 0.8% thiobarbituric acid. The samples were kept for 45 min in a boiling water bath, and then 1 ml of 2% KCl was added to each sample. The colored complex was extracted with butanol-pyridine (15:1, *v/v*) and quantified at 532 nm. Malondialdehyde was used as standard (extinction coefficient: $1.56 \text{ \AA} \sim 105 \text{ cm}^{-1} \text{ M}^{-1}$). LP *in vivo* was determined by conjugated dienes in liver homogenate and subcellular fractions: lipidic fraction was separated with Folch reactive (chloroform-methanol 2:1, *v/v*); samples were dried, reconstituted in hexane, and measured at 233 nm [17].

2.8. Liver Enzymatic Activities. Glutamine synthetase (GS) activity was measured in both liver homogenate and mitochondrial fraction by measuring NADH oxidation in a coupled-enzymatic reaction according to the procedure reported by Kingdon [18]. Briefly, the ATP consumed during glutamine synthesis from glutamate and NH_4^+ is regenerated by pyruvate kinase and phosphoenolpyruvate included in the incubations; the resulting pyruvate is reduced to lactate by the added lactate dehydrogenase. This step is coupled to the oxidation of NADH, which is recorded spectrophotometrically at 340 nm. The GS activity was assayed in a final volume of 3 ml using 0.2 mg of total homogenate protein or 0.5 mg of

total mitochondrial protein. The reaction was followed for 5 min (to ensure linearity), and the results were expressed as $\mu\text{mol}/\text{min}/\text{mg}$ using a value of 6.22 as the extinction coefficient for $\beta\text{-NADH}$ at 340 nm.

Glutamate dehydrogenase (GDH) activity was measured by an enzyme-coupled reaction according to Schmidt and Schmidt [19]. The redox reaction was followed spectrophotometrically by the oxidation of NADH to NAD^+ at 340 nm coupled to the conversion of α -ketoglutarate to glutamate in the presence of ammonium. Results were calculated using the extinction coefficient of $6220 \text{ M}^{-1} \text{ cm}^{-1}$. GDH activity was quantified in liver homogenate as well as in liver mitochondrial and cytosolic fractions.

Caspase-3 is a cysteine-aspartic acid protease with a key role in the executive phase of apoptosis, derived from both extrinsic and intrinsic pathways. The activity of caspase-3 was assayed by a colorimetric method based on the spectrophotometric quantification of chromophore p-nitroaniline (pNA) after cleavage from the labeled substrate DEVD-pNA (Colorimetric kit ABCAM ab39401).

2.9. Mitochondrial Fluorescent Probes. MitoTracker (membrane potential), Rhod-2 (matrix calcium), and MitoSOX (superoxide production) were obtained from Molecular Probes, now Thermo Fisher. $50 \mu\text{g}$ of each dye was diluted in $200 \mu\text{l}$ of dimethyl sulfoxide. From this stock, $1 \mu\text{l}$ was taken and diluted in 100 ml of ringer solution. Liver slices ($\sim 0.5 \text{ cm}$) were oxygenated and incubated with the dyes for 15 min at room temperature. After incubation, the tissues were fixed in a 4% paraformaldehyde solution for 24 h; subsequently, the samples were placed in different concentrations of sucrose (10, 20, and 30%) for 24 h in each concentration. The tissues were cut to $10 \mu\text{m}$ in cryostat and observed in the Olympus DP70 fluorescence microscope; then they were quantified at 40X with the ImageJ program.

2.10. Indirect Calorimetry. Indirect calorimetry analyses were performed in sham and PCA rats using an OxyletPro System (Panlab Harvard Apparatus, Barcelona, Spain). For this purpose, the animals were placed in individual acrylic cages (Oxylet LE 1305 Physiocage, PANLAB) in a controlled temperature environment ($23 \pm 2^\circ\text{C}$) with a photoperiod of 12 h:12 h (lights on at 07:00 h). At week 12 after surgery, a set of 6 rats was acclimated in the Oxylet cages for 48 h before experimental measurements. Oxygen consumption (VO_2) and carbon dioxide production (VCO_2) were measured every 12 min for 72 h by an O_2 and CO_2 analyzer (Oxylet LE 405-gas analyzer, PANLAB) at a controlled flow rate of 900 ml/min (Oxylet LE 400-air supplier, PANLAB). At each point of analysis, the Metabolism v3.0.01 software (Panlab Harvard Apparatus, Barcelona, Spain) automatically calculated the respiratory quotient (RQ) as the VCO_2/VO_2 ratio and energy expenditure (EE) in $\text{kcal}/\text{day}/\text{kg}^{0.75}$ as $\text{VO}_2 \times 1.44 \times [3.815 + (1.232 \times \text{RQ})]$, according to the Weir formula [20]. During all procedures, rats had access to food and water *ad libitum*. Activity and food and drink intake were also measured by a continuous recording using Panlab's weight transducer (LE1305 sensor platform, Panlab).

TABLE 1: Morphometric and biochemical parameters in rats with PCA.

	Sham		PCA	
	Mean	SEM	Mean	SEM
Body weight (g)	444.0	15.0	335.6*	16.0
Liver weight (g)	15.5	0.7	7.3*	0.4
Liver dry weight (%)	71.7	0.8	72.4	1.1
<i>Blood</i>				
Ammonium ($\mu\text{g/ml}$)	2.1	0.2	4.0*	0.4
Urea (mg/dl)	56.8	2.9	51.2	1.6
Glucose (mg/dl)	135.4	7.0	113.3*	3.2
TAG (mg/dl)	46.4	6.6	44.5	4.2
ALT (U/l)	10.6	1.1	17.7*	3.0
AST (U/l)	282.5	13.6	191.8*	2.9
<i>Liver</i>				
Glutamine synthetase (cytosol) ($\mu\text{moles NADH/min/mg}$)	10.9	1.4	6.6*	1.2
Glutamate dehydrogenase (mitochondria) ($\mu\text{moles NADH/min/mg}$)	317.6	40.6	190.5*	12.6
Caspase 3 (absorbance at 405 nm)	1.5	0.3	2.2*	0.2

Body and liver weight, blood parameters, and liver enzymatic activities were determined in rats with PCA 13 weeks after surgery. Blood determinations were performed in the serum and liver determinations were done in homogenate and subcellular fractions. TAG: triacylglycerols; ALT: alanine aminotransferase; ASP: aspartate aminotransferase. Significant differences were detected in cytoplasmic glutamine synthetase activity and in mitochondrial glutamate dehydrogenase activity. No changes were detected in the activity of both enzymes in the liver homogenate. Values correspond to 7-12 sham rats and 15-19 PCA rats. Statistical significance (*) was calculated by the Student *t*-test; *P* value was set at 0.05.

2.11. Statistics. Data are presented as mean \pm standard error of the mean (SEM). Student's *t*-test was done with the significance threshold set at $P < 0.05$. Statistical analyses were performed with GraphPad Prism 5 and graphs were made with SigmaPlot 10.0.

3. Results

3.1. Morphometric, Blood, and Hepatic Parameters in PCA Rats. Experimental PCA animals after 13 weeks of surgical procedure showed a variety of morphometric and biochemical alterations, indicating an important shrinkage of the liver and the expected hyperammonemia, but not a clear hepatic necrotic damage (Table 1). PCA promoted a significant reduction in body weight ($\downarrow 24\%$) that was even more accentuated in the weight of the liver ($\downarrow 53\%$). Therefore, the liver/body weight ratio showed an important reduction ($\downarrow 37\%$) in the PCA group. In contrast, no changes were detected in the dry weight of the liver. The most conspicuous alteration measured in the blood was the significant elevation of ammonium ($\uparrow 90\%$). No gross signs of hepatic encephalopathy were noted, but fine motor coordination test in a rotating rod was deficient in the PCA rats (data not shown). Table 1 also shows some parameters that indicate the metabolic performance of the liver (circulating glucose and triacylglycerides) as well as markers of cellular liability (serum transaminases and liver caspase-3 activity) and hepatic NH_4^+ -intracellular handling. The glycemic level was discretely reduced ($\downarrow 16\%$) whereas circulating urea and TAG were similar to the values observed in sham rats.

Interestingly, PCA rats showed divergent tendencies in ALT and AST blood levels: whereas ALT increased ($\uparrow 67\%$), AST decreased ($\downarrow 32\%$). The activity of caspase-3 in liver homogenate, as an indicator of ongoing apoptosis, was importantly enhanced ($\uparrow 47\%$). Glutamine synthetase (cytosol) and glutamate dehydrogenase (mitochondria), both enzymes involved in hepatic intracellular ammonium-handling, showed significant changes: the 2 enzymatic activities were equally reduced ($\downarrow 40\%$).

These data indicate that our experimental surgical model of PCA successfully reproduced the principal alterations reported for this protocol, specifically the enhancement in circulating ammonium levels and an anatomical atrophy of the liver. In addition, the experimental group also showed reduced glycemic values in *ad libitum* conditions suggesting dietary/endocrinal alterations. Modifications in liver glutamine synthetase and glutamate dehydrogenase activities could be related to the ongoing hyperammonemia, and elimination of cellular types by programmed cell death is highly suggestive of metabolic adaptations in the livers from PCA rats. Because only one serum transaminase was elevated (AST), an active necrotic cell disappearance in the liver can be discarded.

3.2. Histological and Ultrastructural Characterization in PCA Rats. It was evident in the histological study using H&E staining that PCA livers showed a remarkable new feature: all operated animals showed an extensive process of neovascularization (approximately 1 in every 20 liver acini) that made it difficult to distinguish the usual hepatic zonation of

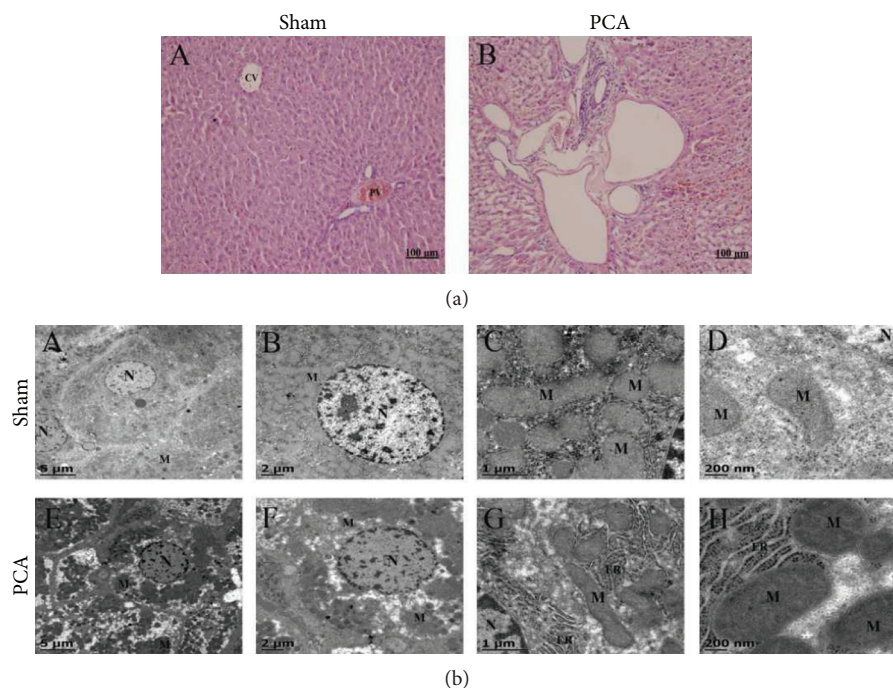


FIGURE 1: Histological and ultrastructural characterization of hepatocytes. (a) Histological characterization in H&E stained section of the liver. (A) Liver from sham operated rat. CV: central vein; PV: portal vein. (B) Experimental animal with PCA showing formation of new blood vessels. (b) Ultrastructural characteristics of hepatic cells. (A–D) Normal hepatocyte of sham-operated rats. (E–H) Hepatocyte cells of PCA-operated rats. N: nucleus; M: mitochondrial; ER: endoplasmic reticulum. Images are representative of 6 independent experimental observations.

pericentral and periportal regions (Figure 1(a), B). Hepatocytes with morphological characteristics of apoptotic activity were also detected, supporting the finding of elevated caspase 3 activity in the liver homogenate (Table 1). Images of electron microscopy displayed some ultrastructural abnormalities: (1) the nuclei did not look as turgid as the nuclei in hepatocytes from sham rats; (2) hepatocytes from PCA rats showed less mitochondrial material (~30%) evidencing extensive zones of protoplasm filled with small vacuoles; and (3) widespread endoplasmic reticulum cisterna with numerous ribosomes (Figure 1(b), E–H).

Analysis of the cellular morphology of PCA rat livers highly suggests that the hepatic gland is adapting to a new equilibrium in response to the hemodynamic challenge that the portal bypass involves: an active angiogenic process that is coincident with an altered subcellular structure, fewer mitochondria, and ongoing apoptotic activity. However, no evidence of necrotic cell destruction was detected.

3.3. Liver Prooxidant Reactions in PCA Rats. Despite the suggestive morphological features of cellular stress observed by electron microscopy (Figure 1(b), E–H), the protocol of experimental PCA for 13 weeks was not associated with any increase in 2 different markers of prooxidant reactions in the livers of PCA rats, namely, conjugated dienes and TBARs (basal levels and Fe^{2+} -supplemented) (Figures 2–4). Indeed, not a single increment in oxidative markers in PCA rats was observed in the whole liver homogenate and all

subcellular fractions tested. Figure 2 shows that conjugated dienes in liver homogenate from PCA rats were similar to the values recorded in sham rats. No conjugated dienes were determined in the serum. In contrast, basal levels of TBARs in liver homogenate from PCA rats showed a very notorious reduction ($\downarrow 87\%$) that was also present when the assay was supplemented with Fe^{2+} ($\downarrow 71\%$). Basal TBARs did not show any change in the serum of PCA rats, but they depicted a significant reduction in the presence of Fe^{2+} ($\downarrow 42\%$). Figure 3 displays the prooxidant status in the mitochondrial and microsomal fractions of the liver. In both fractions, the changes in conjugated dienes were discreet and did not reach statistical significance. However, in basal TBARs, values of mitochondrial and microsomal fractions from PCA rats showed evident diminutions: $\downarrow 82\%$ in the mitochondria and $\downarrow 70\%$ in microsomes. With the Fe^{2+} supplementation, the TBAR value decreased in the mitochondrial fraction ($\downarrow 43\%$), whereas in the microsomal fraction it showed only a tendency to be reduced but without statistical significance. Data from the liver plasma membrane and cytosolic fractions from PCA rats are shown in Figure 4. As with the other subcellular fractions, conjugated diene levels were very similar between sham and PCA rats in these fractions. Similar to the data from Figures 2 and 3, basal TBARs showed a reduction: $\downarrow 22\%$ in plasma membrane and $\downarrow 59\%$ in cytosol. A more notorious decrease was observed when Fe^{2+} was present in the assay. In this condition, the reduction in the plasma membrane fraction was $\downarrow 67\%$, whereas in the cytosolic fraction it was $\downarrow 87\%$.

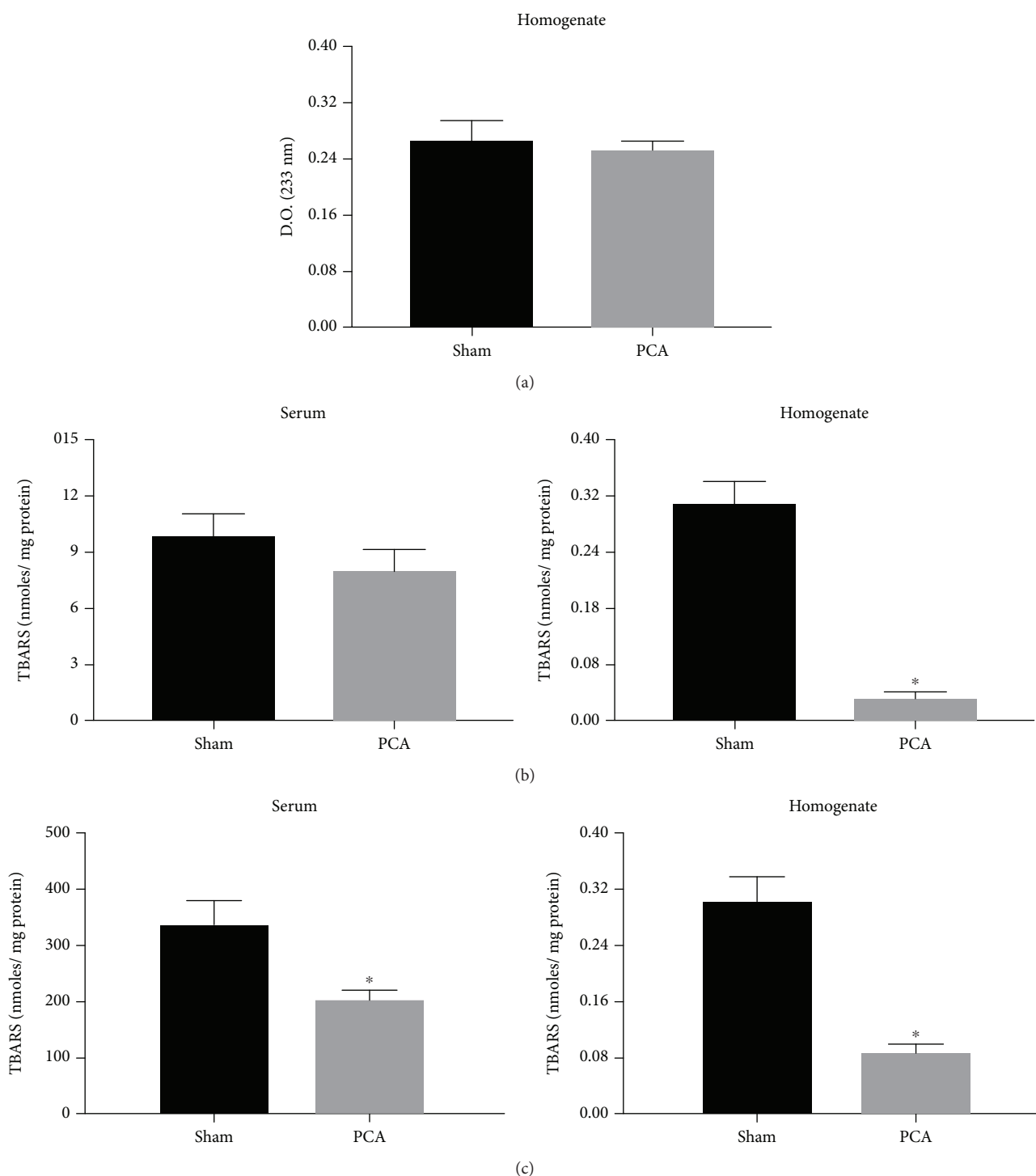


FIGURE 2: Prooxidant reactions in the serum and liver homogenate. (a) Conjugated dienes (not measured in serum). (b) Basal TBARS. (c) TBARS supplemented with FeSO_4 $50 \mu\text{M}$. Data obtained from sham and PCA rats after 13 weeks of surgical procedures. Values represent mean \pm SEM of 12-15 independent experimental observations; $P < 0.05$.

Hence, despite the histological and cellular alterations in the liver of PCA rats, the structural abnormalities were not coincident with an elevation in the levels and activity of prooxidant markers.

3.4. Mitochondrial Fluorescent Probes. Experiments with MitoTracker, Rhod-2, and MitoSOX were done to study the

functional and prooxidant status of the hepatic mitochondria in PCA rats. Data are shown in Figure 5. In the 3 panels the results were comparable, a significant diminution of 21-25% in the fluorescent signal.

Taken together, the ultrastructural analysis of the mitochondrial presence and the functional mitochondrial probes resulted in a similar degree of reduction suggesting that

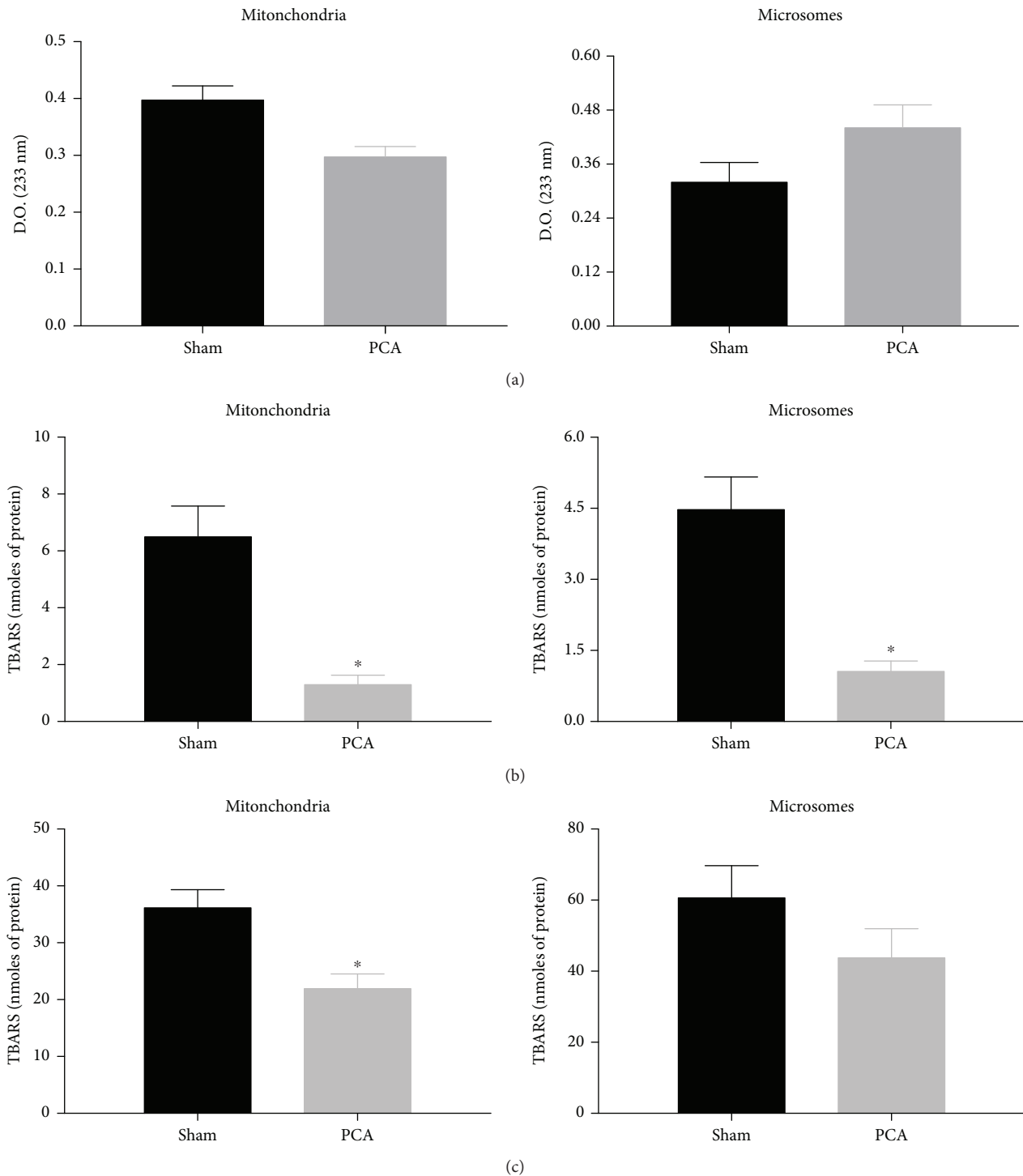


FIGURE 3: Prooxidant reactions in mitochondrial and microsomal fractions of the liver. (a) Conjugated dienes. (b) Basal TBARS. (c) TBARS supplemented with FeSO₄ 50 μM. Subcellular fractions were obtained by differential centrifugation (see Methods). Data obtained from sham and PCA rats after 13 weeks of surgical procedures. Values represent mean ± SEM of 12-15 independent experimental observations; $P < 0.05$.

PCA surgery affects more the liver mitochondrial number than their functional status.

3.5. Metabolic Performance in PCA Rats. By using open-flow indirect calorimetry, we evaluated in PCA rats the individual components of energy demand such as the respiratory

coefficient, cumulative food intake, water drinking, and ambulatory activity. The results involving 24-48 h of continuous recording are depicted in Figure 6. It can be seen that rats after 13 weeks of PCA surgery displayed a reduced pattern of metabolic performance, evidenced by lower energy expenditure and lower respiratory quotient

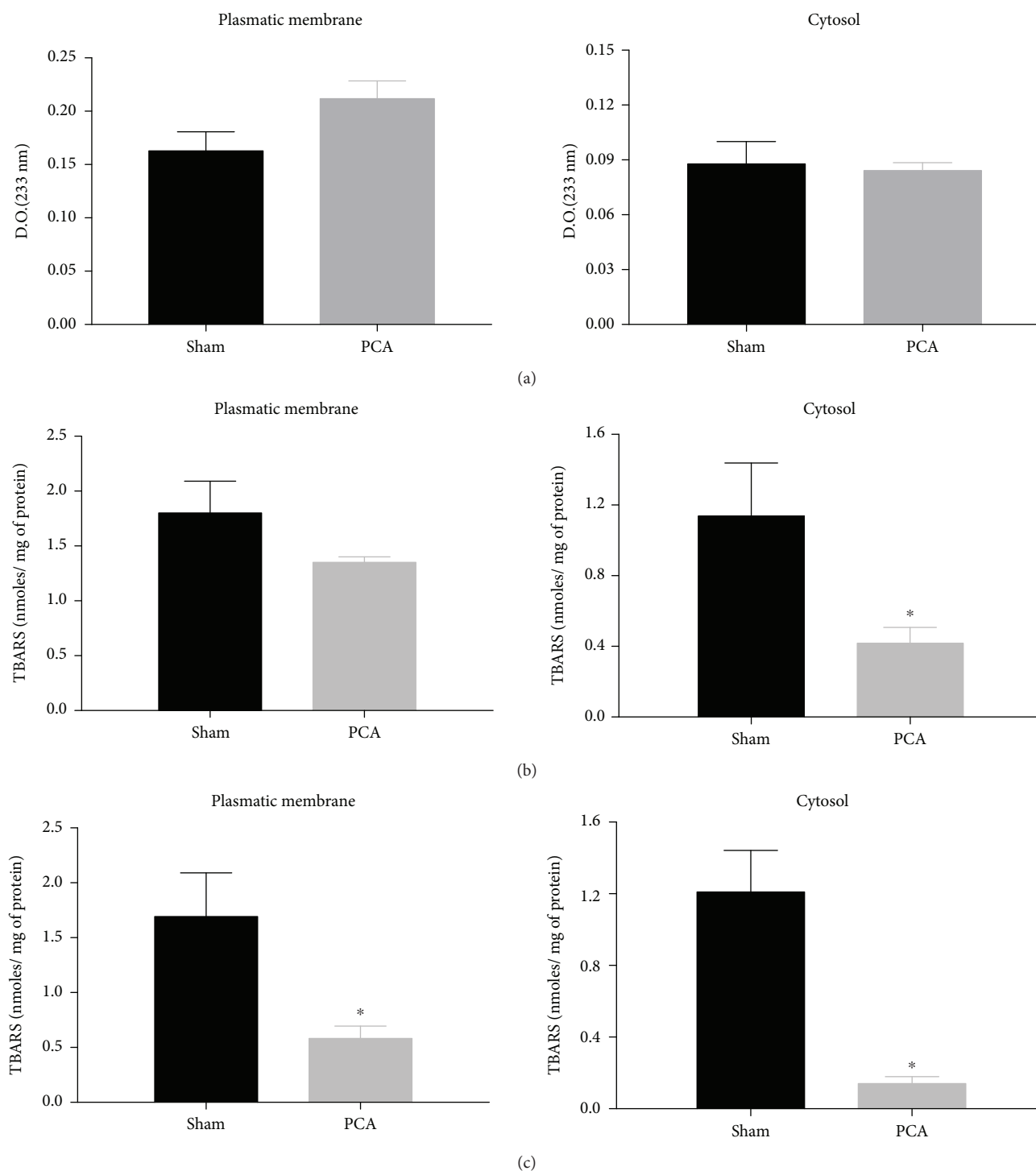


FIGURE 4: Prooxidant reactions in the plasma membrane and cytosolic microsomal fractions of the liver. (a) Conjugated dienes. (b) Basal TBARS. (c) TBARS supplemented with FeSO_4 $50 \mu\text{M}$. Subcellular fractions were obtained by differential centrifugation (see Methods). Data obtained from sham and PCA rats after 13 weeks of surgical procedures. Values represent mean \pm SEM of 12-15 independent experimental observations; $P < 0.05$.

in comparison to sham rats (Figures 6(a) and 6(b)). In both, the diminution was more evident during the dark period which is the time nocturnal rodents are awake. The reduced metabolic activity shown by the PCA rats was accompanied by a significant decrease in the 24h

pattern of food intake (Figure 3(c)). Again, the difference was more accentuated during the dark period. No changes related to the experimental surgery were observed in the daily pattern of water drinking and ambulatory activity (data not shown).

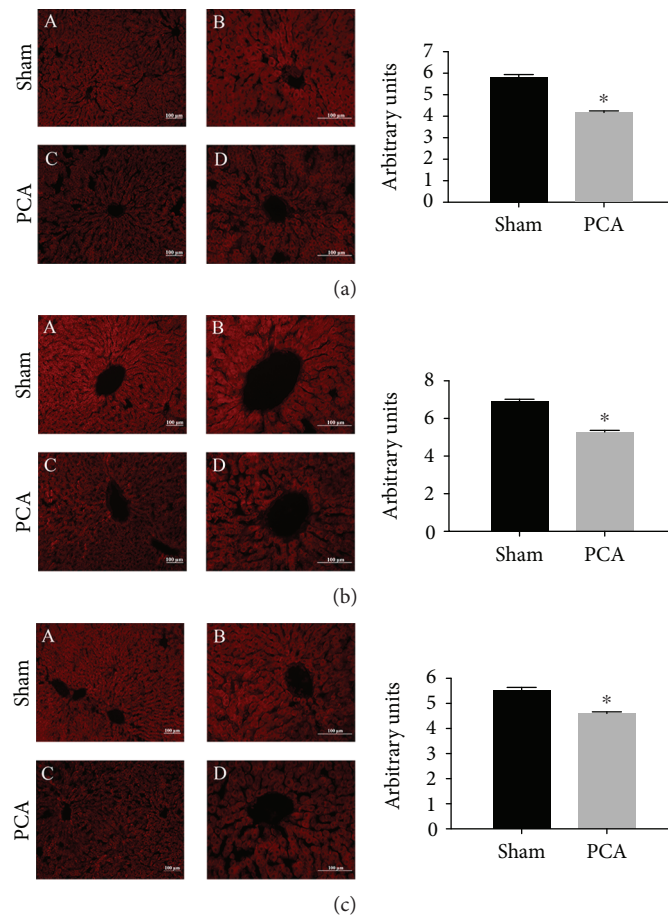


FIGURE 5: Mitochondrial parameters by fluorescent dyes. (a) MitoTracker for assessment of mitochondrial membrane potential $\Delta\Psi_m$. (b) Rhod-2 to measure mitochondrial calcium. (c) MitoSOX for mitochondrial reactive oxygen species (ROS) detection. Histograms at the right side show the quantification of the fluorescent signals, expressed as average \pm SEM. Statistical analysis was done by Student's *t*-test with $P < 0.05$; * means a significant difference. Graphics are representative of 12-15 independent experimental observations.

4. Discussion

4.1. Experimental Protocol. PCA as an experimental model has been mainly focused on characterizing brain alterations associated with hyperammonemic encephalopathy [3]. In contrast, much fewer reports exist regarding the modifications that take place in the liver after the surgery. In particular, the portal bypass involved in PCA importantly influences the uptake, processing, and distribution of nutrients that take place in the hepatic gland. Therefore, it is expected that the liver oxidant metabolism becomes affected as part of the bioenergetic adaptations that are triggered by the loss of the normal hepatic hemodynamics. In this context, previous reports have shown that oxidative stress is developed in cerebral tissues because of the PCA surgery related with high levels of ammonium [21], but none exists regarding the prooxidant status in the liver. Other striking feature associated to the PCA was the notorious reduction of the liver size (Table 1), reduction that was accompanied by an increased apoptotic activity, but at the same time by an enhanced formation of blood vessels without active necrosis (Table 1 and Figure 1(a)).

Previous reports have associated the altered hepatic nutrient arrival caused by the portal deprivation to an active angiogenesis [22]. Damage to the liver cells was discreet at most, since only serum ALT was elevated whereas circulating AST was reduced, and urea levels did not change. Active necrotic cell death is usually associated to the elevation of both transaminases in the serum [23]. All these data are suggestive of an emergent balance in which the morphological changes observed in the liver coexist with a functional hepatic activity.

An important parameter to take into consideration in the PCA model is the elapsed time postsurgery. Because the protocol involves a progressive adaptation and modification of the metabolic and physiological activities, it is necessary to clearly establish the time in which the experiments are done. For example, 3.5 months after PCA surgery were necessary to promote discreet changes in the properties of the liver mitochondria [24], whereas only 3 weeks were enough to affect gene expression and lipogenic activity in the adipose tissue [25]. In particular, our experiments were done after 13 weeks of PCA surgery to ensure a well-established chronic adaptation in the

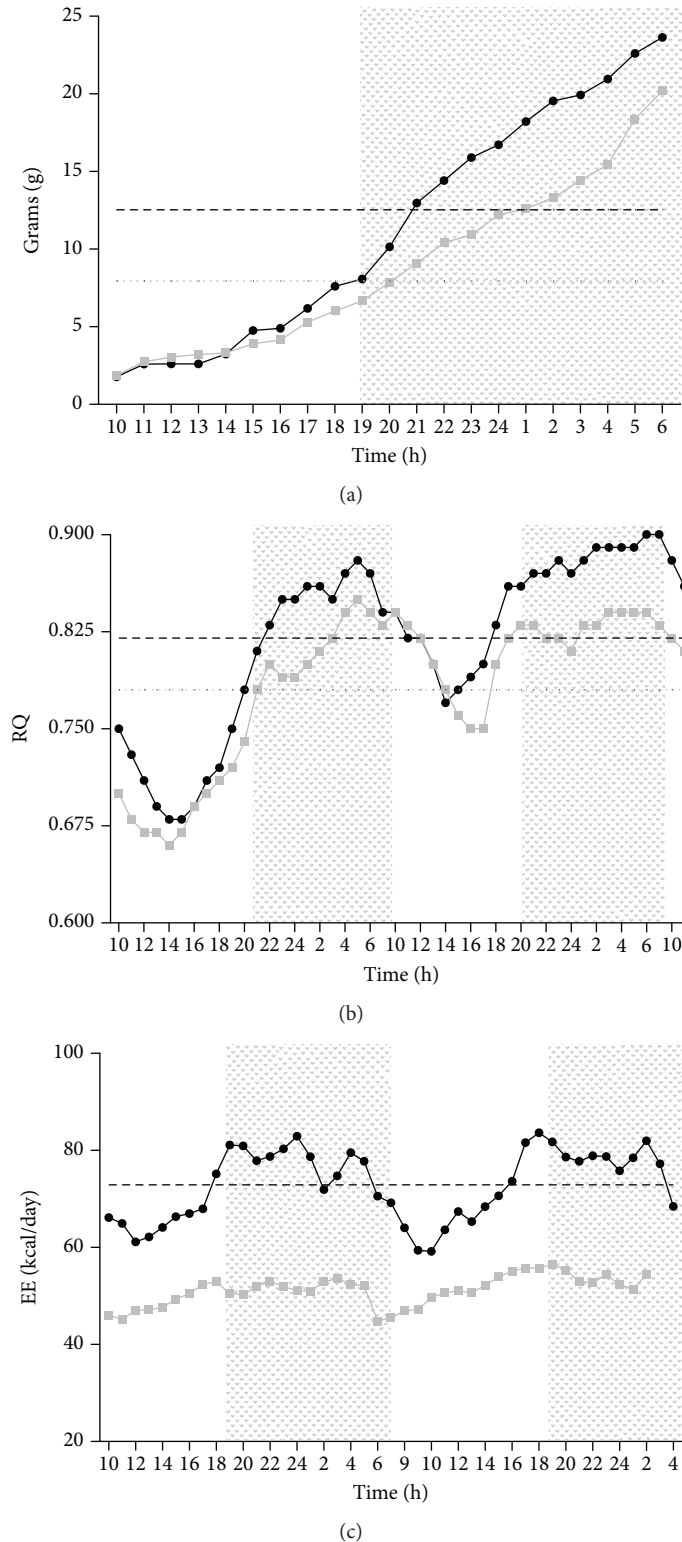


FIGURE 6: Food intake, respiratory quotient, and energy expenditure in rats with PCA. Data were collected over a period of 1-2 days using metabolic cages (PANLAB, Spain). Darker section depicts period with light off. (a) Cumulative food intake, expressed in g, during 24 h. (b) Respiratory quotient (ratio of CO_2 produced by the O_2 consumed) recorded for 2 days. (c) Energy expenditure recorded for 2 days. Data from panels (b) and (c) were recorded every 12 min and the results shown in the graphics correspond to values calculated with the average of every hour. To make simpler the display of the data, only the mean of 6 independent experimental observations are represented; SEM values (corresponding from 8 to 13% of the mean) were omitted. PCA rats showed significant reduction in food intake and respiratory quotient during the dark period and along the 24 h recording in energy expenditure.

metabolic and oxidative capacities of the liver in response to the new hemodynamic circumstances.

4.2. Histological and Cellular Changes. The principal consequence of PCA is to disconnect the portal circulation to the liver. Indeed, this is a major manoeuvre to drastically change the hepatic hemodynamics. One of the most notorious outcomes was the proliferation of new blood vessels in the liver parenchyma (1 in every 20 liver acini in PCA rats). Proangiogenic factors in the liver are numerous and very complex in their mechanisms of action. Some proangiogenic factors are angiopoietin, VEGF, FGF, EGF, and thrombospondin; the role played by the stellate cells is also relevant [26]. Further experiments are needed to learn which factors are involved in the proangiogenic response observed in the PCA livers after 13 weeks of surgery (Figure 1(a)).

Another conspicuous modification detected in the ultrastructural study of the hepatocytes from PCA livers was the reduced presence of mitochondrial bodies (\downarrow 30%) (Figure 1(b)). A possible explanation to this effect is that the disturbed oxygenated blood flow resulting from the PCA (portal blood is more oxygenated than the blood circulating in the central vein) could affect the hepatic oxidative metabolism and thus the hepatic zonation. The presence of fewer mitochondria could explain the generalized and similar reduction observed with the 3 mitochondrial fluorescent probes (MitoTracker, MitoSOX, and Rhod-2) tested in Figure 5. The coincidence in the degree of diminution of mitochondrial corpuscles and the functional fluorescent probes strongly suggest that PCA alters mainly the mitochondrial number but not their properties. The interesting possibility that hepatic zonation (metabolically specialized hepatocytes in the periportal and pericentral regions) could be modified by the PCA remains to be tested.

4.3. Prooxidant Reactions. In our experiments, we measured 2 markers of oxidative stress in liver subcellular fractions and serum (Figure 2): (1) conjugated dienes as a measure of an ongoing lipid peroxidation, also considered by some authors as an “in vivo” lipid peroxidation and (2) TBARs, in basal conditions and Fe^{2+} -supplemented, to evaluate the prooxidant potential of the sample. In addition, the tests were done in liver homogenate and subcellular fractions, since it has been demonstrated that lipid peroxidation can be increased differentially only in some endomembranes, according to the physiological or pharmacological condition studied [12].

Concerning the oxidative activity, PCA surgery involved a clear reduction in the prooxidant activity, confirmed by 2 different markers of lipid peroxidation (Figure 2). These data ruled out a condition of oxidative stress in the liver and serum of the rats after 13 weeks of PCA surgery, despite the evident histological and ultrastructural alterations such as the process of neovascularization, the abnormalities in the nuclear morphology, the reduced mitochondrial number, and the ongoing apoptosis (Figure 2). A putative interpretation to the lower lipoperoxidative activity in the subcellular fractions of the liver from PCA rats is to consider that the liver could be adapting a hypofunctional state

because of the reduced metabolic demands caused by the portal deprivation [22].

These results could also be explained supposing that the appearance of new blood vessels is a regulated process. Hence, the prooxidant reactions are reduced as an adaptation for the liver to properly function despite an ongoing apoptosis. In particular, the reduction of TBAR values in the livers from PCA rats in the presence of Fe^{2+} is suggestive of minor availability of unsaturated acyl groups in the membrane phospholipids. This situation could be related to a hepatocyte membrane restructuring, in both plasma membrane and endomembranes.

Further experiments are needed to clarify the molecular mechanisms underlying these possibilities.

4.4. Metabolic Performance. PCA is an experimental protocol that greatly affects the wellness of rats under the condition of our study and after 13 weeks of the surgical procedure. Data in Table 1 showed a significant reduction in body weight in PCA rats. This alteration was sustained by the confirmation of a reduced daily food intake (Figure 6(a), especially during the dark period). Interestingly, this diminution was not associated with alterations in the ambulatory behavior of PCA rats (data not shown). PCA rats showed an altered hepatic histology since it is coincident with an ongoing angiogenic and apoptotic activities (Table 1 and Figure 1(a)). This circumstance associated with the hyperammonemic condition and the reduced food intake may be related to the minor energy expenditure and respiratory quotient (Figures 6(b) and 6(c)) as well as to the lower glycemia (Table 1) recorded in PCA rats. The altered metabolic performance shown by the PCA rats was not associated with their lighter weight since the energy expenditure and the respiratory quotient were similar in intact rats weighing \sim 430 g and \sim 320 g (data not shown). Taken together, the parameters obtained in the metabolic cages are indicative of a hypometabolic status in the PCA rats that provides novel perspectives regarding this experimental surgical model.

5. Conclusions

After 13 weeks of surgery, experimental PCA promoted hyperammonemia and a reduction of liver mass. A process neovascularization and apoptosis in the liver were evident whereas hepatocytes showed diminished mitochondrial content. However, no active necrotic cell destruction was detected. Lower levels of blood glucose were detected. Hepatic prooxidant reactions measured as TBARs showed a notorious reduction in the PCA group, especially in whole homogenate as well as in microsomal and mitochondrial fractions (at basal conditions), and in whole homogenate and cytosolic fraction (supplemented with Fe^{2+}). Changes in conjugated dienes were discreet. Active energy expenditure as well as food intake was reduced in the PCA group. Overall, data are suggestive of a hypometabolic response that is associated with a lower prooxidant reaction in the liver of PCA rats after 13 weeks of surgery.

Data Availability

All the experimental protocols, material, and data obtained to support the findings and to sustain the conclusions of this study are available from the corresponding author upon request.

Conflicts of Interest

The authors declare that there is no conflict of interest regarding the publication of this paper.

Authors' Contributions

Olivia Vázquez-Martínez and Héctor Valente-Godínez contributed equally to the project.

Acknowledgments

The authors thank Ms. Jessica González-Norris for carefully editing the manuscript. L.N. Fernando López-Barrera was responsible for the artistic version of all figures. The technical assistance of Vet Martín García-Servín, Leonor Casanova, and Lourdes Lara is also thankfully acknowledged. We also thank Dr. Abraham Osornio-Núñez for his kind donation of surgical implements. This work was supported by grants IN201618 (DGAPA-UNAM, PAPIIT) and 284-557 (CONACYT) to MD-M.

References




- [1] N. Toshikuni, Y. Takuma, and M. Tsutsumi, "Management of gastroesophageal varices in cirrhotic patients: current status and future directions," *Annals of Hepatology*, vol. 15, no. 3, pp. 314–325, 2016.
- [2] M. Guevara and J. Rodés, "Hepatorenal syndrome," *International Journal of Biochemistry and Cell Biology*, vol. 37, no. 1, pp. 22–26, 2005.
- [3] K. D. Mullen, S. Birgisson, R. C. Gacad, and H. Conjeevaram, "Animal models of hepatic encephalopathy and hyperammonemia," *Adv. Exp. Med. Biol.*, vol. 368, pp. 1–10, 1994.
- [4] S. Lee, J. G. Chandler, C. E. Broelsch, Y. M. Flamant, and M. J. Orloff, "Portal-systemic anastomosis in the rat," *Journal of Surgical Research*, vol. 17, no. 1, pp. 53–73, 1974.
- [5] N. Hashimoto, M. Nishiwaki, A. Nishioka, H. Ashida, Y. Kotoura, and J. Utsunomiya, "A comparison of the metabolic changes after the distal splenocaval and portacaval shunts," *Surgery Today*, vol. 23, no. 10, pp. 897–901, 1993.
- [6] R. F. Butterworth, "Pathogenesis of hepatic encephalopathy in cirrhosis: the concept of synergism revisited," *Metabolic Brain Disease*, vol. 31, no. 6, pp. 1211–1215, 2016.
- [7] G. Federspil, A. Boninsegna, G. Picchi, G. Zanon, and C. De Palo, "Effect of portacaval shunt on circulating free fatty acids and ketone bodies in rats," *Metabolism*, vol. 29, no. 6, pp. 495–497, 1980.
- [8] A. D. Proia, K. D. Edwards, D. J. McNamara, and K. E. Anderson, "Dietary influences on the hepatic mixed-function oxidase system in the rat after portacaval anastomosis," *Gastroenterology*, vol. 86, no. 4, pp. 618–626, 1984.
- [9] J. C. Pector, J. Winand, J. P. Dehaye, V. Leclercq-Meyer, and J. Christophe, "Effects of portacaval shunt on the genetically obese Zucker rat," *Gastroenterology*, vol. 81, no. 5, pp. 923–927, 1981.
- [10] W. Rokicki, M. Rokicki, and K. Czyzewski, "The effect of "end to side" portacaval anastomosis on regeneration ability of white rat liver," *Zeitschrift für Experimentelle Chirurgie, Transplantation und Künstliche Organe*, vol. 23, no. 3, pp. 175–179, 1990.
- [11] S. H. Lee and B. Fisher, "Portacaval shunt in the rat," *Surgery*, vol. 50, pp. 668–672, 1961.
- [12] I. Aguilar-Delfín, F. López-Barrera, and R. Hernández-Muñoz, "Selective enhancement of lipid peroxidation in plasma membrane in two experimental models of liver regeneration: partial hepatectomy and acute CCl₄ administration," *Hepatology*, vol. 24, no. 3, pp. 657–662, 1996.
- [13] E. G. Loten and J. C. Redshaw-Loten, "Preparation of rat liver plasma membranes in a high yield," *Analytical Biochemistry*, vol. 154, no. 1, pp. 183–185, 1986.
- [14] H. U. Bergmeyer and E. Bernt, "Glutamate-oxalacetate / glutamate-pyruvate transaminases," in *Methods of Enzymatic Analysis*, H. U. Bergmeyer, Ed., Academic Press, New York, NY, USA, 1965.
- [15] E. J. Giamarellos-Bourboulis, S. Skiathitis, A. Dionyssiou-Asteriou et al., "Lipid peroxidation by *Pseudomonas aeruginosa* in the pathogenesis of nosocomial sepsis," *Journal of Postgraduate Medicine*, vol. 49, no. 1, pp. 11–16, 2003.
- [16] R. Hernández-Muñoz, W. Glender, M. Díaz Muñoz, J. Adolfo, J. A. García-Sáinz, and V. Chagoya de Sánchez, "Effects of adenosine on liver cell damage induced by carbon tetrachloride," *Biochemical Pharmacology*, vol. 33, no. 16, pp. 2599–2604, 1984.
- [17] C. D. Klaassen and G. L. Plaa, "Comparison of the biochemical alterations elicited in livers from rats treated with carbon tetrachloride, chloroform, 1,1,2-trichloroethane and 1,1,1-trichloroethane," *Biochemical Pharmacology*, vol. 18, no. 8, pp. 2019–2027, 1969.
- [18] H. S. Kingdon, "Feedback inhibition of glutamine synthetase from green pea seeds," *Archives of Biochemistry and Biophysics*, vol. 163, no. 1, pp. 429–431, 1974.
- [19] E. S. Schmidt and F. W. Schmidt, "Glutamate dehydrogenase: biochemical and clinical aspects of an interesting enzyme," *Clinica Chimica Acta*, vol. 173, no. 1, pp. 43–55, 1988.
- [20] J. B. V. Weir, "New methods for calculating metabolic rates with special reference to protein metabolism," *Journal of Physiology*, vol. 109, no. 1-2, pp. 1–9, 1949.
- [21] P. Carbonero-Aguilar, M. d. M. Díaz-Herrero, O. Cremades, M. Romero-Gómez, and J. Bautista, "Brain biomolecules oxidation in portacaval-shunted rats," *Liver International*, vol. 31, no. 7, pp. 964–969, 2011.
- [22] F. Guérin, M. Wagner, A. Liné et al., "Hepatic proliferation and angiogenesis markers are increased after portal deprivation in rats: a study of molecular, histological and radiological changes," *PLoS One*, vol. 10, no. 5, article e125493, 2015.
- [23] A. Arora and P. Sharma, "Non-invasive diagnosis of fibrosis in non-alcoholic fatty liver disease," *Journal of Clinical and Experimental Hepatology*, vol. 2, no. 2, pp. 145–155, 2012.
- [24] W. Andrzejewski, T. Wróbel-Wybrzak, and S. W. Andrzejewski, "The effect of various types of portocaval anastomoses

and hepatic artery ligation on the metabolism of hepatic mitochondria in rats,” *Acta Physiologica Polonica*, vol. 36, no. 2, pp. 92–97, 1985.

- [25] S. Dasarathy, S. Muc, A. Runkana, K. D. Mullen, K. Kaminsky-Russ, and A. J. McCullough, “Alteration in body composition in the portacaval anastomosis rat is mediated by increased expression of myostatin,” *American Journal of Physiology-Gastrointestinal and Liver Physiology*, vol. 301, no. 4, pp. G731–G738, 2011.
- [26] D. Leyva-Illades, M. McMillin, M. Quinn, and S. Demorrow, “Cholangiocarcinoma pathogenesis: role of the tumor micro-environment,” *Translational Gastrointestinal Cancer*, vol. 1, no. 1, pp. 71–80, 2012.

Research Article

Antifibrotic Effect of Marine Ovothiol in an *In Vivo* Model of Liver Fibrosis

Mariarita Brancaccio,¹ Giuseppe D'Argenio,^{2,3} Vincenzo Lembo ,² Anna Palumbo ,¹ and Immacolata Castellano ¹

¹Department of Biology and Evolution of Marine Organisms, Stazione Zoologica Anton Dohrn, Naples, Italy

²Gastroenterology Unit, Department of Clinical Medicine and Surgery, School of Medicine, Federico II University, Naples, Italy

³IBAF Institute, National Research Council (CNR), via P. Castellino, Naples, Italy

Correspondence should be addressed to Immacolata Castellano; immacolata.castellano@szn.it

Received 5 June 2018; Accepted 18 September 2018; Published 17 December 2018

Guest Editor: Anna M. Giudetti

Copyright © 2018 Mariarita Brancaccio et al. This is an open access article distributed under the Creative Commons Attribution License, which permits unrestricted use, distribution, and reproduction in any medium, provided the original work is properly cited.

Liver fibrosis is a complex process caused by chronic hepatic injury, which leads to an excessive increase in extracellular matrix protein accumulation and fibrogenesis. Several natural products, including sulfur-containing compounds, have been investigated for their antifibrotic effects; however, the molecular mechanisms underpinning their action are partially still obscure. In this study, we have investigated for the first time the effect of ovothiol A, π -methyl-5-thiohistidine, isolated from sea urchin eggs on an *in vivo* murine model of liver fibrosis. Mice were intraperitoneally injected with carbon tetrachloride (CCl₄) to induce liver fibrosis and treated with ovothiol A at the dose of 50 mg/kg 3 times a week for 2 months. Treatment with ovothiol A caused a significant reduction of collagen fibers as observed by histopathological changes and serum parameters compared to mice treated with control solution. This antifibrotic effect was associated to the decrease of fibrogenic markers involved in liver fibrosis progression, such as the transforming growth factor (TGF- β), the α -smooth muscle actin (α -SMA), and the tissue metalloproteinases inhibitor (TIMP-1). Finally, we provided evidence that the attenuation of liver fibrosis by ovothiol A treatment can be regulated by the expression and activity of the membrane-bound γ -glutamyl-transpeptidase (GGT), which is a key player in maintaining intracellular redox homeostasis. Overall, these findings indicate that ovothiol A has significant antifibrotic properties and can be considered as a new marine drug or dietary supplement in potential therapeutic strategies for the treatment of liver fibrosis.

1. Introduction

In the last decades, the need to face complex challenges, i.e., the supply of sustainable food, human health, and aging population has stimulated research efforts to discover new active compounds from natural sources. In particular, the need to develop more efficient products and benefits for mankind, in order to treat or prevent many human disorders and to overcome the side effects of most of the approved drugs, has stimulated a great interest from pharmaceutical and nutraceutical industrial field to search for new natural products from less explored sources. In the last years, growing attention has been focused on the ocean characterized by a higher biodiversity compared to the earth [1]. In particular,

marine natural products have inspired several approved pharmaceutical products, which are now in clinical use and/or in various stages of clinical development [2].

Liver fibrosis represents a worldwide health problem for its growing incidence and prevalence, and its evolution towards cirrhosis, which is associated with high morbidity and mortality. Thus, there is an urgent need to develop antifibrotic treatments that can prevent, halt, or even reverse liver fibrosis or cirrhosis [3]. Liver fibrosis results from chronic liver injury during a long-term wound-healing response, which causes increasing excessive accumulation of extracellular matrix (ECM) proteins, leading to fibrogenesis and later cirrhosis [4]. It represents a complex process that includes apoptosis of hepatocytes, infiltration of inflammatory cells,

induction of inflammatory cytokines, and proliferation of nonparenchymal cells producing ECM, mainly hepatic stellate cells (HSCs) [5]. Active HSCs are characterized by increased proliferation, migration, and contractility, and a relative resistance to apoptosis. At the molecular level, they show increased expression of α -smooth muscle actin (α -SMA) and procollagen-I; both associated with the ability of the activated HSCs to deposit collagens and other matrix proteins in the extracellular space [6]. Indeed, activated HSCs present an altered regulation of matrix remodeling enzymes, such as metalloproteinases (MMPs) and their tissue inhibitors (TIMPs), modulating matrix degradation and production, respectively [7]. Another key player in fibrosis development is the pleiotropic cytokine TGF- β 1, which is secreted in the latent form and when active, induces the activation of HSCs and modulates the expression and secretion of a number of proteases and their regulators, including MMPs and TIMPs [8]. TGF- β 1 can also auto-induce its own production thus subsequently amplifying its actions [9, 10].

Moreover, liver functionality is finely regulated by glutathione (GSH) levels, the most abundant cellular thiol in the cells. GSH is synthesized inside the cell and partially secreted in the extracellular space along a concentration gradient. In the extracellular space, GSH is hydrolyzed by γ -glutamyl-transpeptidase (GGT), a dimeric enzyme located on the membrane surface, and highly expressed in the liver and kidney [11]. This enzyme is therefore involved in GSH metabolism, amino acids recycling, and detoxification mechanisms. In detail, it catalyzes the hydrolysis of the γ -glutamyl bond in GSH and the transfer of the γ -glutamyl group to amino acids and small peptides. It often catalyzes the γ -glutamylation of the administered drugs, allowing the liver and the kidney to detoxify the organism [11, 12].

Several studies demonstrated the efficacy of different natural products and phytochemicals present in foods and used as food extracts (such as sulforaphane, S-allylcysteine, curcumin, proanthocyanidins, garlic extract, coffee, and grape skin or seeds) to prevent or reduce liver fibrosis progression by different mechanisms in several animal models [10, 13–17]. However, despite the striking progress in understanding the molecular mechanisms involved in liver fibrosis and cirrhosis, the antifibrotic therapies are still lacking. In this context, methyl-5-thiohistidines, also called ovothiols, isolated in huge amounts from the eggs of marine invertebrate species, represent promising bioactive compounds [18–20]. First of all, they display unusual antioxidant properties due to the peculiar position of the thiol group on the imidazole ring of histidine [21, 22]. Thanks to their chemical properties, ovothiols can recycle oxidized GSH and play a key role in controlling the cellular redox balance [23, 24]. These molecules were found in different methylated forms at the amino group of the lateral chain of histidine in several marine invertebrates [19, 20, 25–27]. For example, ovothiol A, unmethylated on the lateral chain, was isolated from the eggs of the sea urchin *Paracentrotus lividus* [25] and the sea cucumber *Holothuria tubulosa* [26]. Ovothiol B, mono-methylated on the lateral chain of histidine, was found in the ovaries of the scallop *Chlamys hastata* [21]. Ovothiol A has also been

recently identified in the green microalga *Euglena gracilis*, which is a rich source of vitamins and antioxidants [28]. Interestingly, the biosynthetic pathway leading to ovothiols lacks in vertebrates [18]; therefore, mammals do not produce autonomously these molecules. Up to date, a very few studies have focused on the biological activities of ovothiols in human model systems. Several years ago, a synthetic analogue of ovothiol was reported as a neuroprotective agent in a murine model of brain injury [29]. Recently, we have claimed the nutraceutical and/or pharmaceutical use of marine ovothiol to relieve pathologies associated with chronic endothelial dysfunction, such as diabetes [30], and suggested a role of the molecule in regulating cell proliferation in human liver tumor cells [31]. In particular, ovothiol A, purified by sea urchin eggs, was shown to induce autophagy in human hepatocarcinoma cell lines.

The aim of this study was to evaluate in depth the effect of ovothiol A in an *in vivo* model of chronic liver inflammation, which can silently progress, leading to cirrhosis and eventually to hepatocarcinoma, which is one of the most aggressive tumors with a very poor prognosis. We used a murine model of liver fibrosis in order to test if the administration of ovothiol A in its disulfide form could induce the recovery of liver functionality. In order to define the molecular mechanism underpinning this process, we tested the gene and protein expression of different fibrogenic markers (α -SMA, TGF- β 1, and TIMP1) and the activity of the mature membrane-bound GGT form. Overall, our experiments point to evaluate the efficacy of ovothiol A as a novel anti-inflammatory and antifibrotic bioactive molecule.

2. Methods

2.1. Experimental Model of Progressive Fibrosis and Animal Treatment. Male balb-c albino mice (20–25 g) were housed in a room at a mean constant temperature of 22°C with a 12 h light–dark cycle and free access to standard pellet chow and water. The study was approved by Federico II University School of Veterinary Medicine Animal Care N° 104/2015-PR. Liver fibrosis was induced in mice by intraperitoneal (ip) injection of carbon tetrachloride (CCl₄) 0.2 mL/100 g body weight (b.w.) in refined olive oil (1:1) twice a week for 7 weeks according to a well-established protocol [32]. Two experimental groups were designed as follows: (1) mice receiving CCl₄ and ip injection of the disulfide form of ovothiol A 50 μ g/g b.w. 3 times a week for 7 weeks ($n = 7$); (2) control group receiving CCl₄ and ip injection of vehicle (aqueous solution) alone ($n = 7$) with the same timing. Ovothiol A was prepared as described by Russo et al., 2014 [31]. The dose of administration was chosen on the basis of a previous work demonstrating that at this posology an ovothiol analogue induced no toxicity in not injured mice and neuroprotection in mice affected by brain injury [29]. A group of 5 normal mice was also included in the study. The animals were then killed under anaesthesia, and their livers were harvested at peak fibrosis (3 days after the final injection of CCl₄). After harvesting, livers were divided with a minimum of two lobes fixed in formalin for histologic analysis and histochemistry, and the remaining tissue was snap-

frozen for RNA and protein extraction. Serum was also collected from each mouse to analyze biochemical parameters.

2.2. Histology and Determination of Serum Biochemical Parameters. Formalin-fixed paraffin-embedded tissue was cut into 4 μm sections by using routine techniques and mounted onto slides with coverslips. Representative sections of each fixed liver were stained with haematoxylin/eosin (H&E) for routinely observations. For the detection of collagen content, sections were stained with Sirius red/Fast green, according to standard protocols. All histological analyses were performed by an experienced histopathologist in a blinded manner. For each mouse, 64 fields of a constant raster of 31 mm^2 were analyzed at 100-fold final magnification. For semiautomated morphometry, a Sony 3CCD (model DXC-950P) video microscope equipped with a motor stage and the Quantimed 500MC (Leica, Germany) software were used. Serum aspartate aminotransferase (AST), alanine aminotransferase (ALT), and alkaline phosphatase (ALP) levels were determined to assess liver function by using standard laboratory techniques and equipment (Roche Diagnostics, Germany).

2.3. RNA Extraction and cDNA Synthesis. Total RNA was extracted from frozen tissue by homogenization in Trizol Reagent according to the manufacturer's protocol (Life Technologies). The amount of total RNA extracted was estimated measuring the absorbance at 260 nm and the purity by 260/280 and 260/230 nm ratios by Nanodrop (ND-1000 UV-Vis Spectrophotometer; NanoDrop Technologies). The integrity of RNA was evaluated by agarose gel electrophoresis. For each sample, 1200 ng of total RNA extracted was retrotranscribed with iScriptTM cDNA synthesis kit (Bio-Rad), following the manufacturer's instructions.

2.4. Gene Expression by Real-Time qPCR. For real-time qPCR experiments, the data from each cDNA sample were normalized using the mouse housekeeping gene GAPDH (glyceraldehyde 3-phosphate dehydrogenase). In the case of GAPDH, TGF- β , α -SMA, Col1a1, and GGT-1, the specific primers were designed based on the nucleotide sequences downloaded by NCBI database (accession numbers) using Primer3WEB v.4.0.0. GAPDH primer forward 5'-GGTG AAGGTCGGTGTGAACG-3', primer reverse 5'-CTCGCT CCTGGAAGATGGTG-3'; TGF- β primer forward 5'-TGC GCTTGCAGAGATTA AAA-3', primer reverse 5'-CTGCC GTACA ACTCCAGTGA-3'; α -SMA primer forward 5'-CT GACAGAGGCACCACTGAA-3', primer reverse 5'-CATC TCCAGAGTCCAGCACA-3'; Col1a1 primer forward 5'-A CAGTCGCTTACCTACAGC-3', primer reverse 5'-TGG GGTGGAGGGAG;TTTACA-3' GGT-1 primer forward 5'-TGCTCGGTGACCCAAAGTTT-3', primer reverse 5'-TT CAGAGGATGGCAGTGCTG-3'. A final concentration of 1.4 pmol/ μL for each primer and 1 FastStart SYBR Green Master Mix (total volume of 10 μL) were used for the reaction mix. PCR amplifications were performed in a ViiATM 7 real-time PCR system (Applied Biosystems) thermal cycler using the following thermal profile: 95°C for 10 min, one

cycle for cDNA denaturation; 95°C for 15 sec and 60°C for 1 min, 40 cycles for amplification; 72°C for 5 min, one cycle for final elongation; and one cycle for melting curve analysis (from 60°C to 95°C) to verify the presence of a single product. Each assay included a no-template control for each primer pair. Specificity of amplification reactions was verified by melting curve analysis. The efficiency of each primer pair was calculated according to standard method curves using the equation $E = 10^{-1/\text{slope}}$. Five serial dilutions were set up to determine Ct values and reaction efficiencies for all primer pairs. Standard curves were generated for each oligonucleotide pair using the Ct values versus the logarithm of each dilution factor, and PCR amplifications were performed in a ViiATM 7 real-time PCR system (Applied Biosystems) thermal cycler using the standard protocol previously reported. To capture intra-assay variability, all real-time qPCR reactions were carried out in triplicate. Fluorescence was measured using ViiATM 7 Software (Applied Biosystems). The expression of the genes was analyzed and internally normalized against GAPDH using relative expression software tool (REST) software based on the Pfaffl method (2002). Relative expression ratios above two cycles were considered significant. Experiments were repeated at least three times.

2.5. Protein Analysis. Liver samples, about 20/30 mg, were homogenized in 1 mL of RIPA lysis buffer (1X) containing a 50 mM Tris-HCl (pH 7.6), 150 mM NaCl, 5 mM EDTA, 0.5% NP-40, 0.5% Sodium deoxycholate, 10% SDS, phosphatase, and protease inhibitor cocktail (Roche). Liver homogenates were run on 12% SDS/polyacrylamide gel according to Laemmli. Following electrophoresis, proteins were transferred onto a PVDF (Millipore) membrane (Bio-Rad Trans-Blot Apparatus) and detected using a mouse anti-TGF- β polyclonal antibody (Sigma-Aldrich, USA), mouse anti-GGT monoclonal antibody (Santa Cruz Biotechnology, USA), rabbit anti- α -SMA monoclonal antibody (Santa Cruz Biotechnology, USA), rabbit TIMP-1 polyclonal antibody (Elabscience), and as an internal control mouse anti-GAPDH monoclonal antibody (Santa Cruz Biotechnology, USA). All primary antibodies were incubated at 4°C overnight. The appropriate secondary antibody was added, and immunoreactive proteins were detected using the ECL (WesternBrightTM detection kit ECL, Advansta, USA) according to the manufacturer's instructions. Protein expression levels were analyzed by means of densitometric analysis using the Image J software.

2.6. Enzyme Isolation—GGT Activity. Tissues were homogenized with Potter-Elvehjem tissue homogenizer at 4°C in 5 volumes of 25 mM Tris-HCl, pH 7.5, 0.2 mM EDTA, containing 0.33 M sucrose, 1 μM leupeptin, and 1.4 $\mu\text{g}/\text{mL}$ aprotinin [33]. The homogenate was centrifuged at 9000 $\times g$ for 20 min; the supernatant was spun at 100,000 $\times g$ for 1 h to spin down nuclei, mitochondria, and cellular debris. The pellet was homogenized in 25 mM Tris-HCl, pH 7.35, 0.5% Triton X-100, 1 μM leupeptin, 1.4 $\mu\text{g}/\text{mL}$ aprotinin, and then centrifuged again at 100,000 $\times g$ for 1 h. The supernatant was aliquoted and stored at -80°C and then assayed for GGT protein expression and activity. GGT activity was

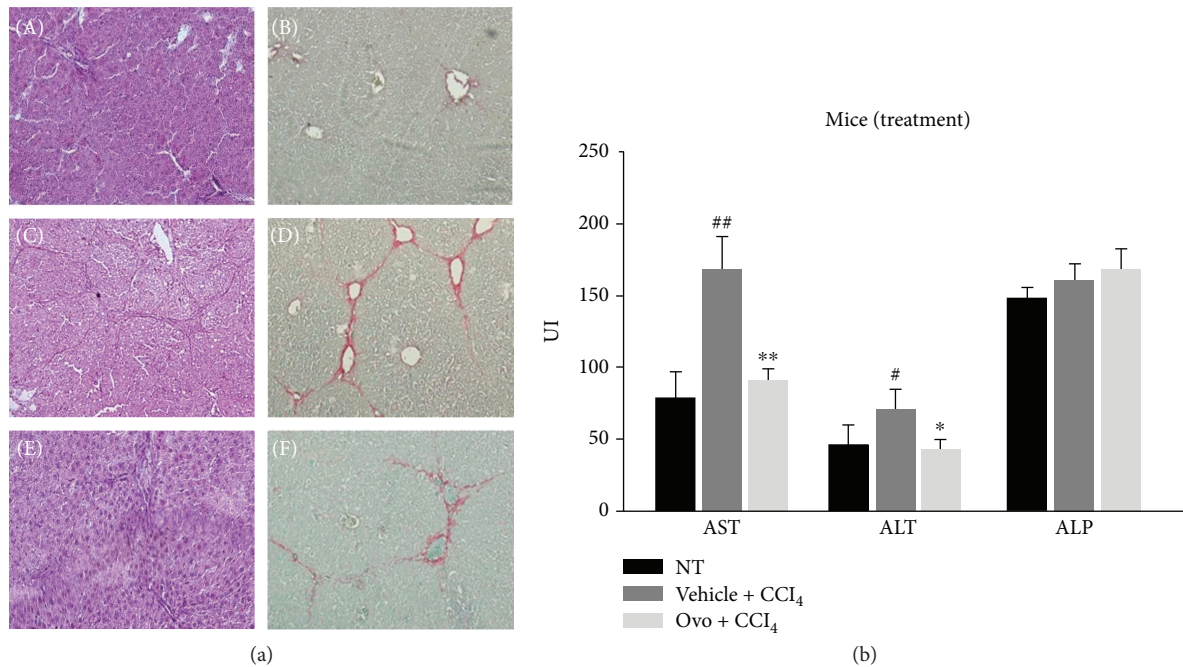


FIGURE 1: (a) Histological analysis. H&E staining and sirius red dye to highlight the collagen fibers of liver section: (A, B) healthy hepatic tissue; (C, D) fibrotic liver tissue induced by CCl₄; (E, F) liver tissue with hepatic fibrosis treated with ovothiol A. (b) Evaluation of serum levels of liver enzymes. The levels of AST, ALT, and ALP were determined in the serum from mice affected by liver fibrosis and treated with ovothiol A or control solution. Data are expressed as mean \pm SD, $n = 7$. The significance was determined by the ANOVA and post hoc analysis: ($*p < 0.05$) and ($**p < 0.01$) represent significance compared to vehicle + CCl₄; ($#p < 0.05$) and ($##p < 0.01$) compared to nontreated (NT) healthy mice.

determined by a colorimetric test. The assay buffer contains 100 mM Tris-HCl pH 7.8 or PBS 1X pH 7.4. Each reaction contains 1 mM of γ -glutamyl-para-nitroanilide as a donor substrate and 40 mM glycylglycine as an acceptor substrate. The product formation, p-nitroaniline, was continuously monitored at room temperature at A405 nm using a Bio-Rad 680 microplate reader with Microplate Manager 5.2 (Bio-Rad) software. One unit of GGT activity was defined as the amount of GGT that released 1 μ mol of p-nitroaniline/min at room temperature.

2.7. Glutathione Assay. Total glutathione levels were determined by Glutathione Assay Kit (Sigma). Briefly, frozen liver tissues were ground with a pestle with a mortar in the presence of liquid nitrogen to prepare a fine powder. Then, 100 mg of powder was added to 3 volumes of 5% 5-sulfosalicylic acid and mixed. Then, other 7 volumes of 5% 5-sulfosalicylic acid were added, mixed, left for 5 min at 4°C, and finally centrifuged at 10,000 $\times g$ for 10 min. Diluted samples of the supernatants were used for the assay procedure, in which following the incubation with glutathione reductase and NADPH, glutathione was totally recovered in the reduced form and thus determined by monitoring the reduction of 5,5-dithiobis (2-nitrobenzoic acid) to 5-thio-2-nitrobenzoic at 412 nm by a Thermo Scientific™ Multiskan™ FC Microplate Photometer.

2.8. Statistical Analysis. As appropriate, comparisons among groups were made by Student's *t*-test or analysis of variance

ANOVA followed by Bonferroni or Tukey's multiple comparison tests. Values of $p < 0.05$ were considered significant.

3. Results

3.1. Effect of Ovothiol on Liver Histology and Serum Biochemical Parameters. In order to evaluate the effect of ovothiol A on relieving induced liver fibrosis, the histology and functionality of the liver were examined in injured mice treated and not treated with ovothiol compared to control animals. Histological analysis of hepatic tissue of mice treated with CCl₄ for 7 weeks compared with healthy mice tissue confirmed that the injection of CCl₄ caused the progression of hepatic fibrosis, as demonstrated by the increase of red colored collagen fibers showing established septa linking hepatic veins (see Figure 1(a), C–D compared to A and B). Ovothiol A treatment significantly reduced hepatic fibrosis as shown by the reduction of red colored collagen fibers (Figure 1(a), E–F compared to C and D). The amount of collagen was reduced in fibrotic mice treated with ovothiol compared to those treated with vehicle alone ($2.7 \pm 0.9\%$ vs $5.8 \pm 1.2\%$, $p < 0.05$).

Serum levels of liver enzymes, aspartate aminotransferase (AST), alanine aminotransferase (ALT), and alkaline phosphatase (ALP) were assayed to evaluate liver functionality. Levels of AST and ALT increased in mice affected by hepatic fibrosis, whereas the treatment with ovothiol A led to a significant reduction in AST and ALT levels (Figure 1(b)). Conversely, serum ALP levels in mice with hepatic fibrosis did not significantly differ among the treatment groups.

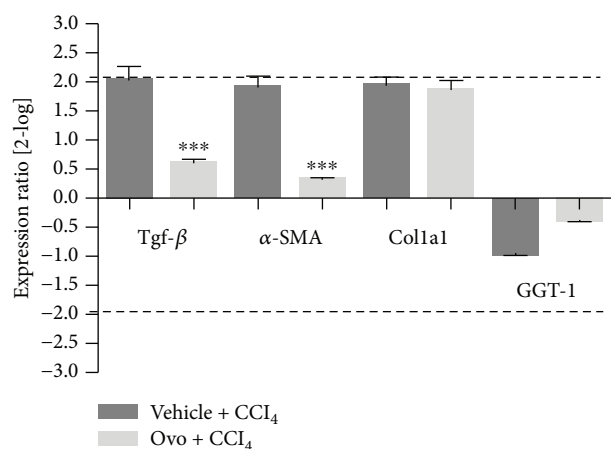


FIGURE 2: Gene expression analysis of markers of liver fibrosis by real-time qPCR. The levels of gene expression of the fibrotic markers in tissues after treatment with ovothiol A or control solution were compared to tissues from healthy mice (reference baseline). Data were analyzed through the REST software, which considers fold differences $\geq +/ -2$ to be significant. (***) $p < 0.001$ represents the significance compared to the treated mice with vehicle + CCl₄.

3.2. Effect of Ovothiol on Gene Expression of Biomarkers of Liver Fibrosis. To evaluate the transcript regulation of specific liver fibrotic markers, gene expression analysis was carried out by real-time qPCR on TGF- β , α -SMA, GGT, and fibrillar type collagen 1 (Col1a1).

A significant increase in gene expression for TGF- β , α -SMA, and Col1a1 was observed in mice affected by liver fibrosis and treated with control solution compared to healthy mice (Figure 2), whereas no significant variation was shown for GGT expression levels. On the other hand, samples from mice treated with ovothiol A showed a significant downregulation of mRNA of the TGF- β and α -SMA, whereas the gene expression of Col1a1 and GGT were not affected.

3.3. Effect of Ovothiol on Protein Expression of Key Players in Liver Fibrosis Progression. The protein expression of the hepatic fibrogenic markers, TGF- β , α -SMA, and TIMP1 was evaluated by Western blot analysis (Figure 3(a)). In mice affected by liver fibrosis, the levels of TGF- β , α -SMA, and TIMP1 significantly increased compared to healthy mice. After treatment with ovothiol A, the protein expression of TGF- β , α -SMA, and TIMP1 significantly decreased compared to mice with hepatic fibrosis (Figures 3(a)–3(d)).

The presence of GGT in the liver tissue was also evaluated by immunoblot of microsomal extracts containing membrane-bound GGT. GGT is synthesized as a single 64 kDa precursor polypeptide, which undergoes self-proteolysis to form the mature protein composed of two subunits, the largest of which is around 50 kDa (Figure 4(a)). The antibody used in this study is directed against a peptide contained in the major subunit; therefore, it is able to recognize both the large subunit and the precursor. In the liver microsomal extracts of healthy mice, 62% of the total GGT is present in the mature form, while in the fibrotic tissues, the mature form

significantly decreased to 36%. Conversely, the treatment with ovothiol A induced an increase in mature protein up to 44% of the total content of GGT (Figures 4(a) and 4(b)). The presence of GGT was also evaluated in mice serum. In all three groups of mice, the serum contained only one band recognized by GGT antibody corresponding to the size of the large subunit of the mature form (Figure 4(c)).

3.4. Ovothiol Affects Membrane-Bound GGT Activity. GGT activity was determined in liver microsomal extracts and normalized against the amount of the mature protein, which represents the active form of the enzyme, compared to the inactive precursor polypeptide [11, 12]. GGT activity significantly increased in fibrotic tissues compared to healthy mice (Figure 5(a)). Treatment with ovothiol A, on the other hand, induced a significant reduction in GGT activity. Since GGT activity is closely related to glutathione metabolism, we also evaluated total glutathione levels in the hepatic tissues. As shown in Figure 5(b), total glutathione levels increased in tissues from mice affected by liver fibrosis and treated with vehicle solution and decreased in liver tissues from mice treated with ovothiol A.

4. Discussion

In the last decade, studies on the isolation and structural characterization of ovothiols have attracted the attention of many scientists [19, 20]. These molecules are sulfur-containing compounds derived from histidine, which, despite the relative structural simplicity, are likely involved in different biological processes in marine organisms [19, 20]. Of particular interest is the finding that vertebrates lack the biosynthetic pathway leading to ovothiol [18], thus envisaging new perspectives on the possible pharmacological applications of the molecule in humans [20, 34]. On this basis, great efforts have been devoted to the chemical synthesis of this class of compounds, lately leading to ovothiols [35, 36] or to 5-thiohistidine, the precursor of ovothiols, unmethylated at the imidazole ring [37]. However, the described chemical procedures are somehow cumbersome and not environmentally friendly; thus, the need to develop an eco-sustainable production of the molecule [20].

Previous studies showed that a synthetic ovothiol analogue exhibited neuroprotective activity in an *in vivo* model of brain injury [29], whereas the natural molecule ovothiol A in disulfide form was tested only in *in vitro* models, showing anti-inflammatory activity in human endothelial cells [30] and antiproliferative effect on human hepatic carcinoma cell lines [31]. These pleiotropic behaviors have been ascribed to different mechanisms of action of these molecules in different cellular contexts [20].

In this study, to deepen the anti-inflammatory properties of this class of molecules, we have evaluated the effect of ovothiol A on an *in vivo* model of liver fibrosis, which is a condition common to many chronic liver diseases, characterized by the presence of parenchymal damage [4, 5]. The chronic activation of the tissue repair response which leads to liver fibrosis is characterized by a significant accumulation of ECM and numerous profibrogenic markers, which is

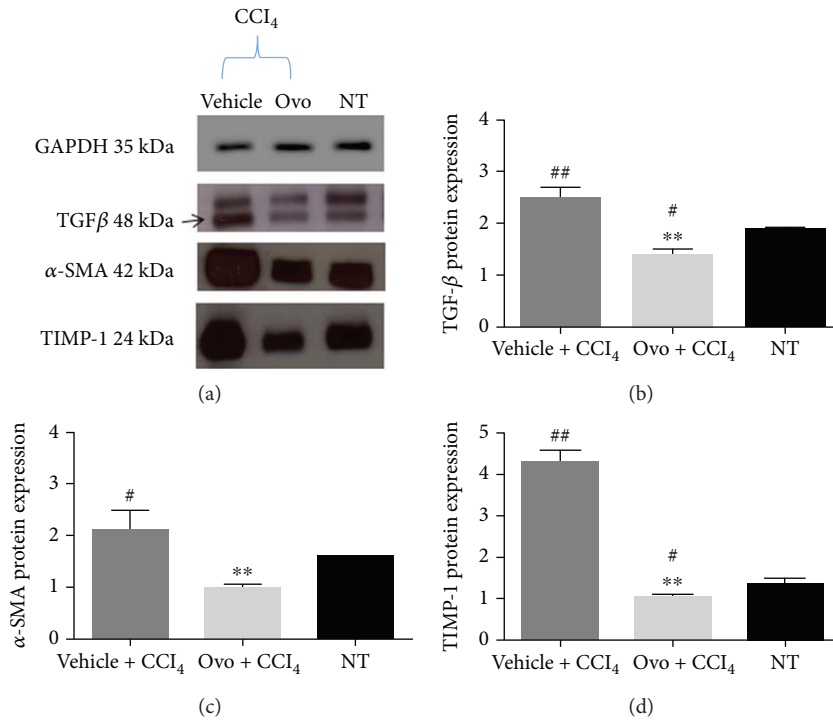


FIGURE 3: Protein expression of liver fibrosis markers. (a) A representative experiment of Western blot analysis of cytosolic extracts obtained from hepatic tissues of mice treated with ovothiol A or vehicle, after induction of liver fibrosis, compared to samples of healthy mice (NT), using antibodies specific for TGF-β, α-SMA, and TIMP1. Histograms of the densitometry analysis of protein bands obtained by Western blot for liver markers: (b) TGF-β; (c) α-SMA; and (d) TIMP1. Data were normalized for GAPDH. Data are expressed as mean ± SD, *n* = 7. The significance was determined by ANOVA test. (#*p* < 0.05) and (##*p* < 0.01) represent significance compared to NT; (***p* < 0.01) represents significance compared to the treated with vehicle + CCl₄.

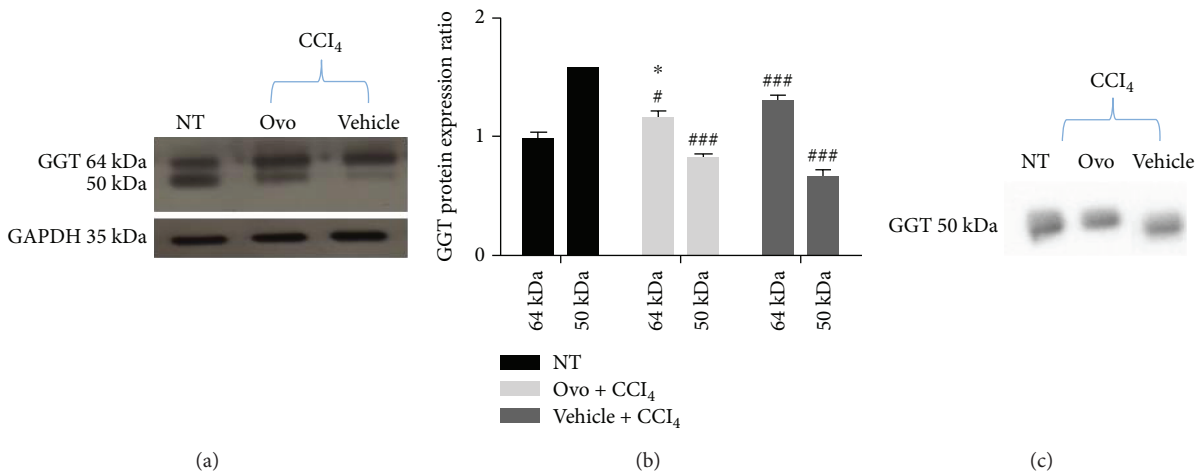


FIGURE 4: Protein expression of GGT. (a) Representative Western blot performed with GGT-specific antibody using microsomal extracts of hepatic tissues of mice with liver fibrosis treated with ovothiol or control solution compared to nontreated healthy mice (NT). (b) Histogram of the densitometric analysis of the GGT bands at 64 and 50 kDa. Data were normalized for GAPDH. (c) Representative Western blot performed on mice serum using GGT-specific antibody. Data are expressed as mean ± SD, *n* = 6. Statistical significance was determined by the one-way ANOVA test; (#*p* < 0.05) and (###*p* < 0.001) represent the significance compared to the corresponding NT band; (**p* < 0.05) represents the significance compared to fibrotic mice treated with control solution.

responsible for the excessive deposition of collagen fibers [6]. Regeneration from liver fibrosis implies key processes, such as the eradication of pathological agents, apoptosis of HSC, remodeling of ECM, and regeneration of parenchyma and liver function. From the clinical perspective, fibrinolytic

therapies reverting advanced fibrosis after the elimination of the causative agent represent a feasible challenge [3]. In fact, in clinical practice, the spontaneous recovery of liver histology, after the elimination of the agent causing chronic liver disease, usually occurs only in some patients and takes more

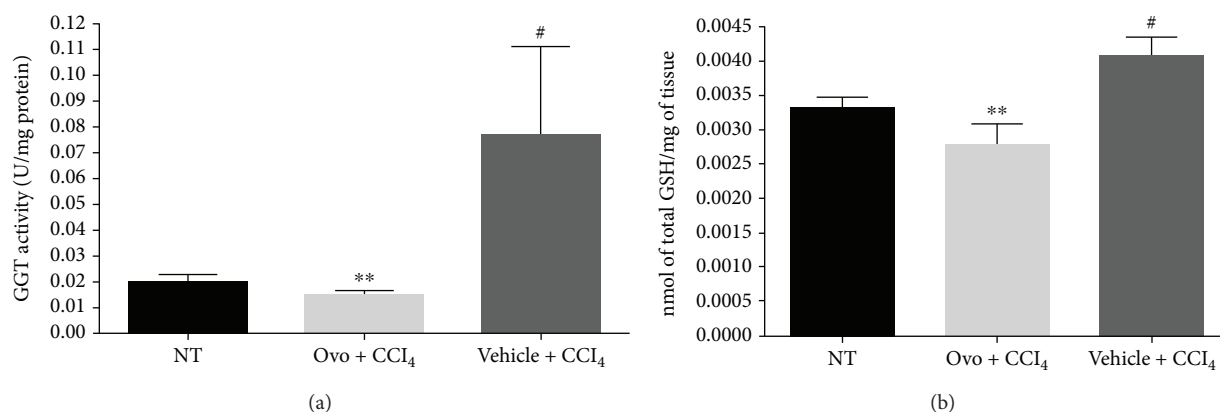


FIGURE 5: GGT activity and glutathione content. (a) The enzymatic activity of GGT was evaluated on liver tissue microsomal extracts containing membrane-bound GGT. The activity of GGT was normalized compared to the mature protein band (50 kDa) detected by Western blot. (b) The levels of glutathione were determined in hepatic tissue of mice treated with ovothiol A or vehicle, after induction of hepatic fibrosis, compared to samples of healthy tissue mice (NT). Data are expressed as mean \pm SD, $n = 6$. The bars indicated the mean of 7 measures \pm SD (standard deviation). The significance was determined by the ANOVA and post hoc analysis: (# $p < 0.05$) represents significance compared to healthy control; (** $p < 0.01$) represents significance compared to mice treated with vehicle + CCl₄.

than 3 years. Several sulfur-containing compounds have been shown to induce the reversion of liver fibrosis [10, 13, 14]. Recently, an ergothioneine-rich diet has been shown to ameliorate liver fibrosis [38]. Ergothioneine is a sulfur-containing histidine produced by some fungi and bacteria [39]. Unlike ovothiol, the sulfur of ergothioneine is localized on position 2 of the imidazole ring of histidine, making it stable in its thionic form. In our study, the methyl-5-thiohistidine (ovothiol A) isolated from sea urchin eggs was administered as disulfide because the reduced form is unstable and very reactive and can be presumably generated in the cell by recycling mechanisms [29]. In the disulfide form, ovothiol A inhibited the onset and/or progression of hepatic fibrosis, highlighting the antifibrotic properties for this type of molecules. Our findings clearly indicate that ovothiol A induced a significant reduction in the accumulation of collagen fibers in injured hepatic tissues associated with the decrease of the serum levels of the liver enzymes AST and ALT (Figure 1). Indeed, ovothiol A activates fibrinolytic processes on the extracellular ECM matrix through the downregulation of different fibrotic markers (Figure 2). In particular, TGF- β , the most important profibrogenic cytokine, was found significantly reduced by ovothiol A treatment also at the protein level (Figure 3). Since the activation of TGF- β is a fundamental step for the activation of HSC and for hepatic fibrogenesis, it is reasonable to infer that a decreased expression of TGF- β , mediated by ovothiol A, is consistent with a reduced amount of activated HSC, remodeling of extracellular matrix, and regeneration of liver function. The reduction of activated HSC after ovothiol A treatment was further confirmed by the reduction of the α -SMA protein isoform, which generally increases in acute hepatopathies, and it is rarely detected in the normal liver.

On the other hand, our results demonstrate that the administration of ovothiol A had no effects on the gene regulation of Col1a1 (Figure 2), a known marker of activation of the fibrogenic process, which encodes the alpha-1 subunit of fibrillar type collagen [6]. The deposition of this protein is

responsible for the significant changes that occur in the composition of the ECM following liver injury and consequent alteration of the liver tissue anatomy. The reduction of collagen fibers observed at histological level is therefore likely caused by an indirect action exerted by ovothiol A on the metalloproteinases and on the inhibitors thereof, which are involved in the degradation of ECM and consequently in the reversion of the pathological condition. Indeed, we found an increased protein expression of the metalloproteinase inhibitor TIMP1 in fibrotic tissues and a decreased expression after treatment with ovothiol A (Figure 3). Under these conditions, in fact, metalloproteases should be free to degrade collagen fibers in the ECM, thus reducing the fibrotic process.

The analysis of protein expression and activity of GGT appeared to be more complex. Our finding indicates that liver fibrosis is characterized by high levels of membrane-bound GGT activity (Figure 5(a)). The total content of GGT protein, consisting of the precursor and the mature form remained unchanged following ovothiol treatment (Figures 4(a) and 4(b)), according to the absence of GGT gene regulation (Figure 2). However, the amount of the membrane-bound mature form decreased in mice affected by liver fibrosis compared to control mice and was restored following ovothiol treatment (Figures 4(a) and 4(b)). The main function of GGT is to regulate the intracellular redox homeostasis by catalyzing the degradation of extracellular GSH and promoting thiols recycling within the cell [11, 12]. The cysteinylglycine, resulting from glutathione hydrolysis, is one of the most reactive thiol compounds able to reduce oxygen by a redox reaction with the iron ion, thus promoting the increase in reactive oxygen species (ROS) and oxidative reactions [40, 41]. Therefore, high levels of GGT activity may induce oxidative stress in the cell, thus contributing to the damage and development of liver fibrosis. It is well known that chronic inflammation of the liver can cause damage to the membranes resulting in the release of GGT into the blood [42]. Indeed, GGT and in particular its

high serum levels are well-known markers of liver damage pathologies. However, the role of GGT anchored to the outer membrane surface of liver cells is not yet clear. Here, we show that during the process of liver fibrosis, the activity of the mature GGT form anchored to the membrane increases (see Figure 4), probably contributing to oxidative stress and membrane damage, which in turn causes the further release of the mature protein in the serum (Figure 4(c)). Treatment with ovothiol A in mice affected by the fibrotic process causes the reversion of this phenomenon, that is, the reduction of membrane GGT activity at the physiological levels of healthy mice. Indeed, by inhibiting GGT activity, ovothiol A should also reduce the amount of cysteinylglycine in the cell, thus avoiding the accumulation of ROS and oxidative damage. In support of this hypothesis, intracellular thiol levels increased in untreated fibrotic tissues and decreased following ovothiol A treatment (Figure 5(b)). This may contribute to maintain membrane integrity and reduce the release of the mature membrane-bound GGT into the serum. Indeed, our data suggest that the mature form of GGT is mostly released in the blood during liver fibrosis and that the treatment with ovothiol A presumably reduces this release, resulting in new mature membrane-bound GGT (Figure 4(c)). Another possible explanation could be that the progression of liver fibrosis negatively affects the auto-catalytic cleavage of the GGT precursor, whereas ovothiol A treatment can reinduce the maturation process. The finding that only the mature form of GGT is released in the serum may depend on the adverse effect of its own overexpression and activity or to a more pronounced anchorage to the membrane of its precursor form. Further studies will be needed to clarify these aspects.

5. Conclusions

Liver fibrosis is known to persist for a long time even after successful pharmacological treatment of hepatitis; therefore, a fibrinolytic therapy to rapidly reverse advanced fibrosis/cirrhosis would be more advisable. This study indicates that, in the experimental model, repeated cycles of hepatic damage have contributed to a significant increase in deposition of collagen fibers mediated by profibrogenic cytokines and that the treatment with the disulfide form of ovothiol A has led to the reversion of this condition. In our model, ovothiol A inhibits GGT activity and affects GSH metabolism. This could be the specific mechanism by which ovothiol negatively regulate redox homeostasis and the activation of key fibrotic markers, TGF- β , α -SMA, and TIMP1, which finally leads to a significant degradation of the collagen fibers in the ECM (see scheme in Figure 6). To our knowledge, this is the first study to highlight the involvement of the membrane-bound GGT form in the evolution of liver fibrosis, thus pointing to this enzyme as a potential target of therapeutic strategies directed to ameliorate liver fibrosis effects.

Overall, these results suggest that ovothiols can be considered a novel class of sulfur-containing molecules endowed with antifibrotic properties with possible applications as drugs or food supplement for the treatment of chronic inflammation of the liver. This study also highlights the key

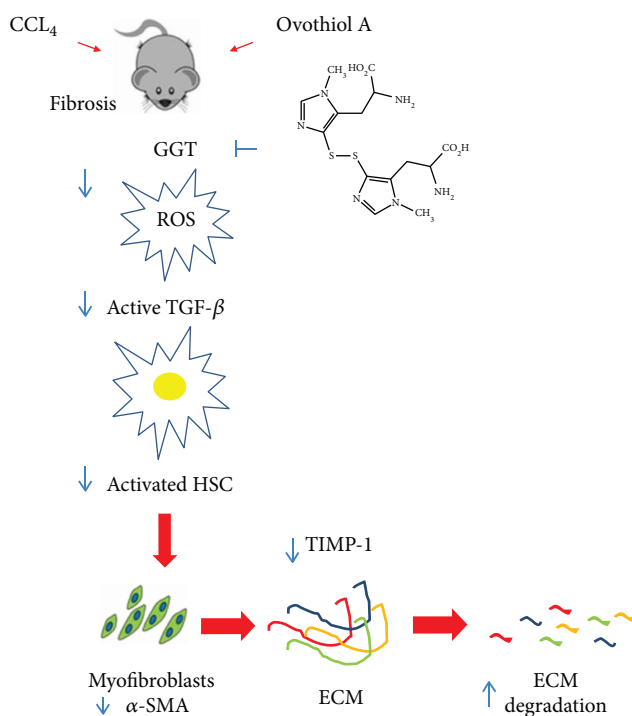


FIGURE 6: Proposed mechanism of action for ovothiol. During the development of liver fibrosis, membrane-bound GGT activity increases, leading to ROS overproduction. ROS can activate TGF- β , which in turn upregulates α -SMA and TIMP1, favoring ECM deposition. Ovothiol acts as a GGT inhibitor and in turn reduces TGF- β activation, thus inducing a cascade of events leading to downregulation of profibrogenic molecules and induction of fibrolytic enzymes.

involvement of sulfur groups in the anti-inflammatory properties of natural products.

Abbreviations

ECM:	Extracellular matrix
HSCs:	Hepatic stellate cells
α -SMA:	α -Smooth muscle actin
TGF- β :	Transforming growth factor
TIMP-1:	Tissue metalloproteinases inhibitor
GGT:	γ -Glutamyl transpeptidase
MMPs:	Metalloproteinases
AST:	Serum aspartate aminotransferase
ALT:	Alanine aminotransferase
ALP:	Alkaline phosphatase
GAPDH:	Glyceraldehyde 3-phosphate dehydrogenase
CCl ₄ :	Carbon tetrachloride
Col1a1:	Fibrillar type collagen 1
NT:	Nontreated.

Data Availability

The data used to support the findings of this study are included within the article.

Disclosure

The content of the present publication is also object of patent application in Italy no. 102018000010907 filed on 10/12/2018.

Conflicts of Interest

The authors declare no conflict of interest.

Authors' Contributions

Mariarita Brancaccio and Giuseppe D'Argenio equally contributed to this work.

Acknowledgments

We thank Davide Caramiello and the service Marine Biological Resources for sea urchin maintenance and gamete collection. A special thanks to Dr. Gian Luigi Russo for critical reading of the final version of the manuscript. Mariarita Brancaccio has been supported by a SZN PhD fellowship. This work was financially supported by Stazione Zoologica Anton Dohrn funds.

References

- [1] J. W. Blunt, A. R. Carroll, B. R. Copp, R. A. Davis, R. A. Keyzers, and M. R. Prinsep, "Marine natural products," *Natural Product Reports*, vol. 35, no. 1, pp. 8–53, 2018.
- [2] K. H. Altmann, "Drugs from the oceans: marine natural products as leads for drug discovery," *CHIMIA International Journal for Chemistry*, vol. 71, no. 10, pp. 646–652, 2017.
- [3] D. Schuppan and Y. O. Kim, "Evolving therapies for liver fibrosis," *The Journal of Clinical Investigation*, vol. 123, no. 5, pp. 1887–1901, 2013.
- [4] C. J. Parsons, M. Takashima, and R. A. Rippe, "Molecular mechanisms of hepatic fibrogenesis," *Journal of Gastroenterology and Hepatology*, vol. 22, Supplement 1, pp. S79–S84, 2007.
- [5] J. E. Puche, Y. Saiman, and S. L. Friedman, "Hepatic stellate cells and liver fibrosis," *Comprehensive Physiology*, vol. 3, no. 4, 2013.
- [6] E. Novo, S. Cannito, E. Morello et al., "Hepatic myofibroblasts and fibrogenic progression of chronic liver diseases," *Histology and Histopathology*, vol. 30, no. 9, pp. 1011–1032, 2015.
- [7] S. Hemmann, J. Graf, M. Roderfeld, and E. Roeb, "Expression of MMPs and TIMPs in liver fibrosis a systematic review with special emphasis on anti-fibrotic strategies," *Journal of Hepatology*, vol. 46, no. 5, pp. 955–975, 2007.
- [8] H.-Y. Li, D. Ju, D.-W. Zhang et al., "Activation of TGF- β 1-CD147 positive feedback loop in hepatic stellate cells promotes liver fibrosis," *Scientific Reports*, vol. 5, no. 1, article 16552, 2015.
- [9] H. L. Weng, Y. Liu, J. L. Chen et al., "The etiology of liver damage imparts cytokines transforming growth factor beta1 or interleukin-13 as driving forces in fibrogenesis," *Hepatology*, vol. 50, no. 1, pp. 230–243, 2009.
- [10] G. D'Argenio, G. Mazzone, M. T. Ribocco et al., "Garlic extract attenuating rat liver fibrosis by inhibiting TGF- β 1," *Clinical Nutrition*, vol. 32, no. 2, pp. 252–258, 2013.
- [11] I. Castellano and A. Merlino, " γ -Glutamyltranspeptidases: sequence, structure, biochemical properties, and biotechnological applications," *Cellular and Molecular Life Sciences*, vol. 69, no. 20, pp. 3381–3394, 2012.
- [12] I. Castellano, A. Merlino, I. Castellano, and A. Merlino, "*Gamma-Glutamyl Transpeptidases: Structure and Function*," in *SpringerBriefs in Biochemistry and Molecular Biology*, Springer, 2013.
- [13] G. D'Argenio, D. C. Amoruso, G. Mazzone et al., "Garlic extract prevents CCl₄-induced liver fibrosis in rats: the role of tissue transglutaminase," *Digestive and Liver Disease*, vol. 42, no. 8, pp. 571–577, 2010.
- [14] C. J. Oh, J. Y. Kim, A. K. Min et al., "Sulforaphane attenuates hepatic fibrosis via NF-E2-related factor 2-mediated inhibition of transforming growth factor- β /Smad signaling," *Free Radical Biology & Medicine*, vol. 52, no. 3, pp. 671–682, 2012.
- [15] P. Vitaglione, F. Morisco, G. Mazzone et al., "Coffee reduces liver damage in a rat model of steatohepatitis: the underlying mechanisms and the role of polyphenols and melanoidins," *Hepatology*, vol. 52, no. 5, pp. 1652–1661, 2010.
- [16] H. Shinkawa, S. Takemura, Y. Minamiyama et al., "S-allylcysteine is effective as a chemopreventive agent against porcine serum-induced hepatic fibrosis in rats," *Osaka City Medical Journal*, vol. 55, no. 2, pp. 61–69, 2009.
- [17] M. O. Shin and J. O. Moon, "Effect of dietary supplementation of grape skin and seeds on liver fibrosis induced by dimethylnitrosamine in rats," *Nutrition Research and Practice*, vol. 4, no. 5, pp. 369–374, 2010.
- [18] I. Castellano, O. Migliaccio, S. D'Aniello, A. Merlino, A. Napolitano, and A. Palumbo, "Shedding light on ovothiol biosynthesis in marine metazoans," *Scientific Reports*, vol. 6, no. 1, article 21506, 2016.
- [19] A. Palumbo, I. Castellano, and A. Napolitano, "Ovothiol: a potent natural antioxidant from marine organisms," in *Blue Biotechnology: Production and Use of Marine Molecules. Part 2: Marine Molecules for Disease Treatment/Prevention and for Biological Research*, S. Barre and S. S. Bates, Eds., pp. 583–610, Wiley VCH, Weinheim, Germany, 2018.
- [20] I. Castellano and F. P. Seebeck, "On ovothiol biosynthesis and biological roles: from life in the ocean to therapeutic potential," *Natural Product Reports*, 2018.
- [21] E. Turner, R. Klevit, L. J. Hager, and B. M. Shapiro, "Ovothiols, a family of redox-active mercaptohistidine compounds from marine invertebrate eggs," *Biochemistry*, vol. 26, no. 13, pp. 4028–4036, 1987.
- [22] T. P. Holler and P. B. Hopkins, "Ovothiols as biological antioxidants. The thiol groups of ovothiol and glutathione are chemically distinct," *Journal of the American Chemical Society*, vol. 110, no. 14, pp. 4837–4838, 1988.
- [23] B. Shapiro, "The control of oxidant stress at fertilization," *Science*, vol. 252, no. 5005, pp. 533–536, 1991.
- [24] E. Turner, L. Hager, and B. Shapiro, "Ovothiol replaces glutathione peroxidase as a hydrogen peroxide scavenger in sea urchin eggs," *Science*, vol. 242, no. 4880, pp. 939–941, 1988.
- [25] A. Palumbo, M. d'Ischia, G. Misuraca, and G. Prota, "Isolation and structure of a new sulphur-containing aminoacid from sea urchin eggs," *Tetrahedron Letters*, vol. 23, no. 31, pp. 3207–3208, 1982.

- [26] A. Palumbo, G. Misuraca, M. d'Ischia, F. Donaudy, and G. Prota, "Isolation and distribution of 1-methyl-5-thiol-L-histidine disulphide and a related metabolite in eggs from echinoderms," *Comparative Biochemistry and Physiology*, vol. 78, no. 1, pp. 81–83, 1984.
- [27] F. Rossi, G. Nardi, A. Palumbo, and G. Prota, "5-thiolhistidine, a new amino acid from eggs of *Octopus vulgaris*," *Comparative Biochemistry and Physiology*, vol. 80, no. 4, pp. 843–845, 1985.
- [28] E. C. O'Neill, M. Trick, L. Hill et al., "The transcriptome of *Euglena gracilis* reveals unexpected metabolic capabilities for carbohydrate and natural product biochemistry," *Molecular BioSystems*, vol. 11, no. 10, pp. 2808–2820, 2015.
- [29] J. Vamecq, P. Maurois, P. Bac et al., "Potent mammalian cerebroprotection and neuronal cell death inhibition are afforded by a synthetic antioxidant analogue of marine invertebrate cell protectant ovolthiols," *The European Journal of Neuroscience*, vol. 18, no. 5, pp. 1110–1120, 2003.
- [30] I. Castellano, P. di Tomo, N. di Pietro et al., "Anti-inflammatory activity of marine ovolthiol A in an *in vitro* model of endothelial dysfunction induced by hyperglycemia," *Oxidative Medicine and Cellular Longevity*, vol. 2018, Article ID 2087373, 12 pages, 2018.
- [31] G. Russo, M. Russo, I. Castellano, A. Napolitano, and A. Palumbo, "Ovolthiol isolated from sea urchin oocytes induces autophagy in the Hep-G2 cell line," *Marine Drugs*, vol. 12, no. 7, pp. 4069–4085, 2014.
- [32] R. Issa, X. Zhou, N. Trim et al., "Mutation in collagen-1 that confers resistance to the action of collagenase results in failure of recovery from CCl₄-induced liver fibrosis, persistence of activated hepatic stellate cells, and diminished hepatocyte regeneration," *The FASEB Journal*, vol. 17, no. 1, pp. 47–49, 2003.
- [33] J. B. King, M. B. West, P. F. Cook, and M. H. Hanigan, "A novel, species-specific class of uncompetitive inhibitors of gamma-glutamyl transpeptidase," *The Journal of Biological Chemistry*, vol. 284, no. 14, pp. 9059–9065, 2009.
- [34] C. Jacob, "A scent of therapy: pharmacological implications of natural products containing redox-active sulfur atoms," *Natural Product Reports*, vol. 23, no. 6, pp. 851–863, 2006.
- [35] T. P. Holler, F. Ruan, A. Spaltenstein, and P. B. Hopkins, "Total synthesis of marine mercaptohistidines: ovolthiols A, B, and C," *The Journal of Organic Chemistry*, vol. 54, no. 19, pp. 4570–4575, 1989.
- [36] A. Mirzahosseini, S. Hosztafi, G. Tóth, and B. Noszá, "A cost-effective synthesis of enantiopure ovolthiol A from L-histidine, its natural precursor," *ARKIVOC*, vol. 2014, no. 6, 2014.
- [37] S. Daunay, R. Lebel, L. Farescour, J. C. Yadan, and I. Erdelmeier, "Short protecting-group-free synthesis of 5-acetylsulfanyl-histidines in water: novel precursors of 5-sulfanyl-histidine and its analogues," *Organic & Biomolecular Chemistry*, vol. 14, no. 44, pp. 10473–10480, 2016.
- [38] Y. Tang, Y. Masuo, Y. Sakai et al., "Localization of xenobiotic transporter OCTN1/SLC22A4 in hepatic stellate cells and its protective role in liver fibrosis," *Journal of Pharmaceutical Sciences*, vol. 105, no. 5, pp. 1779–1789, 2016.
- [39] B. Halliwell, I. K. Cheah, and R. M. Y. Tang, "Ergothioneine - a diet-derived antioxidant with therapeutic potential," *FEBS Letters*, 2018.
- [40] S. Dominici, A. Visvikis, L. Pieri et al., "Redox modulation of NF- κ B nuclear translocation and DNA binding in metastatic melanoma. The role of endogenous and γ -glutamyl transferase-dependent oxidative stress," *Tumori*, vol. 89, no. 4, pp. 426–433, 2003.
- [41] S. Dominici, A. Paolicchi, A. Corti, E. Maellaro, and A. Pompella, "Prooxidant reactions promoted by soluble and cell-bound γ -glutamyltransferase activity," *Methods in Enzymology*, vol. 401, pp. 484–501, 2005.
- [42] Y. Yu, Y. Fan, Z. Yang, Y. Lu, Q. Xu, and X. Chen, "Elevated serum gamma-glutamyltransferase predicts advanced histological liver damage in chronic hepatitis B," *Discovery Medicine*, vol. 21, no. 113, pp. 7–14, 2016.

Research Article

Protective Effects of Aqueous Extracts of *Flos loniceræ Japonicæ* against Hydroquinone-Induced Toxicity in Hepatic L02 Cells

Yanfang Gao,¹ Huanwen Tang,² Liang Xiong,¹ Lijun Zou,¹ Wenjuan Dai,^{1,3} Hailong Liu,^{1,3} and Gonghua Hu¹ 

¹Department of Preventive Medicine, Gannan Medical University, 1 Yixueyuan Road, Ganzhou, 341000 Jiangxi, China

²Department of Environmental and Occupational Health, Dongguan Key Laboratory of Environmental Medicine, School of Public Health, Guangdong Medical University, Dongguan, 523808 Guangdong, China

³Department of Occupational Health and Toxicology, School of Public Health, Nanchang University, BaYi Road 461, Nanchang, 3300061 Jiangxi, China

Correspondence should be addressed to Gonghua Hu; hgh0129@163.com

Received 20 June 2018; Revised 21 August 2018; Accepted 4 October 2018; Published 18 November 2018

Academic Editor: Daniele Vergara

Copyright © 2018 Yanfang Gao et al. This is an open access article distributed under the Creative Commons Attribution License, which permits unrestricted use, distribution, and reproduction in any medium, provided the original work is properly cited.

Hydroquinone (HQ) is widely used in food stuffs and is an occupational and environmental pollutant. Although the hepatotoxicity of HQ has been demonstrated both *in vitro* and *in vivo*, the prevention of HQ-induced hepatotoxicity has yet to be elucidated. In this study, we focused on the intervention effect of aqueous extracts of *Flos loniceræ Japonicæ* (FLJ) on HQ-induced cytotoxicity. We demonstrated that HQ reduced cell viability in a concentration-dependent manner by administering 160 $\mu\text{mol/L}$ HQ for 12 h as the positive control of cytotoxicity. The aqueous FLJ extracts significantly increased cell viability and decreased LDH release, ALT, and AST in a concentration-dependent manner compared with the corresponding HQ-treated groups in hepatic L02 cells. This result indicated that aqueous FLJ extracts could protect the cytotoxicity induced by HQ. HQ increased intracellular MDA and LPO and decreased the activities of GSH, GSH-Px, and SOD in hepatic L02 cells. In addition, aqueous FLJ extracts significantly suppressed HQ-stimulated oxidative damage. Moreover, HQ promoted DNA double-strand breaks (DSBs) and the level of 8-hydroxy-2'-deoxyguanosine and apoptosis. However, aqueous FLJ extracts reversed HQ-induced DNA damage and apoptosis in a concentration-dependent manner. Overall, our results demonstrated that the toxicity of HQ was mediated by intracellular oxidative stress, which activated DNA damage and apoptosis. The findings also proved that aqueous FLJ extracts exerted protective effects against HQ-induced cytotoxicity in hepatic L02 cells.

1. Introduction

Hydroquinone (HQ) is a ubiquitous environmental chemical in cosmetics, medicines, the environment, and human diet; HQ can be metabolized from benzene as potentially hematotoxic, genotoxic, and carcinogenic compounds [1]. Humans are exposed to HQ through various channels, including oral administration, inhalation, and through the skin [2, 3]. Although the effects of HQ exposure on human health have been extensively studied and reported, the actual mechanisms of such effects remain unclear. The involved mechanisms trigger oxidative stress, which causes DNA damage,

mutation in cellular transformation, *in vivo* tumorigenesis, gene toxicity, and epigenetic changes [1, 4–8]. In our previous experiments, HQ induced apoptosis in hepatic L02 cells by changing the cellular redox status by reducing the cellular thiol level and increasing the cellular reactive oxygen species (ROS) level. In addition, ROS can lead to DNA damage by breaking DNA or producing lipid peroxidation in the membrane, thereby increasing the degrees of apoptosis and necrosis of L02 hepatocytes [1, 9–11]. These findings indicated that HQ can damage L02 hepatocytes through a series of oxidative stress reactions, so it is possible to use some antioxidants for reducing HQ toxicity.

Flos loniceræ Japonicæ (FLJ) is the flower of *Lonicera japonica Thunb.*, which is widely planted in China [12]. FLJ is used worldwide as a popular traditional herbal medicine with various pharmacological activities [13, 14]. In traditional Chinese medicine, FLJ is typically used to treat common colds and fevers. FLJ exerts various effects, such as antioxidant, anti-inflammatory, antihyperlipidemic, and anticancer [15–18]. In addition, FLJ protects cells against hydrogen peroxide-induced apoptosis by phosphorylating MAPKs and PI3K/Akt. FLJ is believed to dispel noxious heat from the blood and neutralize poisonous effects. FLJ significantly increases blood neutrophil activity and promotes neutrophil phagocytosis at appropriate concentrations [12]. Some investigators posited that the methanol extract of FLJ induces protective effects against rat hepatic injuries caused by carbon tetrachloride and aqueous extracts of FLJ flowers may act as therapeutic agents for inflammatory disease through the selective regulation of NF- κ B activation in rat liver [19]. FLJ is characterized by high biomass, easy cultivation, extensive competitive ability, wide geographic distribution, and strong resistance to environmental stresses, including bacterial, viral, and oxidative stresses [20]. However, the protective effects of aqueous FLJ extracts against HQ-induced cytotoxicity have not been demonstrated.

In this study, we examined the protective effects of aqueous FLJ extracts against HQ-induced cytotoxicity and their involvement in oxidative stress, DNA damage, and apoptosis. For this reason, we investigated the MDA and LPO levels as indexes of lipid peroxidation; the activities of SOD, GSH, and GSH-Px as antioxidant enzymes; DNA double-strand breaks (DSBs) and 8-hydroxy-2'-deoxyguanosine (8-OHdG) level as specific markers of oxidative damage of DNA; HQ-induced apoptosis; and the cytoprotective effect of aqueous FLJ extracts in hepatic L02 cells.

2. Materials and Methods

2.1. Chemicals. HQ, 3-(4,5-dimethylthiazol-2-yl)2,5-diphenyl-tetrazolium bromide (MTT), Hoechst33258, low-melting agarose (LMA), normal-melting agarose (NMA), 8-OHdG, deoxyguanosine (dG), and propidium iodide (PI) were purchased from Sigma (St. Louis, MO, USA). Fetal bovine serum (FBS) and RPMI-1640 medium were acquired from HyClone (Logan, UT, USA). Penicillin-streptomycin for the cell culture and trypsin were procured from Gibco/Invitrogen (Carlsbad, CA, USA). Other chemicals and reagents were of the highest analytical grade and bought from Sangon Biotech Co. Ltd. (Shanghai, China).

2.2. Plant Material and Preparation of Extract. The aqueous FLJ extracts were prepared by adopting the standard method used for treating patients with liver disease in traditional Chinese medicine. In brief, dried FLJ fruits (100 g) were boiled in 500 mL of distilled water for 3 h. The total extract was centrifuged at 5000 rcf for 30 min. The supernatant was filtered with filter paper, and the residue was further extracted twice under the same conditions. The filtrates were evaporated to dryness under vacuum and weighed. The final yield was 12.5% (w/w). The lyophilized extract was dissolved

in distilled water to produce a final concentration of 100 g/mL FLJ extract, which was stored at -20°C .

2.3. Cell Lines and Culture. The immortalized human normal hepatocyte L02 cell line was provided by Dr. Zhixiong Zhuang (Shenzhen Center for Disease Control and Prevention, Guangdong, China). L02 cells were cultured in RPMI-1640 medium supplemented with 10% (v/v) heat-inactivated FBS and antibiotic supplement (100 U/mL of penicillin and 100 $\mu\text{g}/\text{mL}$ of streptomycin) in a humidified incubator at 37°C under 95% air and 5% CO_2 . After each specified treatment time of incubation, the cells were harvested for further analysis.

2.4. Assessment of L02 Cell Viability. The cell viability of L02 cells was determined by MTT assay. The cells were seeded into 96-well flat-bottomed plates overnight at 37°C under 5% CO_2 and immediately treated with HQ (5, 10, 20, 40, 80, and 160 μM) for 6, 12, 24, and 48 h; 160 $\mu\text{mol}/\text{L}$ HQ was administered for 12 h as the positive control of oxidative damage. The samples were classified under five groups, namely, control (without HQ and FLJ), 160 $\mu\text{mol}/\text{L}$ HQ, 0.25 g/mL FLJ + HQ, 0.50 g/mL FLJ + HQ, and 1.00 g/mL FLJ + HQ for 12 h. Subsequently, 20 μL of MTT solution (5 mg/mL) was added to the culture medium for 4 h before the end of the treatment time to allow the formation of formazan crystals. The supernatant was discarded, and 100 μL of cell lysis buffer (50% DMF, 20% SDS, pH 4.6–4.7) was added to dissolve the intracellular crystalline formazan products. After constant and gentle shaking for 10 min at room temperature, the absorbance was recorded at 570 nm. Cell viability was calculated using the equation cellular relative viability = $(\text{OD}_{\text{treated wells}} - \text{OD}_{\text{blank}}) / (\text{OD}_{\text{control wells}} - \text{OD}_{\text{blank}})$.

2.5. Measurement of Intracellular Cytotoxicity and Oxidative Damage. The toxic effect of HQ in hepatic L02 cells was estimated in terms of LDH release and the activities of ALT and AST by using commercial kits (Nanjing Jiancheng Bioengineering Institute, China) in accordance with the manufacturer's protocol.

Commercial kits (Nanjing Jiancheng Bioengineering Institute, China) were utilized to assess the activities of SOD, GSH-Px, and GSH and the levels of MDA and LPO. The activities of SOD, GSH-Px, and GSH were expressed as units/milligram of protein. MDA and LPO contents were expressed as nmol/milligram of protein. The protein concentration was estimated using a BCA kit.

2.6. DNA Damage Assay. DNA damage was determined by the following assays. (i) DNA damage was evaluated using alkaline single-cell gel electrophoresis (comet assay). In brief, after 24 h of exposure, followed by washing with PBS, a 1.2×10^5 cell suspension was mixed with 0.8% LMA at 37°C and spread on a fully frosted microscope slide precoated with 0.65% NMA. After the agarose solidified, the slide was covered with another 75 μL of 0.8% LMA and then immersed in lysis solution (2.5 M NaCl, 100 mM Na_2EDTA , 10 mM Tris base, 1% Triton-X 100, 10% DMSO, pH 10) for 2 h at 4°C . The slides were placed in a gel-electrophoresis apparatus containing 300 mM NaOH and 1 mM Na_2EDTA (pH 13) for 30 min at 4°C

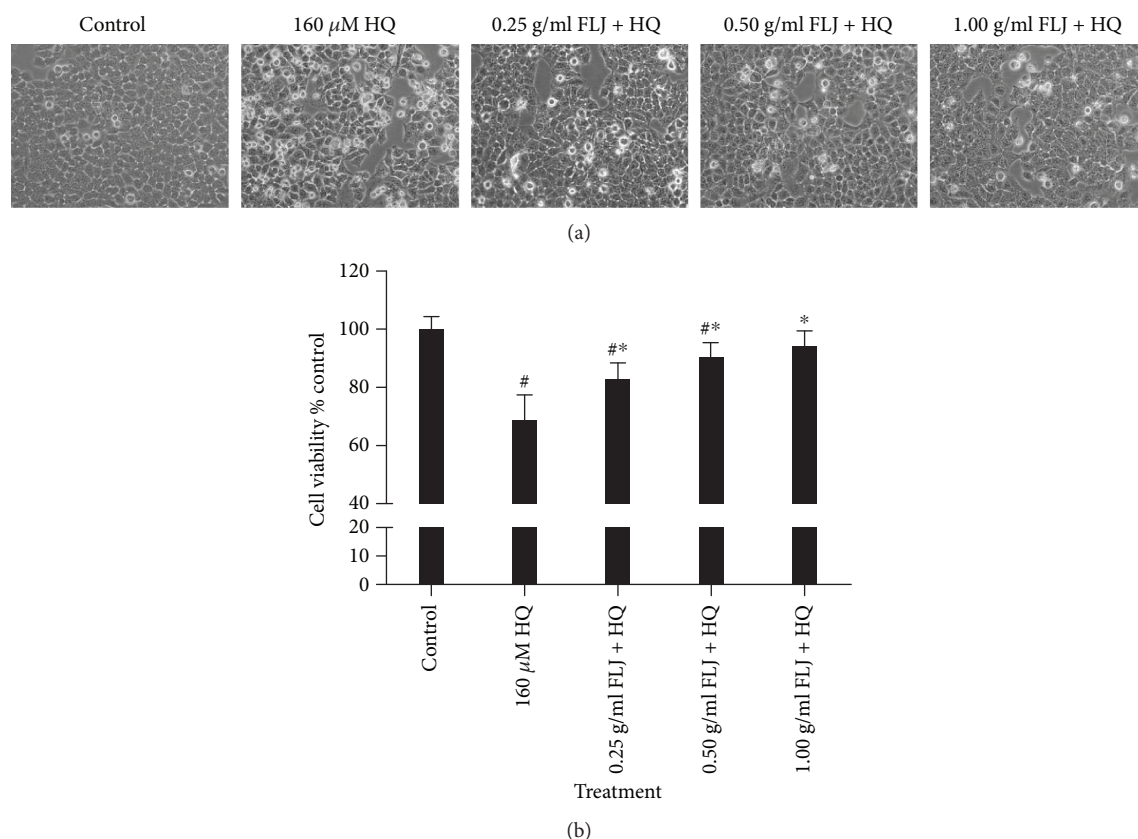


FIGURE 1: Protective effects of aqueous FLJ extracts against HQ-induced cytotoxicity (a) L02 cells treated with 0 and 160 μ M HQ and 0.25, 0.50, and 1.00 g/mL FLJ + HQ for 12 h. Morphological features of L02 cells were observed by inverted microscope. (b) L02 cells treated with 0 and 160 μ M HQ and 0.25, 0.50, and 1.00 g/mL FLJ + HQ for 12 h. Cell proliferation was detected by using the MTT proliferating reagent. All data were representative of at least three independent experiments. # $P < 0.05$ compared with the control. * $P < 0.05$ compared with 160 μ M HQ treatment.

to allow DNA unwinding and alkali labile damage. Electrophoresis was performed at 25 V (300 mA) and 4°C for 20 min. Subsequently, all slides were washed three times with a neutralizing buffer (0.4 M Tris, pH 7.5) for 5 min each time and stained with 80 μ L of PI (5 μ g/mL). A total of 100 randomly chosen cells (comets) were visually scored using a fluorescence microscope (Nikon Eclips TE-S, Japan) equipped with an excitation filter of 515–560 nm and a barrier filter of 590 nm. The “tail length and tail moment” of each comet were calculated using casp-1.2.2 analysis software. (ii) 8-OHdG was evaluated by high-performance liquid chromatography with electrochemical detection (HPLC-ECD) [21]. In brief, genomic DNA was extracted using a Genomic DNA Purification Kit in 500 μ g hydrolyzed DNA samples through the nuclease P1 and alkaline phosphatase hydrolysis of DNA. The samples were then filtered through 0.22 μ m nylon filters. 8-OHdG and dG levels were measured by using HPLC-ECD and HPLC with variable wavelength detector (HPLC-UV) systems as previously described. About 100 μ L of final hydrolysates was analyzed by HPLC-ECD with reverse phase-C18 (RP-C18) analytical column as the column. The mobile phase consisted of 50 mM KH_2PO_4 buffer (pH 5.5 and containing 10% methanol). The separations were performed at a flow rate of

1 mL/min. The amount of 8-OHdG in DNA was calculated as the number of 8-OHdG molecules/ 10^6 unmodified dG molecules.

2.7. Apoptosis Assay. Apoptosis was assessed by flow cytometry using PI assay. In brief, the cells were incubated in RPMI 1640 with 10% FBS. The cells consisted of the control group, the group treated with 160 μ M HQ, and the group coincubated in the absence or presence of FLJ (0.25, 0.50, and 1.00 g/mL) for 12 h. Subsequently, the cells were washed with cold PBS and incubated with PI (0.5 μ g) for 20 min at room temperature in the dark. The cells were immediately analyzed on a FACSCanto II flow cytometer (Becton and Dickinson, San Jose, CA, USA), and data from 10,000 events were obtained. The results were expressed as the percentage of cells labeled with PI (apoptotic).

2.8. Statistical Analysis. All data are presented as the mean \pm standard deviation (SD). Statistical evaluation of data analysis was performed using SPSS 16.0 for Windows. The differences between the mean values of multiple groups were analyzed by one-way ANOVA, followed by SNK test. $P < 0.05$ was considered statistically significant.

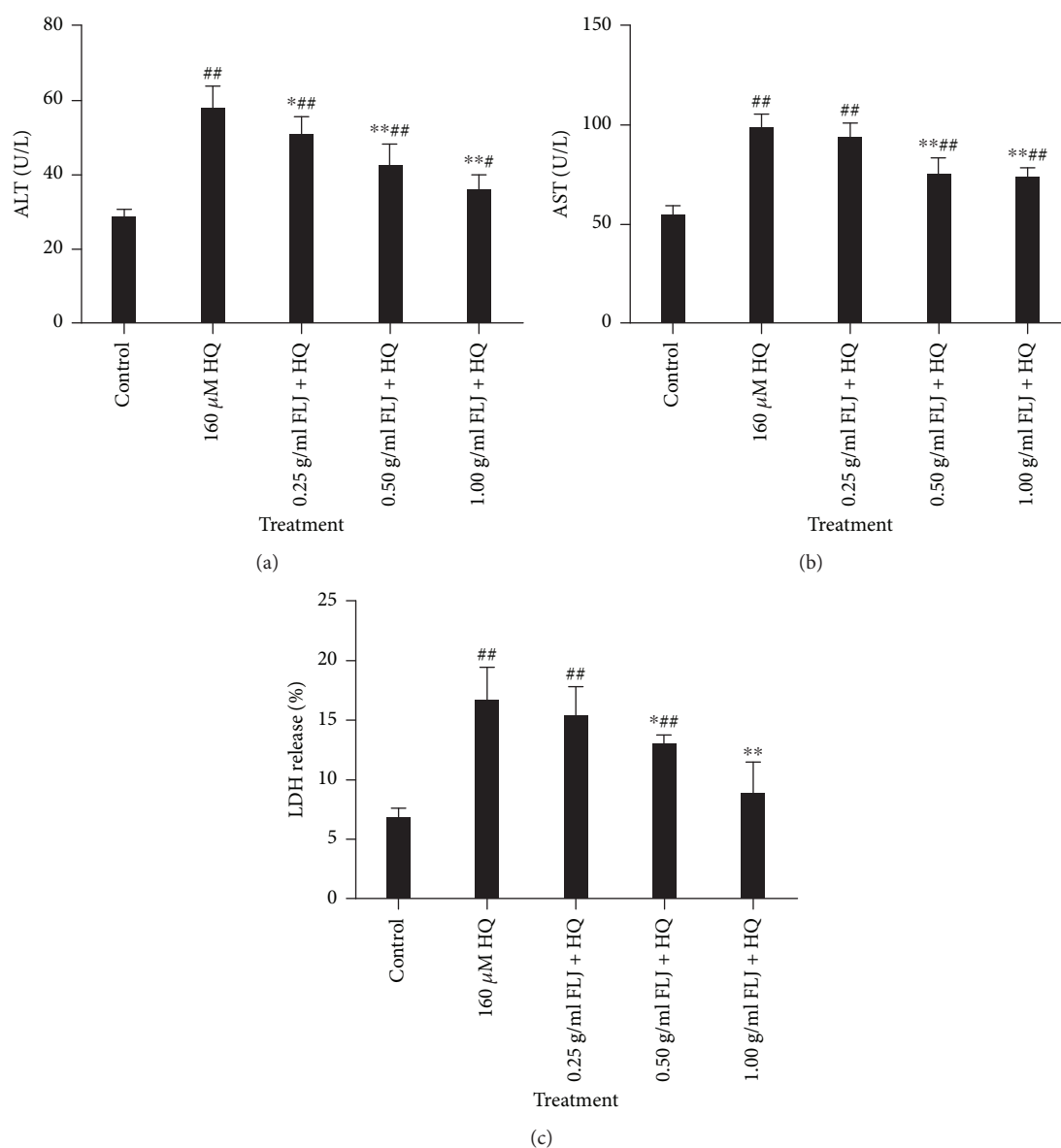


FIGURE 2: Protective effects of aqueous FLJ extracts against HQ-induced cytotoxicity L02 cells treated with 0 and 160 μM HQ and 0.25, 0.50, and 1.00 g/mL FLJ + HQ for 12 h. LDH release and the activities of aminotransferase (ALT) and aspartate aminotransferase (AST) were detected by using commercial kits. All data were representative of at least three independent experiments. # $P < 0.05$ compared with the control. * $P < 0.05$ compared with 160 μM HQ treatment.

3. Results

3.1. Protective Effects of Aqueous FLJ Extracts against HQ-Induced Cytotoxicity. As the first step in determining the necessary HQ concentration to induce cytotoxicity, the viability of L02 cells was assessed by MTT assay. HQ induced a concentration- and time-dependent reduction in L02 cell viability compared with untreated control cells. We administered 160 $\mu\text{mol/L}$ HQ for 12 h as the positive control of cytotoxicity. After 12 h of coexposure to aqueous FLJ extracts at the specified concentrations, the cell significantly increased compared with that in the corresponding HQ-treated groups (Figures 1(a) and 1(b)). These results revealed that aqueous FLJ extracts intervened the HQ-induced cytotoxicity.

To evaluate the protective effects of aqueous FLJ extracts against HQ, we examined cytotoxicity in terms of the LDH release and the ALT and AST levels. The results showed that aqueous FLJ extracts significantly downregulated LDH release, ALT, and AST in a concentration-dependent manner compared with the corresponding HQ-treated groups (Figure 2). Thus, aqueous FLJ extracts could reverse HQ-induced cytotoxicity.

3.2. Protective Effects of Aqueous FLJ Extracts against HQ-Induced Cellular Oxidative Damage. Oxidative stress can mediate apoptosis in various cell models and is considered an important apoptotic signal. Therefore, we investigated whether intracellular oxidative damage is involved in HQ-

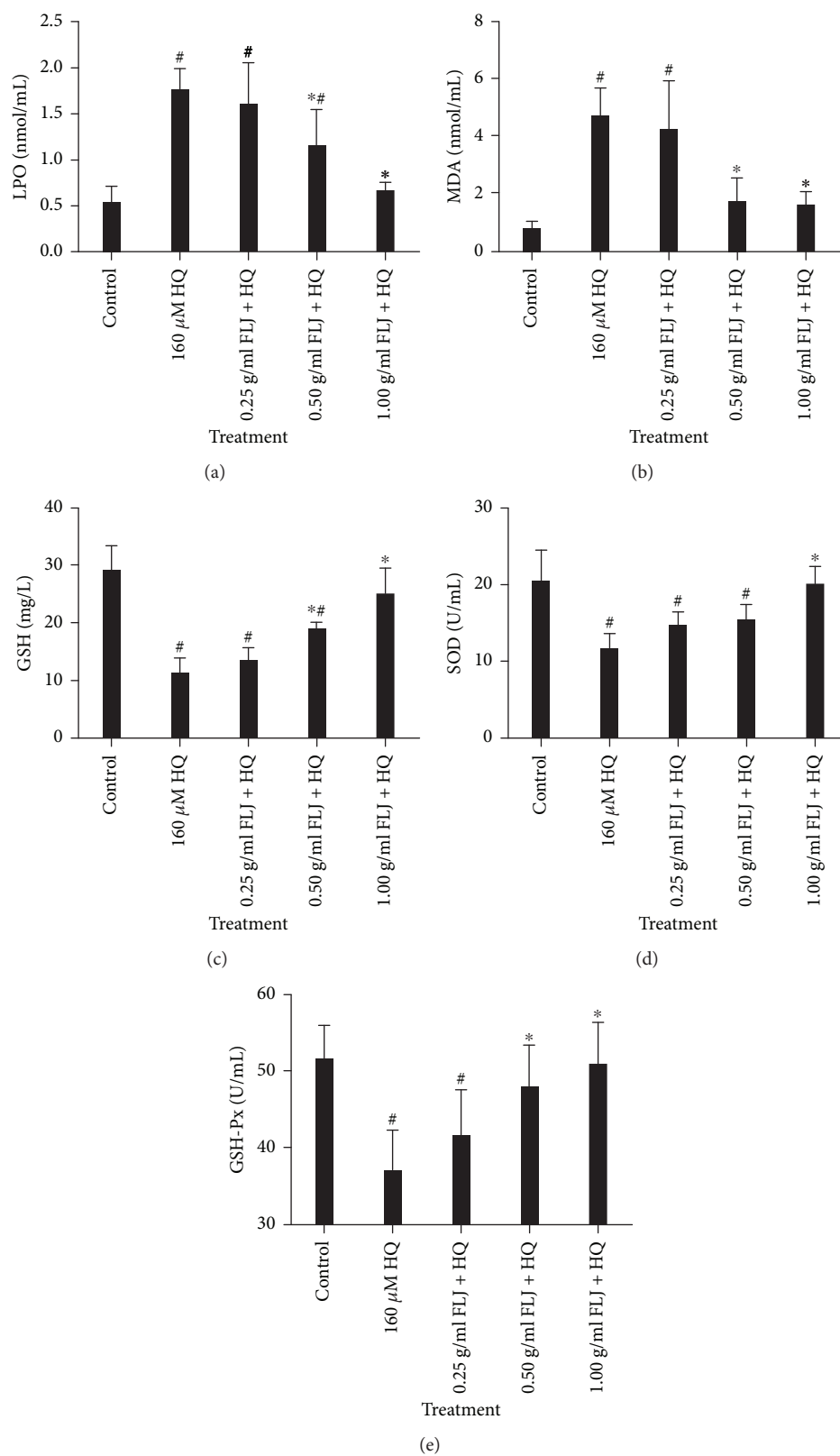


FIGURE 3: Protective effects of aqueous FLJ extracts against HQ-induced oxidative damage L02 cells treated with 0 and 160 μ M HQ and 0.25, 0.50, and 1.00 g/mL FLJ + HQ for 12 h. MDA and LPO levels as the indexes of lipid peroxidation and the SOD, GSH, and GSH-Px activities as antioxidant enzymes were detected by using commercial kits for oxidative stress. All data were representative of at least three independent experiments. [#] $P < 0.05$ compared with the control. ^{*} $P < 0.05$ compared with 160 μ M HQ treatment.

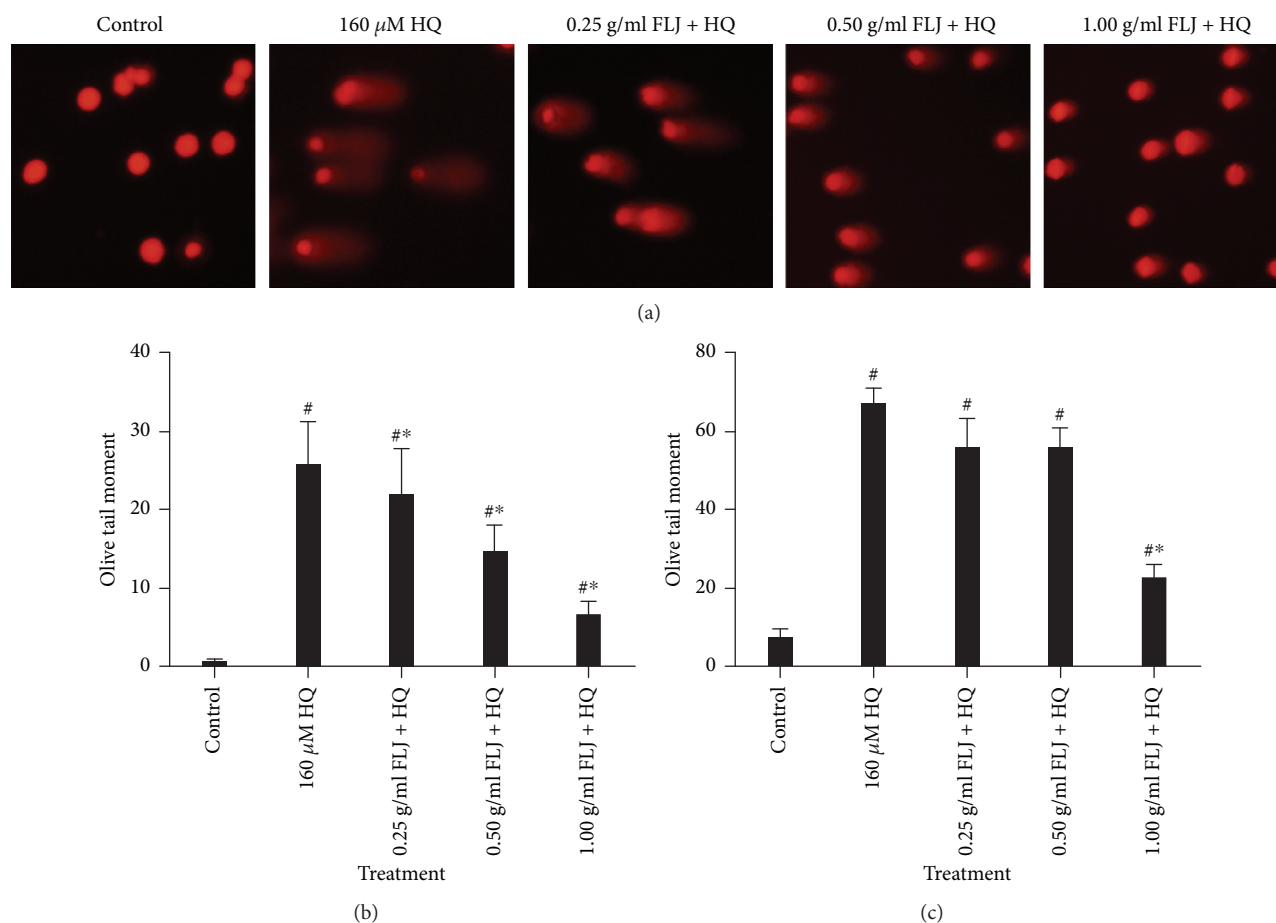


FIGURE 4: Protective effects of aqueous FLJ extracts against HQ-induced DNA damage (a, b) L02 cells treated with 0 and 160 μ M HQ and 0.25, 0.50, and 1.00 g/mL FLJ + HQ for 12 h. DNA damage was evaluated by alkaline single-cell gel electrophoresis (comet assay). (c) L02 cells treated with 0 and 160 μ M HQ and 0.25, 0.50, and 1.00 g/mL FLJ + HQ for 12 h. 8-Hydroxy-2'-deoxyguanosine (8-OHdG) level as a specific marker of oxidative damage of DNA. 8-OHdG was evaluated using high-performance liquid chromatography with electrochemical detection (HPLC-ECD). All data were representative of at least three independent experiments. [#] $P < 0.05$ compared with the control. ^{*} $P < 0.05$ compared with 160 μ M HQ treatment.

induced cell death and found that HQ exposure increased MDA and LPO production, but aqueous FLJ extracts reduced the production of MDA and LPO in a concentration-dependent manner. In addition, aqueous FLJ extracts reversed the production of antioxidant enzymes (such as GSH, SOD, and GSH-Px), indicating that aqueous FLJ extracts exerted a protective effect against HQ-induced oxidative stress in L02 cells (Figure 3).

3.3. Protective Effects of Aqueous FLJ Extracts against HQ-Induced DNA Damage. To elucidate the protective effects of aqueous FLJ extracts against HQ-induced DNA damage, L02 cells were exposed to various treatments: 0 and 160 μ M HQ and 0.25, 0.5, and 1.0 g/mL FLJ + HQ for 12 h. DNA damage was assessed. We performed comet assay, which is a commonly used indicator of genomic instability and genotoxic exposure. As shown in Figure 4(a), HQ induced a marked increase in DNA damage. However, aqueous FLJ extracts significantly decreased DNA damage compared with the corresponding HQ-treated groups as measured in terms of the tail moment and tail length. To further validate our

findings regarding the protective effects of aqueous FLJ extracts against HQ-induced DNA damage, we used HPLC-ECD to measure the level of 8-OHdG, which is a widely used marker of oxidative DNA damage. The results revealed a concentration-dependent decrease in 8-OHdG levels in the samples treated with aqueous FLJ extracts (Figure 4(b)), implying that aqueous FLJ extracts exerted a protective effect against HQ-induced DNA damage.

3.4. Protective Effects of Aqueous FLJ Extracts against HQ-Induced Apoptosis. Given that apoptosis is regulated by oxidative stress and DNA damage, the apoptosis rate in the L02 cells was also investigated by flow cytometry using PI assay. The apoptosis rate significantly decreased in the HQ-intoxicated L02 cells compared with that in the control. To further evaluate whether the protective effect of aqueous FLJ extracts on the L02 cells involves cell apoptosis, the L02 cells were incubated with aqueous FLJ extracts and HQ, and the apoptosis rate was then assessed. The results revealed that the apoptosis rate of the group exposed to both aqueous FLJ extracts and HQ was lower than that of the HQ group,

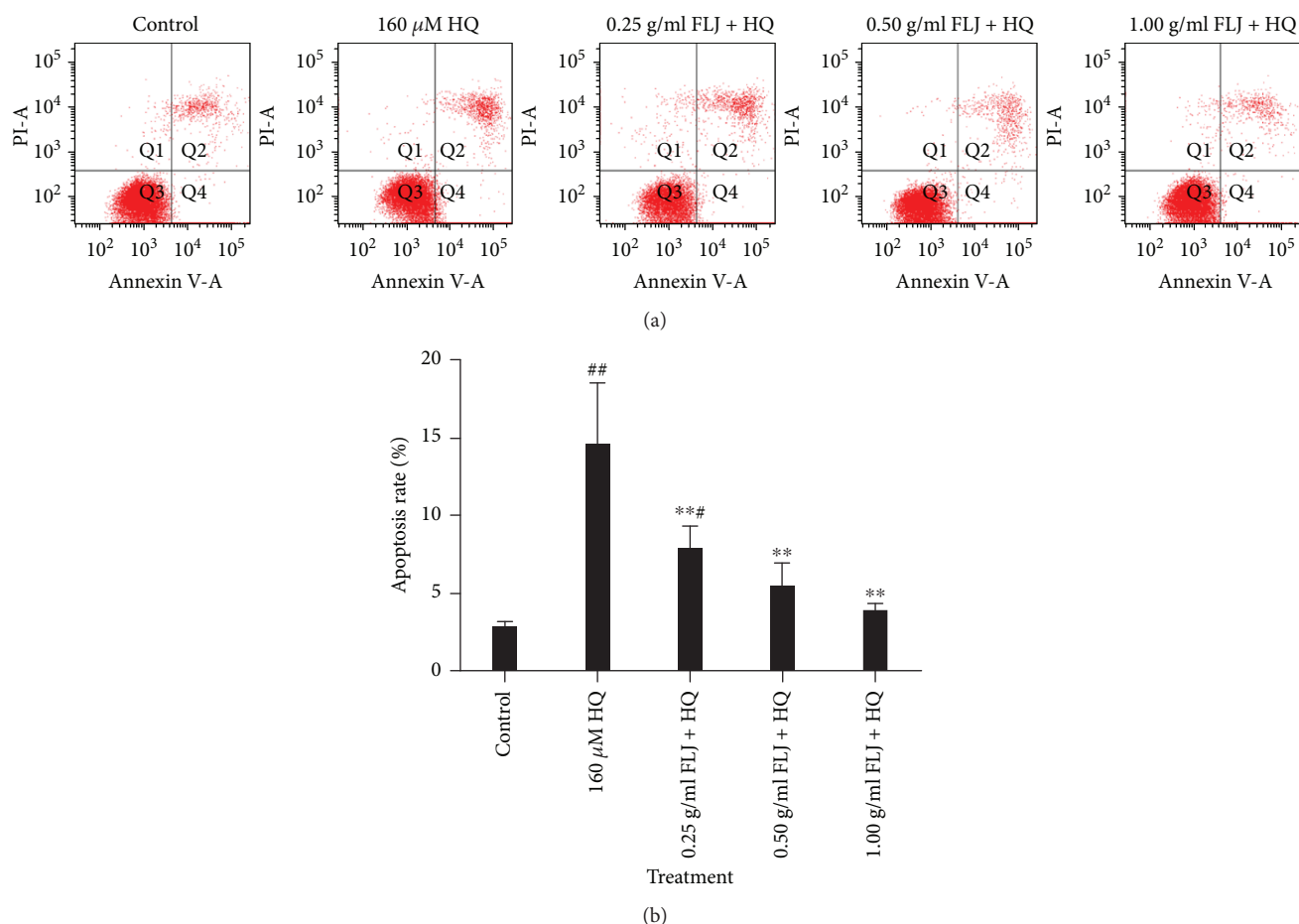


FIGURE 5: Protective effects of aqueous FLJ extracts against HQ-induced apoptosis in L02 cells treated with 0 and 160 μ M HQ and 0.25, 0.50, and 1.00 g/mL FLJ + HQ for 12 h. Apoptosis was assessed by flow cytometry using propidium iodide (PI) assay. All data were representative of at least three independent experiments. # $P < 0.05$ compared with the control. * $P < 0.05$ compared with 160 μ M HQ treatment.

indicating that aqueous FLJ extracts played an important role in reducing apoptosis in HQ-exposed L02 cells (Figure 5).

4. Discussion

HQ is a well-known toxicant of liver and induces many effects on the hepatic system. Although many studies have explored HQ, the actual mechanisms underlying these effects remain poorly understood. FLJ, which is also known as *Jinyinhua* or *Japanese honeysuckle*, is the dried flower bud or open flower of *Lonicera japonica Thunb* [22]. It is one of the most popular traditional Chinese medicines, and it has been applied in the healthcare of China and other East Asian countries for a long time. It has been proven to display antioxidant, antiviral, anticarcinogenic, anti-inflammatory, analgesic, antipyretic, and antimicrobial functions [23]. This study focused on the protective effects of aqueous FLJ extracts against HQ-induced cytotoxicity.

Serum ALT and AST levels are used as biochemical markers of liver damage, as the membrane destruction of hepatocytes releases hepatic enzymes, such as ALT and AST, into blood circulation [24]. The water extracts of FLJ containing 20% chlorogenic acid are protective against

alcohol-induced chemical liver injury in mice [12, 24], which was similar to the protection conferred by aqueous FLJ extracts to the L02 hepatic cell model induced by HQ.

Oxidative stress plays a critical role in the development of drug-induced liver damage [25] and in HQ-induced toxicity. Intercellular ROS may cause detrimental alterations in cell membranes, DNA, and other cellular structures. ROS are critical intermediates under normal physiological conditions that contribute to pathophysiological events in liver injury. Intracellular oxidative stress balance is crucial in maintaining normal cellular function in response to exogenous and endogenous factors [26]. MDA is a key marker of lipid peroxidation. The progression of liver damage was correlated with oxidative stress, as confirmed by MDA measurements [27]. FLJ polyphenol extracts were protective against the lipid peroxidation of erythrocyte and lipid membranes [28]. Consistent with the literature, the levels of MDA and LPO in our study were significantly higher in the HQ-treated group than in the controls. The levels of MDA and LPO concentrations were lower in aqueous FLJ extracts than in the HQ group.

The primary antioxidant defense systems include SOD and the GSH redox cycle [29]. SOD, which is produced from the mitochondrion electron transfer chain and scavenges

superoxide anions, is an important antioxidant enzyme. SOD can transform superoxide anions into H_2O_2 and catalase and then continuously detoxify them to H_2O [30]. The GSH redox cycle, which mainly includes GSH and GPx, modulates the redox-mediated responses of hepatic cells induced by external or intracellular stimulation. GSH is the main non-enzymatic regulator of intracellular redox homeostasis. GSH directly scavenges hydroxyl radicals and is a cofactor in detoxifying hydrogen peroxide, lipid peroxides, and alkyl peroxides. GPx, which is a selenocysteine-containing enzyme, reduces lipid hydroperoxides to their corresponding alcohols and hydrogen peroxide to water in the liver. Therefore, enhancing the hepatic antioxidant system capacity may be an effective therapeutic strategy for alleviating and treating liver damage [25]. Our study showed that the cytotoxicity of HQ is mediated by intracellular oxidative stress and confirmed the protective effects exerted by aqueous FLJ extracts as an antioxidant against HQ-induced cytotoxicity in L02 cells.

DNA damage is caused by multiple factors, including oxidative stress, vitamin B12 deficiency, and ischemia-reperfusion injury [31]. The ratio of 8-OHdG/dG is correlated with the severity of oxidative stress. The high activity of an antioxidant enzyme may be a compensatory regulation in response to increased oxidative stress. In our previous study, we demonstrated that DNA damage is related to HQ-induced hepatotoxicity [11]. ROS causes oxidative stress, which leads to DNA damage. Cells have evolved elaborate mechanisms to respond to DNA damage, at the core of which is the signaling pathway known as the DNA damage checkpoint [32]. This pathway initiates many aspects of the DNA damage response (DDR), including activation of DNA repair and induction of apoptosis [33, 34]. DNA damage is an early event in DDR. Thus, we examined DNA damage through the comet assay and 8-OHdG level, which is a specific marker of oxidative damage of DNA. In different kinds of cells, HQ induces the production of superoxides and hydroperoxides, which are implicated in the initiation and promotion stages of apoptosis and DNA damage. In the present study, although HQ induced DNA damage and apoptosis, we observed a concentration-dependent reverse in 8-OHdG levels, DDBs in the nucleus, and apoptosis in the group treated with aqueous FLJ extracts.

In conclusion, the results of this study strongly suggested that aqueous FLJ extracts played a role in protecting against HQ-induced cytotoxicity. On the basis of our results, we suggest a possible mechanism involved in the protective effects of aqueous FLJ extracts against HQ-induced cytotoxicity. HQ induced MDA and LPO formation, which activated antioxidant enzyme production. Intracellular oxidative stress balance was disturbed, thereby inducing DNA damage and apoptosis and promoting HQ-induced cytotoxicity. However, aqueous FLJ extracts could increase the activation of the antioxidant, which may reduce DNA damage and apoptosis and exert a protective effect against HQ-induced cytotoxicity. The molecular mechanism could further elucidate the antioxidant role of aqueous FLJ extracts.

Abbreviations

DDR:	DNA-damage response
HQ:	Hydroquinone
MDA:	Malondialdehyde
LPO:	Lipid peroxidation
ROS:	Reactive oxygen species
FLJ:	Flos <i>Lonicerae Japonicae</i>
LDH:	Lactic dehydrogenase
ALT:	Alanine transaminase
AST:	Aspartate aminotransferase
PI:	Propidium iodide
HPLC-EC:	High-performance liquid chromatography with electrochemical
DSBs:	DNA double-strand breaks
8-OHdG:	8-hydroxy-2'-deoxyguanosine.

Data Availability

The data used to support the findings of this study are included within the article.

Conflicts of Interest

The authors declare no conflict of interest.

Authors' Contributions

Yanfang Gao, Huanwen Tang, and Liang Xiong contributed equally to this work.

Acknowledgments

This work was supported by grants from National Natural Science Foundation of China (81460504, 81260434, 81273116, and 81060241), the Traditional Chinese Medicine Scientific Research Project funded by the Health Department of Jiangxi Province (2009A074), the Science and Technology Project funded by the Education Department of Jiangxi Province (GJJ13689, GJJ170862), the Natural Science Foundation of Jiangxi Province (20132BAB205071, 20114BAB205041, and 20142BAB215014), and supported by Doctor Initial Funding for Gannan Medical University (QD201302 and QD201701).

References

- [1] S. Chen, H. Liang, G. Hu et al., "Differently expressed long noncoding RNAs and mRNAs in TK6 cells exposed to low dose hydroquinone," *Oncotarget*, vol. 8, no. 56, pp. 95554–95567, 2017.
- [2] C. B. Hebeda, F. J. Pinedo, S. M. Bolonheis et al., "Intracellular mechanisms of hydroquinone toxicity on endotoxin-activated neutrophils," *Archives of Toxicology*, vol. 86, no. 11, pp. 1773–1781, 2012.
- [3] S. H. Inayat-Hussain, H. A. Ibrahim, E. L. Siew et al., "Modulation of the benzene metabolite hydroquinone induced toxicity: evidence for an important role of *fau*," *Chemico-Biological Interactions*, vol. 184, no. 1-2, pp. 310–312, 2010.

- [4] F. J. Enguita and A. L. Leitao, "Hydroquinone: environmental pollution, toxicity, and microbial answers," *BioMed Research International*, vol. 2013, Article ID 542168, 14 pages, 2013.
- [5] Z. Li, C. Wang, J. Zhu et al., "The possible role of liver kinase B1 in hydroquinone-induced toxicity of murine fetal liver and bone marrow hematopoietic stem cells," *Environmental Toxicology*, vol. 31, no. 7, pp. 830–841, 2016.
- [6] J. Liu, Q. Yuan, X. Ling et al., "PARP-1 may be involved in hydroquinone-induced apoptosis by poly ADP-ribosylation of ZO-2," *Molecular Medicine Reports*, vol. 16, no. 6, pp. 8076–8084, 2017.
- [7] J. Zhu, H. Wang, S. Yang et al., "Comparison of toxicity of benzene metabolite hydroquinone in hematopoietic stem cells derived from murine embryonic yolk sac and adult bone marrow," *PLoS One*, vol. 8, no. 8, article e71153, 2013.
- [8] H. Bahadar, F. Maqbool, S. Mostafalou et al., "The molecular mechanisms of liver and islets of Langerhans toxicity by benzene and its metabolite hydroquinone *in vivo* and *in vitro*," *Toxicology Mechanisms and Methods*, vol. 25, no. 8, pp. 628–636, 2015.
- [9] G. H. Hu, Z. X. Zhuang, H. Y. Huang, L. Yu, J. H. Yuan, and L. Q. Yang, "Effect of hydroquinone on expression of ubiquitin-ligating enzyme Rad18 in human L-02 hepatic cells," *Zhonghua Lao Dong Wei Sheng Zhi Ye Bing Za Zhi*, vol. 27, no. 4, pp. 222–225, 2009.
- [10] G. H. Hu, Z. X. Zhuang, H. Y. Huang, L. Yu, L. Q. Yang, and W. D. Ji, "Relationship between polymerase eta expression and DNA damage-tolerance in human hepatic cells by hydroquinone," *Zhonghua Yu Fang Yi Xue Za Zhi*, vol. 43, no. 1, pp. 56–60, 2009.
- [11] G. Hu, H. Huang, L. Yang et al., "Down-regulation of Polh expression leads to increased DNA damage, apoptosis and enhanced S phase arrest in L-02 cells exposed to hydroquinone," *Toxicology Letters*, vol. 214, no. 2, pp. 209–217, 2012.
- [12] Y. Nam, J. M. Lee, Y. Wang, H. S. Ha, and U. D. Sohn, "The effect of *Flos Lonicerae Japonicae* extract on gastro-intestinal motility function," *Journal of Ethnopharmacology*, vol. 179, pp. 280–290, 2016.
- [13] Y. P. Guo, L. G. Lin, and Y. T. Wang, "Chemistry and pharmacology of the herb pair *Flos Lonicerae japonicae*-*Forsythiae fructus*," *Chinese Medicine*, vol. 10, no. 1, p. 16, 2015.
- [14] W. Zhou, A. Yin, J. Shan, S. Wang, B. Cai, and L. Di, "Study on the rationality for antiviral activity of *Flos Lonicerae Japonicae*-*Fructus Forsythiae* herb couple preparations improved by chito-oligosaccharide via integral pharmacokinetics," *Molecules*, vol. 22, no. 4, p. 654, 2017.
- [15] Y. Yang, L. Wang, Y. Wu et al., "On-line monitoring of extraction process of *Flos Lonicerae Japonicae* using near infrared spectroscopy combined with synergy interval PLS and genetic algorithm," *Spectrochimica Acta Part A: Molecular and Biomolecular Spectroscopy*, vol. 182, pp. 73–80, 2017.
- [16] W. Zhou, J. Shan, S. Wang, B. Cai, and L. di, "Transepithelial transport of phenolic acids in *Flos Lonicerae Japonicae* in intestinal Caco-2 cell monolayers," *Food & Function*, vol. 6, no. 9, pp. 3072–3080, 2015.
- [17] S. T. Kao, C. J. Liu, and C. C. Yeh, "Protective and immunomodulatory effect of *flos Lonicerae japonicae* by augmenting IL-10 expression in a murine model of acute lung inflammation," *Journal of Ethnopharmacology*, vol. 168, pp. 108–115, 2015.
- [18] Y. Li, W. Cai, X. Weng et al., "*Lonicerae Japonicae* Flos and *Lonicerae* Flos: a systematic pharmacology review," *Evidence-Based Complementary and Alternative Medicine*, vol. 2015, Article ID 905063, 16 pages, 2015.
- [19] B. C. Y. Cheng, H. Yu, H. Guo et al., "A herbal formula comprising *Rosae Multiflorae Fructus* and *Lonicerae Japonicae* Flos, attenuates collagen-induced arthritis and inhibits TLR4 signalling in rats," *Scientific Reports*, vol. 6, no. 1, article 20042, 2016.
- [20] J. W. Kang, N. Yun, H. J. Han, J. Y. Kim, J. Y. Kim, and S. M. Lee, "Protective effect of *Flos Lonicerae* against experimental gastric ulcers in rats: mechanisms of antioxidant and anti-inflammatory action," *Evidence-Based Complementary and Alternative Medicine*, vol. 2014, Article ID 596920, 11 pages, 2014.
- [21] Y. Kaya, A. Çebi, N. Söylemez, H. Demir, H. H. Alp, and E. Bakan, "Correlations between oxidative DNA damage, oxidative stress and coenzyme Q10 in patients with coronary artery disease," *International Journal of Medical Sciences*, vol. 9, no. 8, pp. 621–626, 2012.
- [22] J. Li, Y. Wang, J. Xue, P. Wang, and S. Shi, "Dietary exposure risk assessment of flonicamid and its effect on constituents after application in *Lonicerae Japonicae* Flos," *Chemical and Pharmaceutical Bulletin*, vol. 66, no. 6, pp. 608–611, 2018.
- [23] Z. Hu, C. Lausted, H. Yoo et al., "Quantitative liver-specific protein fingerprint in blood: a signature for hepatotoxicity," *Theranostics*, vol. 4, no. 2, pp. 215–228, 2014.
- [24] S. E. Fomenko, N. F. Kushnerova, V. G. Sprygin, and T. V. Momot, "Hepatorotective activity of honeysuckle fruit extract in carbon tetrachloride intoxicated rats," *Eksperimental'naia i Klinicheskaia Farmakologija*, vol. 77, no. 10, pp. 26–30, 2014.
- [25] J. Arauz, E. Ramos-Tovar, and P. Muriel, "Redox state and methods to evaluate oxidative stress in liver damage: from bench to bedside," *Annals of Hepatology*, vol. 15, no. 2, pp. 160–173, 2016.
- [26] C. Wang, J. D. Harwood, and Q. Zhang, "Oxidative stress and DNA damage in common carp (*Cyprinus carpio*) exposed to the herbicide mesotrione," *Chemosphere*, vol. 193, pp. 1080–1086, 2018.
- [27] S. Ullah, Z. Li, Z. Hasan, S. U. Khan, and S. Fahad, "Malathion induced oxidative stress leads to histopathological and biochemical toxicity in the liver of rohu (*Labeo rohita*, Hamilton) at acute concentration," *Ecotoxicology and Environmental Safety*, vol. 161, pp. 270–280, 2018.
- [28] D. Bonarska-Kujawa, H. Pruchnik, S. Cyboran, R. Żyłka, J. Oszmiański, and H. Kleszczyńska, "Biophysical mechanism of the protective effect of blue honeysuckle (*Lonicera caerulea* L. var. *kamtschatica* Sevest.) polyphenols extracts against lipid peroxidation of erythrocyte and lipid membranes," *The Journal of Membrane Biology*, vol. 247, no. 7, pp. 611–625, 2014.
- [29] T. Fukai and M. Ushio-Fukai, "Superoxide dismutases: role in redox signaling, vascular function, and diseases," *Antioxidants & Redox Signaling*, vol. 15, no. 6, pp. 1583–1606, 2011.
- [30] Y. Nojima, K. Ito, H. Ono et al., "Superoxide dismutases, SOD1 and SOD2, play a distinct role in the fat body during pupation in silkworm *Bombyx mori*," *PLoS One*, vol. 10, no. 2, article e0116007, 2015.
- [31] Y. Nakabepu, K. Sakumi, K. Sakamoto, D. Tsuchimoto, T. Tsuzuki, and Y. Nakatsu, "Mutagenesis and carcinogenesis caused by the oxidation of nucleic acids," *Biological Chemistry*, vol. 387, no. 4, pp. 373–379, 2006.

- [32] C. Park, S. Hong, S. Shin et al., "Activation of the Nrf2/HO-1 signaling pathway contributes to the protective effects of *Sargassum serratifolium* extract against oxidative stress-induced DNA damage and apoptosis in SW1353 human chondrocytes," *International Journal of Environmental Research and Public Health*, vol. 15, no. 6, article 1173, 2018.
- [33] S. Khan, A. Zafar, and I. Naseem, "Copper-redox cycling by coumarin-di(2-picoly)amine hybrid molecule leads to ROS-mediated DNA damage and apoptosis: a mechanism for cancer chemoprevention," *Chemico-Biological Interactions*, vol. 290, pp. 64–76, 2018.
- [34] D. Liu, R. Li, X. Guo et al., "DNA damage regulated autophagy modulator 1 recovers the function of apoptosis-stimulating of p53 protein 2 on inducing apoptotic cell death in Huh7.5 cells," *Oncology Letters*, vol. 15, no. 6, pp. 9333–9338, 2018.

Review Article

Aberrant Metabolism in Hepatocellular Carcinoma Provides Diagnostic and Therapeutic Opportunities

Serena De Matteis,¹ Andrea Ragusa ,^{2,3} Giorgia Marisi,¹ Stefania De Domenico,⁴ Andrea Casadei Gardini ,⁵ Massimiliano Bonafè,^{1,6} and Anna Maria Giudetti ⁷

¹Biosciences Laboratory, Istituto Scientifico Romagnolo per lo Studio e Cura dei Tumori (IRST) IRCCS, Meldola, Italy

²Department of Engineering for Innovation, University of Salento, Lecce, Italy

³CNR Nanotec, Institute of Nanotechnology, via Monteroni, 73100 Lecce, Italy

⁴Italian National Research Council, Institute of Sciences of Food Production (ISPA), Lecce 73100, Italy

⁵Department of Medical Oncology, Istituto Scientifico Romagnolo per lo Studio e Cura dei Tumori (IRST) IRCCS, Meldola, Italy

⁶Department of Experimental, Diagnostic & Specialty Medicine, Alma Mater Studiorum, University of Bologna, Bologna, Italy

⁷Department of Biological and Environmental Sciences and Technologies, University of Salento, Lecce, Italy

Correspondence should be addressed to Anna Maria Giudetti; anna.giudetti@unisalento.it

Received 27 July 2018; Accepted 3 October 2018; Published 4 November 2018

Academic Editor: Javier Egea

Copyright © 2018 Serena De Matteis et al. This is an open access article distributed under the Creative Commons Attribution License, which permits unrestricted use, distribution, and reproduction in any medium, provided the original work is properly cited.

Hepatocellular carcinoma (HCC) accounts for over 80% of liver cancer cases and is highly malignant, recurrent, drug-resistant, and often diagnosed in the advanced stage. It is clear that early diagnosis and a better understanding of molecular mechanisms contributing to HCC progression is clinically urgent. Metabolic alterations clearly characterize HCC tumors. Numerous clinical parameters currently used to assess liver functions reflect changes in both enzyme activity and metabolites. Indeed, differences in glucose and acetate utilization are used as a valid clinical tool for stratifying patients with HCC. Moreover, increased serum lactate can distinguish HCC from normal subjects, and serum lactate dehydrogenase is used as a prognostic indicator for HCC patients under therapy. Currently, the emerging field of metabolomics that allows metabolite analysis in biological fluids is a powerful method for discovering new biomarkers. Several metabolic targets have been identified by metabolomics approaches, and these could be used as biomarkers in HCC. Moreover, the integration of different omics approaches could provide useful information on the metabolic pathways at the systems level. In this review, we provided an overview of the metabolic characteristics of HCC considering also the reciprocal influences between the metabolism of cancer cells and their microenvironment. Moreover, we also highlighted the interaction between hepatic metabolite production and their serum revelations through metabolomics researches.

1. Introduction

Hepatocellular carcinoma (HCC) is the most common type of primary liver cancer. It represents the fifth most common cancer worldwide and the second most frequent cause of cancer-related deaths [1]. HCC occurs most often in people with chronic liver diseases related to viral (chronic hepatitis B and C), toxic (alcohol and aflatoxin), metabolic (diabetes, hemochromatosis, and nonalcoholic fatty liver disease), and immune (autoimmune hepatitis and primary biliary) factors [1].

Effective management of HCC depends on early diagnosis and proper monitoring of the patients' response to therapy through the identification of pathways and mechanisms that are modulated during the process of tumorigenesis. In this context, the interest towards the concept of tumor metabolism is growing for several reasons: (i) metabolic alteration is a recognized hallmark of cancer, (ii) oncogenes drive alterations in cancer metabolism, (iii) metabolites can regulate gene and protein expressions, and (iv) metabolic proteins and/or metabolites represent diagnostic and prognostic biomarkers [2–6].

Metabolic alterations constitute a selective advantage for tumor growth, proliferation, and survival as they provide support to the crucial needs of cancer cells, such as increased energy production, macromolecular biosynthesis, and maintenance of redox balance. Although this is a common feature for all tumor types, it is still not completely clear how the tumor metabolic demand can really influence the metabolic profile and homeostasis of other tissues. Can they act as tumor bystanders or do they have an active role in supporting tumor growth? In this scenario, the liver represents a perfect metabolic model that governs body energy metabolism through the physiological regulation of different metabolites including sugars, lipids, and amino acids [7]. How can HCC metabolic alterations support tumor growth and influence systemic metabolism?

In this review, we take a detailed look at the alterations in intracellular and extracellular metabolites and metabolic pathways that are associated with HCC and describe the functional contribution on cancer progression and metabolic reprogramming of tumor microenvironment including immune cells. The analysis of circulating metabolites by metabolomics may provide us with novel data about this systemic crosstalk.

2. Reprogramming of Glucose Metabolism: Increased Uptake of Glucose and Lactate Production

In physiological conditions, the liver produces, stores, and releases glucose depending on the body's need for this substrate. After a meal, blood glucose enters the hepatocytes via the plasma membrane glucose transporter (GLUT). Human GLUT protein family includes fourteen members which exhibit different substrate specificities and tissue expression [8]. Once inside the cell, glucose is first converted, by glycolysis, into pyruvate and then completely oxidized into the mitochondrial matrix by the tricarboxylic acid (TCA) cycle and the oxidative phosphorylation. Alternatively, it can be channelled in the fatty acid synthesis pathway through the *de novo* lipogenesis (DNL). Glucose-6-phosphate dehydrogenase, the rate-limiting enzyme of the pentose phosphate pathway, is used in the liver to generate reduced nicotinamide adenine dinucleotide phosphate (NADPH) that is required for lipogenesis and biosynthesis of other bioactive molecules. In pathological conditions, glucose energy metabolism is altered. Important changes have been observed not only in the expression of specific transporters and enzyme isoforms but also in the flux of metabolites.

HCC tumors display a high level of glucose metabolism [9] (Figure 1). This enhanced metabolic demand is important for metabolic imaging and well supported by the ability of 18F-fluodeoxyglucose (18F-FDG) positron emission tomography (PET) to correlate with unfavorable histopathologic features [10] and with the proliferative activity of tumor [11]. Moreover, high glucose levels as observed in patients with diabetes can accelerate tumorigenesis in HCC cells by generating advanced glycation

end-products and O-GlcNAcylation of the Yes-associated protein (YAP) and c-Jun [12, 13].

The common feature of these alterations is an increased glucose uptake and production of lactate even in the presence of oxygen and fully functioning mitochondria (Warburg effect) [2, 3], but it is not correlated with enhanced gluconeogenesis as the expression of phosphoenolpyruvate carboxykinases 1 and 2 and fructose 1,6-bisphosphatase 1 (FBP1), has been reported to be downregulated in HCC [14]. Overall, this metabolic reprogramming promotes growth, survival, proliferation, and long-term maintenance [15]. To respond to this metabolic requirement, HCC tumors enhance glucose uptake [16] by upregulating GLUT1 and GLUT2 isoforms [17–19]. siRNA-mediated abrogation of GLUT1 expression inhibits proliferative and migratory potential of HCC cells [20], while GLUT2 overexpression was correlated to a worse prognosis [21, 22].

Once inside the cell, glucose is converted in glucose-6-phosphate (G6P) by the hexokinase (HK), which is the first enzyme of the glycolytic pathway. Five major hexokinase isoforms are expressed in mammalian tissues and denoted as HK1, HK2, HK3, HK4, and the isoform hexokinase domain containing 1 (HKDC1). HCC tumors express high levels of the HK2 isoform, and its expression is correlated with the pathological stage of the tumor [23, 24]. In HCC, HK2 knockdown inhibited the flux of glucose to pyruvate and lactate, increased oxidative phosphorylation, and sensitized to metformin [24]. Moreover, HK2 silencing also synergized with sorafenib to inhibit tumor growth in mice [24]. Interestingly, a new member of the HK family the isoform HKDC1 was upregulated in HCC tissues compared with the adjacent normal tissues. HCC patients with high expression levels of HKDC1 had poor overall survival. Silencing HKDC1 suppressed HCC cell proliferation and migration *in vitro*, probably by the repression of the Wnt/ β -catenin pathway [25].

The transition to glucose metabolism involves alterations in different glycolytic enzymes. A well-characterized example is the decreased expression of FBP1 [26]. FBP1 downregulation by promoter methylation and copy-number loss contributed to HCC progression by altering glucose metabolism [26]. An increased expression of glyceraldehyde-3-phosphate dehydrogenase (GAPDH) [27, 28] and pyruvate kinases 2 (PKM2) [9, 29, 30] was also described. The altered expression of these enzymes supports the flux of glucose in the glycolytic pathway leading to the generation of pyruvate that may be either used to generate lactate or be directed towards the TCA cycle. The high glutamine utilization and the high levels of lactate observed in HCC tissues are both in accordance with the first hypothesis, suggesting an increased TCA carbon anaplerosis in HCC cells [24, 31]. Glutamine represents the most abundant amino acid in blood and tissues and represents the major hepatic gluconeogenic substrate. A metabolic shift towards glutamine regulates tumor growth in HCC [14]. Hepatoma cells have an accelerated metabolism and net glutamine consumption, with potential implication at the systemic level [32].

Glutamine is metabolized in several distinct pathways. By glutaminolysis, glutamine can be converted to α -ketoglutarate

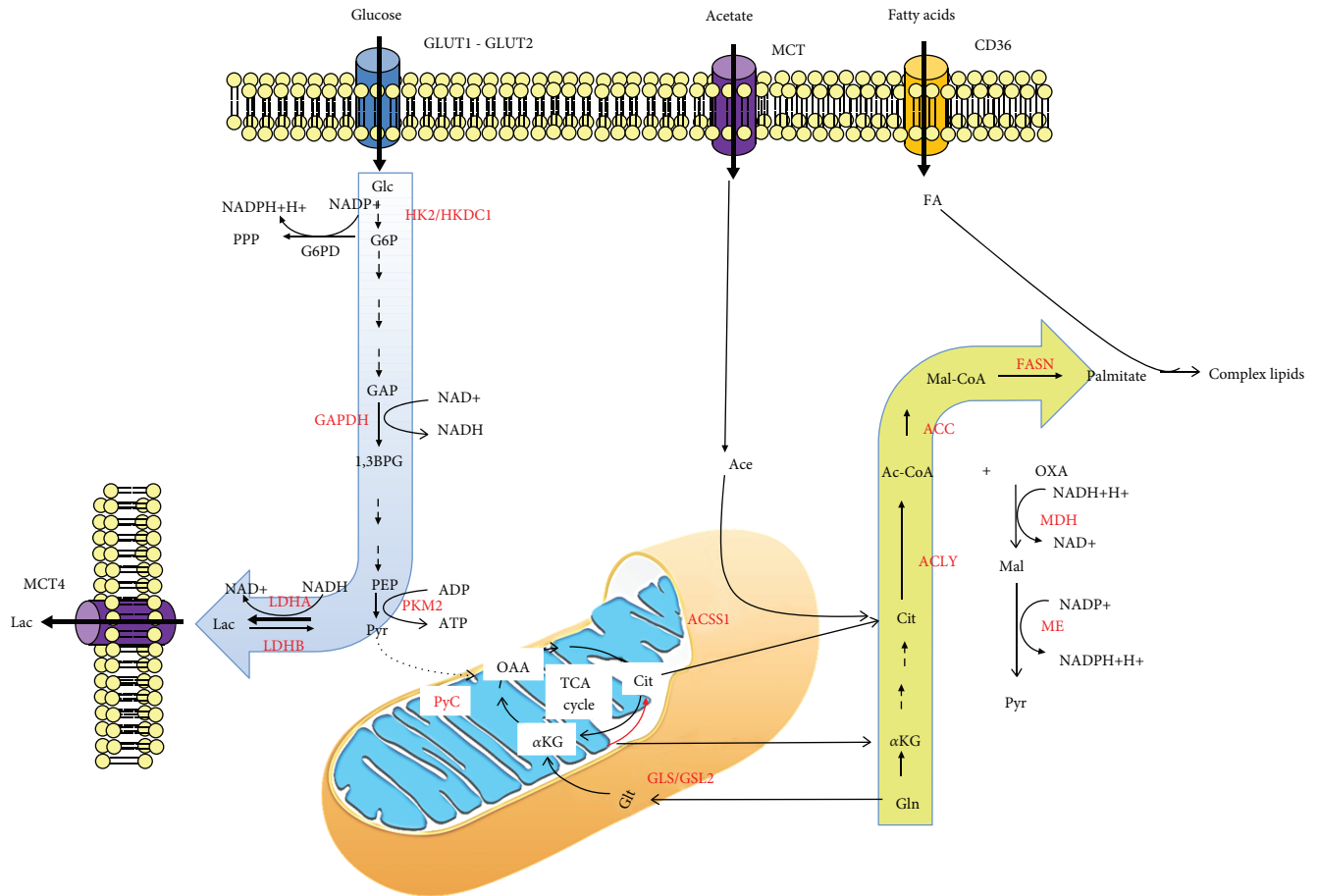


FIGURE 1: Metabolic reprogramming in HCC. Glucose enters the cancer cell via glucose transporters 1 and 2 (GLUT1 and GLUT2), and it is mainly used in the glycolytic pathway due to the overexpression of enzymes such as hexokinase 2 (HK2) and hexokinase domain containing 1 (HKDC1), glyceraldehyde-3-phosphate dehydrogenase (GAPDH), and pyruvate kinase 2 (PK2). The glycolytic pathway mainly produces, by the overexpression of lactate dehydrogenase A (LDHA) isoform, lactate (Lac) which is transported outside of the cell mainly throughout the monocarboxylate transporter isoform 4 (MCT4). Fatty acids enter cancer cells thanks to the upregulation of fatty acid translocase CD36. Nevertheless, fatty acid synthesis can also start from acetate (Ace), which is transported in the cell by MCT and converted into acetyl-CoA (Ac-CoA) by the mitochondrial isoform of acetyl-CoA synthase 1 (ACSS1). Moreover, glutamine (Gln) takes part in lipid synthesis after conversion into glutamate by mitochondrial glutaminase enzymes (GLS/GLS2). Glutamate is then converted into α -ketoglutarate (α KG) which can enter the tricarboxylic acid (TCA) cycle. Alternatively, α KG can undergo a reductive carboxylation by which it is transformed in citrate in the mitochondria (red arrow) or in the cytosol. In glutamine-free conditions, pyruvate (Pyr) can be converted into oxaloacetate (OAA) by the anaplerotic reaction catalysed by pyruvate carboxylase (PyC) enzyme. The *de novo* fatty acids synthesis is increased in cancer cells, and it is associated with a high expression of key enzymes such as acetyl-CoA carboxylase (ACC) and fatty acid synthase (FASN). This latter metabolic pathway is associated to a high production of reducing equivalents in the form of reduced nicotinamide adenine dinucleotide phosphate (NADPH) that is mainly produced in the first reaction of the pentose phosphate pathway (PPP) catalysed by glucose-6-phosphate dehydrogenase (G6PD) and by the malic enzyme (ME).

to replenish TCA cycle thus supporting energy production and providing intermediates for other biosynthetic pathways. By reductive carboxylation, glutamine moves in reverse of the TCA cycle from α -ketoglutarate to citrate to sustain lipid synthesis. So far, conflicting data have been reported on the role of glutamine in HCC. In fact, a study demonstrated that glutamine is metabolized mainly via glutaminolysis and not via reductive carboxylation to be converted into lactate [24]. Another study did not support this hypothesis as the great majority of enzymes involved in the conversion of glutamine to α -ketoglutarate were significantly downregulated in HCC compared to the normal liver [14]. This highlights the heterogeneous behaviour of this pathway that might be

influenced by specific conditions of the microenvironment or its correlation to specific genetic alterations. For instance, glutamine metabolism in HCC varied in relation to the initiating lesion. Mouse liver tumors induced by MYC overexpression significantly increased both glucose and glutamine catabolism, whereas MET-induced liver tumors used glucose to produce glutamine [33].

The metabolic reaction that generates lactate from pyruvate is catalysed by lactate dehydrogenase (LDH). In humans, five active LDH isoenzymes are present and each of which is a tetrameric enzyme composed of two major subunits, M and H (formally A and B), encoded by *Ldh-A* and *Ldh-B*, respectively. The M subunit is predominantly

found in the skeletal muscle, whereas the H subunit in the heart. LDHA and LDHB are upregulated in human cancers and associated with aggressive tumor outcomes [34–36].

In human HCC, LDHA expression was upregulated as a consequence of the downregulation of the microRNA-383 [37]. LDHA knockdown induced apoptosis and cell growth arrest in HCC cells and suppressed metastasis in a xenograft mouse model [38]. Serum LDH has been used as a prognostic indicator for patients with HCC treated with sorafenib, undergoing transcatheter arterial chemoembolization (TACE), or curative resection [39–42].

Lactate, the product of LDH activity, is exported in the extracellular milieu by monocarboxylate transporters (MCT). In HCC samples, an overexpression of MCT4 has been reported [43] and was also associated with Ki-67 expression [44]. Basigin, a transmembrane glycoprotein also called CD147, was found to be involved in the reprogramming of glucose metabolism in HCC cells. In particular, CD147 promoted glycolysis and facilitated the cell surface expression of MCT1 and lactate export [45]. Interestingly, blocking CD147 and/or MCT1 was reported to suppress HCC proliferation [45].

At a metabolic level, a high level of lactate with a low level of glucose was detected by nuclear magnetic resonance analysis in HCC samples [46]. This confirms the glycolytic shift toward lactate and provides a correlation between enzymatic alterations and metabolite expression [46]. The increased lactate concentration observed in the serum of HCC patients, compared to normal subjects, seems to be a consequence of this metabolic change [47]. However, the role of this secreted lactate still remains largely unclear. Nevertheless, increased lactate production was observed in patients with steatosis and steatohepatitis (NASH) compared to normal patients suggesting that the shift toward and anaerobic glucose metabolism can be involved in the first steps of liver carcinogenesis [48].

3. Altered Anabolic and Catabolic Lipid Pathways in HCC

The liver plays a key role in the metabolism of lipids and lipoproteins, and the anomalies in these metabolic pathways underlie HCC pathogenesis as demonstrated by increased risks observed in patients with obesity [49], diabetes [50], and hepatic steatosis [51]. After a carbohydrate rich meal, fatty acids can be synthesized from glycolytic pyruvate by *DNL*. Thus, entering the mitochondria, pyruvate is converted into acetyl-CoA by the pyruvate dehydrogenase enzyme. In the mitochondrial matrix, acetyl-CoA condenses with oxaloacetate to form citrate which, in conditions of high energetic charge, is conveyed to the cytoplasm throughout the citrate carrier for lipid synthesis. Key enzymes of cytosolic *DNL* are acetyl-CoA carboxylase (ACC), which catalyses the ATP-dependent carboxylation of acetyl-CoA to malonyl-CoA, and the multifunctional enzyme fatty acid synthase (FASN), which utilizes malonyl-CoA for synthesizing palmitoyl-CoA [52]. *DNL* also needs reducing power in the form of NADPH + H⁺, which is mainly generated through the glucose metabolism

in the pentose phosphate pathway and in the malic enzyme reaction. *DNL* alterations were observed in HCC samples [53] and in other liver diseases, including nonalcoholic fatty liver disease (NAFLD) [54]. A combinatorial network-based analysis revealed that many enzymes involved in *DNL*, as well as enzymes related to NADPH production, such as glucose-6-phosphate dehydrogenase and malic enzyme, were upregulated in HCC with respect to the noncancerous liver samples [14].

During cancer progression, an overexpression of FASN is important for promoting tumor cell survival and proliferation [54], and it was also associated with poor patient prognosis [55]. In line with what observed in other types of tumors, recent studies described a functional association among lipogenesis, FASN, sterol regulatory element-binding protein-1 (SREBP-1), a transcription factor regulating FASN expression, and HCC [56–64]. The therapeutic effects of targeting FASN were investigated in several works. For instance, HCC induced by AKT/c-Met was fully inhibited in FASN knockout mice [65].

Alternative carbon sources can support the generation of acetyl-CoA required for *DNL*. This can derive from exogenous acetate, which is transported into cells by members of the MCT family and then converted to acetyl-CoA by acetyl-CoA synthase enzymes (mitochondrial ACSS1 and ACSS3 or cytosolic ACSS2) to fuel fatty acid synthesis (Figure 1). Mitochondrial ACSS1 expression, but not ACSS2 or ACSS3 ones, is significantly upregulated in HCC compared to noncancerous liver and associated with increased tumor growth and malignancy under hypoxic conditions [14].

Tumors can be addicted or independent from *DNL* by the activation of complementary pathways. In fact, both *de novo* synthesized and exogenous fatty acids can support the growth of HCC tumors [66]. The studies performed on animal models demonstrated that the inhibition of lipogenesis via genetic deletion of ACC genes increased susceptibility to tumorigenesis in mice treated with the hepatocellular carcinogen diethylnitrosamine, demonstrating that lipogenesis is essential for liver tumorigenesis [67].

The liver is able to take up nonesterified fatty acids from the blood, in proportion to their concentration, either via specific transporters (fatty acid transport protein (FATP) or fatty acid translocase/CD36) or by diffusion. The activation of the CD36 pathway has been associated with tumor aggressiveness by the induction of the epithelial-mesenchymal transition (EMT) program [68], which is a process that contributes to cancer progression [69, 70]. This is mediated through the involvement of specific pathways. The analysis of the Cancer Genome Atlas (TCGA) dataset revealed a significant association between CD36 and EMT markers, potentially by the activation of Wnt and TGF- β signaling pathways [71].

The liver is able to oxidize fatty acids by both mitochondrial and peroxisomal β -oxidation. The entry of fatty acids into the mitochondria is regulated by the activity of the enzyme carnitine palmitoyltransferase-I (CPT-I) [72], which catalyses the synthesis of acylcarnitines from very long acyl-CoA and carnitine, thus allowing the entry of polar fatty

acids in the mitochondrial matrix. In a rat model of NASH, a decreased mitochondrial CPT-I activity [73] and dysfunction of both complex I and II of the mitochondrial respiratory chain [74] have been demonstrated. Moreover, deregulation of mitochondrial β -oxidation with downregulation of many enzymes involved in fatty acid oxidation has been reported in HCC patients [14]. Accordingly, the urinary level of short- and medium-chain acylcarnitines was found to be different in HCC vs. cirrhosis, and butyrylcarnitine (carnitine C4:0) was defined as a potential marker for distinguishing between HCC and cirrhosis [75]. All together, these data indicate that mitochondrial alterations can represent an early determinant in HCC.

The liver represents also a major site of synthesis and metabolism of endogenous cholesterol. The pool of cholesterol is tightly regulated, and it reflects the input of cholesterol from the diet, its biosynthesis, the secretion and uptake of cholesterol from plasma lipoproteins, the conversion of cholesterol into bile, and the reuptake of biliary cholesterol and bile acids from the intestine to the liver. The rate-limiting enzyme in the cholesterol synthesis is the 3-hydroxy-3-methylglutaryl-CoA reductase, which catalyses the synthesis of mevalonate.

There is increasing evidence that the mevalonate pathway is implicated in the pathogenesis of HCC [76, 77]. To this respect, clinical studies demonstrated that statins, widely used to reduce cholesterol levels, were able to reduce the risk of HCC [78] and showed antiproliferative effects *in vitro* on HepG2 cells and *in vivo* on rats with HCC [79]. Data from a meta-analysis report that the use of statins could significantly cut the risk of liver cancer and that fluvastatin is the most effective drug for reducing HCC risk compared to other statin interventions [80].

Cholesterol is also used in the liver for the synthesis of bile acids, which are hydroxylated steroids that, once secreted in the intestine, provide for solubilisation of dietary cholesterol, lipids, fat-soluble vitamins, and other essential nutrients, thus promoting their delivery to the liver. Primary bile acids, such as cholic acid and chenodeoxycholic acid, are synthesized in hepatocytes and can be conjugated to glycine or taurine [81]. Cholic acid conjugated to glycine, in the form of glycocholic acid, represents a secondary bile acid that is synthesized by microbiota in the small intestine [81]. It has been reported that intrahepatic bile acid may have a stimulatory effect of hepatic tumorigenesis [82] and abnormal bile acid metabolism has been correlated with HCC [83–86]. The hepatic deregulation of bile acid metabolism can result in increased serum level of glycolic acid, as reported by Guo and collaborators [87].

Modification in the activity of enzymes related to phospholipid remodelling has been reported in a rat model of cirrhosis [88]. Moreover, an altered lipid metabolism, including phospholipids, fatty acids, and bile metabolites, was observed in serum samples from HCC patients [89, 90]. In particular, higher phosphatidylcholines (PC) concentrations were observed in HCC patients at early and late stage compared to cirrhotic and control subjects, indicating

a disturbance of the phospholipid catabolism [85]. This result significantly correlated with higher levels of PC observed at tissue level [91].

4. Alterations in Amino Acid and Protein Metabolism Underlying HCC

The liver carries out many functions in protein metabolism. A broad spectrum of proteins responsible for the maintenance of hemostasis, oncotic pressure, hormone, lipid transport, and acute phase reactions are synthesized in the liver. Among these proteins, albumin is synthesized almost exclusively by the liver, and alone, it accounts for 40% of hepatic protein synthesis. Moreover, the liver is also able to synthesize thyroid-binding globulin, VLDL apoB 100, and complement.

A very recent work reports that patients with lower serum albumin levels have significantly larger maximum tumor diameters, greater prevalence of portal vein thrombosis, increased tumor multifocality, and higher α -fetoprotein levels with respect to patients with higher albumin levels. These data indicate that decreased serum albumin correlates with increased parameters of HCC aggressiveness, therefore, having a role in HCC aggressiveness [92].

In the liver, the synthesized nonessential amino acids (AA) play a pivotal role in the maintenance of diverse homeostatic functions such as gluconeogenesis. Both synthesized amino acids and those derived from the diet are utilized either for protein synthesis or catabolized (except branched chain amino acids) by transamination or oxidative deamination reactions. These processes produce keto acids that can be oxidized to produce energy in the form of ATP. Several enzymes used in these pathways (for example, alanine transaminase and aspartate transaminase) are commonly assayed in serum to assess liver damage. Moreover, the oxidative deamination of amino acids produces ammonium ions, a toxic product whose detoxification can either occur in extrahepatic tissues, throughout the synthesis of glutamine when combined with glutamate, or in the liver, to make urea which is then transported to the kidneys where it can be directly excreted in urine.

An increased AA metabolism is generally observed in human tumors, in line with the role of AA and enzymes responsible for their production in cancer initiation and progression [93–96]. The shift toward an increased amino acid production is considered as a consequence of the described altered glucose metabolism. In the condition of increased consumption of glucose by aerobic glycolysis, amino acids can be used as glucose precursors or activators of glycolytic enzymes [97].

An altered AA metabolism characterizes HCC compared to other liver diseases. For instance, serum levels of alanine, serine, glycine, cysteine, aspartic acid, lysine, methionine, tyrosine, phenylalanine, tryptophan, and glutamic acid were dramatically increased in HCC compared with healthy subjects, together with a lower ratio of branched-chain amino acids (valine, leucine, and isoleucine) to aromatic amino acids (tyrosine, phenylalanine, and tryptophan) [98, 99].

Furthermore, AA bioavailability not only contributes to anabolic and catabolic pathways but it is also essential during HCC pathogenesis by supporting cellular hypoxic responses [100].

5. Oxidative Metabolism Imbalance in HCC

Oxidative stress occurs when reactive oxygen species (ROS) production overwhelms the normal antioxidant capacity of cells [101]. ROS are short-lived and very reactive molecules that rapidly react with cellular biomolecules yielding oxidatively modified products that eventually lead to cell injury and death. Due to the high instability of ROS, they cannot be easily detected, and protein carbonyls, 8-hydroxydeoxyguanosine, and 4-hydroxynonenal (which are oxidatively modified products of proteins, DNA, and lipids, respectively) have been widely used as markers for oxidative stress [102].

Accumulating evidence suggests that many types of cancer cells have increased levels of oxidative stress and ROS production with respect to normal cells [103]. As a consequence of this, redox homeostasis is finely regulated in cancer cells with an underappreciated role in the control of cell signaling and metabolism. For instance, ROS-mediated inhibition of PKM2 allows cancer cells to sustain antioxidant responses by diverting glucose flux into the pentose phosphate pathway and increasing the production of reducing equivalents for ROS detoxification [104]. Understanding the mechanisms at the basis of ROS homeostasis might have therapeutic implications.

Oxidative damage is considered a key pathway in HCC progression and increases patient vulnerability for HCC recurrence [105]. Oxidative stress closely correlates with HCV- and NASH-related HCC, but relatively weakly with HBV-related HCC [106]. Moreover, it has been reported that NASH-related HCC patients had a diminished serum antioxidative function compared with nonalcoholic fatty liver disease patients [107].

Glutathione is a nonenzymatic tripeptide that plays a central role in the cellular antioxidant defense system, and it represents the most abundant antioxidant in hepatocytes. Glutathione is synthesized intracellularly from cysteine, glycine, and glutamate, and it is abundantly found in the cytosol and mitochondria and in a smaller percentage in the endoplasmic reticulum [108]. During glutathione antioxidant function, the reduced form of glutathione (GSH) is oxidized to the glutathione disulfide dimer (GSSG). The regeneration of the reduced form requires the enzymatic action of glutathione reductase and reducing equivalents in the form of NADPH + H⁺. A significant increase in all amino acids related to the GSH synthesis, including 5-oxoproline, was observed in the serum of HCC patients, and an increase of G6P that represents an important source of NADPH for the generation of GSH has been also reported [109]. Moreover, signs of DNA and lipid oxidative damages were found in HCC. Indeed, an increased level of 8-hydroxydeoxyguanosine was found in chronic hepatitis, corresponding to an increased risk of HCC [110, 111]. In addition, a mass spectrometry study highlighted an increased level of

4-hydroxynonenal in human tissues of HCC compared to peripheral noncancerous tissues [112].

The GSH:GSSG ratio is considered an important indicator of the redox balance in cells, with a higher ratio representing low oxidative stress [107]. Upon depletion of GSH, ROS induce oxidative stress which causes liver damage, and reduced GSH levels have been reported in various liver diseases [113]. By-products of GSH synthesis are represented by γ -glutamyl peptides that are biosynthesized through a reaction of ligation of glutamate with various amino acids and amines by the action of γ -glutamylcysteine synthetase. Serum level of γ -glutamyl peptides, measured by capillary chromatography-MS/MS, was increased in patients with virus-related HCC [114, 115], and it was considered a reliable potential biomarker for this pathology [115]. The 2-hydroxybutyric acid is another compound considered in relation to GSH metabolism. It is primarily produced in mammalian hepatic tissues, which catabolize threonine or synthesize glutathione. Under conditions of intense oxidative stress, hepatic glutathione synthesis is increased, and there is a high demand for cysteine. In such cases, homocysteine is diverted from the transmethylation pathway and instead it is used to produce cystathionine, which is then cleaved into cysteine and finally incorporated into glutathione. 2-Hydroxybutyric acid is then produced from reduction of α -ketobutyrate, which is released as a by-product of the cystathionine conversion to cysteine. An increased serum concentration of 2-hydroxybutyric acid as well as of xanthine, an intermediate in the purine degradation process producing H₂O₂, and several γ -glutamyl peptides, were found in HCC with respect to control subjects [116, 117].

6. Metabolic Reprogramming of HCC Microenvironment

HCC microenvironment consists of stromal cells, hepatic stellate cells, and endothelial and immune cells. The crosstalk between tumor cells and their surrounding microenvironment is required for sustaining HCC development by promoting angiogenesis, EMT, or by modulating the polarization of immune cells. Tumor-associated macrophages (TAM) and myeloid-derived suppressor cells (MDSC) are the major components of tumor-infiltrate and are abundant in HCC microenvironment (Figure 2) [118–120]. Metabolites released from tumor cells can have an impact on immune cells.

Inflammatory stimuli promote the switching of macrophages towards an M1-like phenotype characterized by the production of inflammatory cytokines. On the contrary, anti-inflammatory stimuli induce these cells to acquire an M2-like phenotype with immunosuppressive functions [121]. Thus, during chronic inflammation, macrophages predispose a given tissue to tumor initiation by releasing themselves factors that promote neoplastic transformation. In the successive phases of inflammation, the macrophage phenotype shifts more toward one that is immunosuppressive and supports tumor growth, angiogenesis, and metastasis [122]. In this respect, both epidemiological and clinical studies have demonstrated that various chronic

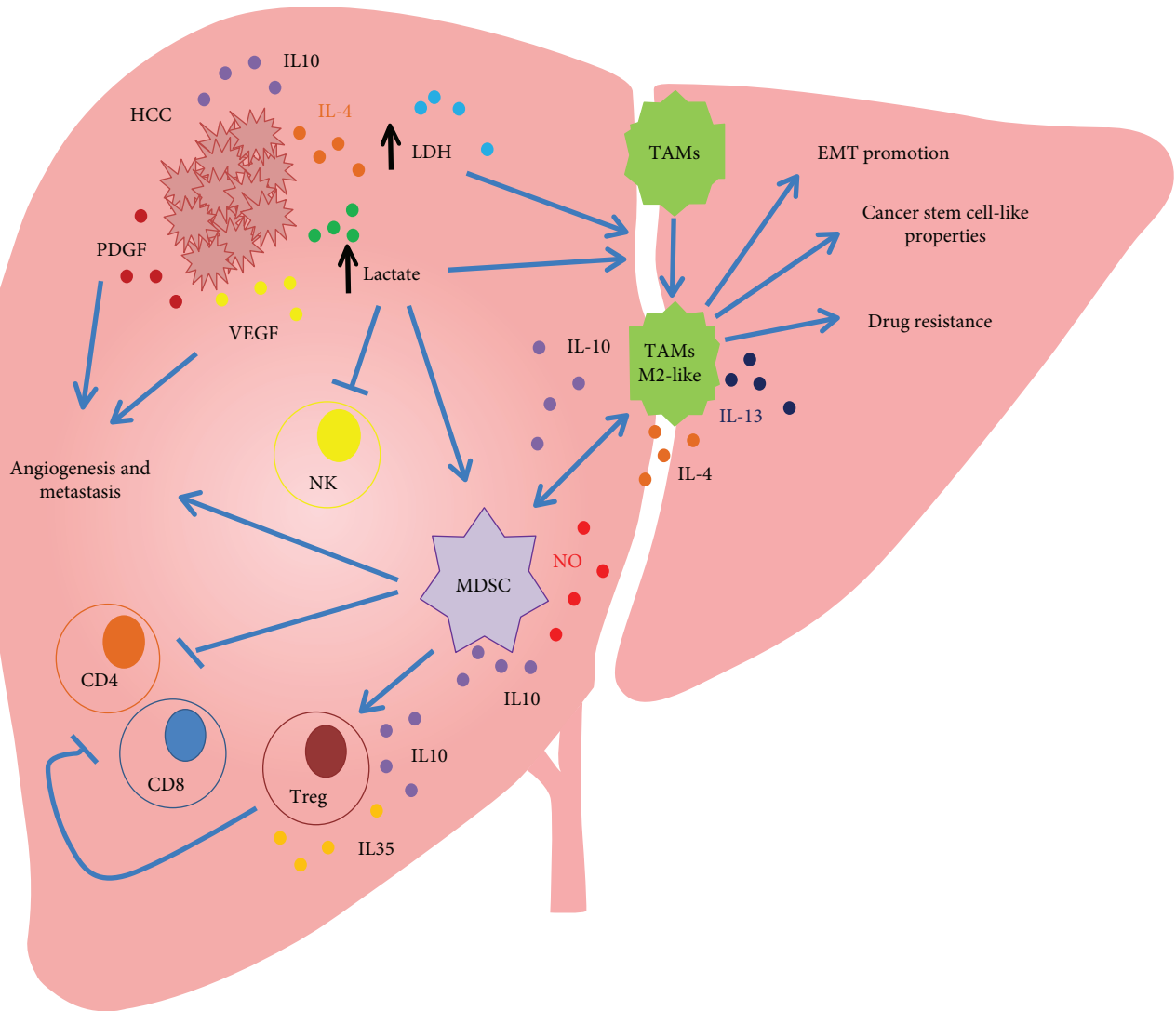


FIGURE 2: Metabolic connections between HCC and immune cells. Tumor-associated macrophages (TAM) and myeloid-derived suppressor cells (MDSC) are the major components of tumor-infiltrate and are abundant in HCC microenvironment, with a key role in supporting tumor initiation, progression, angiogenesis, metastasis, and drug resistance. HCC cells acquire an altered metabolism resulting in increased levels of LDH and lactate that, on the one hand, promote TAM polarization in M2-like phenotype, favoring the EMT, cancer stem cell-like properties, and drug resistance, and, on the other hand, increase the number of MDSC and inhibit NK cell function.

inflammatory diseases can predispose to increased risk of cancer at the same site of inflammation, and HCC is a clear example of inflammation-related cancer.

TAM originate from circulating monocytic precursors, and they are recruited to tumor cells by tumor-derived signals. It has been reported that, in the early phase of the tumor, TAM acquire an inflammatory phenotype and shift their metabolism toward an anaerobic glycolytic pathway [122, 123]. This allows polarized macrophages to rapidly fuel themselves with energy and to cope with hypoxic tissue microenvironment. The interplay between M2-like TAM and cancer is complex, and it is involved in each step of HCC development. It has been demonstrated that this TAM subset promotes migration and EMT. It also induces cancer stem cell-like properties and drug resistance in human HCC, thus highlighting the importance of targeting

the immune microenvironment as a mechanism to inhibit HCC recurrence and metastasis (Figure 2) [124]. Moreover, it has been shown that an increase in the M2-macrophage population is associated with poor prognosis in HCC [125]. TAM can use metabolites released from cancer cells to modulate their polarization status. This is supported by the findings that demonstrated that tumor-released lactate is utilized by TAM to increase the expression of vascular endothelial growth factor and to induce an M2-like status [126]. Lactate can also have effects on other cell types by increasing the number of MDSC, thus inhibiting NK cell function (Figure 2) [127]. The immunosuppressive functions of MDSC can also be regulated by other metabolites, including fatty acids. In MDSC, increased fatty acid uptake and fatty acid oxidation are induced by a STAT3/STAT5-mediated pathway leading

to an increased expression of CD36. Accumulation of lipids increases the oxidative metabolism of MDSC and activates their immunosuppressive mechanisms [128].

7. Concluding Remarks and Perspectives

Global changes in metabolic pathways were identified across different tumor types [129, 130]. The picture that emerged for the comparison between tumors and normal tissue revealed common demands in biochemical pathways associated with biomass production, such as glycolysis, pentose phosphate pathway, purine, and pyrimidine biosynthesis, irrespective of the cell of origin. This cancer tissue-specific metabolic signature is well defined in HCC, where the high glucose demand supports PPP pathway, lactate production by anaerobic glycolysis, and fatty acid production by FASN. Glucose utilization is regulated at multiple levels, including the transcriptional regulation of metabolic enzymes and transporters whose expression is altered in HCC tissues, and consistent with the identification of mitochondrial DNA alterations which was associated with a reduced oxidative phosphorylation and enhanced glycolysis [131].

HCC cells also rely on other carbon substrates to support anaplerotic pathways. A role for glutamine and acetate in sustaining HCC bioenergetics has been proposed. Alternative anaplerotic pathways exist that rely on the transformation of pyruvate to oxaloacetate by pyruvate carboxylase to support the growth of HCC cells in glutamine-free conditions [132]. The dependence of HCC cells from lipid uptake should be also considered, suggesting the existence of a metabolic flexibility and of a possible cross-talk between metabolic pathways that might result by changes imposed by the tumor microenvironment or by the activation of specific signaling pathways. HCC cells can, for instance, modulate fatty acids uptake by the upregulation of CD36 and caveolin 1 that is mediated by the activation of Wnt and TGF- β pathways.

More unique metabolic features were also defined by TCGA studies where significant alterations by mutation or downregulation by hypermethylation in albumin, apolipoprotein B, and carbamoyl phosphate synthase I metabolic genes were observed in HCC [71].

Overall, this metabolic program seems to be essential for HCC biology to sustain tumor growth and progression, and targeting of these pathways might have significant clinical implications. For instance, clinical effects of dexamethasone are explicated *in vivo* by restoring gluconeogenesis [133], inhibition of proline production and targeting of transketolase significantly enhances the cytotoxic effect of sorafenib *in vivo* [134], and insights into nucleotide and lipid metabolism of HCC may provide novel clinical opportunities [135].

However, the design of therapeutic metabolic targeted strategies should be carefully evaluated taking into account tumor heterogeneity and tumor interaction with the microenvironment. Several approaches were applied to address these complexities, including computational, proteomics, and metabolomics. Specifically, these methods tried to move forward the analysis of a single metabolite to obtain not a

static snapshot of tumor biology but a more dynamic picture of metabolic changes in cancer. In this context, the field has expanded to bypass some classical limitations as the small number of samples to be analyzed and the number of analytes to be revealed. By the integration of different omics approaches, genome-scale metabolic models (GEMM) provided a way to study metabolic pathways at systems level [136] and to predict the action of a pathway inhibition at multiple layers of biological complexity. A personalized GEMM has been realized for NAFLD patients [137, 138] and HCC patients [14, 139] to characterize a specific disease-related metabolic phenotype. Moreover, the detailed analysis of a specific metabolic status provides the opportunity to study network perturbations after drug treatment. GEMM built from six HCC patients has been used to predict the action of antimetabolites on cancer growth. The model identified 147 antimetabolites that can inhibit growth in any of the studied HCC tumors, and a smaller group of antimetabolites that were predicted to be effective in only some of the HCC patients, showing a more personalized mechanism of action [139]. Moreover, GEMM has become an informative approach to elucidate tumor heterogeneity at the metabolic level [14].

Although most studies were centered on tumor tissue, metabolomics analyses at the blood level showed to be promising in predicting metabolic alterations at the tissue level. Solid results were obtained with some metabolites, such as lactate and AA, and their altered expression in serum clearly mirrors a metabolic alteration of tumor tissue. The same is probably true for other metabolites such as fatty acids but not yet clarified.

Conflicts of Interest

The authors declare that there is no conflict of interest regarding the publication of this paper.

References

- [1] A. Forner, M. Reig, and J. Bruix, "Hepatocellular carcinoma," *The Lancet*, vol. 391, no. 10127, pp. 1301–1314, 2018.
- [2] N. N. Pavlova and C. B. Thompson, "The emerging hallmarks of cancer metabolism," *Cell Metabolism*, vol. 23, no. 1, pp. 27–47, 2016.
- [3] R. J. DeBerardinis and N. S. Chandel, "Fundamentals of cancer metabolism," *Science Advances*, vol. 2, no. 5, article e1600200, 2016.
- [4] A. J. Wolpaw and C. V. Dang, "Exploiting metabolic vulnerabilities of cancer with precision and accuracy," *Trends in Cell Biology*, vol. 28, no. 3, pp. 201–212, 2018.
- [5] D. Vergara, E. Stanca, F. Guerra et al., " β -Catenin knock-down affects mitochondrial biogenesis and lipid metabolism in breast cancer cells," *Frontiers in Physiology*, vol. 8, p. 544, 2017.
- [6] C. Agostinelli, S. Carloni, F. Limarzi et al., "The emerging role of GSK-3 β in the pathobiology of classical Hodgkin lymphoma," *Histopathology*, vol. 71, no. 1, pp. 72–80, 2017.
- [7] L. Rui, "Energy metabolism in the liver," *Comprehensive Physiology*, vol. 4, no. 1, pp. 177–197, 2014.

- [8] C. C. Barron, P. J. Bilan, T. Tsakiridis, and E. Tsiani, "Facilitative glucose transporters: implications for cancer detection, prognosis and treatment," *Metabolism*, vol. 65, no. 2, pp. 124–139, 2016.
- [9] R. Z. Shang, S. B. Qu, and D. S. Wang, "Reprogramming of glucose metabolism in hepatocellular carcinoma: progress and prospects," *World Journal of Gastroenterology*, vol. 22, no. 45, pp. 9933–9943, 2016.
- [10] A. Kornberg, M. Freesmeyer, E. Bärthel et al., "18F-FDG-uptake of hepatocellular carcinoma on PET predicts microvascular tumor invasion in liver transplant patients," *American Journal of Transplantation*, vol. 9, no. 3, pp. 592–600, 2009.
- [11] K. Kitamura, E. Hatano, T. Higashi et al., "Proliferative activity in hepatocellular carcinoma is closely correlated with glucose metabolism but not angiogenesis," *Journal of Hepatology*, vol. 55, no. 4, pp. 846–857, 2011.
- [12] X. Zhang, Y. Qiao, Q. Wu et al., "The essential role of YAP O-GlcNAcylation in high-glucose-stimulated liver tumorigenesis," *Nature Communications*, vol. 8, article 15280, 2017.
- [13] Y. Qiao, X. Zhang, Y. Zhang et al., "High glucose stimulates tumorigenesis in hepatocellular carcinoma cells through AGER-dependent O-GlcNAcylation of c-Jun," *Diabetes*, vol. 65, no. 3, pp. 619–632, 2016.
- [14] E. Björnson, B. Mukhopadhyay, A. Asplund et al., "Stratification of hepatocellular carcinoma patients based on acetate utilization," *Cell Reports*, vol. 13, no. 9, pp. 2014–2026, 2015.
- [15] N. Hay, "Reprogramming glucose metabolism in cancer: can it be exploited for cancer therapy?," *Nature Reviews Cancer*, vol. 16, no. 10, pp. 635–649, 2016.
- [16] U. Parikh, C. Marcus, R. Sarangi, M. Taghipour, and R. M. Subramaniam, "FDG PET/CT in pancreatic and hepatobiliary carcinomas: value to patient management and patient outcomes," *PET Clinics*, vol. 10, no. 3, pp. 327–343, 2015.
- [17] T. Yamamoto, Y. Seino, H. Fukumoto et al., "Over-expression of facilitative glucose transporter genes in human cancer," *Biochemical and Biophysical Research Communications*, vol. 170, no. 1, pp. 223–230, 1990.
- [18] R. Grobholz, H. J. Hacker, B. Thorens, and P. Bannasch, "Reduction in the expression of glucose transporter protein GLUT 2 in preneoplastic and neoplastic hepatic lesions and reexpression of GLUT 1 in late stages of hepatocarcinogenesis," *Cancer Research*, vol. 53, no. 18, pp. 4204–4211, 1993.
- [19] T. S. Su, T. F. Tsai, C. W. Chi, S. H. Han, and C. K. Chou, "Elevation of facilitated glucose-transporter messenger RNA in human hepatocellular carcinoma," *Hepatology*, vol. 11, no. 1, pp. 118–122, 1990.
- [20] T. Amann and C. Hellerbrand, "GLUT1 as a therapeutic target in hepatocellular carcinoma," *Expert Opinion on Therapeutic Targets*, vol. 13, no. 12, pp. 1411–1427, 2009.
- [21] K. Daskalow, D. Pfander, W. Weichert et al., "Distinct temporospatial expression patterns of glycolysis-related proteins in human hepatocellular carcinoma," *Histochemistry and Cell Biology*, vol. 132, no. 1, pp. 21–31, 2009.
- [22] Y. H. Kim, D. C. Jeong, K. Pak et al., "SLC2A2 (GLUT2) as a novel prognostic factor for hepatocellular carcinoma," *Oncotarget*, vol. 8, no. 40, pp. 68381–68392, 2017.
- [23] L. Gong, Z. Cui, P. Chen, H. Han, J. Peng, and X. Leng, "Reduced survival of patients with hepatocellular carcinoma expressing hexokinase II," *Medical Oncology*, vol. 29, no. 2, pp. 909–914, 2012.
- [24] D. DeWaal, V. Nogueira, A. R. Terry et al., "Hexokinase-2 depletion inhibits glycolysis and induces oxidative phosphorylation in hepatocellular carcinoma and sensitizes to metformin," *Nature Communications*, vol. 9, no. 1, p. 446, 2018.
- [25] Z. Zhang, S. Huang, H. Wang et al., "High expression of hexokinase domain containing 1 is associated with poor prognosis and aggressive phenotype in hepatocarcinoma," *Biochemical and Biophysical Research Communications*, vol. 474, no. 4, pp. 673–679, 2016.
- [26] H. Hirata, K. Sugimachi, H. Komatsu et al., "Decreased expression of fructose-1,6-bisphosphatase associates with glucose metabolism and tumor progression in hepatocellular carcinoma," *Cancer Research*, vol. 76, no. 11, pp. 3265–3276, 2016.
- [27] S. Liu, Y. Sun, M. Jiang et al., "Glyceraldehyde-3-phosphate dehydrogenase promotes liver tumorigenesis by modulating phosphoglycerate dehydrogenase," *Hepatology*, vol. 66, no. 2, pp. 631–645, 2017.
- [28] S. Ganapathy-Kanniappan, R. Kunjithapatham, and J. F. Geschwind, "Glyceraldehyde-3-phosphate dehydrogenase: a promising target for molecular therapy in hepatocellular carcinoma," *Oncotarget*, vol. 3, no. 9, pp. 940–953, 2012.
- [29] C. C.-L. Wong, S. L.-K. Au, A. P.-W. Tse et al., "Switching of pyruvate kinase isoform L to M2 promotes metabolic reprogramming in hepatocarcinogenesis," *PLoS One*, vol. 9, no. 12, article e115036, 2014.
- [30] K. Nakao, H. Miyaaki, and T. Ichikawa, "Antitumor function of microRNA-122 against hepatocellular carcinoma," *Journal of Gastroenterology*, vol. 49, no. 4, pp. 589–593, 2014.
- [31] A. A. Cluntun, M. J. Lukey, R. A. Cerione, and J. W. Locasale, "Glutamine metabolism in cancer: understanding the heterogeneity," *Trends in Cancer*, vol. 3, no. 3, pp. 169–180, 2017.
- [32] B. P. Bode and W. W. Souba, "Glutamine transport and human hepatocellular transformation," *Journal of Parenteral and Enteral Nutrition*, vol. 23, 5_Supplement, pp. S33–S37, 1999.
- [33] M. O. Yuneva, T. W. M. Fan, T. D. Allen et al., "The metabolic profile of tumors depends on both the responsible genetic lesion and tissue type," *Cell Metabolism*, vol. 15, no. 2, pp. 157–170, 2012.
- [34] H. Xie, J. I. Hanai, J. G. Ren et al., "Targeting lactate dehydrogenase-A inhibits tumorigenesis and tumor progression in mouse models of lung cancer and impacts tumor-initiating cells," *Cell Metabolism*, vol. 19, no. 5, pp. 795–809, 2014.
- [35] D. Vergara, P. Simeone, P. del Boccio et al., "Comparative proteome profiling of breast tumor cell lines by gel electrophoresis and mass spectrometry reveals an epithelial mesenchymal transition associated protein signature," *Molecular BioSystems*, vol. 9, no. 6, pp. 1127–1138, 2013.
- [36] L. Brisson, P. Bański, M. Sboarina et al., "Lactate dehydrogenase B controls lysosome activity and autophagy in cancer," *Cancer Cell*, vol. 30, no. 3, pp. 418–431, 2016.
- [37] Z. Fang, L. He, H. Jia, Q. Huang, D. Chen, and Z. Zhang, "The miR-383-LDHA axis regulates cell proliferation, invasion and glycolysis in hepatocellular cancer," *Iranian Journal of Basic Medical Sciences*, vol. 20, no. 2, pp. 187–192, 2017.
- [38] S. L. Sheng, J. J. Liu, Y. H. Dai, X. G. Sun, X. P. Xiong, and G. Huang, "Knockdown of lactate dehydrogenase A suppresses tumor growth and metastasis of human

- hepatocellular carcinoma,” *FEBS Journal*, vol. 279, no. 20, pp. 3898–3910, 2012.
- [39] L. Faloppi, M. Scartozzi, M. Bianconi et al., “The role of LDH serum levels in predicting global outcome in HCC patients treated with sorafenib: implications for clinical management,” *BMC Cancer*, vol. 14, no. 1, p. 110, 2014.
- [40] M. Scartozzi, L. Faloppi, M. Bianconi et al., “The role of LDH serum levels in predicting global outcome in HCC patients undergoing TACE: implications for clinical management,” *PLoS One*, vol. 7, no. 3, article e32653, 2012.
- [41] J. P. Zhang, H. B. Wang, Y. H. Lin et al., “Lactate dehydrogenase is an important prognostic indicator for hepatocellular carcinoma after partial hepatectomy,” *Translational Oncology*, vol. 8, no. 6, pp. 497–503, 2015.
- [42] L. Faloppi, M. Bianconi, R. Memeo et al., “Lactate dehydrogenase in hepatocellular carcinoma: something old, something new,” *BioMed Research International*, vol. 2016, Article ID 7196280, 7 pages, 2016.
- [43] H. J. Gao, M. C. Zhao, Y. J. Zhang et al., “Monocarboxylate transporter 4 predicts poor prognosis in hepatocellular carcinoma and is associated with cell proliferation and migration,” *Journal of Cancer Research and Clinical Oncology*, vol. 141, no. 7, pp. 1151–1162, 2015.
- [44] V. A. Alves, C. Pinheiro, F. Morais-Santos, A. Felipe-Silva, A. Longatto-Filho, and F. Baltazar, “Characterization of monocarboxylate transporter activity in hepatocellular carcinoma,” *World Journal of Gastroenterology*, vol. 20, no. 33, pp. 11780–11787, 2014.
- [45] Q. Huang, J. Li, J. Xing et al., “CD147 promotes reprogramming of glucose metabolism and cell proliferation in HCC cells by inhibiting the p53-dependent signaling pathway,” *Journal of Hepatology*, vol. 61, no. 4, pp. 859–866, 2014.
- [46] C. Teilhet, D. Morvan, J. Joubert-Zakeyeh et al., “Specificities of human hepatocellular carcinoma developed on non-alcoholic fatty liver disease in absence of cirrhosis revealed by tissue extracts ¹H-NMR spectroscopy,” *Metabolites*, vol. 7, no. 4, p. 49, 2017.
- [47] Y. Chen, J. Zhou, J. Li, J. Feng, Z. Chen, and X. Wang, “Plasma metabolomic analysis of human hepatocellular carcinoma: diagnostic and therapeutic study,” *Oncotarget*, vol. 7, no. 30, pp. 47332–47342, 2016.
- [48] S. C. Kalhan, L. Guo, J. Edmison et al., “Plasma metabolomic profile in nonalcoholic fatty liver disease,” *Metabolism*, vol. 60, no. 3, pp. 404–413, 2011.
- [49] L. Gan, Z. Liu, and C. Sun, “Obesity linking to hepatocellular carcinoma: a global view,” *Biochimica et Biophysica Acta (BBA) - Reviews on Cancer*, vol. 1869, no. 2, pp. 97–102, 2018.
- [50] X. Li, X. Wang, and P. Gao, “Diabetes mellitus and risk of hepatocellular carcinoma,” *BioMed Research International*, vol. 2017, Article ID 5202684, 10 pages, 2017.
- [51] A. Borrelli, P. Bonelli, F. M. Tuccillo et al., “Role of gut microbiota and oxidative stress in the progression of non-alcoholic fatty liver disease to hepatocarcinoma: current and innovative therapeutic approaches,” *Redox Biology*, vol. 15, pp. 467–479, 2018.
- [52] S. Smith, A. Witkowski, and A. K. Joshi, “Structural and functional organization of the animal fatty acid synthase,” *Progress in Lipid Research*, vol. 42, no. 4, pp. 289–317, 2003.
- [53] D. F. Calvisi, “De novo lipogenesis: role in hepatocellular carcinoma,” *Der Pathologe*, vol. 32, no. S2, pp. 174–180, 2011.
- [54] K. L. Donnelly, C. I. Smith, S. J. Schwarzenberg, J. Jessurun, M. D. Boldt, and E. J. Parks, “Sources of fatty acids stored in liver and secreted via lipoproteins in patients with nonalcoholic fatty liver disease,” *The Journal of Clinical Investigation*, vol. 115, no. 5, pp. 1343–1351, 2005.
- [55] C. Mounier, L. Bouraoui, and E. Rassart, “Lipogenesis in cancer progression (review),” *International Journal of Oncology*, vol. 45, no. 2, pp. 485–492, 2014.
- [56] L. Li, L. Che, C. Wang et al., “[¹C]acetate PET imaging is not always associated with increased lipogenesis in hepatocellular carcinoma in mice,” *Molecular Imaging and Biology*, vol. 18, no. 3, pp. 360–367, 2016.
- [57] Y. Gao, L. P. Lin, C. H. Zhu, Y. Chen, Y. T. Hou, and J. Ding, “Growth arrest induced by C75, a fatty acid synthase inhibitor, was partially modulated by p38 MAPK but not by p53 in human hepatocellular carcinoma,” *Cancer Biology & Therapy*, vol. 5, no. 8, pp. 978–985, 2006.
- [58] D. F. Calvisi, C. Wang, C. Ho et al., “Increased lipogenesis, induced by AKT-mTORC1-RPS6 signaling, promotes development of human hepatocellular carcinoma,” *Gastroenterology*, vol. 140, no. 3, pp. 1071–1083.e5, 2011.
- [59] T. Y. Na, Y. K. Shin, K. J. Roh et al., “Liver X receptor mediates hepatitis B virus X protein-induced lipogenesis in hepatitis B virus-associated hepatocellular carcinoma,” *Hepatology*, vol. 49, no. 4, pp. 1122–1131, 2009.
- [60] X. Zhu, X. Qin, M. Fei et al., “Combined phosphatase and tensin homolog (PTEN) loss and fatty acid synthase (FAS) overexpression worsens the prognosis of Chinese patients with hepatocellular carcinoma,” *International Journal of Molecular Sciences*, vol. 13, no. 8, pp. 9980–9991, 2012.
- [61] L. Che, M. G. Pilo, A. Cigliano et al., “Oncogene dependent requirement of fatty acid synthase in hepatocellular carcinoma,” *Cell Cycle*, vol. 16, no. 6, pp. 499–507, 2017.
- [62] Q. Wang, W. Zhang, Q. Liu et al., “A mutant of hepatitis B virus X protein (HBxDelta127) promotes cell growth through a positive feedback loop involving 5-lipoxygenase and fatty acid synthase,” *Neoplasia*, vol. 12, no. 2, pp. 103–IN3, 2010.
- [63] T. Yamashita, M. Honda, H. Takatori et al., “Activation of lipogenic pathway correlates with cell proliferation and poor prognosis in hepatocellular carcinoma,” *Journal of Hepatology*, vol. 50, no. 1, pp. 100–110, 2009.
- [64] C. Li, W. Yang, J. Zhang et al., “SREBP-1 has a prognostic role and contributes to invasion and metastasis in human hepatocellular carcinoma,” *International Journal of Molecular Sciences*, vol. 15, no. 5, pp. 7124–7138, 2014.
- [65] J. Hu, L. Che, L. Li et al., “Co-activation of AKT and c-Met triggers rapid hepatocellular carcinoma development via the mTORC1/FASN pathway in mice,” *Scientific Reports*, vol. 6, no. 1, article 20484, 2016.
- [66] D. Cao, X. Song, L. Che et al., “Both *de novo* synthesized and exogenous fatty acids support the growth of hepatocellular carcinoma cells,” *Liver International*, vol. 37, no. 1, pp. 80–89, 2017.
- [67] M. E. Nelson, S. Lahiri, J. D. Y. Chow et al., “Inhibition of hepatic lipogenesis enhances liver tumorigenesis by increasing antioxidant defence and promoting cell survival,” *Nature Communications*, vol. 8, article 14689, 2017.
- [68] A. Nath, I. Li, L. R. Roberts, and C. Chan, “Elevated free fatty acid uptake via CD36 promotes epithelial-mesenchymal transition in hepatocellular carcinoma,” *Scientific Reports*, vol. 5, no. 1, article 14752, 2015.

- [69] G. Giannelli, P. Koudelkova, F. Dituri, and W. Mikulits, "Role of epithelial to mesenchymal transition in hepatocellular carcinoma," *Journal of Hepatology*, vol. 65, no. 4, pp. 798–808, 2016.
- [70] D. D. Stefania and D. Vergara, "The many-faced program of epithelial-mesenchymal transition: a system biology-based view," *Frontiers in Oncology*, vol. 7, p. 274, 2017.
- [71] A. Ally, M. Balasundaram, R. Carlsen et al., "Comprehensive and integrative genomic characterization of hepatocellular carcinoma," *Cell*, vol. 169, no. 7, pp. 1327–1341.e23, 2017.
- [72] J. Kerner and C. Hoppel, "Fatty acid import into mitochondria," *Biochimica et Biophysica Acta (BBA) - Molecular and Cell Biology of Lipids*, vol. 1486, no. 1, pp. 1–17, 2000.
- [73] G. Serviddio, A. M. Giudetti, F. Bellanti et al., "Oxidation of hepatic carnitine palmitoyl transferase-I (CPT-I) impairs fatty acid beta-oxidation in rats fed a methionine-choline deficient diet," *PLoS One*, vol. 6, no. 9, article e24084, 2011.
- [74] G. Serviddio, F. Bellanti, R. Tamborra et al., "Alterations of hepatic ATP homeostasis and respiratory chain during development of non-alcoholic steatohepatitis in a rodent model," *European Journal of Clinical Investigation*, vol. 38, no. 4, pp. 245–252, 2008.
- [75] Y. Shao, B. Zhu, R. Zheng et al., "Development of urinary pseudotargeted LC-MS-based metabolomics method and its application in hepatocellular carcinoma biomarker discovery," *Journal of Proteome Research*, vol. 14, no. 2, pp. 906–916, 2015.
- [76] A. Wada, K. Fukui, Y. Sawai et al., "Pamidronate induced anti-proliferative, apoptotic, and anti-migratory effects in hepatocellular carcinoma," *Journal of Hepatology*, vol. 44, no. 1, pp. 142–150, 2006.
- [77] Y. Honda, H. Aikata, F. Honda et al., "Clinical outcome and prognostic factors in hepatocellular carcinoma patients with bone metastases medicated with zoledronic acid," *Hepatology Research*, vol. 47, no. 10, pp. 1053–1060, 2017.
- [78] S. Singh, P. P. Singh, A. G. Singh, M. H. Murad, and W. Sanchez, "Statins are associated with a reduced risk of hepatocellular cancer: a systematic review and meta-analysis," *Gastroenterology*, vol. 144, no. 2, pp. 323–332, 2013.
- [79] E. Ridruejo, G. Romero-Caími, M. J. Obregón, D. Kleiman de Pisarev, and L. Alvarez, "Potential molecular targets of statins in the prevention of hepatocarcinogenesis," *Annals of Hepatology*, vol. 17, no. 3, pp. 490–500, 2018.
- [80] Y. Y. Zhou, G. Q. Zhu, Y. Wang et al., "Systematic review with network meta-analysis: statins and risk of hepatocellular carcinoma," *Oncotarget*, vol. 7, no. 16, pp. 21753–21762, 2016.
- [81] J. Y. L. Chiang, "Bile acids: regulation of synthesis," *Journal of Lipid Research*, vol. 50, no. 10, pp. 1955–1966, 2009.
- [82] E. Lozano, L. Sanchez-Vicente, M. J. Monte et al., "Cocarcinogenic effects of intrahepatic bile acid accumulation in cholangiocarcinoma development," *Molecular Cancer Research*, vol. 12, no. 1, pp. 91–100, 2014.
- [83] T. Takahashi, U. Deuschle, S. Taira et al., "Tsumura-Suzuki obese diabetic mice-derived hepatic tumors closely resemble human hepatocellular carcinomas in metabolism-related genes expression and bile acid accumulation," *Hepatology International*, vol. 12, no. 3, pp. 254–261, 2018.
- [84] S. Yamada, Y. Takashina, M. Watanabe et al., "Bile acid metabolism regulated by the gut microbiota promotes non-alcoholic steatohepatitis-associated hepatocellular carcinoma in mice," *Oncotarget*, vol. 9, no. 11, pp. 9925–9939, 2018.
- [85] S. H. Jee, M. Kim, M. Kim et al., "Metabolomics profiles of hepatocellular carcinoma in a Korean prospective cohort: the Korean cancer prevention study-II," *Cancer Prevention Research*, vol. 11, no. 5, pp. 303–312, 2018.
- [86] W. Jia, G. Xie, and W. Jia, "Bile acid-microbiota crosstalk in gastrointestinal inflammation and carcinogenesis," *Nature Reviews Gastroenterology & Hepatology*, vol. 15, no. 2, pp. 111–128, 2018.
- [87] C. Guo, C. Xie, P. Ding et al., "Quantification of glycocholic acid in human serum by stable isotope dilution ultra performance liquid chromatography electrospray ionization tandem mass spectrometry," *Journal of Chromatography B*, vol. 1072, pp. 315–319, 2018.
- [88] E. Stanca, G. Serviddio, F. Bellanti, G. Vendemiale, L. Siculella, and A. M. Giudetti, "Down-regulation of LPCAT expression increases platelet-activating factor level in cirrhotic rat liver: potential antiinflammatory effect of silybin," *Biochimica et Biophysica Acta (BBA) - Molecular Basis of Disease*, vol. 1832, no. 12, pp. 2019–2026, 2013.
- [89] Y. Liu, Z. Hong, G. Tan et al., "NMR and LC/MS-based global metabolomics to identify serum biomarkers differentiating hepatocellular carcinoma from liver cirrhosis," *International Journal of Cancer*, vol. 135, no. 3, pp. 658–668, 2014.
- [90] T. Chen, G. Xie, X. Wang et al., "Serum and urine metabolite profiling reveals potential biomarkers of human hepatocellular carcinoma," *Molecular & Cellular Proteomics*, vol. 10, no. 7, article M110.004945, 2011.
- [91] Q. Huang, Y. Tan, P. Yin et al., "Metabolic characterization of hepatocellular carcinoma using nontargeted tissue metabolomics," *Cancer Research*, vol. 73, no. 16, pp. 4992–5002, 2013.
- [92] B. I. Carr and V. Guerra, "Serum albumin levels in relation to tumor parameters in hepatocellular carcinoma patients," *The International Journal of Biological Markers*, vol. 32, no. 4, pp. e391–e396, 2017.
- [93] J. Luo, "Cancer's sweet tooth for serine," *Breast Cancer Research*, vol. 13, no. 6, p. 317, 2011.
- [94] J. W. Locasale, A. R. Grassian, T. Melman et al., "Phosphoglycerate dehydrogenase diverts glycolytic flux and contributes to oncogenesis," *Nature Genetics*, vol. 43, no. 9, pp. 869–874, 2011.
- [95] R. Possemato, K. M. Marks, Y. D. Shaul et al., "Functional genomics reveal that the serine synthesis pathway is essential in breast cancer," *Nature*, vol. 476, no. 7360, pp. 346–350, 2011.
- [96] M. Jain, R. Nilsson, S. Sharma et al., "Metabolite profiling identifies a key role for glycine in rapid cancer cell proliferation," *Science*, vol. 336, no. 6084, pp. 1040–1044, 2012.
- [97] B. Chaneton, P. Hillmann, L. Zheng et al., "Serine is a natural ligand and allosteric activator of pyruvate kinase M2," *Nature*, vol. 491, no. 7424, pp. 458–462, 2012.
- [98] R. Gao, J. Cheng, C. Fan et al., "Serum metabolomics to identify the liver disease-specific biomarkers for the progression of hepatitis to hepatocellular carcinoma," *Scientific Reports*, vol. 5, no. 1, article 18175, 2016.
- [99] M. Stepien, T. Duarte-Salles, V. Fedirko et al., "Alteration of amino acid and biogenic amine metabolism in hepatobiliary cancers: findings from a prospective cohort study," *International Journal of Cancer*, vol. 138, no. 2, pp. 348–360, 2016.

- [100] L. Tang, J. Zeng, P. Geng et al., "Global metabolic profiling identifies a pivotal role of proline and hydroxyproline metabolism in supporting hypoxic response in hepatocellular carcinoma," *Clinical Cancer Research*, vol. 24, no. 2, pp. 474–485, 2018.
- [101] P. Muriel, "Role of free radicals in liver diseases," *Hepatology International*, vol. 3, no. 4, pp. 526–536, 2009.
- [102] J. Arauz, E. Ramos-Tovar, and P. Muriel, "Redox state and methods to evaluate oxidative stress in liver damage: from bench to bedside," *Annals of Hepatology*, vol. 15, no. 2, pp. 160–173, 2016.
- [103] G. Y. Liou and P. Storz, "Reactive oxygen species in cancer," *Free Radical Research*, vol. 44, no. 5, pp. 479–496, 2010.
- [104] D. Anastasiou, G. Poulogiannis, J. M. Asara et al., "Inhibition of pyruvate kinase M2 by reactive oxygen species contributes to cellular antioxidant responses," *Science*, vol. 334, no. 6060, pp. 1278–1283, 2011.
- [105] A. I. Fitian and R. Cabrera, "Disease monitoring of hepatocellular carcinoma through metabolomics," *World Journal of Hepatology*, vol. 9, no. 1, pp. 1–17, 2017.
- [106] A. Takaki and K. Yamamoto, "Control of oxidative stress in hepatocellular carcinoma: helpful or harmful?," *World Journal of Hepatology*, vol. 7, no. 7, pp. 968–979, 2015.
- [107] Y. Shimomura, A. Takaki, N. Wada et al., "The serum oxidative/anti-oxidative stress balance becomes dysregulated in patients with non-alcoholic steatohepatitis associated with hepatocellular carcinoma," *Internal Medicine*, vol. 56, no. 3, pp. 243–251, 2017.
- [108] S. C. Lu, "Glutathione synthesis," *Biochimica et Biophysica Acta (BBA) - General Subjects*, vol. 1830, no. 5, pp. 3143–3153, 2013.
- [109] L. Andrisic, D. Dudzik, C. Barbas, L. Milkovic, T. Grune, and N. Zarkovic, "Short overview on metabolomics approach to study pathophysiology of oxidative stress in cancer," *Redox Biology*, vol. 14, pp. 47–58, 2018.
- [110] S. Tanaka, K. Miyaniishi, M. Kobune et al., "Increased hepatic oxidative DNA damage in patients with nonalcoholic steatohepatitis who develop hepatocellular carcinoma," *Journal of Gastroenterology*, vol. 48, no. 11, pp. 1249–1258, 2013.
- [111] N. Nishida, T. Arizumi, M. Takita et al., "Reactive oxygen species induce epigenetic instability through the formation of 8-hydroxydeoxyguanosine in human hepatocarcinogenesis," *Digestive Diseases*, vol. 31, no. 5–6, pp. 459–466, 2013.
- [112] M. Xiao, H. Zhong, L. Xia, Y. Tao, and H. Yin, "Pathophysiology of mitochondrial lipid oxidation: role of 4-hydroxynonenal (4-HNE) and other bioactive lipids in mitochondria," *Free Radical Biology and Medicine*, vol. 111, pp. 316–327, 2017.
- [113] S. Li, H.-Y. Tan, N. Wang et al., "The role of oxidative stress and antioxidants in liver diseases," *International Journal of Molecular Sciences*, vol. 16, no. 11, pp. 26087–26124, 2015.
- [114] T. Soga, M. Sugimoto, M. Honma et al., "Serum metabolomics reveals γ -glutamyl dipeptides as biomarkers for discrimination among different forms of liver disease," *Journal of Hepatology*, vol. 55, no. 4, pp. 896–905, 2011.
- [115] T. Saito, M. Sugimoto, K. Okumoto et al., "Serum metabolome profiles characterized by patients with hepatocellular carcinoma associated with hepatitis B and C," *World Journal of Gastroenterology*, vol. 22, no. 27, pp. 6224–6234, 2016.
- [116] J. Zeng, P. Yin, Y. Tan et al., "Metabolomics study of hepatocellular carcinoma: discovery and validation of serum potential biomarkers by using capillary electrophoresis-mass spectrometry," *Journal of Proteome Research*, vol. 13, no. 7, pp. 3420–3431, 2014.
- [117] A. I. Fitian, D. R. Nelson, C. Liu, Y. Xu, M. Ararat, and R. Cabrera, "Integrated metabolomic profiling of hepatocellular carcinoma in hepatitis C cirrhosis through GC/MS and UPLC/MS-MS," *Liver International*, vol. 34, no. 9, pp. 1428–1444, 2014.
- [118] S. K. Biswas, P. Allavena, and A. Mantovani, "Tumor-associated macrophages: functional diversity, clinical significance, and open questions," *Seminars in Immunopathology*, vol. 35, no. 5, pp. 585–600, 2013.
- [119] B. Z. Qian and J. W. Pollard, "Macrophage diversity enhances tumor progression and metastasis," *Cell*, vol. 141, no. 1, pp. 39–51, 2010.
- [120] T. Kapanadze, J. Gamrekashvili, C. Ma et al., "Regulation of accumulation and function of myeloid derived suppressor cells in different murine models of hepatocellular carcinoma," *Journal of Hepatology*, vol. 59, no. 5, pp. 1007–1013, 2013.
- [121] S. K. Biswas and A. Mantovani, "Macrophage plasticity and interaction with lymphocyte subsets: cancer as a paradigm," *Nature Immunology*, vol. 11, no. 10, pp. 889–896, 2010.
- [122] S. K. Biswas and A. Mantovani, "Orchestration of metabolism by macrophages," *Cell Metabolism*, vol. 15, no. 4, pp. 432–437, 2012.
- [123] S. K. Biswas, A. Sica, and C. E. Lewis, "Plasticity of macrophage function during tumor progression: regulation by distinct molecular mechanisms," *Journal of Immunology*, vol. 180, no. 4, pp. 2011–2017, 2008.
- [124] S. Wan, E. Zhao, I. Kryczek et al., "Tumor-associated macrophages produce interleukin 6 and signal via STAT3 to promote expansion of human hepatocellular carcinoma stem cells," *Gastroenterology*, vol. 147, no. 6, pp. 1393–1404, 2014.
- [125] A. Budhu, M. Forgues, Q. H. Ye et al., "Prediction of venous metastases, recurrence, and prognosis in hepatocellular carcinoma based on a unique immune response signature of the liver microenvironment," *Cancer Cell*, vol. 10, no. 2, pp. 99–111, 2006.
- [126] O. R. Colegio, N. Q. Chu, A. L. Szabo et al., "Functional polarization of tumour-associated macrophages by tumour-derived lactic acid," *Nature*, vol. 513, no. 7519, pp. 559–563, 2014.
- [127] Z. Husain, Y. Huang, P. Seth, and V. P. Sukhatme, "Tumor-derived lactate modifies antitumor immune response: effect on myeloid-derived suppressor cells and NK cells," *Journal of Immunology*, vol. 191, no. 3, pp. 1486–1495, 2013.
- [128] A. A. Al-Khami, L. Zheng, L. Del Valle et al., "Exogenous lipid uptake induces metabolic and functional reprogramming of tumor-associated myeloid-derived suppressor cells," *Oncotarget*, vol. 6, no. 10, article e1344804, 2017.
- [129] J. Hu, J. W. Locasale, J. H. Bielas et al., "Heterogeneity of tumor-induced gene expression changes in the human metabolic network," *Nature Biotechnology*, vol. 31, no. 6, pp. 522–529, 2013.
- [130] E. Gaude and C. Frezza, "Tissue-specific and convergent metabolic transformation of cancer correlates with metastatic potential and patient survival," *Nature Communications*, vol. 7, article 13041, 2016.
- [131] C. C. Hsu, H. C. Lee, and Y. H. Wei, "Mitochondrial DNA alterations and mitochondrial dysfunction in the progression

- of hepatocellular carcinoma,” *World Journal of Gastroenterology*, vol. 19, no. 47, pp. 8880–8886, 2013.
- [132] T. Cheng, J. Sudderth, C. Yang et al., “Pyruvate carboxylase is required for glutamine-independent growth of tumor cells,” *Proceedings of the National Academy of Sciences of the United States of America*, vol. 108, no. 21, pp. 8674–8679, 2011.
- [133] R. Ma, W. Zhang, K. Tang et al., “Switch of glycolysis to gluconeogenesis by dexamethasone for treatment of hepatocarcinoma,” *Nature Communications*, vol. 4, no. 1, article 2508, 2013.
- [134] I. M.-J. Xu, R. K.-H. Lai, S.-H. Lin et al., “Transketolase counteracts oxidative stress to drive cancer development,” *Proceedings of the National Academy of Sciences of the United States of America*, vol. 113, no. 6, pp. E725–E734, 2016.
- [135] M. J. Kim, Y. K. Choi, S. Y. Park et al., “PPAR δ reprograms glutamine metabolism in sorafenib-resistant HCC,” *Molecular Cancer Research*, vol. 15, no. 9, pp. 1230–1242, 2017.
- [136] C. Zhang and Q. Hua, “Applications of genome-scale metabolic models in biotechnology and systems medicine,” *Frontiers in Physiology*, vol. 6, p. 413, 2016.
- [137] A. Mardinoglu, R. Agren, C. Kampf, A. Asplund, M. Uhlen, and J. Nielsen, “Genome-scale metabolic modelling of hepatocytes reveals serine deficiency in patients with non-alcoholic fatty liver disease,” *Nature Communications*, vol. 5, no. 1, article 3083, 2014.
- [138] A. Mardinoglu, E. Bjornson, C. Zhang et al., “Personal model-assisted identification of NAD⁺ and glutathione metabolism as intervention target in NAFLD,” *Molecular Systems Biology*, vol. 13, no. 3, p. 916, 2017.
- [139] R. Agren, A. Mardinoglu, A. Asplund, C. Kampf, M. Uhlen, and J. Nielsen, “Identification of anticancer drugs for hepatocellular carcinoma through personalized genome-scale metabolic modeling,” *Molecular Systems Biology*, vol. 10, no. 3, p. 721, 2014.

Research Article

Heme Oxygenase-1 May Affect Cell Signalling via Modulation of Ganglioside Composition

Václav Šmíd ^{1,2}, Jakub Šuk ¹, Neli Kachamakova-Trojanowska^{3,4}, Jana Jašprová,¹
Petra Valášková ¹, Alicja Józkwicz ³, Józef Dulak,³ František Šmíd,¹ Libor Vítek ^{1,2}
and Lucie Muchová ¹

¹Institute of Medical Biochemistry and Laboratory Diagnostics, 1st Faculty of Medicine and General University Hospital in Prague, Charles University, Katerinska 32, 12108 Prague, Czech Republic

²4th Department of Internal Medicine, 1st Faculty of Medicine and General University Hospital in Prague, Charles University, U Nemocnice 499/2, 12801 Prague, Czech Republic

³Department of Medical Biotechnology, Faculty of Biochemistry, Biophysics and Biotechnology, Jagiellonian University, 7 Gronostajowa St., 30-387 Krakow, Poland

⁴Malopolska Centre for Biotechnology, Jagiellonian University, Gronostajowa str 7a, 30-387 Krakow, Poland

Correspondence should be addressed to Lucie Muchová; lucie.muchova@lf1.cuni.cz

Received 14 May 2018; Revised 28 July 2018; Accepted 5 August 2018; Published 19 September 2018

Academic Editor: Daniele Vergara

Copyright © 2018 Václav Šmíd et al. This is an open access article distributed under the Creative Commons Attribution License, which permits unrestricted use, distribution, and reproduction in any medium, provided the original work is properly cited.

Heme oxygenase 1 (Hmox1), a ubiquitous enzyme degrading heme to carbon monoxide, iron, and biliverdin, is one of the cytoprotective enzymes induced in response to a variety of stimuli, including cellular oxidative stress. Gangliosides, sialic acid-containing glycosphingolipids expressed in all cells, are involved in cell recognition, signalling, and membrane stabilization. Their expression is often altered under many pathological and physiological conditions including cell death, proliferation, and differentiation. The aim of this study was to assess the possible role of Hmox1 in ganglioside metabolism in relation to oxidative stress. The content of liver and brain gangliosides, their cellular distribution, and mRNA as well as protein expression of key glycosyltransferases were determined in *Hmox1* knockout mice as well as their wild-type littermates. To elucidate the possible underlying mechanisms between Hmox1 and ganglioside metabolism, hepatoblastoma HepG2 and neuroblastoma SH-SY5Y cell lines were used for *in vitro* experiments. Mice lacking *Hmox1* exhibited a significant increase in concentrations of liver and brain gangliosides and in mRNA expression of the key enzymes of ganglioside metabolism. A marked shift of GM1 ganglioside from the subsinusoidal part of the intracellular compartment into sinusoidal membranes of hepatocytes was shown in *Hmox1* knockout mice. Induction of oxidative stress by chenodeoxycholic acid *in vitro* resulted in a significant increase in GM3, GM2, and GD1a gangliosides in SH-SY5Y cells and GM3 and GM2 in the HepG2 cell line. These changes were abolished with administration of bilirubin, a potent antioxidant agent. These observations were closely related to oxidative stress-mediated changes in sialyltransferase expression regulated at least partially through the protein kinase C pathway. We conclude that oxidative stress is an important factor modulating synthesis and distribution of gangliosides *in vivo* and *in vitro* which might affect ganglioside signalling in higher organisms.

1. Introduction

Heme oxygenase 1 (Hmox1) is a highly inducible antioxidant and cytoprotective enzyme in the heme catabolic pathway generating equimolar amounts of iron, carbon monoxide, and biliverdin which is immediately reduced to bilirubin [1]. Hmox1 activity—also due to the effect of

its bioactive products—affects pathophysiology of many neurologic, cardiovascular, and pulmonary diseases [2–4]. In the liver, Hmox1 plays an important role in hepatic fat accumulation, fibrogenesis, ischemia-reperfusion, and oxidative injury [5]. Moreover, upon *Hmox1* knockout, the cells and/or animals become more vulnerable to oxidative stress. Free radical formation as well as oxidative stress-

associated cytotoxicity are increased in *Hmox1* knockouts due to reduced antioxidant bilirubin and vasoactive carbon monoxide formation, disruption of iron homeostasis, and accumulation of prooxidative heme [6]. Due to iron accumulation, liver is one of the tissues most affected by an increased oxidative stress in *Hmox1* knockout mice and increased lipid peroxidation, fibrosis, and hepatic injury have been described in these animals [5]. Furthermore, an increase in some key cytoprotective genes such as NAD(P)H dehydrogenase quinone 1 and glutathione S-transferase P1 and marked decrease in peroxyl radical scavenging activity have been described in *Hmox1* knockouts even under basal (unstimulated) conditions [7]. Bilirubin per se is considered a potent endogenous antioxidant protecting against diseases associated with oxidative stress [8] and counteracting harmful effects of various prooxidants including hydrophobic bile acids (BA) on cells and tissues [9]. In fact, both bilirubin and BA are accumulated in plasma and tissues during cholestasis and while BA are responsible for increased lipid peroxidation and oxidative liver damage, bilirubin has a protective effect [10].

Gangliosides are ubiquitously found in all tissues, but most abundantly in the nervous system [11]. They substantially influence the organization of the membrane and the function of specific membrane-associated proteins due to lipid-lipid and lipid-protein lateral interactions [12]. In the brain, ganglioside expression correlates with neurogenesis, synaptogenesis, synaptic transmission, and cell proliferation [13, 14].

It is known that gangliosides form so called caveolae or “detergent resistant microdomains” (DRM), which are crucial elements for cell-cell recognition, adhesion, and especially membrane stabilization [15, 16]. There is also evidence that caveolin-1, an important component of caveolae, interacts with *Hmox1*, modulates its activity, and can act as a natural competitive inhibitor of *Hmox1* with heme [17]. Moreover, gangliosides have been found to inhibit hydroxyl radical formation *in vitro* [18] and also modulate ROS formation in human leukocytes [19] and neuronal cells [20].

Despite the close relationship of gangliosides and *Hmox1* in DRM, there are only few reports discussing the possible role of *Hmox1* or oxidative stress in ganglioside metabolism [21, 22]. The aim of this study was to assess the role of *Hmox1* knockout and associated oxidative stress on ganglioside metabolism and to identify the possible underlying mechanisms.

2. Materials and Methods

2.1. Materials. Paraformaldehyde, biotin, bovine serum albumin (BSA), phorbol 12-myristate 13-acetate (protein kinase C (PKC) activator), Ro 31-0432 (PKC inhibitor), chenodeoxycholic acid (CDCA), diaminobenzidine tetrahydrochloride tablets, NADPH, and sulfosalicylic acid were supplied by Sigma-Aldrich (St. Louis, MO, USA); avidin was obtained from Fluka (Buchs, Switzerland), the cholera toxin B subunit (CTB) peroxidase conjugated came from List Biological Laboratories (CA, USA), and the HPTLC silica-gel plates came from Merck (Darmstadt, Germany). Cell plates were supplied by Corning (NY, USA). The TaqMan® Gene Expression Master Mix, High-Capacity RNA-to-cDNA Kit,

and the TaqMan Gene Expression Assay kit for mouse and human genes were obtained from Life Technologies (Carlsbad, CA, USA). The QIAshredder kit and RNeasy Plus Mini Kit were supplied by Qiagen (USA). All other chemicals were purchased locally from Penta (Prague, Czech Republic).

2.2. Animals. *Hmox1*^{-/-} ($n = 9$; KO—knockout) mice and *Hmox1*^{+/+} ($n = 6$; Wt—wild type) littermates (C57Bl/6xFVB, 8-week-old males) were used for all the experiments. Breeding heterozygote pairs of *Hmox1*-deficient mice were initially kindly provided by Anupam Agarwal, University of Alabama (Birmingham, AL). The *Hmox1*^{-/-} strain poorly breeds on pure C57/Bl6 background (5.1% of expected *Hmox1*^{-/-} pups) and therefore is maintained on mixed C57/Bl6 × FVB background (20.1% of expected *Hmox1*^{-/-} pups, when *Hmox1*^{-/-} males are crossed with *Hmox1*^{+/-} females) [23]. All *Hmox1*^{+/+} controls were C57/Bl6xFVB littermates from the same breeders used to obtain *Hmox1*^{-/-} mice. They had free access to food and water and were kept in individually ventilated cages with a 12:12 day/night cycle, under a specific pathogen-free regime. All aspects of the study met the accepted criteria of experimental use of laboratory animals, and all protocols were approved by the Animal Research Committee of the 1st Faculty of Medicine, Charles University, Prague, Czech Republic, and by the 1st Local Ethics Committee for Animal Research, Krakow, Poland.

2.3. Tissue Preparation. Mice were intraperitoneally anesthetized with ketamine (90 mg/kg) and xylazine (10 mg/kg) and sacrificed by cervical dislocation at day 5. The inferior vena cava was cannulated through laparotomy, and blood samples were collected, transferred to EDTA-containing tubes, mixed, and placed on ice. An aliquot was centrifuged to separate out the plasma. The livers and brains were then harvested and weighed. Pieces of liver tissues were appropriately processed for further biochemical and histochemical analyses (see below). For quantitative histochemical analysis of GM1 ganglioside, the liver specimens were collected using a systematic uniform random sampling method [24].

For the RNA analysis, 100 mg of tissue was immediately placed in 1.5 mL microcentrifuge tubes containing RNeasy Lysis Buffer (Qiagen, Valencia, CA, USA). The tubes were stored at -80°C until total RNA isolation.

2.4. Extraction and TLC Densitometry of Liver and Brain Gangliosides. The chloroform-methanol extraction of gangliosides from the liver tissue was used—the procedure previously described by Majer et al. [25]—and gangliosides were finally purified on a small silica gel column [26]. Brain gangliosides were isolated as described previously [27, 28]. All ganglioside samples were separated in a solvent system (chloroform/methanol/0.2% aqueous CaCl_2 , 55/45/10, v/v/v) and detected with resorcinol-HCl reagent. The densitometry was performed according to Majer et al. [25] using a CATS3 Software, CAMAG (Switzerland).

GSL are abbreviated according to recommendations of the IUPAC-IUB Commission on Biochemical Nomenclature [29]: glycosyltransferases: *GlcT*, UDP-glucose ceramide

glucosyltransferase; *GalTI*, UDP-Gal:betaGlcNAc beta-1,4-galactosyltransferase; *ST3GalV* (*GM3 synthase*), ST3 beta-galactoside alpha-2,3-sialyltransferase 5; *ST8Sial* (*GD3 synthase*), ST8 alpha-*N*-acetylneuraminide alpha-2,8-sialyltransferase 1; *B4GalNTI* (*GM2/GD2 synthase*), beta-1,4-*N*-acetyl-galactosaminyltransferase 1; and *B3GalTIV* (*GM1 synthase*), UDP-Gal:betaGlcNAc beta 1,3-galactosyltransferase.

2.5. GM1 Histochemistry. GM1 was determined using a modified procedure according to Jirkovská et al. [30]. In brief, 4% formaldehyde was freshly prepared by depolymerization of paraformaldehyde (pH = 7.2). Frozen 6 μ m thin sections were first fixed in dry cold acetone (-20°C) for 15 min and then in 4% freshly prepared paraformaldehyde for 5 min. Endogenous peroxidase activity was blocked by incubation for 15 min in phosphate-buffered saline (PBS) supplemented by 1% H_2O_2 and 0.1% sodium azide. Endogenous biotin was blocked by means of a DakoCytomation blocking kit (DakoCytomation, Denmark). In order to block nonspecific binding, sections were treated with 3% BSA in PBS for 15 min. GM1 ganglioside was detected in liver sections using CTB biotin labelled (Sigma, USA), diluted 1:300 in PBS, plus 3% BSA at 8°C for 16.5 h, followed with streptavidin-peroxidase polymer at room temperature for 1 h. Peroxidase activity was visualized with diaminobenzidine tetrahydrochloride for 20 min in the dark. Sections were mounted in mounting medium Dako S3025 (Dako North America, CA, USA).

Two negative control tests were performed for each group. First, CTB was omitted in immunohistochemical staining. Second, fixed sections were extracted with chloroform:methanol 2:1 at room temperature for 30 minutes followed by standard immunohistochemical staining.

2.6. Densitometric Analysis of GM1 Ganglioside in Sinusoidal Membrane and Adjacent Cytoplasm Areas. Six liver specimens were used from each animal. One section from each specimen was used for GM1 ganglioside detection with CTB as described above. From each section, four hepatic lobules with a clearly discernible central vein were selected. In each lobule, one measuring frame in the central lobular zone III and one measuring frame in the corresponding peripheral lobular zone I were selected for analysis. In each frame, 15 areas of sinusoidal surface and 15 areas of adjacent hepatocyte cytoplasm were selected by the stratified random sampling method [24] and marked out. The reaction product was quantified as the mean optical density of the analyzed areas (determined by the densitometric program ACC 6.0, SOFO, Czech Republic) at objective magnification of 40x (NA = 0.7). The ratios of densities measured in the sinusoidal membrane and subsinusoidal intracellular compartment were measured and compared together (sin/int).

2.7. Cell Culture Experiments. Human neuroblastoma cell line SH-SY5Y (ATCC, Manassas, VA, USA) was cultured in the Minimum Essential Medium Eagle (MEM) and Ham's F-12 medium (1:1, v/v) with 15% of fetal bovine serum and human hepatoblastoma cell line HepG2 (ATCC, Manassas, VA, USA) in MEM with 10% of fetal bovine serum in a

humidified atmosphere (containing 5% CO_2 and 37°C). Authentication of used cell lines was confirmed by an independent laboratory using a method based on an accredited short tandem repeat analysis.

Cells were seeded onto 6-well plates (Corning, NY, USA) at a concentration of 50,000 cells per 1 cm^2 and treated with CDCA and bilirubin for 4 h. SH-SY5Y cells were also treated with PKC activator (phorbol 12-myristate 13-acetate) or PKC inhibitor (Ro 31-0432) for 4 h. After the incubation period, cells were harvested into the lysis buffer and stored at -80°C for further experiments.

2.8. Measurement of Intracellular ROS Production. ROS production was determined using a fluorescent probe 5-(and-6)-chloromethyl-2',7'-dichlorodihydrofluorescein diacetate acetyl ester (CM-H₂DCFDA, Life Technologies, USA). Briefly, SH-SY5Y cells were grown in 12-well plates to 80% confluence. Cells were then incubated with CDCA and/or antioxidant (bilirubin) for 24 h. After the incubation, the cells were washed twice with PBS and loaded with 10 μM CM-H₂DCFDA at 37°C for 30 min in the dark, then washed with PBS to remove excess dye. Fluorescence was measured using 485 nm excitation and 540 nm emission wavelengths in microplate reader (Synergy HTX, BioTek, USA). Cells were then lysed with Cell Lysis Buffer (Cell Signaling Technology, USA), and protein concentration was measured using DC Protein Assay (Bio-Rad, USA) according to the manufacturer's instruction. Data were normalized to protein content and expressed as % of controls.

2.9. Lipid Peroxidation. Lipid peroxidation was measured according to the method by Vreman et al. [31]. Twenty microliters of 10% liver or brain sonicates in 0.1 M phosphate buffer, pH = 7.4, were incubated at 37°C with 100 μM ascorbate (80 μL) and 6 μM Fe^{2+} (0.5 μL) in a septum-sealed vial. Butylated hydroxytoluene (10 μM) was added to the blank reaction. The reaction was terminated by adding 2 μL of 60% sulfosalicylic acid. CO produced into the vial headspace was quantified by gas chromatography with a reduction gas analyzer (Peak Laboratories LLC, Mountain View, CA, USA). The amount of CO produced served as an index of lipid peroxidation, was measured as picomoles of CO per hour per milligram of fresh tissue, and was expressed as % of control.

2.10. Western Blotting. Cells grown to 60% confluency were lysed using RIPA buffer supplemented with phosphatase and protease inhibitors (Protease Inhibitor Mix G and Phosphatase Inhibitor Mix I, Serva, Heidelberg, Germany). Samples were separated by SDS-PAGE on 12% polyacrylamide gel and then transferred to nitrocellulose membrane (Bio-Rad Laboratories, Hercules, CA, USA). After blocking in Tween-PBS with 5% BSA (Sigma-Aldrich, St. Louis, MO, USA) for at least 1.5 h, membranes were incubated with GM3 synthase and GM2/GD2 synthase antibody (1:2000; Santa Cruz sc-365329 and sc-376505, Dallas, TX, USA), or β -actin (1:2000; Cell Signaling Technology, Danvers, MA, USA) overnight at 4°C . After washing, membranes were incubated with anti-mouse m-IgG κ BP-HRP (Santa Cruz

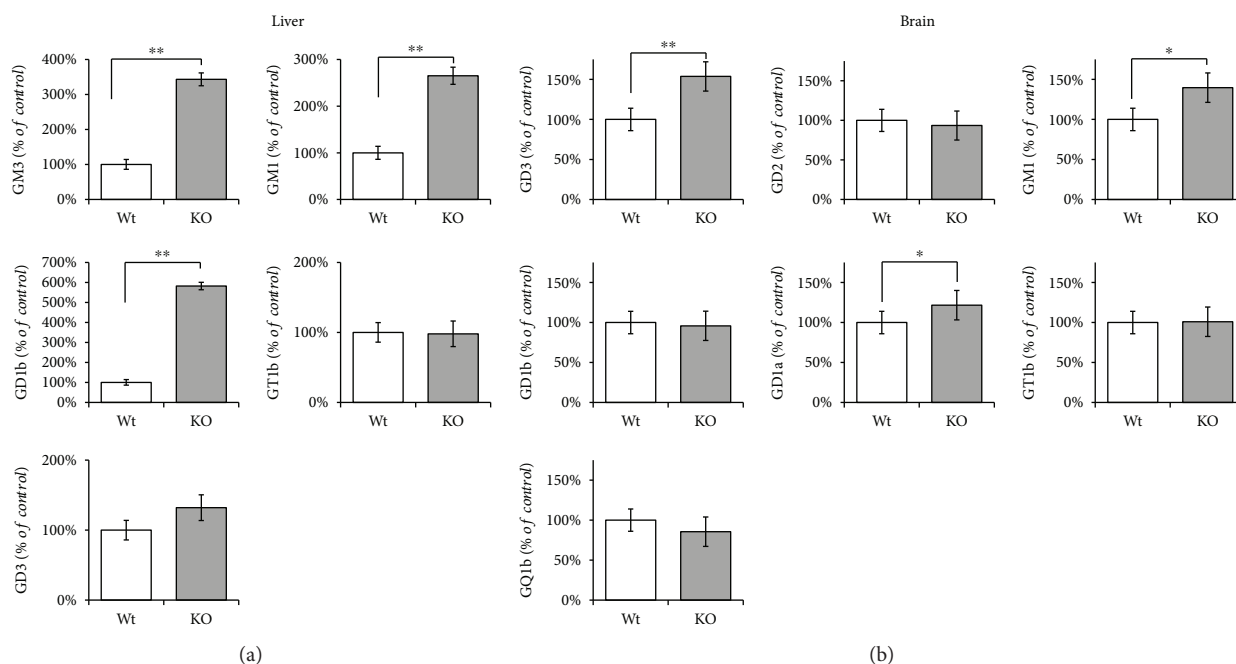


FIGURE 1: The impact of *Hmox1* knockout on ganglioside composition in mouse (a) liver and (b) brain. Isolated hepatic (a) and brain (b) gangliosides were separated in a solvent system and analyzed by a densitometric method after TLC separation and detection using resorcinol-HCl reagent. Values are expressed as % of control and represent mean SD. Wt: wild-type ($n = 6$); KO: *Hmox1* knockout ($n = 9$). * $P < 0.05$ and ** $P < 0.01$.

sc-516102, Dallas, TX, USA) for 1 h. Immunocomplexes on the membranes were visualized with ECL Western Blotting Detection Reagents (Cell Signaling Technology) using an Odyssey infrared imaging system (LI-COR Biosciences, Lincoln, NE, USA).

2.11. Quantitative Real-Time PCR. The liver samples were stored frozen at -80°C in RNAlater (Sigma-Aldrich, St. Louis, USA), and total RNA was isolated using a Qiagen RNeasy Plus kit and QIAshredder (Qiagen, USA). Cell culture samples were stored in lysis buffer at -80°C , and total RNA was isolated using PerfectPure RNA Cell Kit (5Prime, USA). A High-Capacity cDNA Reverse Transcription Kit (Life Technologies, Carlsbad, CA, USA) was used to generate cDNA. Quantitative real-time PCR was performed using TaqMan[®] Gene Expression Assay Kit (Life Technologies, Carlsbad, CA, USA) for the following genes: *GlcT* (Hs00234293_m1), *GalTI* (Hs00191135_m1), GM3 synthase (*St3GalV*, Mm00488237_m1, and Hs01105379_m1), GD3 synthase (*STSia8*, Mm00456915_m1, and Hs00268157_m1), GM2/GD2 synthase (*B4GalNT1*, Mm00484653_m1, and Hs01110791_g1), and GM1 synthase (*B3GalT4*, Mm00546324_s1, and Hs00534104_s1), all provided by Life Technologies (Carlsbad, CA, USA). The data were normalized to HPRT and expressed as percent of control levels.

2.12. Statistical Analysis. Normally distributed data are presented as mean \pm SD and analyzed by the Student *t*-test. The Mann-Whitney *U* test or Kruskal-Wallis test were used in skewed data. Differences with $P < 0.05$ were considered significant.

3. Results

3.1. The Impact of *Hmox1* Knockout on the Liver and Brain Ganglioside Content. To investigate the role of *Hmox1* knockout on the ganglioside pattern, we measured changes in ganglioside composition in the liver as well as the brain, the tissue with the highest glycolipid content *in vivo*. As the ganglioside spectra differ within specific tissues, only major gangliosides and representatives of two main biosynthetic pathways, *a*- and *b*-series, were determined.

In the liver, mice lacking *Hmox1* exhibited marked increases in the concentrations of individual gangliosides. Specifically, *Hmox1* knockout led to a significant increase in GM3 ($343 \pm 76\%$, $P < 0.001$) and GM1 ($265 \pm 62\%$, $P < 0.001$) representing *a*-series, and GD1b ($582 \pm 176\%$, $P < 0.001$) from *b*-series of gangliosides (Figure 1(a)).

In the brain, the most abundant ganglioside was GD1a in both wild-type as well as knockout animals. Together with GM1, GD1a content was significantly higher (GD1a 122% vs. Wt, $P < 0.05$; GM1 140% vs. Wt, $P < 0.05$) in *Hmox1* knockout mice as compared to wild types. The other two major brain gangliosides (GM3, GT1b) stayed unchanged after *Hmox1* knockout. The amount of minor GD3 ganglioside was also significantly increased (154% vs. Wt, $P < 0.01$) (Figure 1(b)). The scheme of *de novo* biosynthesis of the oligosaccharide moieties of gangliosides is illustrated in Figure 2.

To confirm the level of oxidative stress in *Hmox1* knockouts, we measured the extent of lipid peroxidation in liver and brain tissue homogenates. Importantly, liver lipid peroxidation was increased in *Hmox1* knockout mice as compared to controls ($155\% \pm 51\%$ *Hmox1*^{-/-}, $n = 7$, vs. $100\% \pm 46\%$

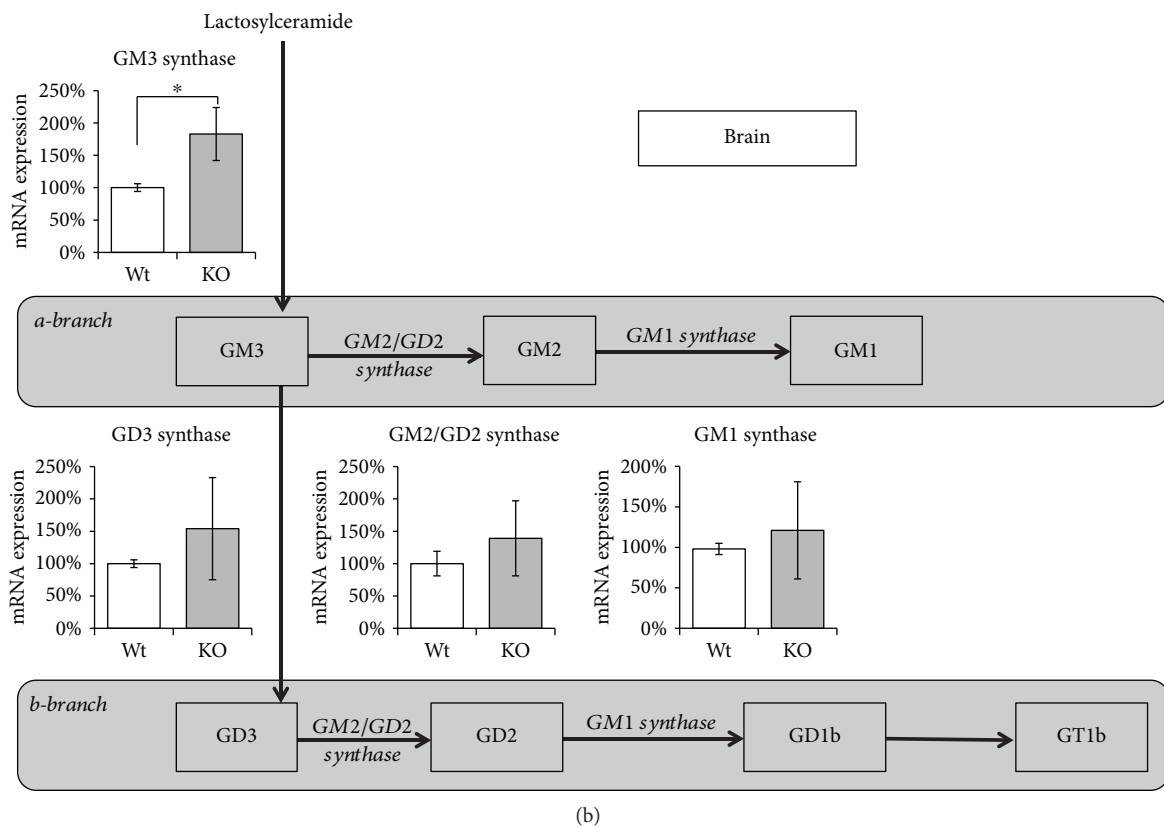
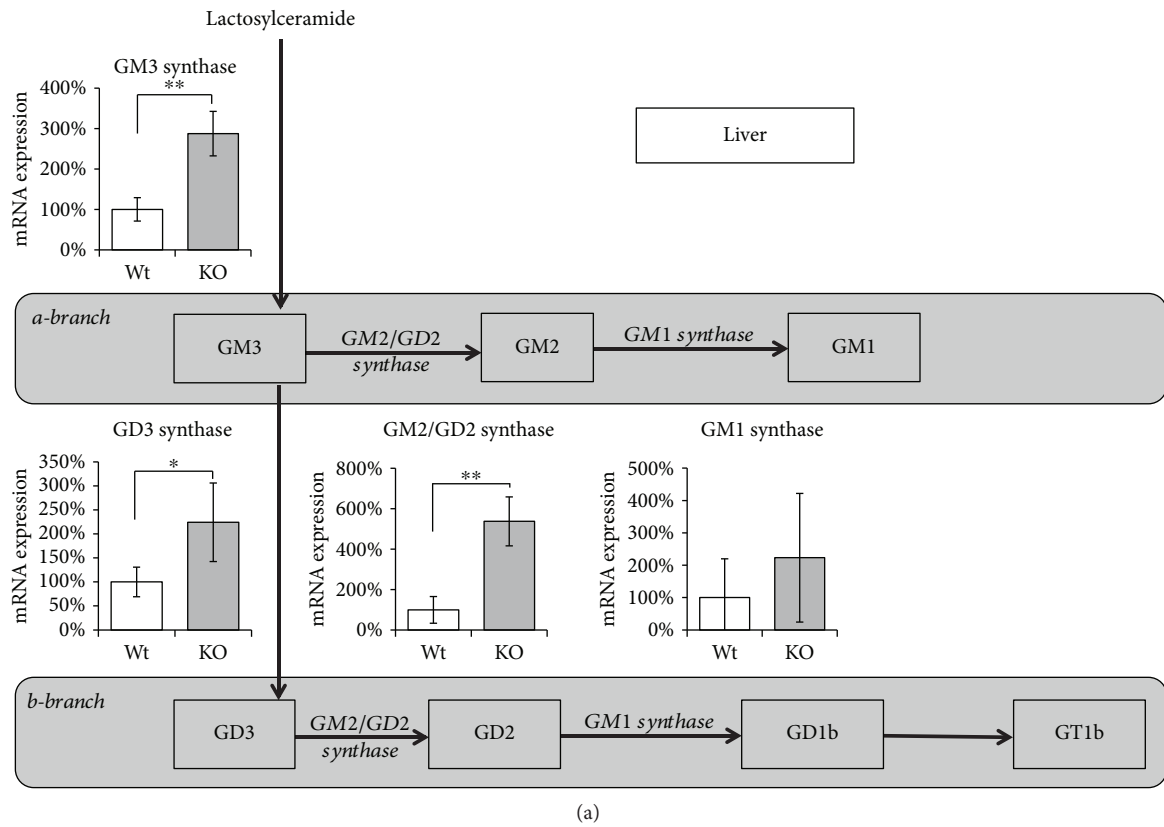


FIGURE 2: *Hmox1* knockout leads to changes in sialyltransferase expression in the liver and brain. Relative mRNA expression of the key enzymes in ganglioside synthesis was measured in the liver (a) and brain (b) tissues of wild-type (Wt) and *Hmox1* knockout (KO) animals. Values are expressed as % of control. Wt: wild-type ($n = 6$); KO: *Hmox1* knockout ($n = 9$). * $P < 0.01$; ** $P < 0.001$.

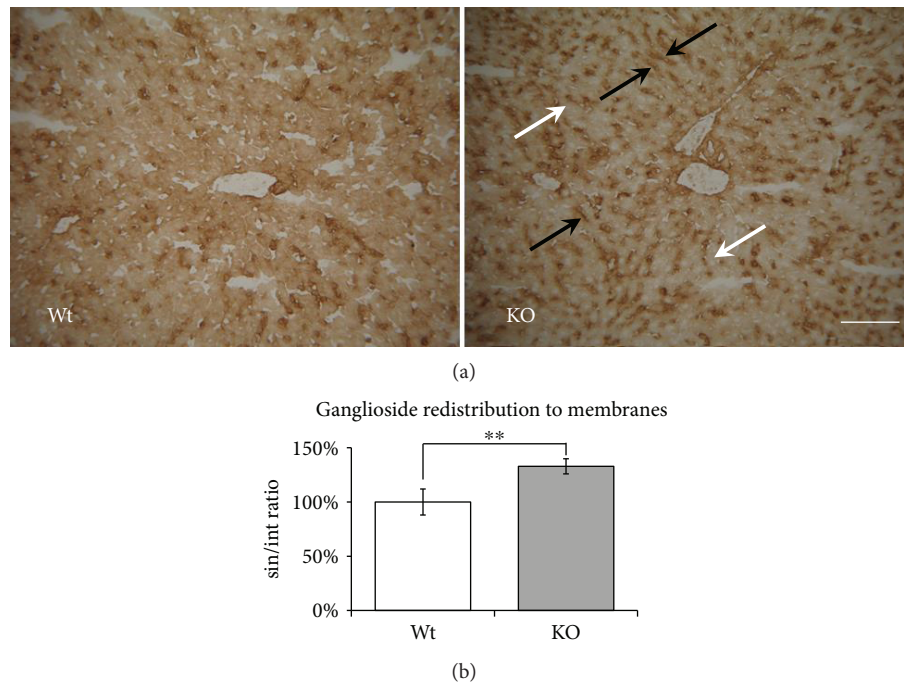


FIGURE 3: The effect of *Hmox1* knockout on distribution/localization of GM1 ganglioside in the liver. (a) Immunohistochemical detection of GM1 ganglioside. In the liver sections, GM1 ganglioside was detected using the cholera toxin B subunit with streptavidin-peroxidase polymer. Diaminobenzidine tetrahydrochloride (brown colour) was used for visualization. The shift of GM1 ganglioside expression from intracellular localization (white arrows) into sinusoidal membranes (black arrows) was observed in *Hmox1* knockout animals. (b) Quantification of GM1 staining in the liver. Image analysis of the distribution of GM1 ganglioside staining in the subsinusoidal part of the intracellular compartment (int) and sinusoidal membranes (sin) of hepatocytes, expressed as the sin/int ratio relative to control (Wt). The reaction product was quantified as the mean optical density of the analyzed areas at objective magnification of 40x (NA = 0.7). Bar represents 100 μ m. Wt: wild-type ($n = 6$); KO: *Hmox1* knockout ($n = 9$). ** $P < 0.01$.

Hmox^{+/+}, $n = 6$, $P = 0.032$). No significant increase was observed in a brain tissue ($115 \pm 46\%$ *Hmox*^{-/-}, $n = 7$, vs. $100 \pm 45\%$ *Hmox*^{+/+}, $n = 6$, $P = 0.311$).

3.2. *Hmox1* Knockout Results in Changes in the Expression of Sialyltransferases. Relative mRNA expression of the key sialyltransferases was determined to elucidate the activation rate of *a*- and *b*-series of a ganglioside biosynthetic pathway in mouse liver and brain homogenates. *Hmox1* knockout led to a significant increase in mRNA expression of GM3 synthase (*ST3GalV*) ($287 \pm 55\%$, $P < 0.001$; $183 \pm 41\%$, $P < 0.01$) in both liver and brain, and GD3 synthase (*St8SiaI*) ($224 \pm 89\%$, $P < 0.01$), the key step in an activation of *b*-biosynthetic branch in the liver. *Hmox1* knockout caused also significant activation of GM2/GD2 synthase (*B4GalNTI*) ($538 \pm 121\%$, $P < 0.001$) in the liver. Expression of GM1 synthase (*B3GalTIV*) stayed unchanged in both liver and brain (Figure 2).

3.3. *Hmox1* Knockout Leads to a Marked Shift of Gangliosides to the Hepatocyte Membrane. To study possible changes in distribution of gangliosides within mouse hepatocytes, histochemical localization of GM1, the representative of gangliosides, was determined in the liver sections. In control liver specimens, GM1 was detected in both sinusoidal and canalicular membranes, as well as in the intracytoplasmic compartment. In *Hmox1* knockout animals, we observed a pronounced shift in GM1 ganglioside expression

from intracellular localization into sinusoidal membranes (Figure 3(a)). To quantify this redistribution pattern of GM1, we measured the GM1 expression under high microscopic magnification expressed as sin/int ratio (GM1 staining in the sinusoidal membrane/subsinusoidal intracellular compartment) ($133 \pm 7\%$, $P < 0.01$, Figure 3(b)).

3.4. Ganglioside Pattern in Neuroblastoma Cells (SH-SY5Y) Is Affected by Oxidative Stress. To find out whether changes in the ganglioside pattern might be affected by an increased oxidative stress associated with *Hmox1* knockout, we investigated the regulation of glycosphingolipid (GSL) synthesis using SH-SY5Y neuroblastoma cells rich in gangliosides. CDCA, a potent inducer of ROS production accumulating in the liver during cholestasis, was used to increase oxidative stress *in vitro*, while addition of bilirubin, a potent antioxidant and a product of the *Hmox* pathway, had an opposite effect (Figure 4).

Administration of CDCA (80 μ M) resulted in a significant increase in the major gangliosides GD1a (141%, $P < 0.01$), GM3 (170%, $P < 0.01$), and GM2 (130%, $P < 0.05$) in SH-SY5Y neuroblastoma cells (Figure 5(a)) and GM3 (233%, $P < 0.01$) and GM2 (251%, $P < 0.05$) in hepatoblastoma HepG2 cells (Figure 5(b)). Interestingly, coadministration of bilirubin (CDCA/bilirubin), a potent antioxidant, resulted in normalization of the ganglioside pattern in both cell lines (Figure 5).

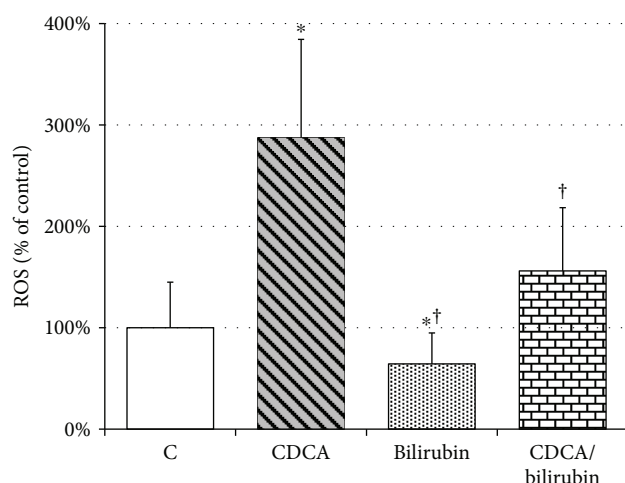


FIGURE 4: The ameliorating effect of bilirubin on CDCA-induced oxidative stress in SH-SY5Y cells. SH-SY5Y cells were incubated with CDCA (80 μ M), bilirubin (1 μ M), or both (CDCA/bilirubin) for 24 h. ROS production was measured using fluorescent CM-H2DCFDA probe. Values are expressed as % of controls. C: control; CDCA: chenodeoxycholic acid (80 μ M); bilirubin: 1 μ M bilirubin; CDCA/bilirubin: CDCA (80 μ M) + bilirubin (1 μ M). * P < 0.05 vs. C; † P < 0.05 vs. CDCA.

3.5. Oxidative Stress-Mediated Changes in Sialyltransferase (*ST3GalV*) Expression Are Regulated through the Protein Kinase C Pathway. To elucidate whether oxidative stress induced by CDCA affects the expression of GM3 synthase (*ST3GalV*), a key enzyme in ganglioside metabolism, *in vitro*, SH-SY5Y as well as HepG2 cell lines were incubated with CDCA and/or bilirubin for 4 h. Significant increases in GM3 synthase mRNA expression were observed upon CDCA treatment while cotreatment with bilirubin abolished this effect in both neuroblastoma (Figure 6(a)) and hepatic (Figure 6(c)) cell lines. The results were confirmed by the detection of GM3 synthase protein expression in the SH-SY5Y cell line (Figure 6(b)).

To investigate the possible role of the PKC pathway on oxidative stress-mediated changes in ganglioside expression, we measured the effect of PKC induction/inhibition (PKC^{+/-}) on the mRNA expression of *GM3 synthase* (*ST3GalV*), in the SH-SY5Y cell line. PKC activators induced the mRNA expression of *ST3GalV*. On the other hand, PKC inhibitors significantly decreased *ST3GalV* mRNA expression. Importantly, cotreatment of CDCA with PKC inhibitor completely abolished the stimulatory effect of CDCA on *ST3GalV* mRNA (Figure 6(d)). Successful PKC activation and/or inhibition was proven by determination of mRNA expression of PKC alpha, PKC beta, and PKC epsilon (Figure 6(e)).

4. Discussion

Gangliosides play a crucial role in signal transduction pathways, regulating many different cell functions such as proliferation, differentiation, adhesion, and cell death [32, 33]. They are responsible for the rigidity of a plasmatic membrane [34] and participate in a protection against

oxidative stress [19, 21]. However, the significance of changes in ganglioside metabolism under oxidative stress remains to be elucidated. To address this issue, we have studied the consequences of the antioxidant enzyme *Hmox1* deficiency for ganglioside metabolism in mouse tissues. Unlike in the brain, we found significantly increased lipid peroxidation in the liver of *Hmox1* knockout animals which is in accordance with the published data showing increased lipid peroxidation and hepatic injury mostly due to iron accumulation in the liver tissue [6]. Our results indicate that oxidative stress plays an important role in ganglioside synthesis resulting in changes in their spectra and cellular distribution.

Gangliosides are ubiquitously found in tissues and body fluid with the most abundant expression in the nervous system [35]. The expression levels of gangliosides undergo dramatic changes during various physiological and pathological conditions including cell death, proliferation, differentiation, development, and oncogenesis [36–38] as well as neurological diseases [39, 40]. These effects are largely attributed to the changes in expression levels of ganglioside synthases (glycosyltransferases) [41, 42]. In our previous experiments on rats, we observed the shift in liver ganglioside synthesis towards more complex ones in various types of cholestatic liver diseases [25, 30]. These changes were associated with the accumulation of detergent and prooxidative bile acids as well as with the increase in oxidative stress in these animals [21, 22].

In the present study, *Hmox1* knockout resulting in the absence of an important antioxidant enzyme in experimental mice was accompanied by significant increases in the brain GM1, GD1a, and GD3 and liver GM1, GM3, and GD1b gangliosides. The tissue specificity of these changes might be explained by the different ganglioside composition of the liver and brain tissues. While GM3 is the main ganglioside in the liver, GD1a is the most abundant in the adult brain [38, 43], where GD1a, GM1, GD1b, GT1b, and GD3 belong to most important glycosphingolipids [44]. Several reports suggest gangliosides to possess antioxidant properties, but very little is known about the function of gangliosides in the liver and therefore most data relates to the nervous tissue [11]. Among these, GM1 ganglioside has neuroprotective functions. Micelles containing GM1 inhibited iron-catalysed hydroxyl radical formation *in vitro* [18], GM1 decreased ROS formation in rat brain synaptosomes [45], or protected cells against H₂O₂-induced oxidative damage [46] while GD1b was able to inhibit lipid peroxidation in human sperm cells [47]. On the other hand, some gangliosides might enhance ROS formation and contribute to the cell death. Sohn et al. [48] found GM3, but not GD3 or GT1b, to mediate oxidative toxicity induced by glutamate in immortalized mouse neuronal HT22 cells. GD3 was described to interact with mitochondria and generate ROS [49, 50], and there is strong evidence for involvement of GD3 in autophagosome formation [51, 52]. GD3 is also considered a key player in apoptosis by Fas, ceramide, and amyloid- β [53, 54]. These findings suggest an important role of gangliosides in processes involved in oxidative stress regulation which might explain their compensatory upregulation in the prooxidative environment of *Hmox1* knockout.

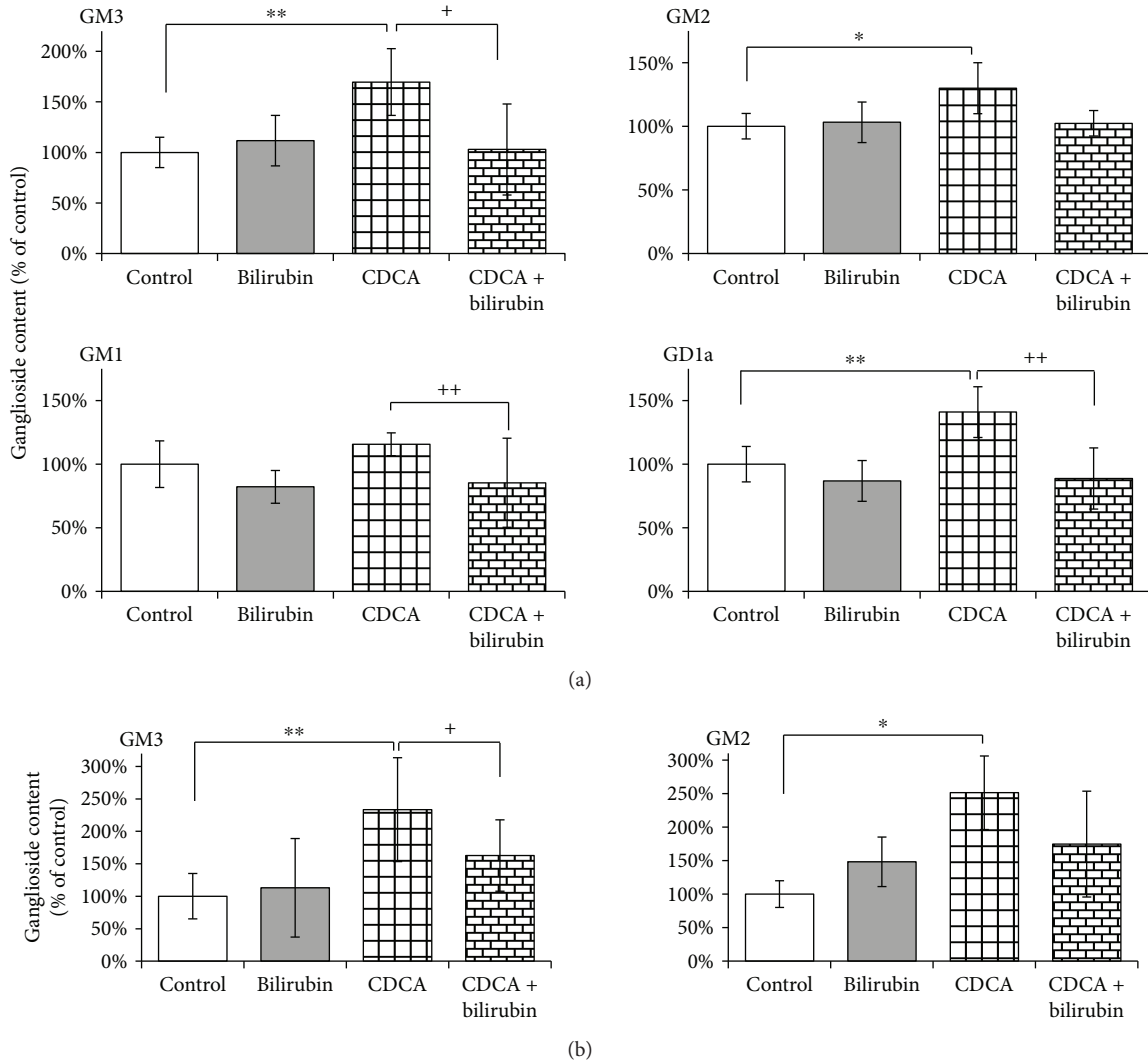


FIGURE 5: The ameliorating effect of bilirubin on CDCA-induced change in ganglioside content in SH-SY5Y cells (a) and HepG2 cells (b). Relative content of individual gangliosides was evaluated using extraction and TLC densitometry after incubation with CDCA or CDCA/bilirubin for 4 in (a) SH-SY5Y cells and (b) HepG2 cells. Values are expressed as % of controls. Bilirubin ($1 \mu\text{M}$); CDCA: chenodeoxycholic acid ($80 \mu\text{M}$); CDCA/bilirubin: CDCA ($80 \mu\text{M}$) + bilirubin ($1 \mu\text{M}$). * $P < 0.05$ vs. C; ** $P < 0.01$ vs. C; + $P < 0.05$ vs. CDCA; ++ $P < 0.01$ vs. CDCA.

The effect of oxidative stress on changes in ganglioside synthesis was further supported by determination of glycosyltransferase mRNA expressions in mouse liver and brain homogenates. The key regulatory enzymes in the synthesis of nearly all gangliosides, *GM3* and *GD3 synthases*, as well as *GalNAcT*, were found to be significantly increased in *Hmox1* knockouts while *GM1* synthase expression stayed unchanged. These data correspond with the observed increases in liver gangliosides and are in accordance with our previous observations on liver glycosyltransferase expression in experimental cholestasis in rats [22]. The increase in liver *GM1* ganglioside content in *Hmox1* knockouts allows speculating that expression of *GM1 synthase* is redundant in wild-type animals and is capable of maintaining the induction of the *GalNAcT* product. Interestingly, only *GM3* synthase has been found to be significantly upregulated in the brain suggesting the tissue-specific regulation of various sialyltransferases. Moreover, different extents of

oxidative stress in particular tissues might affect the final sialyltransferase expression.

Furthermore, in our earlier reports, we described not only an increase in ganglioside synthesis but also their shift into the sinusoidal membranes of hepatocytes upon oxidative stress induced by bile acids [21]. This mechanism could protect hepatocytes against detergent and prooxidant effects of bile acids. A very similar effect was observed in the present study. We have used a selective histochemical approach based on the high binding affinity of *Cholera toxin* B subunit to *GM1* ganglioside [6], the representative of the complex gangliosides. A significant shift of *GM1* gangliosides from intracellular localization to the membrane compartment was found in *Hmox1* knockout which is also associated with prooxidative condition.

To investigate the mechanism of oxidative stress-mediated changes in ganglioside metabolism, we used the *in vitro* model of the SH-SY5Y neuroblastoma cell line rich

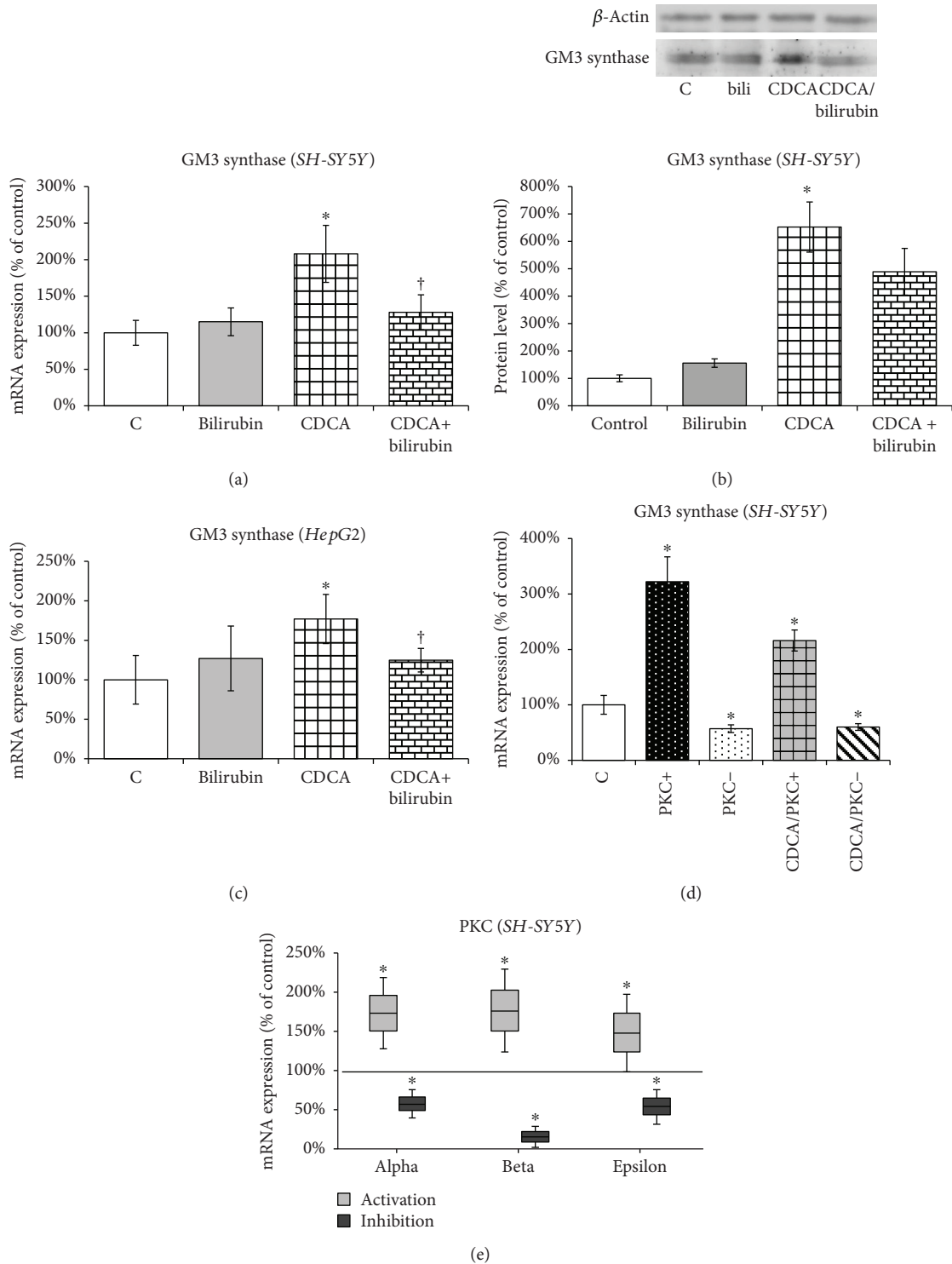


FIGURE 6: The opposite effects of CDCA and bilirubin on regulation of GM3 synthase expression in SH-SY5Y and HepG2 cells. (a) Relative GM3 synthase (ST3GalV) mRNA expression was determined in control cells (C), after 4 h incubation with chenodeoxycholic acid (CDCA) and/or bilirubin in SH-SY5Y cells. (b) Relative GM3 synthase (ST3GalV) protein expression by Western blot was determined in control cells (C), after 4 h incubation with chenodeoxycholic acid (CDCA) and/or bilirubin in SH-SY5Y cells. (c) Relative GM3 synthase (ST3GalV) mRNA expression was determined in control cells (C), after 4 h incubation with chenodeoxycholic acid (CDCA) and/or bilirubin in HepG2 cells. (d) PKC activity was modulated by incubating SH-SY5Y cells with PKC activator (PKC⁺) or PKC inhibitor (PKC⁻) or their combination with CDCA (CDCA/PKC⁺, CDCA/PKC⁻) for 4 h. (e) PKC activation and/or inhibition was proven by determination of mRNA expression vs. control (100% line) of PKC alpha, PKC beta, and PKC epsilon in SH-SY5Y cells. Values are expressed as % of controls. C: control; PKC⁺: PKC activation by phorbol 12-myristate 13-acetate (5 μ M); PKC⁻: PKC inhibition by Ro 31-0432 (5 μ M); CDCA: chenodeoxycholic acid (80 μ M); CDCA/bilirubin: CDCA (80 μ M) + bilirubin (1 μ M). **P* < 0.05 vs. C; †*P* < 0.05 vs. CDCA.

in glycosphingolipids and, for the comparison, the human hepatoblastoma HepG2 cell line. Interestingly, the HepG2 cell line was found to be very poor in ganglioside content and completely lacking GD3 synthase. Exposure of SH-SY5Y to oxidative stress induced by chenodeoxycholic acid [55] resulted in a significant increase in all major gangliosides of this cell line—GD1a, GM3, and GM2—while addition of a potent antioxidant, bilirubin [56], resulted in normalization of the ganglioside content. Importantly, the same pattern was observed in the HepG2 cell line in GM3 and GM2 gangliosides. These results are in accordance with our earlier observations [10] that bilirubin may counteract a prooxidative effect of BA on hepatocytes in the model of obstructive cholestasis in rats. Furthermore, accumulation of hydrophobic BA in the brain and their possible involvement in hepatic encephalopathy associated with cholestatic liver diseases has been reported [57]. BA can act as cell signalling effectors through binding and activating receptors on both the cell membrane and nucleus. BA signalling encompasses both direct (FXR, TGR5) and indirect (FGF19, GLP-1) pathways. The role of BA in extrahepatic diseases is becoming more important, and increasing amount of reports suggests that BA might play an important role in neurological function and diseases [58, 59].

To elucidate the mechanism of oxidative stress-induced changes of ganglioside metabolism, we focused on regulation of the main enzyme in complex ganglioside synthesis, GM3 synthase (*ST3GalV*).

PKC appeared to be a logical candidate regulating the expression of GM3 synthase. Hydrophobic bile acids are considered potent inducers of PKC while antioxidants inhibit PKC activity [60, 61]. For more than 30 years, it has been known that ganglioside metabolism is in tight connection to PKC activity [62–64], and the action of glycosyltransferases is controlled through posttranslational modification. Glycosyltransferase activities have been demonstrated to be significantly modulated by the action of PKC [65]. Another study suggested the role of PKC as an activator of GM3 synthase (*ST3GalV*) [66]. Our *in vitro* data support this hypothesis. While PKC activators and oxidative stress induced the expression of *ST3GalV*, PKC inhibitors as well as antioxidants completely abolished this effect.

There are some limitations of our study. First, we were primarily interested in the shift of GSL to the cytoplasmic membrane; however, more studies are needed to assess whether subcellular localization and trafficking of gangliosides are affected as well. Second, in histochemical analyses, we used GM1 as a GSL representative but further studies with individual gangliosides are needed to confirm that the shift of GM1 from the intracellular compartment to the cytoplasmic membrane is a general reaction to loss of Hmox1 action. Finally, the PKC pathway is an important but probably not the only pathway regulating GSL metabolism affected by oxidative stress.

5. Conclusions

We conclude that oxidative stress is an important factor modulating synthesis and distribution of gangliosides *in vivo* and *in vitro*. Knockout of *Hmox1*, an important

antioxidant enzyme, results in tissue-specific increases in main gangliosides together with changes in mRNA expression of key enzymes of ganglioside synthesis. We demonstrate that these changes might be, at least partially, mediated through modulation of the PKC pathway.

Data Availability

The raw data used to support the findings of this study are available from the corresponding author upon request.

Conflicts of Interest

The authors declare that there is no conflict of interest regarding the publication of this paper.

Acknowledgments

The study was supported by Grant RVO-VFN64165/2018 given by the Czech Ministry of Health; PROGRES Q25/LF1, GAUK 516912, and SVV 260370-2017 provided by the Charles University, Prague, Czech Republic; and the statutory funds from the Jagiellonian University. The Faculty of Biochemistry, Biophysics and Biotechnology of Jagiellonian University is a partner of the Leading National Research Centre (KNOW) supported by the Ministry of Science and Higher Education. The authors wish to thank Janusz Drobot and Witold Nowak for their help with the animal experiments, Kateřina Žižalová for her help with cell culture experiments, and Olga Švejsová and Marie Kolářová for their excellent technical assistance.

References

- [1] L. E. Otterbein, M. P. Soares, K. Yamashita, and F. H. Bach, “Heme oxygenase-1: unleashing the protective properties of heme,” *Trends in Immunology*, vol. 24, no. 8, pp. 449–455, 2003.
- [2] P. Ayuso, C. Martínez, P. Pastor et al., “An association study between *Heme oxygenase-1* genetic variants and Parkinson’s disease,” *Frontiers in Cellular Neuroscience*, vol. 8, p. 298, 2014.
- [3] H. Schipper and W. Song, “A heme oxygenase-1 transducer model of degenerative and developmental brain disorders,” *International Journal of Molecular Sciences*, vol. 16, no. 12, pp. 5400–5419, 2015.
- [4] L. E. Fredenburgh, A. A. Merz, and S. Cheng, “Haeme oxygenase signalling pathway: implications for cardiovascular disease,” *European Heart Journal*, vol. 36, no. 24, pp. 1512–1518, 2015.
- [5] K. D. Poss and S. Tonegawa, “Reduced stress defense in heme oxygenase 1-deficient cells,” *Proceedings of the National Academy of Sciences of the United States of America*, vol. 94, no. 20, pp. 10925–10930, 1997.
- [6] S. T. Fraser, R. G. Midwinter, B. S. Berger, and R. Stocker, “Heme oxygenase-1: a critical link between iron metabolism, erythropoiesis, and development,” *Advances in Hematology*, vol. 2011, Article ID 473709, 6 pages, 2011.
- [7] T. Mamiya, F. Katsuoka, A. Hirayama et al., “Hepatocyte-specific deletion of heme oxygenase-1 disrupts redox homeostasis in basal and oxidative environments,” *The Tohoku Journal of Experimental Medicine*, vol. 216, no. 4, pp. 331–339, 2008.

- [8] L. Novotny and L. Vitek, "Inverse relationship between serum bilirubin and atherosclerosis in men: a meta-analysis of published studies," *Experimental Biology and Medicine*, vol. 228, no. 5, pp. 568–571, 2003.
- [9] J. Zelenka, L. Muchova, M. Zelenkova et al., "Intracellular accumulation of bilirubin as a defense mechanism against increased oxidative stress," *Biochimie*, vol. 94, no. 8, pp. 1821–1827, 2012.
- [10] L. Muchova, K. Vanova, J. Zelenka et al., "Bile acids decrease intracellular bilirubin levels in the cholestatic liver: implications for bile acid-mediated oxidative stress," *Journal of Cellular and Molecular Medicine*, vol. 15, no. 5, pp. 1156–1165, 2011.
- [11] R. K. Yu, Y. Nakatani, and M. Yanagisawa, "The role of glycosphingolipid metabolism in the developing brain," *Journal of Lipid Research*, vol. 50, pp. S440–S445, 2009.
- [12] A. Regina Todeschini and S. I. Hakomori, "Functional role of glycosphingolipids and gangliosides in control of cell adhesion, motility, and growth, through glycosynaptic microdomains," *Biochimica et Biophysica Acta (BBA) - General Subjects*, vol. 1780, no. 3, pp. 421–433, 2008.
- [13] H. Rahmann, "Brain gangliosides and memory formation," *Behavioural Brain Research*, vol. 66, no. 1-2, pp. 105–116, 1995.
- [14] B. Wang, "Sialic acid is an essential nutrient for brain development and cognition," *Annual Review of Nutrition*, vol. 29, no. 1, pp. 177–222, 2009.
- [15] L. J. Pike, "Rafts defined: a report on the keystone symposium on lipid rafts and cell function," *Journal of Lipid Research*, vol. 47, no. 7, pp. 1597–1598, 2006.
- [16] D. Lingwood and K. Simons, "Lipid rafts as a membrane-organizing principle," *Science*, vol. 327, no. 5961, pp. 46–50, 2010.
- [17] J. Taira, M. Sugishima, Y. Kida, E. Oda, M. Noguchi, and Y. Higashimoto, "Caveolin-1 is a competitive inhibitor of heme oxygenase-1 (HO-1) with heme: identification of a minimum sequence in caveolin-1 for binding to HO-1," *Biochemistry*, vol. 50, no. 32, pp. 6824–6831, 2011.
- [18] M. Gavella, M. Kveder, V. Lipovac, D. Jurašin, and N. Filipovi-Vinceković, "Antioxidant properties of ganglioside micelles," *Free Radical Research*, vol. 41, no. 10, pp. 1143–1150, 2007.
- [19] M. Gavella, M. Kveder, and V. Lipovac, "Modulation of ROS production in human leukocytes by ganglioside micelles," *Brazilian Journal of Medical and Biological Research*, vol. 43, no. 10, pp. 942–949, 2010.
- [20] N. F. Avrova, I. V. Victorov, V. A. Tyurin et al., "Inhibition of glutamate-induced intensification of free radical reactions by gangliosides: possible role in their protective effect in rat cerebellar granule cells and brain synaptosomes," *Neurochemical Research*, vol. 23, no. 7, pp. 945–952, 1998.
- [21] T. Petr, V. Smíd, V. Kučerová et al., "The effect of heme oxygenase on ganglioside redistribution within hepatocytes in experimental estrogen-induced cholestasis," *Physiological Research*, vol. 63, no. 3, pp. 359–367, 2014.
- [22] V. Šmíd, T. Petr, K. Váňová et al., "Changes in liver ganglioside metabolism in obstructive cholestasis - the role of oxidative stress," *Folia Biologica*, vol. 62, no. 4, pp. 148–159, 2016.
- [23] A. Szade, W. N. Nowak, K. Szade et al., "Effect of crossing C57BL/6 and FVB mouse strains on basal cytokine expression," *Mediators of Inflammation*, vol. 2015, Article ID 762419, 10 pages, 2015.
- [24] P. W. Hamilton, "Designing a morphometric study," in *Quantitative Clinical Pathology*, P. W. Hamilton and D. C. Allen, Eds., Blackwell Science, Cambridge, MA, USA, 1995.
- [25] F. Majer, L. Trnka, L. Vitek, M. Jirkovská, Z. Mareček, and F. Šmíd, "Estrogen-induced cholestasis results in a dramatic increase of b-series gangliosides in the rat liver," *Biomedical Chromatography*, vol. 21, no. 5, pp. 446–450, 2007.
- [26] R. K. Yu and R. W. Ledeen, "Gangliosides of human, bovine, and rabbit plasma," *Journal of Lipid Research*, vol. 13, no. 5, pp. 680–686, 1972.
- [27] K. Suzuki, "The pattern of mammalian brain gangliosides-II evaluation of the extraction procedures, postmortem changes and the effect of formalin preservation," *Journal of Neurochemistry*, vol. 12, no. 7, pp. 629–638, 1965.
- [28] J. Folch, M. Lees, and G. H. Sloane Stanley, "A simple method for the isolation and purification of total lipides from animal tissues," *The Journal of Biological Chemistry*, vol. 226, no. 1, pp. 497–509, 1957.
- [29] M. A. Chester, "IUPAC-IUB Joint Commission on Biochemical Nomenclature (JCBN). Nomenclature of glycolipids—recommendations 1997," *European Journal of Biochemistry*, vol. 257, no. 2, pp. 293–298, 1998.
- [30] M. Jirkovská, F. Majer, J. Šmídová et al., "Changes in GM1 ganglioside content and localization in cholestatic rat liver," *Glycoconjugate Journal*, vol. 24, no. 4-5, pp. 231–241, 2007.
- [31] H. J. Vreman, R. J. Wong, C. A. Sanesi, P. A. Dennery, and D. K. Stevenson, "Simultaneous production of carbon monoxide and thiobarbituric acid reactive substances in rat tissue preparations by an iron-ascorbate system," *Canadian Journal of Physiology and Pharmacology*, vol. 76, no. 12, pp. 1057–1065, 1998.
- [32] S. Hakomori, "Carbohydrate-to-carbohydrate interaction, through glycosynapse, as a basis of cell recognition and membrane organization," *Glycoconjugate Journal*, vol. 21, no. 3/4, pp. 125–137, 2004.
- [33] R. L. Schnaar, "Glycolipid-mediated cell–cell recognition in inflammation and nerve regeneration," *Archives of Biochemistry and Biophysics*, vol. 426, no. 2, pp. 163–172, 2004.
- [34] I. Pascher, M. Lundmark, P. G. Nyholm, and S. Sundell, "Crystal structures of membrane lipids," *Biochimica et Biophysica Acta (BBA) - Reviews on Biomembranes*, vol. 1113, no. 3-4, pp. 339–373, 1992.
- [35] R. K. Yu, Y. T. Tsai, and T. Ariga, "Functional roles of gangliosides in neurodevelopment: an overview of recent advances," *Neurochemical Research*, vol. 37, no. 6, pp. 1230–1244, 2012.
- [36] S. Hakomori, "Structure, organization, and function of glycosphingolipids in membrane," *Current Opinion in Hematology*, vol. 10, no. 1, pp. 16–24, 2003.
- [37] M. Bektas and S. Spiegel, "Glycosphingolipids and cell death," *Glycoconjugate Journal*, vol. 20, no. 1, pp. 39–47, 2004.
- [38] S. Ngamukote, M. Yanagisawa, T. Ariga, S. Ando, and R. K. Yu, "Developmental changes of glycosphingolipids and expression of glycogenes in mouse brains," *Journal of Neurochemistry*, vol. 103, no. 6, pp. 2327–2341, 2007.
- [39] Y. H. Xu, S. Barnes, Y. Sun, and G. A. Grabowski, "Multi-system disorders of glycosphingolipid and ganglioside metabolism," *Journal of Lipid Research*, vol. 51, no. 7, pp. 1643–1675, 2010.
- [40] S. Lobasso, P. Tanzarella, D. Vergara, M. Maffia, T. Cocco, and A. Corcelli, "Lipid profiling of *parkin*-mutant human skin

- fibroblasts,” *Journal of Cellular Physiology*, vol. 232, no. 12, pp. 3540–3551, 2017.
- [41] A. Ishii, T. Ikeda, S. Hitoshi et al., “Developmental changes in the expression of glycogenes and the content of N-glycans in the mouse cerebral cortex,” *Glycobiology*, vol. 17, no. 3, pp. 261–276, 2007.
- [42] Y. Suzuki, M. Yanagisawa, T. Ariga, and R. K. Yu, “Histone acetylation-mediated glycosyltransferase gene regulation in mouse brain during development,” *Journal of Neurochemistry*, vol. 116, no. 5, pp. 874–880, 2011.
- [43] A. Yamamoto, M. Haraguchi, S. Yamashiro et al., “Heterogeneity in the expression pattern of two ganglioside synthase genes during mouse brain development,” *Journal of Neurochemistry*, vol. 66, no. 1, pp. 26–34, 1996.
- [44] H. Dreyfus, B. Guérol, L. Freysz, and D. Hicks, “Successive isolation and separation of the major lipid fractions including gangliosides from single biological samples,” *Analytical Biochemistry*, vol. 249, no. 1, pp. 67–78, 1997.
- [45] N. F. Avrova, I. O. Zakharova, V. A. Tyurin, Y. Y. Tyurina, I. A. Gamaley, and I. A. Schepetkin, “Different metabolic effects of ganglioside GM1 in brain synaptosomes and phagocytic cells,” *Neurochemical Research*, vol. 27, no. 7/8, pp. 751–759, 2002.
- [46] I. A. Vlasova, I. O. Zakharova, T. V. Sokolova, and N. F. Avrova, “Metabolic effects of ganglioside GM1 on PC12 cells at oxidative stress depend on modulation of activity of tyrosine kinase of trk receptor,” *Zhurnal Evoliutsionnoï Biokhīmii i Fiziologii*, vol. 49, no. 1, pp. 15–23, 2013.
- [47] M. Gavella, V. Lipovac, R. Rakos, and B. Colak, “Reduction of oxidative changes in human spermatozoa by exogenous gangliosides,” *Andrologia*, vol. 37, no. 1, pp. 17–24, 2005.
- [48] H. Sohn, Y. S. Kim, H. T. Kim et al., “Ganglioside GM3 is involved in neuronal cell death,” *The FASEB Journal*, vol. 20, no. 8, pp. 1248–1250, 2006.
- [49] C. García-Ruiz, A. Colell, R. Paris, and J. C. Fernández-Checa, “Direct interaction of GD3 ganglioside with mitochondria generates reactive oxygen species followed by mitochondrial permeability transition, cytochrome *c* release, and caspase activation,” *The FASEB Journal*, vol. 14, no. 7, pp. 847–858, 2000.
- [50] M. R. Rippo, F. Malisan, L. Ravagnan et al., “GD3 ganglioside directly targets mitochondria in a bcl-2-controlled fashion,” *The FASEB Journal*, vol. 14, no. 13, pp. 2047–2054, 2000.
- [51] M. R. Rippo, F. Malisan, L. Ravagnan et al., “GD3 ganglioside as an intracellular mediator of apoptosis,” *European Cytokine Network*, vol. 11, no. 3, pp. 487–488, 2000.
- [52] P. Matarrese, T. Garofalo, V. Manganelli et al., “Evidence for the involvement of GD3 ganglioside in autophagosome formation and maturation,” *Autophagy*, vol. 10, no. 5, pp. 750–765, 2014.
- [53] F. Malisan and R. Testi, “The ganglioside GD3 as the Greek goddess Hecate: several faces turned towards as many directions,” *IUBMB Life*, vol. 57, no. 7, pp. 477–482, 2005.
- [54] A. Dhanushkodi and M. P. McDonald, “Intracranial *V. cholerae* sialidase protects against excitotoxic neurodegeneration,” *PLoS One*, vol. 6, no. 12, article e29285, 2011.
- [55] L. Fuentes-Broto, E. Martínez-Ballarín, J. Miana-Mena et al., “Lipid and protein oxidation in hepatic homogenates and cell membranes exposed to bile acids,” *Free Radical Research*, vol. 43, no. 11, pp. 1080–1089, 2009.
- [56] L. Vitek and J. Ostrow, “Bilirubin chemistry and metabolism; harmful and protective aspects,” *Current Pharmaceutical Design*, vol. 15, no. 25, pp. 2869–2883, 2009.
- [57] V. Tripodi, M. Contin, M. A. Fernández, and A. Lemberg, “Bile acids content in brain of common duct ligated rats,” *Annals of Hepatology*, vol. 11, no. 6, pp. 930–934, 2012.
- [58] M. McMillin and S. DeMorrow, “Effects of bile acids on neurological function and disease,” *The FASEB Journal*, vol. 30, no. 11, pp. 3658–3668, 2016.
- [59] K. L. Mertens, A. Kalsbeek, M. R. Soeters, and H. M. Eggink, “Bile acid signaling pathways from the enterohepatic circulation to the central nervous system,” *Front Neurosci*, vol. 11, p. 617, 2017.
- [60] Y. P. Rao, R. T. Stravitz, Z. R. Vlahcevic, E. C. Gurley, J. J. Sando, and P. B. Hylemon, “Activation of protein kinase C alpha and delta by bile acids: correlation with bile acid structure and diacylglycerol formation,” *Journal of Lipid Research*, vol. 38, no. 12, pp. 2446–2454, 1997.
- [61] S. F. Steinberg, “Mechanisms for redox-regulation of protein kinase C,” *Front Pharmacol*, vol. 6, p. 128, 2015.
- [62] D. Kreutter, J. Y. Kim, J. R. Goldenring et al., “Regulation of protein kinase C activity by gangliosides,” *Journal of Biological Chemistry*, vol. 262, no. 4, pp. 1633–1637, 1987.
- [63] X. J. Xia, X. B. Gu, A. C. Sartorelli, and R. K. Yu, “Effects of inducers of differentiation on protein kinase C and CMP-N-acetylneuraminic acid:lactosylceramide sialyltransferase activities of HL-60 leukemia cells,” *Journal of Lipid Research*, vol. 30, no. 2, pp. 181–188, 1989.
- [64] J. Aguilera, C. Padrós-Giralt, W. H. Habig, and E. Yavin, “GT1b ganglioside prevents tetanus toxin-induced protein kinase C activation and down-regulation in the neonatal brain in vivo,” *Journal of Neurochemistry*, vol. 60, no. 2, pp. 709–713, 1993.
- [65] R. K. Yu and E. Bieberich, “Regulation of glycosyltransferases in ganglioside biosynthesis by phosphorylation and dephosphorylation,” *Molecular and Cellular Endocrinology*, vol. 177, no. 1–2, pp. 19–24, 2001.
- [66] T. W. Chung, H. J. Choi, Y. C. Lee, and C. H. Kim, “Molecular mechanism for transcriptional activation of ganglioside GM3 synthase and its function in differentiation of HL-60 cells,” *Glycobiology*, vol. 15, no. 3, pp. 233–244, 2005.

Review Article

Role of Oxidative Stress in Pathophysiology of Nonalcoholic Fatty Liver Disease

Mario Masarone ¹, Valerio Rosato,¹ Marcello Dallio,² Antonietta Gerarda Gravina ¹,
Andrea Aglitti ¹, Carmelina Loguercio,² Alessandro Federico ², and Marcello Persico ¹

¹Internal Medicine and Hepatology Division, Department of Medicine, University of Medicine of Salerno, Salerno, Italy

²Hepatogastroenterology Division, University of Campania “Luigi Vanvitelli”, Naples, Italy

Correspondence should be addressed to Mario Masarone; mmasarone@unisa.it

Received 16 March 2018; Accepted 23 May 2018; Published 11 June 2018

Academic Editor: Daniele Vergara

Copyright © 2018 Mario Masarone et al. This is an open access article distributed under the Creative Commons Attribution License, which permits unrestricted use, distribution, and reproduction in any medium, provided the original work is properly cited.

Liver steatosis without alcohol consumption, namely, nonalcoholic fatty liver disease (NAFLD), is a common hepatic condition that encompasses a wide spectrum of presentations, ranging from simple accumulation of triglycerides in the hepatocytes without any liver damage to inflammation, necrosis, ballooning, and fibrosis (namely, nonalcoholic steatohepatitis) up to severe liver disease and eventually cirrhosis and/or hepatocellular carcinoma. The pathophysiology of fatty liver and its progression is influenced by multiple factors (environmental and genetics), in a “multiple parallel-hit model,” in which oxidative stress plays a very likely primary role as the starting point of the hepatic and extrahepatic damage. The aim of this review is to give a comprehensive insight on the present researches and findings on the role of oxidative stress mechanisms in the pathogenesis and pathophysiology of NAFLD. With this aim, we evaluated the available data in basic science and clinical studies in this field, reviewing the most recent works published on this topic.

1. Introduction

The presence of a significant (>5% of hepatocytes) fat accumulation in the liver, in the absence of an “unsafe” quantity of alcohol consumption and any other cause of liver diseases, is a potentially pathological condition that is defined as non-alcoholic fatty liver disease (NAFLD) [1]. In the last two decades, it has become the most “emerging” liver disease worldwide, since we are moving towards a gradual reduction of viral hepatitis and a progressive increase of obesity, following the spread of a “western lifestyle” [2, 3]. A wide pathological spectrum of liver injury is associated with NAFLD, ranging from indolent steatosis, usually characterized by an asymptomatic benign clinical course, to nonalcoholic steatohepatitis (NASH), which can lead to fibrosis with an evolutionary course in cirrhosis and hepatocellular carcinoma (HCC) [4–6]. Alarmingly, in patients with NASH, HCC can also develop itself without first progressing to cirrhosis [7].

The prevalence of NAFLD is estimated to be as high as 17–33% in the general population, while it reaches 75% in obese individuals and even more in patients with type 2 diabetes mellitus (T2DM) [3, 8]. The concomitant presence of T2DM increases the risk of progression of liver damage and constitutes a significant risk for cardiovascular diseases [9].

Although obesity, particularly central (abdominal) obesity, is a well-recognized risk factor for it, NAFLD has been also reported in lean individuals (body mass index < 30 kg/m²) [10]. Furthermore, the prevalence of NAFLD differs depending on the gender, ethnicity, and race as a proof of probable involvement of genetic and epigenetic factors in the pathogenesis of the disease [3, 11, 12].

Insulin resistance (IR) is the major pathophysiological factor implicated in NAFLD, as well as metabolic syndrome (MS), a cluster of cardiovascular risk factors comprising visceral obesity, blood hypertension, glucose intolerance, and dyslipidemia [13]. In this way, NAFLD has been considered

as the liver expression of MS, not only burdened with high cardiovascular risk but also responsible of a progressive metabolic, cardiovascular, and/or kidney disease, even without an overt MS [14].

IR is thought to play a pivotal role both to the initiation of the disease and the pathogenic switch of fatty liver to advanced forms of NAFLD, even if the mechanisms underlying this process are still partially unknown [15]. The pathophysiologic mechanism was firstly hypothesized by Day and James who proposed the “two-hit model,” in which the simple steatosis (the first “hit”) in addition to other factors (that were primarily linked to the increase in oxidative stress) were needed for the development of NASH (the second “hit”) [16]. This first hypothesis has been subsequently revised in a “multiple parallel-hit” model in which, in the presence of a significant accumulation of fat in hepatocytes and systemic and hepatic insulin resistance, multiple simultaneous alterations lead to an imbalance between the antilipotoxic protection system of the liver (mitochondrial betaoxidation) and the free radical production in gut and adipose tissue, resulting in endoplasmic stress, oxidative stress, and hepatocyte apoptosis [17].

In this paper, we will review the main evidences on the strict pathophysiologic linkage between oxidative stress mechanisms and the presence NAFLD and its progression, particularly focusing on the most reported pathophysiologic mechanisms: mitochondrial dysfunction, endoplasmic reticulum (ER) stress, iron metabolism derangements, gut-liver axis, insulin resistance, and endothelial dysfunction.

2. Mitochondrial Dysfunction

Since the first studies on NAFLD, many evidences pointed out that it was primarily characterized by the presence of mitochondrial dysfunction [18]. The homeostasis of fat and energy in hepatic cells is regulated by mitochondrial activities, including betaoxidation of free fatty acids (FFAs), electron transfer and production of ATP, and reactive oxygen species (ROS) [19]. Mitochondrial abnormalities alter the balance between prooxidant and antioxidant mechanisms, leading to an increase of nonmetabolized fatty acids in the cytosol as a result of the blockade of fatty acid betaoxidation and the consequent induction of ROS production [20]. The alteration of mitochondrial functions is evident with electron microscopy analysis by some ultrastructural changes such as megamitochondria, loss of cristae, and paracrystalline inclusion bodies in the matrix [21].

An intriguing hypothesis is that a “primary” mitochondrial dysfunction may be the initiator of accumulation of fatty acids in the hepatocytes during insulin-resistance-associated NAFLD particularly if a fat-rich diet provides an increased supply to the liver [22]. The “primary” mitochondrial dysfunction should be due to multiple mechanisms, ranging from mitochondrial DNA damage to sirtuin imbalance. Damage of mitochondrial DNA (mtDNA) and nucleic genes encoding mitochondrial proteins may involve a progressive increase of oxidative stress levels, as in Alpers-Huttenlocher disease, an autosomal-recessive hepatocerebral syndrome, due to a polymerase gamma mutation and mtDNA depletion,

that causes the development of liver steatosis until end-stage liver failure [23]. Moreover, in a murine model was shown that the mutation of the gene encoding for mitochondrial isobutyryl-CoA-dehydrogenase is associated with a hepatic steatosis [24]. Sirtuins are a group of NAD(+)-dependent deacetylase, involved in oxidative damage of both alcoholic and nonalcoholic fatty liver diseases [25]. SIRT1, the most studied of these enzymes, has an indirect regulatory effect on oxidative stress, activating forkhead proteins and PGC-1, transcription factors involved in transcription of antioxidant enzyme genes and in ROS-detoxifying capacity [26]. SIRT3 can increase betaoxidation of FFAs by activation of long-chain acyl-CoA dehydrogenases, and its activity was found decreased in animal models with fatty liver [27]. In this way, a primary decrease of SIRT3, associated with a fat-rich diet, can initiate a pathological process. Sirtuins 1 and 3 using NAD+ as the cosubstrate elicits various metabolic improvements in many tissues (lung, spleen, brain, and small intestine) [28]. In this way, NAD+ depletion may contribute to mitochondrial dysfunction obstructing the adaptive response mediated by sirtuins to high FFA hepatic levels [29].

Besides the hypothesis of a primary mitochondrial dysfunction, it is noted that, during the early phase of fatty infiltration in the hepatocytes, several adaptive metabolic mechanisms are mediated by mitochondrial activity, with the aim of partitioning the lipotoxic FFAs into stable intracellular triglyceride stores, in order to prevent oxidative stress and ROS production [30]. This hypothesis was confirmed in an experimental model of NAFLD in which the mice were subjected to a methionine- and choline-deficient diet, after inhibiting the expression of diacylglycerol O-acyltransferase 2 (DGAT2), the enzyme catalyzing the final step of conversion of FFAs into triglycerides. In this study, despite a reduction of hepatic steatosis, it showed an increase of lipid oxidant stress markers and a worsening of lobular necroinflammation and fibrosis compared to controls, suggesting that steatosis may be a protective mechanism to prevent the progression of liver damage in NAFLD [31].

An overload of FFAs into mitochondria, subsequent to an increased intake or an insulin-resistance condition, even if it reduces the FAA cytosolic concentration, may lead to an increase in the permeability of the inner mitochondrial membrane. This occurrence leads to the dissipation of the membrane potential and the loss of ATP synthesis capacity, resulting in a mitochondrial function impairment and an enhanced ROS generation. The increase of fatty acid oxidation, inducing an increased electron flux in the electron transport chain (ETC), may generate an “electron leakage” (due to reduction of the activity of ETC complexes), thus ensuring a direct reaction between electrons and oxygen, leading to the formation of ROS, rather than the normal reaction mediated by cytochrome C oxidase that combines oxygen and protons in order to form water [19]. The incomplete or suboptimal betaoxidation leads to accumulation of long-chain acylcarnitines, ceramides, and diacylglycerols, lipotoxic intermediates that may promote inflammation and alter the insulin signaling [32]. It was demonstrated that these prooxidant mechanisms act as indirect sources of ROS. The loss of cytochrome C by mitochondria produces threefold more

hydrogen peroxide (H_2O_2) than nondepleted mitochondria [33]; an impaired function of complex I-linked respiration, in a rodent model fed with choline-deficient diet, showed an abnormal ROS production [34]. Alpha-ketoglutarate dehydrogenase, growth factor adapter p66-Shc, monoamine oxidase, and pyruvate dehydrogenase may be other indirect sources of ROS, contributing to increased oxidative stress (Figure 1). Moreover, mitochondrial cytochrome P450 2E1 (CYP2E1), which is a potential direct source of ROS, has been demonstrated to have an increased activity in an animal model of NASH and also in NASH patients [35, 36]. Also CYP2E1, which is responsible for long-chain fatty acid metabolism, produces oxidative radicals and could act as a part of the “second hit” of the pathophysiological mechanism of NAFLD [37]. Furthermore, some CYP2E1 polymorphisms, particularly the c2 allele, has been shown to be associated with the development of NASH in obese, nondiabetic subjects, paving the way for a possible explanation about why not all the subjects with NAFLD go on to develop NASH [38].

In addition to prooxidant mechanism, in an experimental model of NASH, a decreased activity of several detoxifying enzymes was observed. Glutathione peroxidase (GPx) activity is reduced probably in consequence of GSH depletion and impaired transport of cytosolic GSH into the mitochondrial matrix [39]. The polymorphism C47T of the SOD2 gene, encoding for manganese superoxide dismutase, is associated with a reduction of activity of this enzyme resulting in an increased ROS production and a high susceptibility to developing NASH and advanced fibrosis in NAFLD [40].

The initial mitochondrial dysfunction can be further exacerbated by the production of mtDNA mutation by ROS and highly reactive aldehydes, such as malondialdehyde (MDA) and 4-hydroxy-2-nonenal (4-HNE), through lipid peroxidation following the interaction between ROS and polyunsaturated FAs. Cytochrome C oxidase may be directly inhibited by MDA while 4-HNE may contribute to “electron leakage” uncoupling the complex 2 of the electron transport chain. The ETC oxidative capacity may be also decreased by derivative damage by interaction between mitochondrial membranes and both MDA and 4-HNE [41].

2.1. Other Mechanisms of Oxidation

2.1.1. ER Stress. Some evidences in the literature indicated that saturated fatty acids may have a more damaging effect on hepatocytes and liver function compared to unsaturated fatty acids, probably because of the ability of the latter to be esterified into triglycerides, which prevents fatty acid toxicity [42–46]. Saturated fatty acids determine several mechanisms of liver injury including the disruption of endoplasmic reticulum (ER) homeostasis, namely, ER stress, from which various proinflammatory pathways can be activated, very often culminating in cell death. ER is involved in folding and assembling proteins to attain their final appropriate conformation, but under stress conditions, such as lipid overload, the unfolded and misfolded proteins accumulate in the ER lumen, activating a specific signaling pathway called the unfolded protein response (UPR), in order to restore ER homeostasis [47]. UPR is regulated by three

transmembrane stress transducers, protein kinase RNA-like ER kinase (PERK), activating transcription factor 6 (ATF6), and inositol-requiring signaling protein 1 (IRE1). First of all, the cumulative response to these signaling pathways blocks the initiation of translation, in order to reduce the load upon ER. Subsequently, it induces the expression of ATP-requiring chaperon protein in order to correct the misfolded protein, creating a further energetic demand on the potentially dysfunctional mitochondrial, and so on. Lastly, it activates the cellular death signaling [48]. Moreover, in response to an excessive ER activity mediated by cellular stressor, the initiation of inflammatory and apoptotic pathways is started through activation of c-Jun N-terminal kinase (JNK), implicated in the expression of hepatic insulin resistance [49]. In fact, it has been demonstrated that the suppression of the JNK1 can prevent the development of steatohepatitis in MCD diet-fed mice, explaining the importance of JNK signaling in the pathogenesis of this disease [50].

Furthermore, ER is a potent source of ROS and the formation of each disulfide bond during the oxidative folding of nascent proteins is associated with the production of a single ROS, and this process accounts for about the 25% of all cellular ROS generation [51]. ER-resident protein oxidoreductin 1 (ERO1) is essential in this process, and the expression of this flavoenzyme was found increased in an animal model of NAFLD, along with the other markers of inflammatory signaling activation, which we will discuss below [52].

A prolonged ER stress may lead to an increased UPR-mediated ROS generation by activation of proapoptotic protein CCAAT/enhancer-binding homologous protein (CHOP), which is regulated by PERK and ATF6 signaling pathways [53]. It was shown that CHOP deletion, in a mouse model of type 2 diabetes, improved glycemic control reducing levels of oxidative damage, suggesting that CHOP activation could enhance oxidative stress [48]. Recently, similar evidences have been produced also in mouse models of steatohepatitis [54]. In contrast of these results, a recent study attested that CHOP knockout mice, fed with a high-fat and cholesterol diet, had more severe histological features of NASH compared to wild types. Moreover, the treatment with liraglutide did not improve the insulin sensitivity in absence of CHOP, demonstrating also hepatoprotective mechanisms of this protein against ER stress [55].

Furthermore, the ER lumen is the main site of calcium storage, and calcium homeostasis plays a critical role in ER stress. Saturated fatty acids may induce a disruption of ER calcium store, which can act on mitochondrial membranes blocking ETC through the formation of permeability transition pores for cytochrome C, resulting in an increased ROS production and apoptosis induction [56, 57]. The calcium homeostasis is regulated also by sarco/endoplasmic reticulum Ca^{2+} -ATPase (SERCA) that pumps Ca^{2+} into ER from the cytoplasm. The expression of SERCA was shown to be reduced in animal models of obesity and diabetes, and its inhibition was associated with the activation of ER stress response, resulting in UPR-mediated apoptotic pathways [58]. Conversely, it has been proven, in a mouse model of insulin resistance and type 2 diabetes, that the activation of SERCA can mediate reduction of adipose tissue,

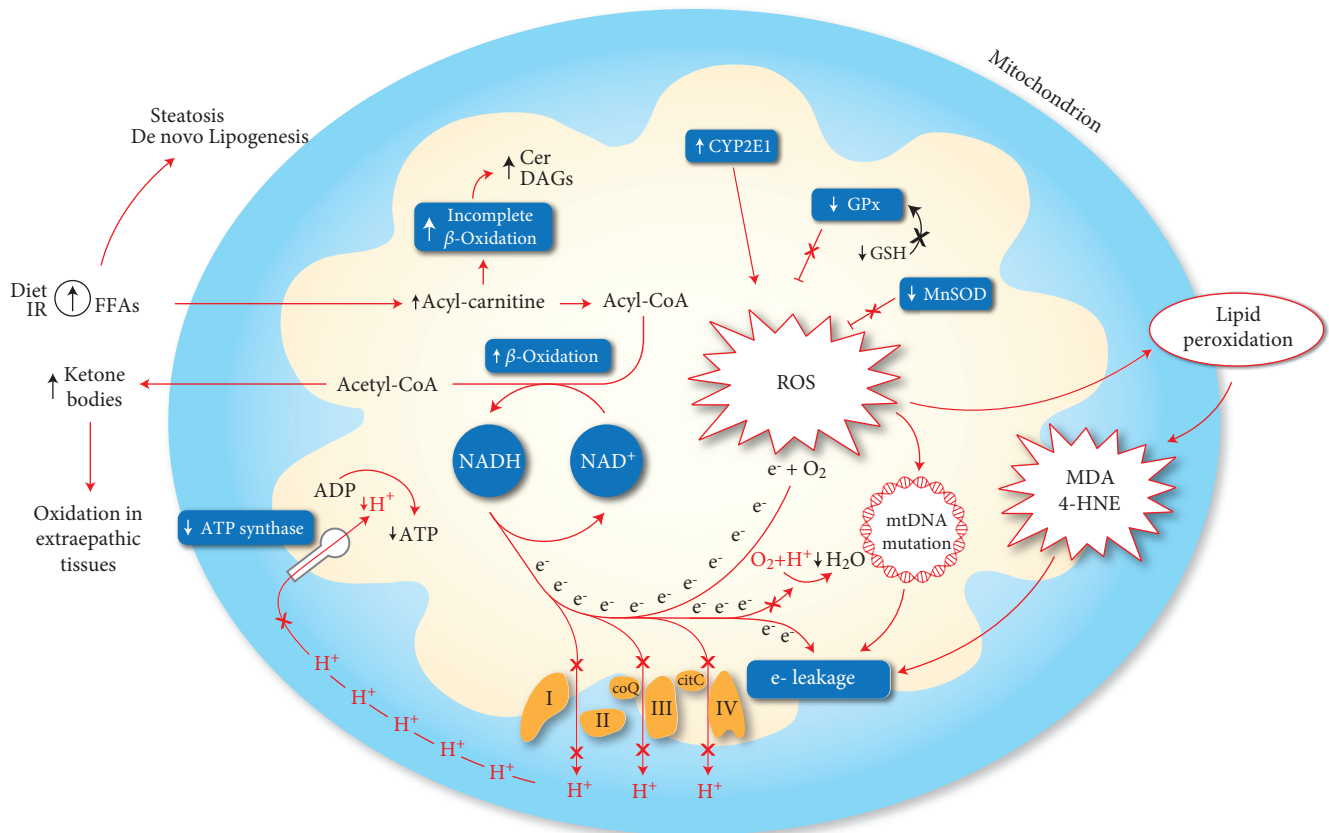


FIGURE 1: Mechanisms of mitochondrial dysfunction involved in the production of oxidative stress. An increase of mitochondrial betaoxidation activity, due to a lipid overload, may induce an impairment of electron transport chain, resulting in an “electron leakage.” The reaction between oxygen and protons catalyzed by cytochrome C oxidase (VI complex) is impaired, and electrons may interact directly with oxygen forming ROS. Furthermore, the generation of mitochondrial membrane potential is reduced following the reduction of proton extrusion from the matrix, weakening the activity of mtDNA ATP synthase. ROS production may exacerbate the mitochondrial dysfunction due to electron leakage following the generation of mtDNA mutation and highly reactive aldehydes (MDA, 4-HNE) produced through lipid peroxidation. Mitochondrial CYP2E1 is a direct source of ROS. A reduction of antioxidant mechanism as GPx and MnSOD was also observed in the NASH model. At last, the incomplete suboptimal oxidation of acyl-carnitine leads to accumulation of lipotoxic intermediates (Cer, DAGs), which can act as an inflammatory intermediate altering the insulin signaling. 4-HNE: 4-hydroxy-2-nonenal; Cer: ceramides; CYP2E1: cytochrome P450 2E1; DAGs: diacylglycerols; FFAs: free fatty acids; GPx: glutathione peroxidase; GSH: glutathione; MDA: malondialdehyde; MnSOD: manganese superoxide dismutase; ROS: reactive oxygen species.

improvement in glucose tolerance, and hepatosteatosis, thus suggesting a promising therapeutic target in metabolic dysfunctions [59]. More recently, in a cellular model of hepatic steatosis, the role of protein kinase C δ (PKC δ) was demonstrated, whose activation by FFAs participates in fatty degeneration of hepatocytes during NASH, inducing ER stress and leading to CHOP-induced cell apoptosis [60]. The silencing of PKC δ was associated with downregulation of CHOP expression and an enhancement of SERCA activity, alleviating ER stress and stabilizing calcium homeostasis [61].

Lastly, UPR was also involved in a decrease in antioxidant mechanism, as the reduction of glutathione levels. UPR mediates via PERK-signaling the inhibition of nuclear factor- (erythroid-derived 2-) like 2 (Nrf2). Nrf2 is a critical effector of cell survival, which activates transcription of antioxidant enzymes (glutathione S-transferase A2 and NADPH: quinone oxidoreductase 1), playing a critical role in elimination of ROS. In a high-fat-diet mouse model, it was

demonstrated that the deletion of Nrf2 is associated with an oxidative stress increase by glutathione level decrease and catalase and superoxide-dismutase activity, resulting in rapid progression to NASH [62]. In Figure 2, these mechanisms are graphically shown.

3. Iron Metabolism Derangements

The first observations of an altered homeostasis of iron metabolism in the clinical profile of NASH date back to 1994, when it was reported that this condition is characterized by the presence of increased levels of ferritin and transferrin [63]. A mild hyperferritinemia is found in at least the half of patients with NAFLD and often represents the only laboratory alteration that leads to the diagnosis of NAFLD. Recently, in a study conducted on 222 NAFLD patients followed for about 15 years, it was demonstrated that an elevated level of ferritin, in addition to being a strong predictor

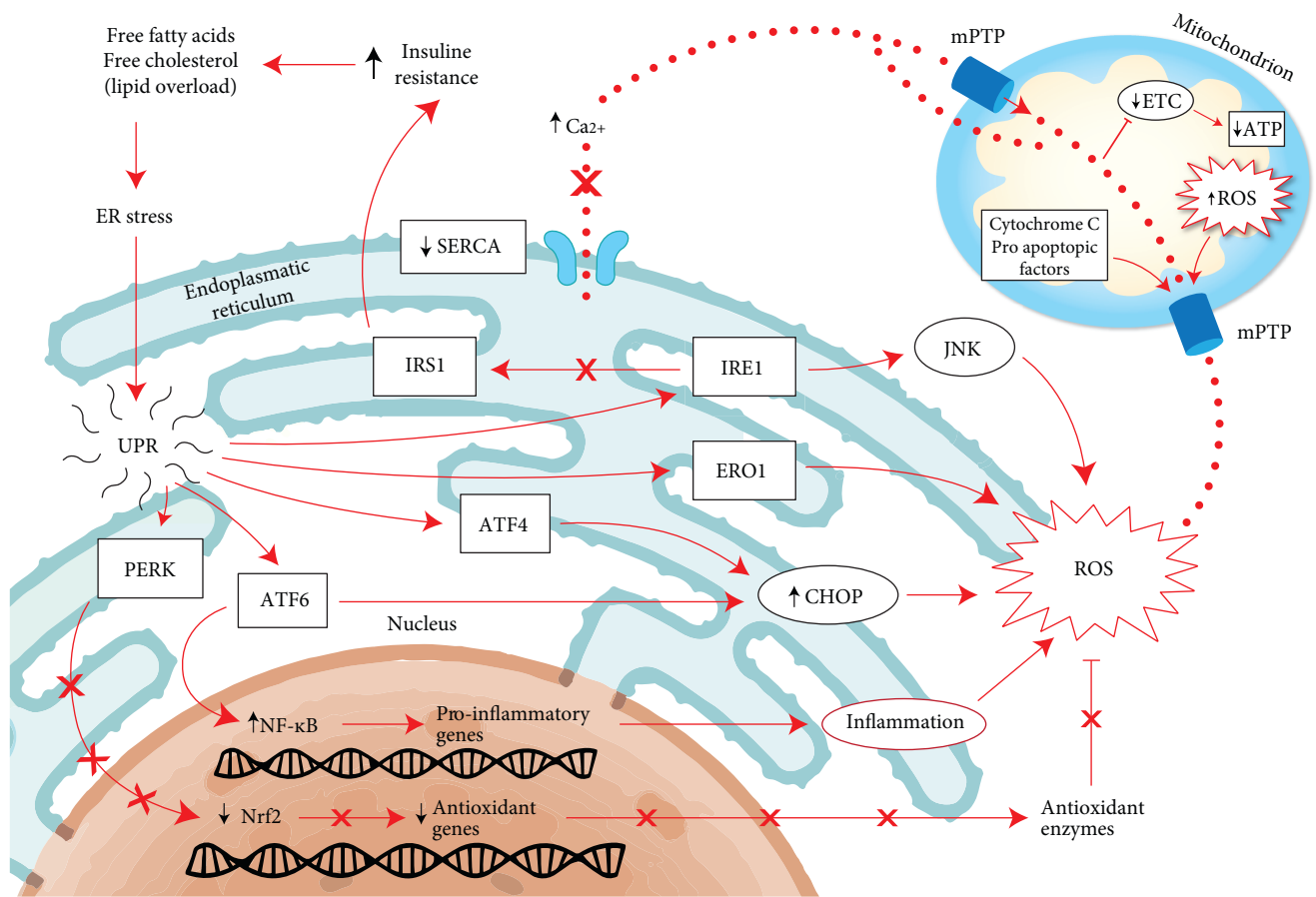


FIGURE 2: Pathway linked to ER stress. Schematic representations of hepatocyte in a fatty liver. A lipid overload, free fatty acids, and cholesterol may induce ER stress leading to “unfolded protein response” in order to reestablish the ER homeostasis. Its prolonged and repetitive activation should trigger a proapoptotic and inflammatory pathway resulting in an increase of oxidative stress. The activity of UPR is fundamentally mediated through three transmembrane stress transducers (PERK, IRE1, and ATF6), which regulate the expression of proinflammatory and antioxidant genes. In a prolonged ER stress condition, the ROS production is also increased by the overexpression of ERO1, an inducible ER oxidoreductase. Saturated fatty acids and ER stress can reduce the activity of SERCA determining a disruption of ER calcium store which can act on mitochondria blocking ETC and forming mPTP resulting in an uncontrolled transition of cytochrome C and other proapoptotic factors into the cytosol. ATF4: activating transcription factor 4; ATF6: activating transcription factor 6; CHOP: C/EBP homologous protein; ER: endoplasmic reticulum; ERO1: ER oxidoreductin 1; ETC: electron transport chain; IRE1: inositol-requiring signaling protein 1; IRS1: insulin receptor substrate 1; mPTP: mitochondrial permeability transition pore; PERK: protein kinase RNA-like ER kinase; ROS: reactive oxygen species; SERCA: sarco/endoplasmic reticulum Ca^{2+} -ATPase; UPR: unfolded protein response.

of advanced liver fibrosis, is associated with an increased long-term risk of death [64]. Iron metabolism is closely related to both oxidative stress and insulin resistance, 2 key points of NAFLD pathogenesis. The hemochromatosis (HFE) gene variants (particularly H63D and C828Y) were evaluated in cohorts of NASH patients in order to find a possible correlation, but it still remains unclear. In a large study on 786 patients, the subjects carrying these two genetic variations, despite showing a higher hepatocellular iron content, had less liver ballooning or NASH [65]. Conversely, in an older study on 51 NASH patients, a linear correlation between hepatic iron and severity of fibrosis in patients homozygous or heterozygous for C282Y was demonstrated. The study concluded that the presence of such mutation in NASH patients was associated with a higher content of hepatic iron and a significantly higher hepatic damage [66].

The hormone hepcidin inhibits the intestinal iron absorption and inactivates the cellular iron exporter ferroportin-1 [67]. In another study on 216 NAFLD patients, an association between the homozygosity for mutation p.Ala736Val in the gene of transmembrane protease serine 6 that led to a loss-of-function mutation of the enzymes matriptase-2 was found. This occurrence resulted in an increase of hepcidin expression, lower hepatic iron stores, and a decreased hepatocellular ballooning, typical features of oxidative stress in NAFLD [68].

The main prooxidizing mechanism generated by an unbound iron overload is characterized by the ability of the ferrous iron to catalyze, via Fenton reaction, the production of hydroxyl radical (OH^{\cdot}) from H_2O_2 , whose cytosolic production derives predominantly by peroxisomal β -oxidation. Unlike the mitochondrial β -oxidation, the peroxisomal

system is more active on long-chain and branched-chain FAs. Moreover, the peroxisomal acyl-CoA oxidase transfers electrons directly to oxygen and not to the respiratory chain (via electron-transferring flavoproteins, such as mitochondrial acyl-CoA dehydrogenase) generating H_2O_2 , subsequently cleaved by catalase. In a mouse model study, it was demonstrated that iron overload can promote the activity of 15-lipoxygenase. This enzyme is able to induce the leakage of peroxisomal membrane, which is normally involved in the physiological turnover of these cytosolic organelles, but in a pathological iron overload as it occurs in NASH, it may be overactivated, resulting in an increase of H_2O_2 production [69]. This oxidative process may result in a lipid peroxidation that modifies the fatty acid profile of cellular membranes, leading to cell organelle damage and impairment of mitochondrial oxidative metabolism. Moreover, iron may directly catalyze lipid peroxidation, resulting in the production of malondialdehyde, which is involved in the fibrogenesis process by activation of hepatic stellate cells [67].

Furthermore, it has also been shown, in a rodent model, that chronic iron overload, obtained by diet enriched with carbonyl-iron, enhances the inducible nitric oxide synthase (iNOS) by extracellular signal-regulated kinase and NF- κ B activation [70]. Iron overload can also reduce the antioxidant capacity decreasing GSH, therefore limiting GPx activity [70]. In the same way, a rat model of NASH was shown that parenteral administration of iron worsened steatosis and induced the development of fibrosis increasing apoptosis [71].

Conversely, it has been proven that iron depletion (rats fed an iron-deficient diet or treated with phlebotomy) may improve diabetic complications of oxidative stress by inhibitions of hepatic superoxide production and lipid peroxidation [72].

Nevertheless, the oxidizing effects of iron may also be indirectly mediated through the inhibition of the antioxidant mechanism, as heme oxygenase-1 (HO-1). HO-1 is the Kupffer cells' inducible isoform of heme oxygenase that possesses antioxidant/anti-inflammatory properties deriving from the elimination of heme and its reactive products, including biliverdin, bilirubin, and iron. HO-1 expression is increased in NAFLD and in mice under iron overload diet, as an adaptive response to oxidative damage [73, 74]. BACH-1 is a heme-binding factor able to repress the transcription of gene encoding for HO-1, and it was shown, in knockout BACH-1 mice fed with a methionine-choline-deficient diet, to have a hepatoprotective effect against steatohepatitis, probably due to failing to inhibit HO-1 [75]. In contrast, it was also demonstrated by Otagawa et al., in a rabbit model of steatohepatitis, a prooxidant mechanism of HO-1 through free iron generation by metabolism of heme, following the phagocytosis of erythrocyte in Kupffer cells, thereby enhancing hydroxyl radicals and lipid peroxides [76]. Interestingly, it has also been shown recently that an intermittent hypoxemia may have a limiting effect on hepatic steatosis. This occurs probably because the increase in hemoglobin levels promotes HO-1 expression with increased iron production, but this latter is rapidly sequestered by ferritin-1 and transferred into the bone marrow for erythropoiesis, limiting the production

of hydroxyl radicals in the liver [77]. An inhibition of proinflammatory transcription factor NF- κ B in mice subjected to intermittent hypoxia was also observed, suggesting that HO-1 contributes to the protection against liver injury, limiting inflammatory response.

In response to the discrepant findings of Otagawa et al.'s study, it can be hypothesized that an increase of oxidative stress could also persist despite the overexpression of HO-1, if the amount of iron exceeds the capacity of iron-detoxification systems, including ferritin-1. In Figure 3, these mechanisms were graphically shown.

4. Gut-Liver Axis

The adult human intestine hosts a complex of enormous populations of bacteria, at least 100 trillion, defined as gut microbiota. The gut microbiota maintains a symbiotic relationship with the organism, providing genetic and metabolic attributes, in order to contribute to various functions, including digestion of otherwise inaccessible nutrients, vitamin synthesis, and resistance to colonization by pathogens [78]. The composition of the gut microbiota is variable and dynamic during human life, being influenced by several factors including diet, environmental hygiene, and antibiotic use and misuse [79]. Qualitative and quantitative modifications of "normal" gut microbiota, namely, dysbiosis, may be involved in development and progression of NAFLD, as well as other chronic metabolic diseases [80, 81]. Gut microbiota ferment some carbohydrates (as cellulose, xylans, and inulin, nondigestible by human enzymes) in order to produce short-chain fatty acids (SCFAs), lipid precursors but also effectors of metabolic pathways, with overall benefits on obesity [82]. In fact, SCFAs, inducing secretion of peptide YY, improve the extraction of calories from the gut, increasing the sense of satiety and thermogenesis, with a reduction of food intake and lipogenesis. Furthermore, SCFA ameliorates gut barrier function, reducing the permeability of bacterial toxins and metabolic endotoxemia that can induce inflammation and insulin resistance [83]. As a result of a condition of dysbiosis, SCFA production is reduced and FFA production from VLDL is increased. This is a consequence of the lack of lipoprotein lipase inhibition through the suppression of angiopoietin-related protein 4 by altered microbiota. Besides a higher lipid accumulation in the liver and the consequent steatosis, a dysbiosis, in human and rodent models, has been shown to be able to alter the integrity of the intestinal barrier, inducing bacteria and bacterial product translocation into the portal circulation, and the activation of proinflammatory pathways. That is the main mechanism associated with the progression of chronic liver disease [84, 85]. The activation of proinflammatory pathways is mediated by some hepatic receptors among which the Toll-like receptors (TLRs) are the best characterized. TLRs may mediate an inflammatory activation in response to recognition of some specific pathogen-associate molecular patterns (PAMPs), including lipopolysaccharide (bound by TLR4), bacterial flagellin (TLR5), double-stranded bacterial DNA (TLR9), or peptidoglycan (TLR2) [86]. The inflammatory signaling activated by TLRs take part in the activation of inflammasomes, a

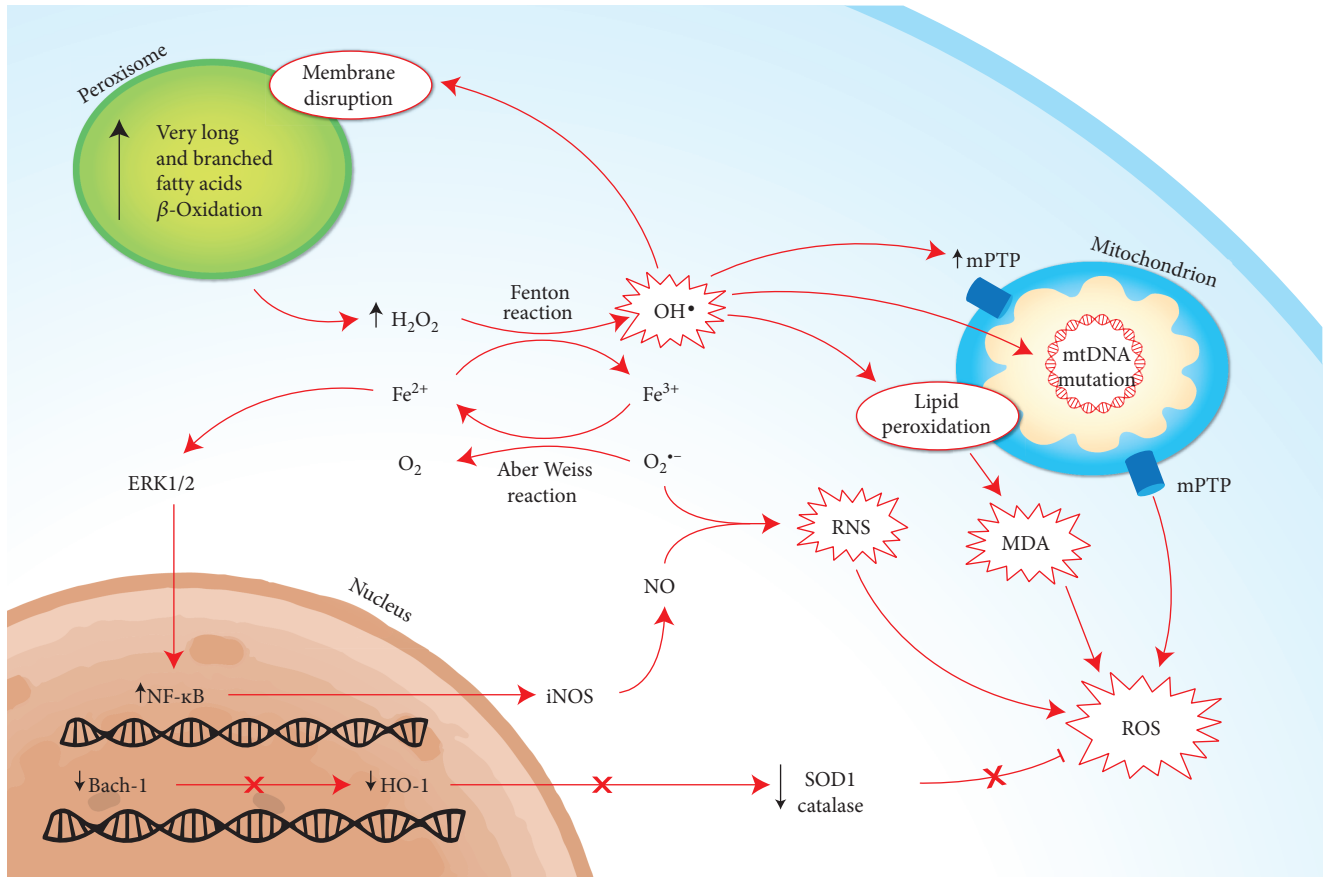


FIGURE 3: Mechanisms of oxidative stress induced by iron metabolism derangements. The main prooxidizing mechanism is characterized by the production of hydroxyl radical from H_2O_2 and Fe^{2+} via Fenton reaction. The main source of H_2O_2 is the peroxisomal betaoxidation of very long and branched fatty acids. The hydroxyl radicals may generate lipid peroxidation of organelle membranes, leading to impairment of mitochondrial metabolism through the production on mPTP and mtDNA mutation, but also increasing the proapoptotic activity with the production of MDA. Furthermore, the chronic iron overload may also enhance the production of iNOS via NF- κ B activation, leading to an increase in nitric oxide and, consequently, to a reaction with the superoxide anion, RNS. At last, the antioxidant mechanism may be inhibited by iron overload, as the activation of BACH-1, a heme-binding factor able to repress the transcription of gene encoding for HO-1, that possesses antioxidant/anti-inflammatory properties. BACH-1: BTB and CNC homology 1; MDA: malondialdehyde; mPTP: mitochondrial permeability transition pore; HO-1: hemoxygenase 1; ROS: reactive oxygen species; RNS: reactive nitrogen species; SOD1: superoxide dismutase 1.

multimeric protein complex regulating the activation of caspase-1 that cleaves the precursor cytokines pro-IL1 β and pro-IL18, whose activated cytokines are involved in inflammation and cell death [86]. Several evidences in literature demonstrated that the inflammasome activity drives NASH progression, and the inhibition of its activation may improve NAFLD pathology and fibrosis [87, 88]. Besides, some evidences from animal studies have shown that deficiency in inflammasome components, specifically NOD-like receptor proteins 3 (NPRL-3) and 6 (NPRL-6), results in reduced inflammatory response, inhibiting IL1 β and IL18, and in alteration of gut homeostasis with loss of epithelial integrity, dysbiosis, and bacteraemia [89, 90]. In this way, the integrity of the gut microbiota composition seems to be closely correlated with the innate immune response mediated by the inflammasome and consequently with the inflammatory response from which may depend the progression of NAFLD. In an animal model study, it was demonstrated that a high-fat diet may increase the percentage of gram-negative

bacteria expressing endotoxins, specifically Proteobacteria, within the gut, resulting in a higher bacterial translocation and in a higher degree of liver injury. Interestingly, though an increase of TLR expression and inflammasome component, as mRNA level of NPRL-3, was found upregulated in the liver of high-fat-diet mice in comparison to controls, an opposite trend was shown in the gut [91]. More recently, these data were reconfirmed in a high-fat- and high-carbohydrate-diet mice model, showing that an abundance of Verrucomicrobia and Proteobacteria was associated to a lack in NPRL-3 inflammasome and a higher hepatic expression of TLR4 and TLR9, resulting in a worse degree of liver injury that was restored after antibiotic treatment [92]. A study on obese and NASH human patients showed abundant representations of Bacteroides and Prevotella and a lower proportion of Firmicutes compared to healthy controls. Furthermore, an elevated blood-ethanol concentration was found exclusively in NASH patients, suggesting an abundance of ethanol-producing bacteria in their gut microbiome

and a role of these bacteria in the pathogenesis of NASH [93]. On this topic, the following hypotheses have been drawn: that NAFLD is indeed an endogenous alcoholic fatty liver disease, considering that gut microbiota can produce daily a quantity of ethanol well above what is considered as safe for humans; that the hepatic first-pass metabolism of ethanol prevents the development of a detectable blood-alcohol concentration; and that, in patients with NASH, genes involved in the metabolism of endogenous ethanol are upregulated. This may particularly be for genes encoding for the hepatic alcohol dehydrogenase (ADH 4) that are strictly involved in liver exposure to high concentrations of ethanol [94].

The close correlation between intestinal dysbiosis and NAFLD has led to the hypothesis that a possible therapeutic option, alongside the use of probiotics and prebiotics, could be the faecal microbiota transplantation, which is already approved for the treatment of *Clostridium difficile* infection, giving promising results also in the treatment of metabolic syndrome and irritable bowel disease [95]. In favor of therapeutic applicability of faecal microbiota transplantation, some promising evidences emerged from preanalytical studies on the effects on insulin sensitivity and systemic inflammation, but the clinical trials are still ongoing.

5. Insulin Resistance and Endothelial Dysfunction

As mentioned above, NAFLD may be considered the liver expression of metabolic syndrome and IR is the mayor pathophysiological implicated in the development of this syndrome [15]. The nitric oxide (NO) production is strictly influenced by the insulin activity, mediating not only the vasodilatation but also the anti-inflammatory, antithrombotic, and antifibrogenic properties of endothelium. The worsening of IR is related to the severity of endothelial dysfunction (ED), whose implication has been evaluated in different models of liver disease [96]. Following the loss of its capacities, ED contributes and promotes the structural and functional changes of liver circulation, impairing the regeneration after liver injury and contributing to progression of liver disease. NO is constitutively synthesized by endothelial nitric oxide synthase (eNOS), whose production of NO plays a fundamental role in the systemic vascular tone, regulating the blood pressure and renal control of extracellular fluid [97]. Insulin signaling leads indirectly to the activation of eNOS through the phosphokinase pathway PI3K/Akt, which may be impaired in the presence of an IR condition, while other pathways remain unaffected, as the Ras/MAPK pathway involved in the control of cell proliferation [98]. The result of this metabolic imbalance reflects the characteristics of ED including the decrease of eNOS activation and then the NO production.

The NO production is also driven through the inducible isoform of NOS (iNOS) that in contrast to eNOS, after its activation, produces large amounts of NO until the exhaustion of substrates or cofactors. The iNOS expression may be upregulated under condition of stress via proinflammatory cytokines (TNF- α , IL1, and IFN- γ), whose expression are increased in obesity and insulin resistance [99]. The excessive

NO formation by iNOS has been shown to be involved in several inflammatory and autoimmune diseases (septic shock, rheumatoid arthritis, osteoarthritis, and multiple sclerosis), but among these, it has been shown that iNOS activity can reduce insulin sensitivity via S-nitrosilation of insulin receptor and modulation of PPAR- γ activation [100, 101]. Furthermore, the overexpression of iNOS contributes to ED with the loss of its anti-inflammatory function. In fact, an impaired generation of NO may promote the production on superoxide and hydroxyl radical intermediates, constituting a state of oxidative stress, which results in cellular apoptosis [102]. In this way, the ED may promote or worsen an inflammatory state, also known as “low-grade inflammation,” that leads to the progression of NAFLD liver injury [103]. Recently, in a mouse model fed with a high-fat diet for 6 weeks, the reduction of the eNOS activity was demonstrated in the early stages of NAFLD, with the result of reducing NO bioavailability, together with an increased oxidative stress and cyclooxygenase activity, resulting in an increase of hepatic vascular resistance unrelated to inflammation or fibrosis [104]. The same evaluation was assessed after cyclooxygenase inhibition therapy with thromboxane receptor antagonist, finding an improvement of endothelial dysfunction. These findings support the fact that the endothelial dysfunction takes part in the pathophysiological process of NAFLD from the early stages and oxidative stress contributes to vascular dysfunction, paving the way for new promising therapeutic strategies. The main pathophysiological mechanisms described above are summarized in Table 1.

6. Clinical Studies in Humans

Although several clinical evidences have highlighted the pathogenic correlation between oxidative stress and obesity-associated metabolic syndrome, its components (hypertension, obesity, and dyslipidemia), and/or diabetes [105–109], which are strictly associated with the presence of NAFLD, fewer clinical studies have investigated the association of oxidative stress and its extent with NAFLD itself. Some of these studies have examined the systemic oxidative alterations by directly evaluating various direct biomarkers of oxidative stress, whereas other studies have investigated the “clinical effects” of such alteration on the cardiovascular system of the patients with steatosis (i.e., with the evaluation of intima-media thickness, epicardial fat measurement, etc.). Others have correlated both serum biomarkers and clinical signs with steatosis and its extent. Moreover, of particular interest are the studies on gut-liver interactions and endothelial dysfunction, oxidative stress, and nitric oxide (NO) metabolism impairment, in particular throughout endothelial nitric oxide synthase (eNOS) activity derangement.

6.1. Studies Evaluating Oxidative Stress Markers. A study by Palmieri et al. demonstrated that serum vitamin C and alpha-tocopherol concentrations were lower and lipid peroxides (thiobarbituric acid reactive substances (TBARS)) were higher in patients with steatosis and metabolic syndrome in contrast with controls. The study concluded that patients with metabolic syndrome and steatosis exhibited a decreased

TABLE 1: Overview of the major pathophysiological mechanisms involved in oxidative stress in NAFLD addressed within the present paper, with the corresponding references.

Pathophysiological mechanisms of oxidative stress	Mechanism (with references)	
	Increasing prooxidant	Decreasing antioxidant
Mitochondrial dysfunction	Impairment of oxidative capacity of ETC, resulting in an “electron leakage” [21]	GSH depletion with reduction of GPx activity [41]
	Accumulation of Cer and DAGs due to incomplete betaoxidation of acyl-carnitine [34]	Reduced activity of MnSOD, polymorphism C47T of SOD2 gene [42]
	mtDNA mutation [25]	
	Production of reactive aldehydes (MDA, 4-HNE) through lipid peroxidation [43]	Impaired activity of cytochrome C [35]
	Increase activity of CYP2E1, polymorphism of C2 allele [37–40]	
ER stress	Prolonged activation of UPR leading to (i) overexpression of ERO1 [49] (ii) calcium disruption due to reduced activity of SERCA [55] (iii) upregulation of CHOP mediated by activation of PERK and ATF6 [50]	Prolonged activation of UPR leading to (i) inhibition of Nrf2 by PERK resulting in the depletion of GSH [59]
	Disruption of peroxisomal membrane [66]	GSH depletion—decreased GPx efficiency [67]
Iron metabolism derangements	Enhanced iNOS expression via NF- κ B activation [67]	Inhibition of HO-1 by activation of BACH-1 [70–74]
	Production of reactive aldehydes (MDA) through lipid peroxidation [64]	Iron actin as a direct competitive antagonist of antioxidant enzymes [69]
Inappropriate inflammatory response mediated by GUT-liver axis	Upregulation of proinflammatory pathways and NADPH oxidase system due to bacterial and bacterial product translocation [80, 81]	
	Activation of inflammasomes resulting in cleavage of cytokines precursors (pro-IL1 β , pro-IL18) [82]	Lack of inhibition of inflammatory response by NPRL-3 and -6 [85, 86]
	Endogenous alcoholic production by alcohol-producing bacteria [89]	
Insulin resistance and endothelial dysfunction	Upregulation of Ras/MAPK pathway involved in cell proliferation [94]	Decrease of eNOS activation due to IR [94]
	Enhanced iNOS activity due to increase expression of proinflammatory cytokines in IR [96]	

4-HNE: 4-hydroxy-2-nonenal; ATF6: activating transcription factor 6; BACH-1: BTB and CNC homology 1; Cer: ceramides; CHOP: C/EBP homologous protein; CYP2E1: cytochrome P 450 2E1; DAGs: diacylglycerols; ER: endoplasmic reticulum; ERO1: ER oxidoreductin 1; ETC: electron transport chain; GPx: glutathione peroxidase; GSH: glutathione; HO-1: hemoxygenase 1; IR: insulin resistance; MDA: malondialdehyde; MnSOD: manganese superoxide dismutase; NPRL: NOD-like receptor protein; Nrf2: nuclear factor- (erythroid-derived 2-) like 2; PERK: protein kinase RNA-like ER kinase; SERCA: sarco/endoplasmic reticulum CA²⁺-ATPase; UPR: unfolded protein response.

antioxidant protection and increased lipid peroxidation [110]. On the same line, a recent paper by Stiuso et al. demonstrated that, not only were there two types of patients, one with higher basal severity of liver steatosis inflammation and fibrosis and the other with milder histological presentations, differing in the extent of oxidative stress (measured with TBARS, nitrite, superoxide dismutase, and catalase), but also that these evaluations could be useful as a prognostic marker of response to an antioxidant treatment [111]. As is clearly explained by the abovementioned pathophysiological mechanism of NAFLD itself (the classical “two-hit” theory [16] or the more up-to date “multiple parallel-hit” theory [17]), the oxidative stress represents the core mechanism at the basis of the “second hit” which conducts to the formation of reactive oxygen species (ROS). This mechanism is a consequence of the excess of fatty acids in the hepatic cells, their energy depletion and consequent mitochondrial dysfunction

leading to increase in oxidative stress and, finally, cellular damage [106]. These mechanisms have been demonstrated by basic science studies on animal experimental models but have also found confirmations in humans [112, 113], giving a precise insight to the importance of the oxidative stress in the pathophysiology of NAFLD. Moreover, these theories found a “clinical” confirmation from the studies that evidenced the association between metabolic syndrome and also its components (hypertension, obesity, and dyslipidemia) taken individually [114–116].

Finally, even more interest in the last few years has risen on two other mechanisms of liver damage in which a major pathogenic role is played by oxidative stress: the gut-liver axis and the endothelial dysfunction. As far as gut-liver axis, recently, some studies have confirmed the already cited findings of experimental animal models in which intestinal dysbiosis is a factor leading to an increase of lipotoxicity. This

occurs, as in animal models, via the stimulation of Toll-like receptors (TLRs) and the consequent activation of inflammasomes that induce cellular injury also by increasing oxidative stress. In particular, it has been demonstrated that in patients with NAFLD, the gut-microbiota impairment (increase in Bacteroidetes, decrease in *Prevotella* spp.) is associated with worse presentations of NASH [117]. Moreover, abundance in ethanol-producing bacteria was also observed in patients with NAFLD, indicating that this issue may lead to an oxidative stress increase and liver injury by “endogenous” production of ethanol in patients with NASH [93].

Finally, also in the frame of endothelial dysfunction, in which, as discussed above, the imbalance in eNOS and iNOS functionality leads to increase in oxidative damage of the liver vasculature leading to inflammation and fibrosis, our group recently published a paper demonstrating that systemic eNOS impairment is significantly associated with NAFLD [118].

7. Conclusions

The present review was aimed at describing the results of the most important studies focused on the explanation of possible pathogenetic theories of oxidative stress as the most important acting factor in all the biological hits able to determine the development and worsening of the complex clinical picture of NAFLD. For this reason, at this level of knowledge, the most important problem is the interpretation and correlation of some results obtained through the clinical studies. A lot of these are difficult to translate in routine clinical practice because of a loss of strong evidences that support their application in the therapy of this disease. Certainly, we must admit that the evolution in the comprehension of the mechanisms that support NAFLD has been very fast in the last decade, and at the same time, the analyzed fields represent some of the most promising topics of scientific research of the future.

Conflicts of Interest

The authors do not have any conflict of interests to declare regarding this paper.

Authors' Contributions

Mario Masarone and Valerio Rosato contributed equally to this work.

Acknowledgments

The authors thank Giulio Mirabella for his contribution in the graphic support of the production of the figures in this paper and Dr. Berardo Guzzi (English Certificate of Proficiency released by University of Cambridge) for his English assistance.

References

[1] P. Angulo, “Nonalcoholic fatty liver disease,” *The New England Journal of Medicine*, vol. 346, no. 16, pp. 1221–1231, 2002.

- [2] G. Bedogni, L. Miglioli, F. Masutti, C. Tiribelli, G. Marchesini, and S. Bellentani, “Prevalence of and risk factors for nonalcoholic fatty liver disease: the Dionysos nutrition and liver study,” *Hepatology*, vol. 42, no. 1, pp. 44–52, 2005.
- [3] M. Masarone, A. Federico, L. Abenavoli, C. Loguercio, and M. Persico, “Non alcoholic fatty liver: epidemiology and natural history,” *Reviews on Recent Clinical Trials*, vol. 9, no. 3, pp. 126–133, 2014.
- [4] C. A. Matteoni, Z. M. Younossi, T. Gramlich, N. Boparai, Y. C. Liu, and A. J. McCullough, “Nonalcoholic fatty liver disease: a spectrum of clinical and pathological severity,” *Gastroenterology*, vol. 116, no. 6, pp. 1413–1419, 1999.
- [5] E. M. Brunt, “Pathology of nonalcoholic fatty liver disease,” *Nature Reviews Gastroenterology & Hepatology*, vol. 7, no. 4, pp. 195–203, 2010.
- [6] F. Nascimbeni, R. Pais, S. Bellentani et al., “From NAFLD in clinical practice to answers from guidelines,” *Journal of Hepatology*, vol. 59, no. 4, pp. 859–871, 2013.
- [7] J. Ertle, A. Dechène, J. P. Sowa et al., “Non-alcoholic fatty liver disease progresses to hepatocellular carcinoma in the absence of apparent cirrhosis,” *International Journal of Cancer*, vol. 128, no. 10, pp. 2436–2443, 2011.
- [8] M. Masarone, V. Rosato, A. Aglitti et al., “Liver biopsy in type 2 diabetes mellitus: steatohepatitis represents the sole feature of liver damage,” *PLoS One*, vol. 12, no. 6, article e0178473, 2017.
- [9] F. Bril and K. Cusi, “Management of nonalcoholic fatty liver disease in patients with type 2 diabetes: a call to action,” *Diabetes Care*, vol. 40, no. 3, pp. 419–430, 2017.
- [10] B. Vos, C. Moreno, N. Nagy et al., “Lean non-alcoholic fatty liver disease (lean-NAFLD): a major cause of cryptogenic liver disease,” *Acta Gastroenterologica Belgica*, vol. 74, no. 3, pp. 389–394, 2011.
- [11] C. Podrini, M. Borghesan, A. Greco, V. Paziienza, G. Mazzoccoli, and M. Vinciguerra, “Redox homeostasis and epigenetics in non-alcoholic fatty liver disease (NAFLD),” *Current Pharmaceutical Design*, vol. 19, no. 15, pp. 2737–2746, 2013.
- [12] C. J. Pirola, T. F. Gianotti, A. L. Burgueno et al., “Epigenetic modification of liver mitochondrial DNA is associated with histological severity of nonalcoholic fatty liver disease,” *Gut*, vol. 62, no. 9, pp. 1356–1363, 2013.
- [13] H. M. Lakka, D. E. Laaksonen, T. A. Lakka et al., “The metabolic syndrome and total and cardiovascular disease mortality in middle-aged men,” *JAMA*, vol. 288, no. 21, pp. 2709–2716, 2002.
- [14] S. Petta, A. Gastaldelli, E. Rebelos et al., “Pathophysiology of non alcoholic fatty liver disease,” *International Journal of Molecular Sciences*, vol. 17, no. 12, article 2082, 2016.
- [15] M. Pasarin, J. G. Abraldes, E. Liguori, B. Kok, and V. La Mura, “Intrahepatic vascular changes in non-alcoholic fatty liver disease: potential role of insulin-resistance and endothelial dysfunction,” *World Journal of Gastroenterology*, vol. 23, no. 37, pp. 6777–6787, 2017.
- [16] C. P. Day and James OF, “Steatohepatitis: a tale of two “hits”?,” *Gastroenterology*, vol. 114, no. 4, pp. 842–845, 1998.
- [17] H. Tilg and A. R. Moschen, “Evolution of inflammation in nonalcoholic fatty liver disease: the multiple parallel hits hypothesis,” *Hepatology*, vol. 52, no. 5, pp. 1836–1846, 2010.

- [18] S. H. Caldwell, R. H. Swerdlow, E. M. Khan et al., "Mitochondrial abnormalities in non-alcoholic steatohepatitis," *Journal of Hepatology*, vol. 31, no. 3, pp. 430–434, 1999.
- [19] I. Grattagliano, O. de Bari, T. C. Bernardo, P. J. Oliveira, D. Q. Wang, and P. Portincasa, "Role of mitochondria in nonalcoholic fatty liver disease—from origin to propagation," *Clinical Biochemistry*, vol. 45, no. 9, pp. 610–618, 2012.
- [20] K. Begriche, J. Massart, M. A. Robin, F. Bonnet, and B. Fromenty, "Mitochondrial adaptations and dysfunctions in nonalcoholic fatty liver disease," *Hepatology*, vol. 58, no. 4, pp. 1497–1507, 2013.
- [21] S. Seki, T. Kitada, T. Yamada, H. Sakaguchi, K. Nakatani, and K. Wakasa, "In situ detection of lipid peroxidation and oxidative DNA damage in non-alcoholic fatty liver diseases," *Journal of Hepatology*, vol. 37, no. 1, pp. 56–62, 2002.
- [22] M. F. Silva, C. C. Aires, P. B. Luis et al., "Valproic acid metabolism and its effects on mitochondrial fatty acid oxidation: a review," *Journal of Inherited Metabolic Disease*, vol. 31, no. 2, pp. 205–216, 2008.
- [23] G. Davidzon, M. Mancuso, S. Ferraris et al., "POLG mutations and Alpers syndrome," *Annals of Neurology*, vol. 57, no. 6, pp. 921–923, 2005.
- [24] N. G. Sabbagha, H. J. Kao, C. F. Yang et al., "Alternative splicing in *Acad8* resulting a mitochondrial defect and progressive hepatic steatosis in mice," *Pediatric Research*, vol. 70, no. 1, pp. 31–36, 2011.
- [25] R. B. Ding, J. Bao, and C. X. Deng, "Emerging roles of SIRT1 in fatty liver diseases," *International Journal of Biological Sciences*, vol. 13, no. 7, pp. 852–867, 2017.
- [26] M. Li, K. Guo, L. Vanella, S. Taketani, Y. Adachi, and S. Ikehara, "Stem cell transplantation upregulates Sirt1 and antioxidant expression, ameliorating fatty liver in type 2 diabetic mice," *International Journal of Biological Sciences*, vol. 11, no. 4, pp. 472–481, 2015.
- [27] A. A. Kendrick, M. Choudhury, S. M. Rahman et al., "Fatty liver is associated with reduced SIRT3 activity and mitochondrial protein hyperacetylation," *Biochemical Journal*, vol. 433, no. 3, pp. 505–514, 2011.
- [28] R. H. Houtkooper, C. Canto, R. J. Wanders, and J. Auwerx, "The secret life of NAD⁺: an old metabolite controlling new metabolic signaling pathways," *Endocrine Reviews*, vol. 31, no. 2, pp. 194–223, 2010.
- [29] K. Gariani, K. J. Menzies, D. Ryu et al., "Eliciting the mitochondrial unfolded protein response by nicotinamide adenine dinucleotide repletion reverses fatty liver disease in mice," *Hepatology*, vol. 63, no. 4, pp. 1190–1204, 2016.
- [30] K. L. Donnelly, C. I. Smith, S. J. Schwarzenberg, J. Jessurun, M. D. Boldt, and E. J. Parks, "Sources of fatty acids stored in liver and secreted via lipoproteins in patients with nonalcoholic fatty liver disease," *The Journal of Clinical Investigation*, vol. 115, no. 5, pp. 1343–1351, 2005.
- [31] K. Yamaguchi, L. Yang, S. McCall et al., "Inhibiting triglyceride synthesis improves hepatic steatosis but exacerbates liver damage and fibrosis in obese mice with nonalcoholic steatohepatitis," *Hepatology*, vol. 45, no. 6, pp. 1366–1374, 2007.
- [32] R. E. Patterson, S. Kalavalapalli, C. M. Williams et al., "Lipotoxicity in steatohepatitis occurs despite an increase in tricarboxylic acid cycle activity," *American Journal of Physiology Endocrinology and Metabolism*, vol. 310, no. 7, pp. E484–E494, 2016.
- [33] Y. Kushnareva, A. N. Murphy, and A. Andreyev, "Complex I-mediated reactive oxygen species generation: modulation by cytochrome c and NAD(P)⁺ oxidation-reduction state," *The Biochemical Journal*, vol. 368, no. 2, pp. 545–553, 2002.
- [34] K. Hensley, Y. Kotake, H. Sang et al., "Dietary choline restriction causes complex I dysfunction and increased H₂O₂ generation in liver mitochondria," *Carcinogenesis*, vol. 21, no. 5, pp. 983–989, 2000.
- [35] N. Chalasani, J. C. Gorski, M. S. Asghar et al., "Hepatic cytochrome P450 2E1 activity in nondiabetic patients with nonalcoholic steatohepatitis," *Hepatology*, vol. 37, no. 3, pp. 544–550, 2003.
- [36] M. D. Weltman, G. C. Farrell, and C. Liddle, "Increased hepatocyte *CYP2E1* expression in a rat nutritional model of hepatic steatosis with inflammation," *Gastroenterology*, vol. 111, no. 6, pp. 1645–1653, 1996.
- [37] J. Aubert, K. Begriche, L. Knockaert, M. A. Robin, and B. Fromenty, "Increased expression of cytochrome P450 2E1 in nonalcoholic fatty liver disease: mechanisms and pathophysiological role," *Clinics and Research in Hepatology and Gastroenterology*, vol. 35, no. 10, pp. 630–637, 2011.
- [38] N. M. Varela, L. A. Quinones, M. Orellana et al., "Study of cytochrome P450 2E1 and its allele variants in liver injury of nondiabetic, nonalcoholic steatohepatitis obese women," *Biological Research*, vol. 41, no. 1, pp. 81–92, 2008.
- [39] F. Caballero, A. Fernandez, N. Matias et al., "Specific contribution of methionine and choline in nutritional nonalcoholic steatohepatitis: impact on mitochondrial S-adenosyl-L-methionine and glutathione," *Journal of Biological Chemistry*, vol. 285, no. 24, pp. 18528–18536, 2010.
- [40] V. Nobili, B. Donati, N. Panera et al., "A 4-polymorphism risk score predicts steatohepatitis in children with nonalcoholic fatty liver disease," *Journal of Pediatric Gastroenterology and Nutrition*, vol. 58, no. 5, pp. 632–636, 2014.
- [41] D. Gao, C. Wei, L. Chen, J. Huang, S. Yang, and A. M. Diehl, "Oxidative DNA damage and DNA repair enzyme expression are inversely related in murine models of fatty liver disease," *American Journal of Physiology Gastrointestinal and Liver Physiology*, vol. 287, no. 5, pp. G1070–G1077, 2004.
- [42] D. Wang, Y. Wei, and M. J. Pagliassotti, "Saturated fatty acids promote endoplasmic reticulum stress and liver injury in rats with hepatic steatosis," *Endocrinology*, vol. 147, no. 2, pp. 943–951, 2006.
- [43] Y. Wei, D. Wang, F. Topczewski, and M. J. Pagliassotti, "Saturated fatty acids induce endoplasmic reticulum stress and apoptosis independently of ceramide in liver cells," *American Journal of Physiology Endocrinology and Metabolism*, vol. 291, no. 2, pp. E275–E281, 2006.
- [44] M. Ricchi, M. R. Odoardi, L. Carulli et al., "Differential effect of oleic and palmitic acid on lipid accumulation and apoptosis in cultured hepatocytes," *Journal of Gastroenterology and Hepatology*, vol. 24, no. 5, pp. 830–840, 2009.
- [45] A. E. Feldstein, N. W. Werneburg, Z. Li, S. F. Bronk, and G. J. Gores, "Bax inhibition protects against free fatty acid-induced lysosomal permeabilization," *American Journal of Physiology Gastrointestinal and Liver Physiology*, vol. 290, no. 6, pp. G1339–G1346, 2006.
- [46] A. K. Leamy, R. A. Egnatchik, M. Shiota et al., "Enhanced synthesis of saturated phospholipids is associated with ER stress and lipotoxicity in palmitate treated hepatic cells," *Journal of Lipid Research*, vol. 55, no. 7, pp. 1478–1488, 2014.

- [47] J. D. Malhotra and R. J. Kaufman, "The endoplasmic reticulum and the unfolded protein response," *Seminars in Cell & Developmental Biology*, vol. 18, no. 6, pp. 716–731, 2007.
- [48] B. Song, D. Scheuner, D. Ron, S. Pennathur, and R. J. Kaufman, "Chop deletion reduces oxidative stress, improves β cell function, and promotes cell survival in multiple mouse models of diabetes," *The Journal of Clinical Investigation*, vol. 118, no. 10, pp. 3378–3389, 2008.
- [49] J. Hirosumi, G. Tuncman, L. Chang et al., "A central role for JNK in obesity and insulin resistance," *Nature*, vol. 420, no. 6913, pp. 333–336, 2002.
- [50] J. M. Schattenberg, R. Singh, Y. Wang et al., "JNK1 but not JNK2 promotes the development of steatohepatitis in mice," *Hepatology*, vol. 43, no. 1, pp. 163–172, 2006.
- [51] Y. Shimizu and L. M. Hendershot, "Oxidative folding: cellular strategies for dealing with the resultant equimolar production of reactive oxygen species," *Antioxidants & Redox Signaling*, vol. 11, no. 9, pp. 2317–2331, 2009.
- [52] M. E. Rinella, M. S. Siddiqui, K. Gardikiotes, J. Gottstein, M. Elias, and R. M. Green, "Dysregulation of the unfolded protein response in db/db mice with diet-induced steatohepatitis," *Hepatology*, vol. 54, no. 5, pp. 1600–1609, 2011.
- [53] P. van Galen, A. Kreso, N. Mbong et al., "The unfolded protein response governs integrity of the haematopoietic stem-cell pool during stress," *Nature*, vol. 510, no. 7504, pp. 268–272, 2014.
- [54] C. D. Fuchs, T. Claudel, H. Scharnagl, T. Stojakovic, and M. Trauner, "FXR controls CHOP expression in steatohepatitis," *FEBS Letters*, vol. 591, no. 20, pp. 3360–3368, 2017.
- [55] K. Rahman, Y. Liu, P. Kumar et al., "C/EBP homologous protein modulates liraglutide-mediated attenuation of non-alcoholic steatohepatitis," *Laboratory Investigation*, vol. 96, no. 8, pp. 895–908, 2016.
- [56] A. Deniaud, O. Sharaf el dein, E. Maillier et al., "Endoplasmic reticulum stress induces calcium-dependent permeability transition, mitochondrial outer membrane permeabilization and apoptosis," *Oncogene*, vol. 27, no. 3, pp. 285–299, 2008.
- [57] Y. Wei, D. Wang, C. L. Gentile, and M. J. Pagliassotti, "Reduced endoplasmic reticulum luminal calcium links saturated fatty acid-mediated endoplasmic reticulum stress and cell death in liver cells," *Molecular and Cellular Biochemistry*, vol. 331, no. 1–2, pp. 31–40, 2009.
- [58] S. Fu, L. Yang, P. Li et al., "Aberrant lipid metabolism disrupts calcium homeostasis causing liver endoplasmic reticulum stress in obesity," *Nature*, vol. 473, no. 7348, pp. 528–531, 2011.
- [59] S. Kang, R. Dahl, W. Hsieh et al., "Small molecular allosteric activator of the sarco/endoplasmic reticulum Ca^{2+} -ATPase (SERCA) attenuates diabetes and metabolic disorders," *Journal of Biological Chemistry*, vol. 291, no. 10, pp. 5185–5198, 2016.
- [60] M. W. Greene, C. M. Burrington, M. S. Ruhoff, A. K. Johnson, T. Chongkraitanakul, and A. Kangwanpornsirir, "PKC δ is activated in a dietary model of steatohepatitis and regulates endoplasmic reticulum stress and cell death," *Journal of Biological Chemistry*, vol. 285, no. 53, pp. 42115–42129, 2010.
- [61] S. Lai, Y. Li, Y. Kuang et al., "PKC δ silencing alleviates saturated fatty acid induced ER stress by enhancing SERCA activity," *Bioscience Reports*, vol. 37, no. 6, article BSR20170869, 2017.
- [62] K. Okada, E. Warabi, H. Sugimoto et al., "Deletion of Nrf2 leads to rapid progression of steatohepatitis in mice fed atherogenic plus high-fat diet," *Journal of Gastroenterology*, vol. 48, no. 5, pp. 620–632, 2013.
- [63] B. R. Bacon, M. J. Farahvash, C. G. Janney, and B. A. Neuschwander-Tetri, "Nonalcoholic steatohepatitis: an expanded clinical entity," *Gastroenterology*, vol. 107, no. 4, pp. 1103–1109, 1994, 7523217.
- [64] H. Hagstrom, P. Nasr, M. Bottai et al., "Elevated serum ferritin is associated with increased mortality in non-alcoholic fatty liver disease after 16 years of follow-up," *Liver International*, vol. 36, no. 11, pp. 1688–1695, 2016.
- [65] J. E. Nelson, E. M. Brunt, and K. V. Kowdley, "Lower serum hepcidin and greater parenchymal iron in nonalcoholic fatty liver disease patients with C282Y HFE mutations," *Hepatology*, vol. 56, no. 5, pp. 1730–1740, 2012.
- [66] D. K. George, S. Goldwurm, G. A. MacDonald et al., "Increased hepatic iron concentration in nonalcoholic steatohepatitis is associated with increased fibrosis," *Gastroenterology*, vol. 114, no. 2, pp. 311–318, 1998.
- [67] P. Dongiovanni, A. L. Fracanzani, S. Fargion, and L. Valenti, "Iron in fatty liver and in the metabolic syndrome: a promising therapeutic target," *Journal of Hepatology*, vol. 55, no. 4, pp. 920–932, 2011.
- [68] L. Valenti, R. Rametta, P. Dongiovanni et al., "The A736V TMPRSS6 polymorphism influences hepatic iron overload in nonalcoholic fatty liver disease," *PLoS One*, vol. 7, no. 11, article e48804, 2012.
- [69] S. Yokota, T. Oda, and H. D. Fahimi, "The role of 15-lipoxygenase in disruption of the peroxisomal membrane and in programmed degradation of peroxisomes in normal rat liver," *Journal of Histochemistry & Cytochemistry*, vol. 49, no. 5, pp. 613–621, 2001.
- [70] P. Cornejo, P. Varela, L. A. Videla, and V. Fernandez, "Chronic iron overload enhances inducible nitric oxide synthase expression in rat liver," *Nitric Oxide*, vol. 13, no. 1, pp. 54–61, 2005.
- [71] N. Imeryuz, V. Tahan, A. Sonsuz et al., "Iron preloading aggravates nutritional steatohepatitis in rats by increasing apoptotic cell death," *Journal of Hepatology*, vol. 47, no. 6, pp. 851–859, 2007.
- [72] Y. Minamiyama, S. Takemura, S. Kodai et al., "Iron restriction improves type 2 diabetes mellitus in Otsuka Long-Evans Tokushima fatty rats," *American Journal of Physiology Endocrinology and Metabolism*, vol. 298, no. 6, pp. E1140–E1149, 2010.
- [73] K. E. Brown, P. A. Dennery, L. A. Ridnour et al., "Effect of iron overload and dietary fat on indices of oxidative stress and hepatic fibrogenesis in rats," *Liver International*, vol. 23, no. 4, pp. 232–242, 2003.
- [74] L. Malaguarnera, R. Madeddu, E. Palio, N. Arena, and M. Malaguarnera, "Heme oxygenase-1 levels and oxidative stress-related parameters in non-alcoholic fatty liver disease patients," *Journal of Hepatology*, vol. 42, no. 4, pp. 585–591, 2005.
- [75] M. Inoue, S. Tazuma, K. Kanno, H. Hyogo, K. Igarashi, and K. Chayama, "Bach1 gene ablation reduces steatohepatitis in mouse MCD diet model," *Journal of Clinical Biochemistry and Nutrition*, vol. 48, no. 2, pp. 161–166, 2011.
- [76] K. Otogawa, K. Kinoshita, H. Fujii et al., "Erythrophagocytosis by liver macrophages (Kupffer cells) promotes oxidative

- stress, inflammation, and fibrosis in a rabbit model of steatohepatitis," *The American Journal of Pathology*, vol. 170, no. 3, pp. 967–980, 2007.
- [77] H. Maeda and K. Yoshida, "Intermittent hypoxia upregulates hepatic heme oxygenase-1 and ferritin-1, thereby limiting hepatic pathogenesis in rats fed a high-fat diet," *Free Radical Research*, vol. 50, no. 7, pp. 720–731, 2016.
- [78] F. Marra and G. Svegliati-Baroni, "Lipotoxicity and the gut-liver axis in NASH pathogenesis," *Journal of Hepatology*, vol. 68, no. 2, pp. 280–295, 2017.
- [79] S. M. Jandhyala, R. Talukdar, C. Subramanyam, H. Vuyyuru, M. Sasikala, and D. Nageshwar Reddy, "Role of the normal gut microbiota," *World Journal of Gastroenterology*, vol. 21, no. 29, pp. 8787–8803, 2015.
- [80] M. Sanduzzi Zamparelli, D. Compare, P. Coccoli et al., "The metabolic role of gut microbiota in the development of non-alcoholic fatty liver disease and cardiovascular disease," *International Journal of Molecular Sciences*, vol. 17, no. 8, 2016.
- [81] A. Federico, M. Dallio, G. G. Caprio, V. M. Ormando, and C. Loguercio, "Gut microbiota and the liver," *Minerva Gastroenterologica e Dietologica*, vol. 63, no. 4, pp. 385–398, 2017.
- [82] N. S. Betrapally, P. M. Gillevet, and J. S. Bajaj, "Changes in the intestinal microbiome and alcoholic and nonalcoholic liver diseases: causes or effects?," *Gastroenterology*, vol. 150, no. 8, pp. 1745–1755.e3, 2016.
- [83] C. Leung, L. Rivera, J. B. Furness, and P. W. Angus, "The role of the gut microbiota in NAFLD," *Nature Reviews Gastroenterology & Hepatology*, vol. 13, no. 7, pp. 412–425, 2016.
- [84] L. W. Peterson and D. Artis, "Intestinal epithelial cells: regulators of barrier function and immune homeostasis," *Nature Reviews Immunology*, vol. 14, no. 3, pp. 141–153, 2014.
- [85] K. Rahman, C. Desai, S. S. Iyer et al., "Loss of junctional adhesion molecule a promotes severe steatohepatitis in mice on a diet high in saturated fat, fructose, and cholesterol," *Gastroenterology*, vol. 151, no. 4, pp. 733–746.e12, 2016.
- [86] H. Guo, J. B. Callaway, and J. P. Ting, "Inflammasomes: mechanism of action, role in disease, and therapeutics," *Nature Medicine*, vol. 21, no. 7, pp. 677–687, 2015.
- [87] A. R. Mridha, A. Wree, A. A. B. Robertson et al., "NLRP3 inflammasome blockade reduces liver inflammation and fibrosis in experimental NASH in mice," *Journal of Hepatology*, vol. 66, no. 5, pp. 1037–1046, 2017.
- [88] J. Henao-Mejia, E. Elinav, C. Jin et al., "Inflammasome-mediated dysbiosis regulates progression of NAFLD and obesity," *Nature*, vol. 482, no. 7384, pp. 179–185, 2012.
- [89] M. H. Zaki, K. L. Boyd, P. Vogel, M. B. Kastan, M. Lamkanfi, and T. D. Kanneganti, "The NLRP3 inflammasome protects against loss of epithelial integrity and mortality during experimental colitis," *Immunity*, vol. 32, no. 3, pp. 379–391, 2010.
- [90] E. Elinav, T. Strowig, A. L. Kau et al., "NLRP6 inflammasome regulates colonic microbial ecology and risk for colitis," *Cell*, vol. 145, no. 5, pp. 745–757, 2011.
- [91] S. De Minicis, C. Rychlicki, L. Agostinelli et al., "Dysbiosis contributes to fibrogenesis in the course of chronic liver injury in mice," *Hepatology*, vol. 59, no. 5, pp. 1738–1749, 2014.
- [92] I. Pierantonelli, C. Rychlicki, L. Agostinelli et al., "Lack of NLRP3-inflammasome leads to gut-liver axis derangement, gut dysbiosis and a worsened phenotype in a mouse model of NAFLD," *Scientific Reports*, vol. 7, no. 1, article 12200, 2017.
- [93] L. Zhu, S. S. Baker, C. Gill et al., "Characterization of gut microbiomes in nonalcoholic steatohepatitis (NASH) patients: a connection between endogenous alcohol and NASH," *Hepatology*, vol. 57, no. 2, pp. 601–609, 2013.
- [94] I. C. de Medeiros and J. G. de Lima, "Is nonalcoholic fatty liver disease an endogenous alcoholic fatty liver disease?—A mechanistic hypothesis," *Medical Hypotheses*, vol. 85, no. 2, pp. 148–152, 2015.
- [95] C. A. Woodhouse, V. C. Patel, A. Singanayagam, and D. L. Shawcross, "Review article: the gut microbiome as a therapeutic target in the pathogenesis and treatment of chronic liver disease," *Alimentary Pharmacology and Therapeutics*, vol. 47, no. 2, pp. 192–202, 2018.
- [96] M. Pasarin, V. La Mura, J. Gracia-Sancho et al., "Sinusoidal endothelial dysfunction precedes inflammation and fibrosis in a model of NAFLD," *PLoS One*, vol. 7, no. 4, article e32785, 2012.
- [97] Y. Yoon, J. Song, S. H. Hong, and J. Q. Kim, "Plasma nitric oxide concentrations and nitric oxide synthase gene polymorphisms in coronary artery disease," *Clinical Chemistry*, vol. 46, no. 10, pp. 1626–1630, 2000.
- [98] M. A. Potenza, F. L. Marasciulo, D. M. Chieppa et al., "Insulin resistance in spontaneously hypertensive rats is associated with endothelial dysfunction characterized by imbalance between NO and ET-1 production," *American Journal of Physiology Heart and Circulatory Physiology*, vol. 289, no. 2, pp. H813–H822, 2005.
- [99] M. Perreault and A. Marette, "Targeted disruption of inducible nitric oxide synthase protects against obesity-linked insulin resistance in muscle," *Nature Medicine*, vol. 7, no. 10, pp. 1138–1143, 2001.
- [100] M. A. Carvalho-Filho, M. Ueno, S. M. Hirabara et al., "S-Nitrosation of the insulin receptor, insulin receptor substrate 1, and protein kinase B/Akt: a novel mechanism of insulin resistance," *Diabetes*, vol. 54, no. 4, pp. 959–967, 2005.
- [101] P. Dallaire, K. Bellmann, M. Laplante et al., "Obese mice lacking inducible nitric oxide synthase are sensitized to the metabolic actions of peroxisome proliferator-activated receptor- γ agonism," *Diabetes*, vol. 57, no. 8, pp. 1999–2011, 2008.
- [102] D. A. Langer, A. Das, D. Semela et al., "Nitric oxide promotes caspase-independent hepatic stellate cell apoptosis through the generation of reactive oxygen species," *Hepatology*, vol. 47, no. 6, pp. 1983–1993, 2008.
- [103] Y. Iwakiri, M. Grisham, and V. Shah, "Vascular biology and pathobiology of the liver: report of a single-topic symposium," *Hepatology*, vol. 47, no. 5, pp. 1754–1763, 2008.
- [104] F. J. Gonzalez-Paredes, G. Hernandez Mesa, D. Morales Arraez et al., "Contribution of cyclooxygenase end products and oxidative stress to intrahepatic endothelial dysfunction in early non-alcoholic fatty liver disease," *PLoS One*, vol. 11, no. 5, article e0156650, 2016.
- [105] J. F. Keaney Jr., M. G. Larson, R. S. Vasan et al., "Obesity and systemic oxidative stress: clinical correlates of oxidative stress in the Framingham study," *Arteriosclerosis, Thrombosis, and Vascular Biology*, vol. 23, no. 3, pp. 434–439, 2003.
- [106] C. Couillard, G. Ruel, W. R. Archer et al., "Circulating levels of oxidative stress markers and endothelial adhesion molecules in men with abdominal obesity," *The Journal of Clinical Endocrinology & Metabolism*, vol. 90, no. 12, pp. 6454–6459, 2005.

- [107] S. Furukawa, T. Fujita, M. Shimabukuro et al., "Increased oxidative stress in obesity and its impact on metabolic syndrome," *The Journal of Clinical Investigation*, vol. 114, no. 12, pp. 1752–1761, 2004.
- [108] K. E. Wellen and G. S. Hotamisligil, "Inflammation, stress, and diabetes," *The Journal of Clinical Investigation*, vol. 115, no. 5, pp. 1111–1119, 2005.
- [109] I. Grattagliano, V. O. Palmieri, P. Portincasa, A. Moschetta, and G. Palasciano, "Oxidative stress-induced risk factors associated with the metabolic syndrome: a unifying hypothesis," *The Journal of Nutritional Biochemistry*, vol. 19, no. 8, pp. 491–504, 2008.
- [110] V. O. Palmieri, I. Grattagliano, P. Portincasa, and G. Palasciano, "Systemic oxidative alterations are associated with visceral adiposity and liver steatosis in patients with metabolic syndrome," *The Journal of Nutrition*, vol. 136, no. 12, pp. 3022–3026, 2006.
- [111] P. Stiuso, I. Scognamiglio, M. Murolo et al., "Serum oxidative stress markers and lipidomic profile to detect NASH patients responsive to an antioxidant treatment: a pilot study," *Oxidative Medicine and Cellular Longevity*, vol. 2014, Article ID 169216, 8 pages, 2014.
- [112] M. Suthanthiran, M. E. Anderson, V. K. Sharma, and A. Meister, "Glutathione regulates activation-dependent DNA synthesis in highly purified normal human T lymphocytes stimulated via the CD2 and CD3 antigens," *Proceedings of the National Academy of Sciences of the United States of America*, vol. 87, no. 9, pp. 3343–3347, 1990.
- [113] N. Chalasani, M. A. Deeg, and D. W. Crabb, "Systemic levels of lipid peroxidation and its metabolic and dietary correlates in patients with nonalcoholic steatohepatitis," *The American Journal of Gastroenterology*, vol. 99, no. 8, pp. 1497–1502, 2004.
- [114] G. Donati, B. Stagni, F. Piscaglia et al., "Increased prevalence of fatty liver in arterial hypertensive patients with normal liver enzymes: role of insulin resistance," *Gut*, vol. 53, no. 7, pp. 1020–1023, 2004.
- [115] A. M. Diehl, "Fatty liver, hypertension, and the metabolic syndrome," *Gut*, vol. 53, no. 7, pp. 923–924, 2004.
- [116] P. M. Gholam, L. Flancbaum, J. T. Machan, D. A. Charney, and D. P. Kotler, "Nonalcoholic fatty liver disease in severely obese subjects," *The American Journal of Gastroenterology*, vol. 102, no. 2, pp. 399–408, 2007.
- [117] J. Boursier, O. Mueller, M. Barret et al., "The severity of non-alcoholic fatty liver disease is associated with gut dysbiosis and shift in the metabolic function of the gut microbiota," *Hepatology*, vol. 63, no. 3, pp. 764–775, 2016.
- [118] M. Persico, M. Masarone, A. Damato et al., "Non alcoholic fatty liver disease and eNOS dysfunction in humans," *BMC Gastroenterology*, vol. 17, no. 1, p. 35, 2017.

Review Article

Hypoxic Signaling and Cholesterol Lipotoxicity in Fatty Liver Disease Progression

Oren Tirosh 

Institute of Biochemistry, Food Science and Nutrition, The R.H. Smith Faculty of Agriculture, Food and Environment, The Hebrew University of Jerusalem, Rehovot, Israel

Correspondence should be addressed to Oren Tirosh; oren.tirosh@mail.huji.ac.il

Received 25 February 2018; Revised 30 April 2018; Accepted 14 May 2018; Published 31 May 2018

Academic Editor: Anna M. Giudetti

Copyright © 2018 Oren Tirosh. This is an open access article distributed under the Creative Commons Attribution License, which permits unrestricted use, distribution, and reproduction in any medium, provided the original work is properly cited.

Cholesterol is the only lipid whose absorption in the gastrointestinal tract is limited by gate-keeping transporters and efflux mechanisms, preventing its rapid absorption and accumulation in the liver and blood vessels. In this review, I explored the current data regarding cholesterol accumulation in liver cells and key mechanisms in cholesterol-induced fatty liver disease associated with the activation of deleterious hypoxic and nitric oxide signal transduction pathways. Although nonalcoholic fatty liver disease (NAFLD) affects both obese and nonobese individuals, the mechanism of NAFLD progression in lean individuals with healthy metabolism is puzzling. Lean NAFLD individuals exhibit normal metabolic responses, implying that liver damage is not associated with impaired metabolism per se and that direct lipotoxic effects are crucial for disease progression. Several redox and oxidant signaling pathways involving cholesterol are at play in fatty liver disease development. These include impairment of the mitochondrial and lysosomal function by cholesterol loading of the inner-cell membranes; formation of cholesterol crystals and hepatocyte degradation; and crown-like structures surrounding degrading hepatocytes, activating Kupffer cells, and evoking inflammation. The current review focuses on the induction of liver inflammation, fibrosis, and steatosis by free cholesterol via the hypoxia-inducible factor 1α (HIF- 1α), a main oxygen-sensing transcription factor involved in all stages of NAFLD. Cholesterol loading in hepatocytes can result in chronic HIF- 1α activity because of the decreased oxygen availability and excessive production of nitric oxide and mitochondrial reactive oxygen species.

1. Nonalcoholic Fatty Liver Disease (NAFLD) and Lipotoxicity

1.1. Pathology. The liver is a major site for the synthesis, oxidation, metabolism, storage, and distribution of lipids and plays an essential role in regulating energy metabolism [1]. NAFLD is a continuum of diseases that includes simple steatosis (lipid accumulation) and nonalcoholic steatohepatitis (NASH) and ultimately leads to cirrhosis, hepatocellular carcinoma (HCC), and end-stage liver failure developing in the absence of excessive alcohol intake. Simple steatosis is considered to have a benign hepatopathological prognosis. In contrast, NASH is characterized by the presence of steatosis, necroinflammation, and liver fibrosis and is associated with higher cardiovascular mortality that is largely caused by liver-related complications. NASH is a leading cause of liver

transplantations [2]. The severity of NAFLD increases in parallel with other features of the metabolic syndrome, supporting the idea that NAFLD in obese individuals represents a hepatic manifestation of the metabolic syndrome. On the other hand, NAFLD has the potential to progress through the inflammatory phase of NASH to fibrosis, cirrhosis, and, in some cases, liver failure or HCC [3]. The disease etiology also involves significant redox and oxidative stress components [4–7].

1.2. Prevalence. The World Health Organization estimates that over one billion adults worldwide are overweight, at least 300 million of which are obese [8]. The percentage of obese individuals in the US increased from 12.0% in 1991 to 35.7% in 2010. In fact, currently, obesity is the second leading cause of preventable death in the US. Obesity represents a

major public health challenge, and NAFLD represents a major complication of obesity. Because of the high prevalence of obesity, NAFLD and NASH have now reached alarming proportions, affecting 10–30% of the world's population. Despite of this, the Food and Drug Administration has not approved any specific treatment for either condition [9–11]. According to a recent study, 417,524 individuals in the US are living with NASH-associated cirrhosis, which represents a major complication of the disease, and approximately 4,104,871 individuals are living with NAFLD-associated advanced fibrosis [12]. Obesity and metabolic syndrome-related NAFLD are characterized by excess fat deposition in the liver, and this is associated with type 2 diabetes mellitus, hyperlipidemia, and insulin resistance [13–15].

1.3. NAFLD in Obese and Nonobese Individuals. The etiology of metabolism-related NAFLD in obese individuals is probably different from that of NAFLD diagnosed in nonobese individuals. The prevalence of NAFLD in nonobese individuals can reach 27% in the lean general population and is particularly common in Asian countries [16]. The pathophysiology of nonobese NAFLD is also possibly quite different from that of obese NAFLD. Genetic predisposition, a fructose- and cholesterol-rich diet, visceral adiposity, and dyslipidemia potentially contribute to the pathogenic process [16, 17]. Distinct causes of nonobese NAFLD, particularly in patients with nonmetabolic syndrome, remain unresolved, but could be connected to cholesterol and toxic bile acid levels in the liver and gastrointestinal (GI) tract. Lipotoxic effects can be mimicked by high-cholesterol diet (HCD), even in the absence of high fat content [18–20].

Categorizing the NAFLD severity is controversial because of contradicting epidemiological reports. NAFLD in the nonobese population has been increasingly reported, and the pathogenesis of nonobese NAFLD is poorly understood [21]. It was previously suggested that the long-term prognosis of nonobese NAFLD patients is worse than that of obese NAFLD patients, with a higher mortality rate among nonobese patients, even in those with a normal metabolic profile [22, 23]. In another report, metabolic syndrome parameters were recorded in nonobese NAFLD but with lesser magnitude relative to those noted in the obese individuals [24]. Obesity was identified as a major risk factor for the deterioration of NAFLD to fibrosis, as determined by a systematic search of Sookoian and Pirola (up to July 2017), which allowed a comparison of 493 nonobese patients and 2209 overweight or obese patients. The analysis revealed that fibrosis scores of overweight or obese-NAFLD patients were higher than those of nonobese NAFLD patients [25].

NAFLD can be detrimental to both obese and nonobese patients. Metabolic effects in nonobese NAFLD patients are less pronounced than the effects of direct liver damage resulting from an exposure of the liver to lipotoxic lipids, especially cholesterol and free fatty acids (FFA). Indeed, in animal models of NASH (methionine- and choline-deficient diet or atherogenic diet), loss of body weight, low levels of glucose, and depletion of the adipose tissue are observed when administered in the absence of high fat. On the other hand, liver damage and inflammation are much prominent in those

models [18]. Therefore, NAFLD progression is not merely associated with excess caloric intake, and lipotoxicity could be the main factor that promotes the fatty liver disease progression, regardless of the metabolic impairment [26]. Lipotoxic effects could be critical in leading up to the nadir of liver function (in terms of clinical parameters) in both nonobese and obese NAFLD patients. Key landmarks in understanding the disease progression in terms of the lipotoxic effect of lipids are listed in Table 1.

2. Involvement of Lipids in Hypoxic Signaling: From Simple Steatosis to HCC

2.1. Hypoxic Signaling. Liver steatosis, inflammation fibrosis, and the formation of HCC are linked with redox signaling and hypoxic signaling via hypoxia-inducible factors (HIFs). HIFs are transcriptional regulators that control gene expression during hypoxia, enabling different cells to survive in the hypoxic environment and under stress conditions [38]. HIFs also regulate cell survival and cancer progression [39]. HIFs are members of the bHLH-PAS family of transcription factors and bind canonical DNA sequences, hypoxia response elements (HREs).

HIFs are heterodimers composed of α (HIF α) and β (ARNT/HIF β) subunits that activate the expression of hundreds of genes that encode proteins regulating cell metabolism, survival, mortality, basement membrane integrity, angiogenesis, vascular tone, hematopoiesis, and other functions [40]. The transcriptional activation and stabilization of HIF-1 α increases when the local oxygen concentration is reduced. HIF-1 α and HIF-2 α undergo posttranslational modifications catalyzed by oxygen-dependent prolyl hydroxylases. These modifications typically stabilize HIF-1 α in cells, proportionally enhancing HIF-1 α activity. In hepatocyte cell lines, HIF-1 α expression is regulated by stress-responsive deacetylase sirtuin 1 [41]. In contrast with the transient nature of HIF-1 α activation and its involvement in the initial response to hypoxia, HIF-2 α protein levels vary to a lesser extent and HIF-2 α stabilization in the liver following its activation lasts longer than that of HIF-1 α [42].

2.2. Hypoxia and Liver Diseases. Most chronic liver conditions are associated with hypoxic conditions linked to metabolic diseases, such as NAFLD. For example, obstructive sleep apnea syndrome (OSAS) and NAFLD are common conditions, frequently encountered in patients with metabolic disorders. OSAS has been associated with an increased risk of cardiovascular and metabolic complications. It was suggested recently that the chronic intermittent hypoxia during OSAS may also affect the occurrence and severity of NAFLD [43]. Chronic exposure of rats to hypoxic conditions resulted in increased activity of the transcription factors HIF-1 α , AP-1, and nuclear factor (NF) κ B, which may be partially involved in hepatic responses to oxidative stress and liver injury under chronic hypoxia. Elevated expression of VEGF, ET-1, inducible nitric oxide synthase (iNOS), and endothelial NOS (eNOS) in response to chronic hypoxia were also reported [44].

TABLE 1: From triglycerides to toxic lipids: key landmarks representing progress in understanding lipotoxicity in NAFLD.

Year	Landmark	Significance	Ref.
1980	NAFLD characterized for the first time	Liver inflammation detected in Mobridge obesity patients	[27]
1998	The two-hit hypothesis	Inflammation occurs after fat (triglyceride) infiltration of the hepatocytes	[28]
2006	Role of free cholesterol (FC) in NASH described: mitochondrial dysfunction, oxidative damage, and proinflammatory effects	Activation of the immune system, inflammation, and cellular apoptosis, and hepatocyte necrosis	[29]
2007	FC and prooxidant effects recognized	Development of the atherogenic diet model for lipid-induced NASH	[30]
2007	Toxicity of free fatty acids described	Increased fibrosis and protective role of triglycerides	[31]
2008	Lipotoxicity of lysophosphatidylcholine determined	Death signals in hepatocytes induced by lipids	[32]
2010	The multiple-parallel hit hypothesis: NAFLD is a multifactorial disease	(a) Inflammation may precede steatosis or may be activated by failure of antilipotoxic protection (b) Other parallel hits derived from the gut and/or the adipose tissue may promote liver inflammation via multiple-organ crosstalk (c) Endoplasmic reticulum (ER) stress and its effect related to signaling networks for steatosis	[33]
2012	Lipids activate NLR family pyrin domain-containing 3 (NLRP3) inflammasomes.	Hepatic long-chain fatty acid composition, a novel determinant in inflammatory response and NASH development	[34]
2012–2014	Ceramide lipotoxicity recognized	Ceramide accumulation and altered acylation pattern in the liver are connected to hepatic steatosis, elevated plasma free fatty acid levels, insulin resistance, and lipotoxicity: these are all noted in NASH	[35, 36]
2017	Cholesterol crystallization within hepatocyte lipid droplets (LDs) observed	Activation of macrophages causes upregulation of tumor necrosis factor (TNF) α , NLRP3, and interleukin 1 β . Cholesterol crystals formed on the LD membrane of degrading hepatocytes facilitate inflammatory activation of Kupffer cells	[37]

NAFLD patients have increased risk to cholelithiasis [45]. Recently, using a NASH model of atherogenic diet supplementation in mice, the connection between hypoxic signaling, liver cholesterol accumulation, and gallstone formation was demonstrated. Protection against gallstone formation was demonstrated in iH-HIFKO mice (mice with specific HIF knockout in hepatocytes). Without HIF-1 α , response to cholesterol lipid concentration was reduced compared with control mice, and bile flow increased due to hepatic expression of aquaporin 8 (AQP8) protein. In addition, liver tissues from patients with NAFLD with gallstones had increased levels of HIF-1 α , HMOX1, and VEGFA mRNAs, compared with livers from patients with NAFLD without gallstones [46].

2.3. Liver Steatosis. The involvement of HIF-1 α in liver steatosis has been linked to hypoxia-inducible protein 2 (HIG2), which is regulated by HIF-1 α . The HIG2 protein is located at the hemimembrane of LDs and colocalizes with the LD proteins adipophilin and TIP47 [47–49]. HIG2 overexpression under normoxic conditions increases neutral lipid deposition in HeLa cells and stimulates cytokine expression [49]. HIG2 is detected in the atherosclerotic arteries and in patients with fatty liver disease, suggesting that this product of the ubiquitously inducible HIF-1 α gene target may play an important

functional role in disease progression and etiology associated with ectopic lipid accumulation [49]. Exposure of human cells to hypoxia reportedly causes accumulation of triglycerides and LD formation [50].

Another mechanism of HIF-1 α -mediated lipid accumulation involves the induction of the lipin 1 gene, whose product is involved in triglyceride biosynthesis. HIF-1 α reportedly binds a single distal HRE in the lipin 1 gene promoter, causing its activation under low-oxygen conditions [50]. Activation of the HIF-1 α pathway by nitric oxide (NO) donors can also lead to lipid accumulation in hepatocytes. Treatment of the AML-12 mouse hepatocytes with the NO donor diethylenetriamine NONOate (DETA-NO) resulted in a dose- and time-dependent increase in lipid accumulation in these cells, as determined by Nile red fluorescence [51]. Further, exposure of the cells to 1 mM DETA-NO for 24 h resulted in elevated reactive oxygen species (ROS) production, mainly peroxides. NO induced HIF-1 α expression, whereas treatment with the HIF-1 α inhibitor YC-1 blocked lipid accumulation in these cells [51].

2.4. Liver Fibrosis. HIF-1 α is also a major regulator of liver fibrosis [52–55]. In the context of progressive chronic liver disease under hypoxic conditions, activated myofibroblasts exhibit both proangiogenic and profibrogenic activities [56].

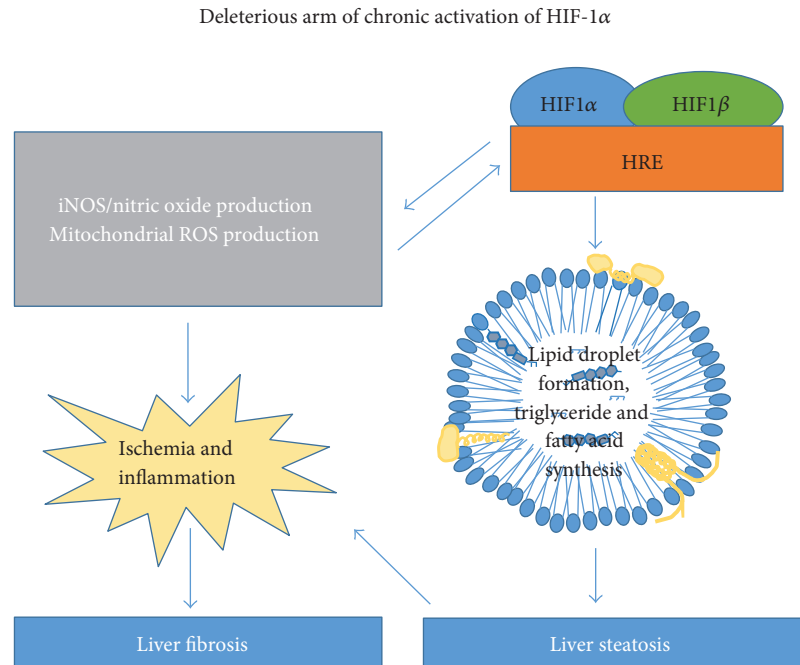


FIGURE 1: Consequences of chronic activation of the HIF-1 α -iNOS axis, and its downstream involvement in lipid metabolism and fatty liver disease formation. HIF-1 α stabilization can be induced by hypoxia or by exclusive NO or mitochondrial ROS production. HIF-1 α stabilization promotes lipid synthesis and LD formation, both of which can aggravate liver steatosis. Chronic, but not transient, expression of HIF-1 α and iNOS can induce inflammatory liver damage and fibrosis.

The product of the lysyl oxidase (LOX) gene, a hypoxia-responsive gene, catalyzes collagen crosslinking and is thought to be important in cancer metastasis and osteoarthritis. LOX is upregulated by both HIF-1 α and HIF-2 α [57]. In addition, LOX has been shown to significantly contribute to collagen stabilization during liver fibrosis [58].

HIF proteins are potential target for treating chronic liver diseases [59]. Studies of a specific model of cholestasis revealed that chronic liver injury activates HIF-1 α in macrophages, regulating the production of mediators of liver fibrosis. In fact, nuclear HIF-1 α is present in macrophages, hepatocytes, and fibroblasts in the cholestatic liver disease, in the livers of patients with primary biliary cholangitis and primary sclerosing cholangitis [60]. Further, the levels of smooth muscle α -actin and type I collagen are lower in the liver of HIF-deficient mouse than those in a mouse with normal HIF levels, in a model of obstructive cholestasis of bile duct ligation [55]. These findings demonstrate that HIFs are important regulators of liver fibrosis [60] (Figure 1) and that their activation may be regulated by cholesterol accumulation in the liver.

2.5. HCC. The final stage of NAFLD is the formation of HCC. HIF-1 α and HIF-2 α were suggested to play pivotal roles in inducing HCC. These two proteins and NF- κ B have been shown to regulate genes involved in carcinogenesis and HCC progression. The von Hippel-Lindau (VHL) protein targets HIF-1/2 α subunits for degradation and participates in modulating the activities of HIFs and NF- κ B. Recently, it was shown that pVHL overexpression synergizes with doxorubicin in the treatment of HCC [61]. Further, in an HCC

model of injecting mouse HCC cells to the liver of immune competent mice, HIF-1 α was shown to be associated with undifferentiation and accumulation of myeloid-derived suppressor cells (MDSCs), which exhibit immunosuppressive activities. In the report, it was suggested that HIF-1 α may regulate tumor growth by regulating ectoenzyme, ectonucleoside triphosphate diphosphohydrolase 2 (ENTPD2), and extracellular levels of 5'-AMP to promote tumor growth through shaping the microenvironment of the HCC tumor in addition to direct impact. Thereby, MDSC accumulation enables cancer cells to escape immune surveillance and to become nonresponsive to immune suppression. Indeed, it was reported that hypoxia causes MDSC accumulation via the HIF-1 α signaling pathway [62].

2.6. Glucose Metabolism and HCC. Under hypoxic conditions, cancer cells, including HCC cells, consume excessive levels of glucose as the major fuel source and produce high levels of lactate (via the Warburg effect, i.e., aerobic glycolysis) [63]. In HCC cells, the Warburg effect is controlled by HIF-1 α [64]. In terms of clinical outcomes, the aggressiveness of HCC tumors may be attributed to the intensity of aerobic glycolysis. An elevated glycolysis enables tumors to survive under conditions of stress and to evade chemotherapy. Indeed, the activation of HIF-1 α -dependent genes that regulate glycolysis is much higher in HCC with venous invasion than in HCC without venous invasion [65]. Another survival benefit is that in certain tumors (including HCC tumors), HIF-1 β /ARNT expression is upregulated by HIF-1 α , resulting in augmented HIF-1 α signaling and better survival [66].

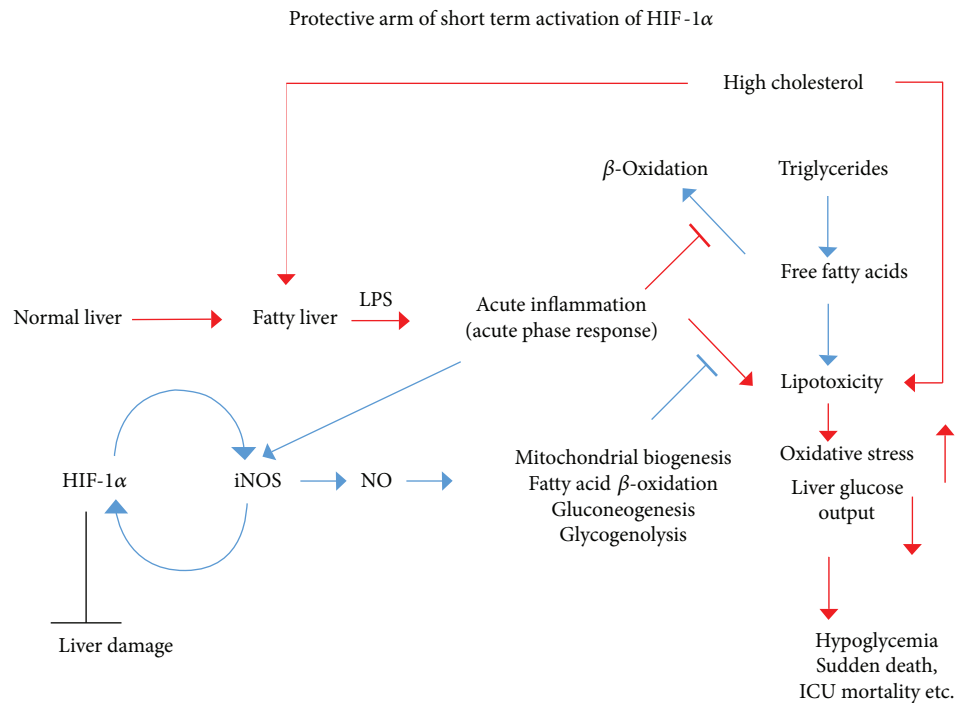


FIGURE 2: Consequences of acute activation of the HIF-1 α -iNOS axis, and its downstream roles in lipid and glucose metabolism. Transient HIF-1 α and iNOS activation in response to acute inflammatory signals can protect against metabolic collapse of the liver. This is especially relevant in the steatotic liver, allowing glucose and energy production under stress. ICU: intensive care unit.

Taken together, these findings indicate that HIFs may serve as a novel and key therapeutic target for treating chronic liver metabolic diseases in human. HIF-1 α inhibition could be relevant to the resolution of all NAFLD-related clinical parameters (including steatosis, chronic hepatitis, and fibrosis) and HCC, whereas its activation is relevant to the protection against ischemia/reperfusion- (I/R-) related injury and acute hepatitis [59]. Interestingly, dietary cholesterol can chronically activate the HIF-1 α pathway even under normoxic conditions [20].

The complex molecular function of HIF-1 α is also relevant to its capacity to activate the expression of iNOS, one of the most important redox-signaling molecules, as well as oxidative and nitrosative stress-related enzymes [67]. iNOS can generate high levels of NO. Chronically produced NO can be deleterious while transiently produced NO can be protective in terms of correcting metabolic inflammatory stress (Figure 2).

Transient iNOS expression and activation of the HIF-1 α -iNOS axis not only protects liver metabolism but also prevents the progression of liver damage [68]. Previously, it was postulated that NO may contribute to hepatotoxicity by mitochondrial activity inhibition, followed by reduced ATP synthesis, increased ROS production, and the inability to adapt to hypoxic stress [69]. It has been suggested that NO can block mitochondrial respiration and thereby prevent HIF-1 α stabilization [70]. However, under normoxia, NO was shown to interact with the catalytic site of prolyl hydroxylase domain proteins and to promote HIF-1 α stabilization [71]. Other observations imply that reduction of NO production by eNOS contributes to liver pathology by dysregulating

the blood flow and oxygen delivery [72]. Furthermore, hepatocytes undergo necrosis and apoptosis after partial hepatectomy in iNOS-knockout mouse, indicating that NO production is essential for protecting hepatocytes from death after liver resection [73]. Knockout mouse models of iNOS or eNOS revealed that NO plays a crucial role in liver regeneration. Mei and Thevananther and Rai et al. reported impaired liver regeneration after partial hepatectomy in the eNOS- and iNOS-knockout mouse models, respectively [73, 74]. The role of NO in a treatment of partial hepatectomy was also demonstrated in animals supplemented with N(G)-nitro-L-arginine methyl ester (L-NAME), a NOS inhibitor. Impaired liver regeneration with simultaneously enhanced liver steatosis and reduced survival was observed in animals treated with L-NAME [75]. These data indicate that NO plays an antisteatotic role. Further, decreased eNOS expression precedes the formation of liver damage following intensive blood infusion of triglycerides in rat [76]. In summary, NO can be toxic or protective, depending on the liver microenvironment (Figure 2).

The specific roles of NO in NAFLD progression and liver fibrosis are ill defined. Marked fibrosis and inflammation are observed in the liver of iNOS-knockout mouse but not in wild-type (WT) mice after 48 weeks on a high-fat diet (HFD) [77]. However, following a short-term (6-week) supplementation of high cholesterol and cholic acid (the designated NASH model), chronic production of NO by iNOS induced liver fibrosis, HIF-1 α stabilization, and DNA damage in WT mice [19].

Lipopolysaccharides (LPS) can promote liver inflammation and NASH [78]. However, conflicting reports fail to

clarify the role of NO production in promoting this association. Although it has been suggested that NO is a mediator of organ dysfunction, some investigators have suggested that NO protects the liver and other organs. Previous studies from the author's laboratory demonstrated that iNOS-deficient mice with fatty liver induced by ethionine supplementation in choline-deficient diet, or a cholesterol/cholic acid-rich diet, are more sensitive to LPS treatment than WT mice are [68, 79]. It is known that fatty liver sensitivity to acute inflammation injury is much higher than that of normal liver. In a mouse model of fatty liver and endotoxemia, iNOS expression plays an important protective role [79].

Taken together, previous findings indicate that a feedback loop exists between HIF-1 α and iNOS, protecting against cholesterol or LPS-induced metabolic collapse under stress (Figure 2). However, chronic activation of HIF-1 α and iNOS can result in liver fibrosis and liver damage (Figure 1).

3. Cholesterol Toxicity and Metabolic Effects in NAFLD

NASH involves hepatic steatosis and necroinflammation. The transition towards hepatic inflammation represents a key step in disease pathogenesis because it promotes liver damage, culminating in hepatic fibrosis, cirrhosis, and liver cancer [3]. It is well known that phytosterol and dietary cholesterol absorption are tightly regulated in the GI tract. While the absorption efficiency of other types of lipids (especially triglycerides) is approximately 98%, the efficiency of cholesterol absorption is on average around 50% [80]. It is controlled by the Niemann-Pick C1-like 1 (NPC1L1), a polytopic transmembrane protein localized at the apical membrane of enterocytes and the canalicular membrane of hepatocytes, which functions as the gatekeeper for cholesterol absorption. NPC1L1 is a transporter that facilitates intestinal free cholesterol (FC) absorption. It also counterbalances hepatobiliary cholesterol excretion [81]. In addition to NPC1L1, two other transporters (ABCG5 and ABCG8) that potentiate plant sterol and cholesterol efflux back into the intestinal and biliary lumen for fecal excretion regulate decreased cholesterol uptake [82]. This unique control mechanism slows down the rate of absorption of FC to the circulation and the bodily tissues. This mechanism prevents atherosclerosis and protects the liver against cholesterol lipotoxicity [81].

Emerging experimental and clinical data link altered hepatic cholesterol homeostasis and FC accumulation with NASH pathogenesis [83, 84]. When the experimental animals receive normal-fat diet supplemented with cholesterol (i.e., without HFD), the dietary cholesterol and liver cholesterol accumulation induce several NASH features with symptoms similar to those seen in nonobese human subjects with NASH. Such characteristics include a moderate loss of body weight, loss of adipose tissue mass, and little or no hyperinsulinemia [18]. Animals with steatohepatitis induced by methionine and choline deficiency and animals receiving an atherogenic (cholesterol + cholate) diet exhibit only minimal systemic insulin resistance. Insulin resistance is exacerbated by increasing the fat content (triglycerides) of the diets

[30, 85]. This indicates that cholesterol is a nutritional factor critical for the development of NASH and that its lipotoxic activity is probably dissociated from the metabolic status of the patient [86, 87]. It has been known for a long time that cholesterol can induce apoptosis and plaque instability in macrophages by causing endoplasmic reticulum (ER) stress to promote thrombotic events [88]. The direct and indirect proapoptotic pathways associated with cholesterol in hepatocytes are shown in Figure 3. Although hepatic accumulation of triglycerides is linked to simple steatosis, it has become clear that cholesterol is involved in hepatic inflammation [89, 90].

The classic mechanism of cholesterol-induced NASH was initially proposed in 2006 [29]. It was suggested that mitochondrial FC loading is involved in precipitating NASH by changing the fluidity of the mitochondrial membranes, which led to the oxidation of mitochondrial glutathione, and sensitized hepatocytes to tumor necrosis factor (TNF) α and Fas-dependent death signaling via mitochondrial glutathione depletion [29]. Regarding the dietary effect on NASH, supplementation of leptin-deficient ob/ob obese mice on a HCD with high-fructose diet resulted in NASH development [91]. Rodents administered diets with high cholesterol content and cholic acid (atherogenic diets) developed steatohepatitis within 4–12 weeks [30].

Cholesterol can also alter the metabolic function and inflammatory status of the liver. Cholesterol in the form of modified plasma lipoproteins represents an important risk factor for the progression to hepatic inflammation in diet-induced NASH [89]. Further, hyperinsulinemia in conjunction with hepatic cholesterol accumulation activates the sterol regulatory element-binding protein 2 (SREBP-2) to upregulate a low-density lipoprotein receptor, which leads to reduced biotransformation of cholesterol to bile acids [92]. These events precipitate hepatocyte injury or apoptosis, macrophage recruitment, liver fibrosis, and progression from steatosis to NASH [92]. SREBP-2 accumulation in the liver was suggested to link between insulin resistance as a risk factor in NASH and necroinflammation. Its accumulation and activation in steatotic hepatocytes may be affected by multiple NASH-related factors including hyperinsulinemia, inflammatory cytokines, and miR dysregulation [92]. Such changes in metabolic conditions are significant contributors to liver FC lipotoxicity by increased cholesterol synthesis through the mevalonate pathway and due to increased cholesterol uptake (free and esterified) by the liver. Activation of SREBP-2 under conditions of insulin resistance can result in inhibition of mitochondrial β -oxidation leading to FFA accumulation. Therefore, insulin resistance can be connected to FFA toxicity.

In addition to direct lipotoxicity of FC, FFA, and other lipids, a mechanism for synergistic toxicity between cholesterol and FFA was suggested to be related to failure to activate the repression factor small heterodimer partner (SHP) upon farnesoid X receptor activation and was shown in obese NAFLD patients [93]. Altogether, this indicates that under NASH conditions there is probably an overaccumulation of cholesterol and bile acids in the liver. In animals, models of high-fat diets from plant source (with no cholesterol)

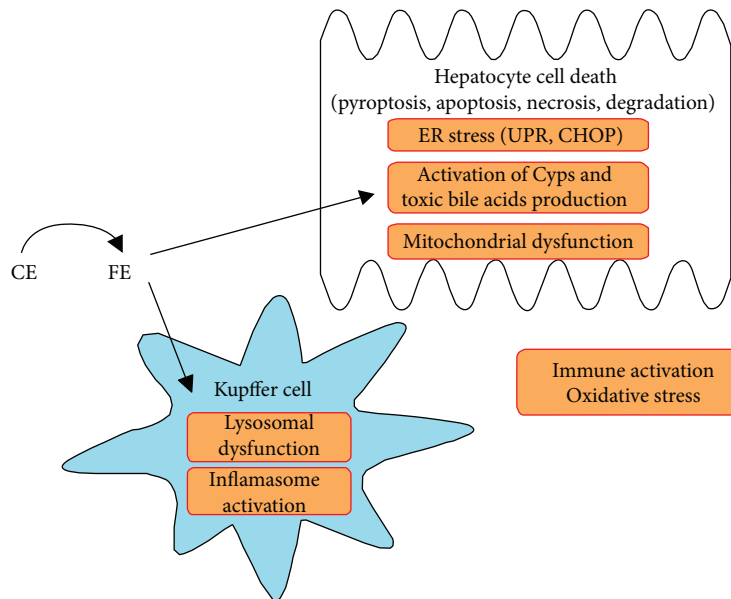


FIGURE 3: FC may directly or indirectly contribute to the development of hepatocyte lipotoxicity through different signaling pathways. Hydrolyzing cholesteryl ester (CE) to free cholesterol in the endosomes of Kupffer cells may lead to inflammation, oxidative stress, immune activation, and cell death. However, dietary FC can directly induce cell death in hepatocytes by different pathways, for example, activation of the Cyps pathway and induction of toxic bile acid production, mitochondrial dysfunction, and ER stress. CE: cholesteryl ester; Cyps: cytochrome P 450 enzymes; CHOP: C/EBP homologous protein; pyroptosis: type of cell death that involves caspase 1 activation and cell swelling [83]; UPR: unfolded protein response.

induced insulin resistance rapidly without significant liver damage [94] indicating that access cholesterol in the liver is not pivotal for induction of insulin resistance but insulin resistance and metabolic syndrome could be important in precipitating lipotoxicity in obesity.

In individuals with metabolic impairment, cholesterol may alter insulin metabolism, which is related to NASH. One study of metabolic syndrome-associated NASH in a rat model demonstrated a possible link between HCD and insulin signaling [95]. The study indicated that the effect of HCD on the development of hepatic insulin resistance is associated with the increased interaction between caveolin-1 and the liver insulin receptor. A mechanism was suggested whereby HCD alters caveolin-1 expression *in vivo*, which is accompanied by altered insulin receptor localization and activity [95]. Supplementation of rat diet with high cholesterol also induced insulin resistance, although elevated insulin receptor autophosphorylation (its activation) was observed in response to insulin [95]. Such contradicting effects of cholesterol on insulin signaling could be explained by a recent observation that both elevated and reduced plasma membrane cholesterol content affects insulin signaling in hepatocytes [96].

4. Signal Transduction Pathways for Dietary Cholesterol That Induce NASH

It is widely recognized that a Western-style diet increases the risk of NASH development and its subsequent progression to HCC [97]. However, the diet-induced changes in the signaling pathways relevant to these pathologies are not well understood. Several mechanisms have been proposed to

explain the dramatic inducing effect of cholesterol on the progression of inflammation and apoptosis/necrosis of hepatocytes and nonparenchymal cells. Some of these mechanisms are related to redox signaling and oxidative stress. It has been suggested that the progression of NAFLD to steatohepatitis is underpinned by mitochondrial dysfunction, glutathione oxidation, and reduced mitochondrial membrane fluidity [29].

The paradoxical effect of cholesterol on hepatocytes and HCC, leading to cell death, was the subject of a recent review [98]. With respect to steatohepatitis, the effect of intracellular trafficking of cholesterol and its contribution to mitochondrial glutathione depletion in association with cell death was demonstrated. The loading of both dietary cholesterol and cholesterol arising from *de novo* synthesis probably affects mitochondrial glutathione carriers, resulting in mitochondrial glutathione depletion and sensitization of hepatocytes to inflammatory and apoptotic cytokines. The ER stress plays a limited role in the progression of NAFLD to NASH and was suggested not to be involved in cholesterol-induced NASH [29]. It was demonstrated that FC distribution in the ER and plasma membrane does not cause ER stress or alter inflammatory signaling [29]. However, the role of ER stress in cholesterol-induced NASH is limited to the steroidogenic acute regulatory protein-related lipid transfer domain protein StARD5, which may affect the ER in Kupffer cells. It was recently evidenced that ER stress induces the transcriptional upregulation of StARD1, facilitating mitochondrial cholesterol loading [98].

Interestingly, simple steatosis enhances the sensitivity of hepatocytes to hypoxic injury [99]. The author's research

group demonstrated that reduced HIF-1 α activation in steatotic hepatocytes compared to nonsteatotic hepatocytes is the reason for their increased vulnerability [99]. The capacity of steatotic cells to express HIF-1 α -dependent genes responsible for the utilization of nutrients for energy production was also impaired. In contrast, overexpression of constitutively active HIF-1 α significantly increased cellular viability and ATP and *GLUT1* mRNA levels in steatotic hepatocytes subjected to hypoxia. Further, in these cells, hypoxia led to the reduction of cellular and nuclear reduced glutathione levels and enhanced accumulation of 4-hydroxynonenal protein adducts. Hypoxia, in combination with hepatic steatosis, was also shown to promote oxidative stress, leading to NF- κ B inactivation and impaired HIF-1 α induction, and thereby increasing cell susceptibility to hypoxic injury [99]. In contrast with steatotic hepatocytes loaded with TGs, hepatocyte treatment with cholesterol dramatically increases HIF-1 α activation *in vitro* and *in vivo* and promotes molecular inflammatory response for cell survival, setting the stage for HCC induction [100]. An adaptive response of HCC cells to cholesterol is to protect mitochondrial glutathione levels from depletion via the 2-oxoglutarate carrier. The regulation of 2-oxoglutarate carrier expression was found to be HIF-dependent [100]. These findings indicate that the exposure of hepatocytes to cholesterol may lead to cell death (because of the effect of cholesterol on the mitochondria) or can activate a survival pathway specially in HCC.

In addition, the oxidative products of cholesterol oxysterols were suggested to contribute to liver injury and mitochondrial dysfunction. A synergistic interaction between FFA and oxysterols was suggested to impair mitochondrial function in NASH. Accumulation of specific nonenzymatic oxysterols and FFA induces mitochondrial damage and depletion of proteins of the respiratory chain complexes and mitochondrial biogenesis both *in vivo* and *in vitro* [101]. Targeted lipidomic analysis of a rat liver with steatohepatitis identified oxysterol triols (e.g., cholestane-3 β ,5 α ,6 β -triol) that were associated with mitochondrial dysfunction and hepatocyte toxicity [102]. It was suggested that the hepatic accumulation of both fatty acids and toxic oxysterols, such as triols, leads to impaired mitochondrial function and biogenesis, contributing to liver pathology in NAFLD [102].

In addition to the classical mitochondrial damage hypothesis for the effect of cholesterol on hepatocytes, the following signaling pathways have been also suggested to mediate the damaging effect of cholesterol:

(1) *Overactivation of the intestinal SREBP-2 transcription factor*: SREBP-2 activation was suggested to promote the progression of hepatic fibrosis associated with diet-induced NASH [103]. Mice specifically overexpressing SREBP-2 in the intestine exhibited greater inflammation and more severe fibrosis of the liver in response to HCD with HFD than their WT littermates. This demonstrates a novel link between the intestinal regulation of cholesterol metabolism and NASH pathogenesis [103].

(2) *Cholesterol crystals in hepatocyte LDs and Kupffer cell activation*: In human and experimental NASH models, the mechanism underlying the enhanced proinflammatory effect of cholesterol was suggested to involve FC crystal formation in hepatocytes. This insight is important for understanding the progression of simple steatosis to NASH. Cholesterol crystals and crown-like structures that are formed in degraded hepatocytes were shown to interact with NLRP3 inflammasomes of Kupffer cells to induce inflammatory responses. This suggests that cholesterol can act as a damage-associated molecular pattern in the liver to promote activation of the NLRP3 inflammasome and other proinflammatory pathways [37, 104].

(3) *Enhanced activation of Kupffer cells by LPS in the presence of toxic lipids*: Kupffer cells in the liver function in LPS clearance. Accumulation of lipids within hepatocytes and Kupffer cells can activate or suppress LPS activity and the bacterial load. Kupffer cells express high levels of class A scavenger receptors (SR-A). These receptors have affinity to modified lipoproteins, and LPS uptake may be overactivated due to the decreased capacity of steatotic hepatocytes to support LPS clearance thereby promoting NASH [105]. In addition, direct recognition of fatty acid moieties by Toll-like receptors (TLRs) is an important mechanism by which lipids regulate the inflammatory pathways and innate immunity in NAFLD/NASH patients [105].

FC metabolism may directly affect the proinflammatory activity of Kupffer cells. For example, in LDL receptor-deficient mice fed HFD, inflammation occurred only if the diet contained cholesterol [90]. The presence of foamy Kupffer cells suggests that scavenging of modified lipoproteins may induce inflammatory responses [90, 105]. In addition, the accumulation of cholesterol in the lysosomal fraction of Kupffer cells was suggested to facilitate liver inflammation [106].

(4) *FC promotes hepatic stellate cell (HSC) activation*: FC accumulation in HSCs induces liver fibrosis in NASH [19]. It has been suggested that FC activates HSCs by rendering them susceptible to transforming growth factor (TGF) β signaling [107]. The role of HSC activation by cholesterol was discussed in a recent review [7]. Indeed, FC activates HSCs in several animal models of NASH; for example, the inclusion of cholesterol in HFD in a methionine choline-deficient model or in models of cholestasis accelerates fibrosis [108]. The signaling mechanism suggested to explain that the activation of HSCs is associated with FC accumulation, which sensitizes the cells to TGF- β through TLR4 upregulation and downregulation of the TGF- β pseudoreceptor BAMBI (bone morphogenetic protein and activin membrane-bound inhibitor), leading to TGF- β -induced liver fibrosis [109].

- (5) *Cholesterol-rich diet-induced protein kinase C β (PKC β) activation:* PKC β activation was suggested as a mechanism to prevent cholesterol accumulation in the liver and to protect against NASH development. Such a scenario indicates that PKC β represents an important mediator in the functional wiring of cholesterol metabolism. Indeed, the loss of PKC β activity induces tumorigenesis by modulating the stability of cell cycle-associated proteins [110]. Further, diets with high fat and high cholesterol content lead to NASH and HCC, and a systemic loss of PKC β promotes hepatic cholesterol accumulation in response to such diets. In addition, compared with nontumorous human liver specimens, reduced PKC β expression is observed in human HCC [110].
- (6) *Chronic activation of hypoxia signaling pathways:* Plasma cholesterol levels correspond to decreased oxygen availability in the hepatic tissue, and the solubility and diffusion of oxygen are impaired in membranes with high cholesterol content [4]. The ability of cholesterol accumulated in the plasma membrane to ameliorate the diffusion of oxygen across membranes and to limit intracellular oxygen availability was demonstrated in several types of cells and in model membranes, as summarized in [4].

A mechanism whereby cholesterol loading of hepatocytes activates HIF-1 α and induces chronic hypoxic responses was revealed *in vitro*, in isolated hepatocytes; *in vivo*, using an atherogenic diet; and in a bile duct ligation model of cholestasis [20, 55, 68]. HIF-1 α activation was dependent on excessive production of reactive oxygen and nitrogen species by cholesterol-mitochondria interactions and iNOS activation [20]. This novel redox-signaling hypothesis can explain the transition from simple steatosis to NASH and liver fibrosis [19].

A possible physiological cause of HIF-NOS pathway activation is to correct and combat acute stress. It should be noted that gluconeogenesis and glycogenolysis are suppressed during acute inflammatory stress. It was suggested that this suppression of glucose production is associated with NO production [111]. However, using iNOS-deficient mouse, the author's research group has shown that NO generation actually supports glucose production in the liver [79]. Culturing hepatocytes with a combination of LPS, TNF- α , interleukin 1 β , and interferon γ inhibits glucose generation by glycogen metabolism and prevents the repletion of glycogen in freshly cultured cells [112]. Further, a pyruvate tolerance test revealed that pretreatment of rats with LPS reduces hepatic gluconeogenesis [111]. The author's group also demonstrated that HIF-1 α activation induces iNOS expression, supporting glucose production by NO signaling in the liver under inflammatory stress conditions [68]. Collectively, these findings indicate that such activation of the HIF-1 α -NOS axis plays a role of a defense mechanism against acute inflammatory responses. This might be important under acute conditions, such as ischemic hepatitis. Ischemic hepatitis, described as "shock liver," is characterized by a massive but transient increase in serum transaminase levels, usually associated with cardiac failure and hypoglycemia [113].

Another physiological situation that might result in glucose production failure is excessive consumption of alcohol during fasting, which can lead to severe hypoglycemia and sudden death [114] (Figure 2). Studies conducted using pharmacological approaches to stabilize HIFs have revealed the protective function of HIFs during I/R-induced liver injury [59]. Therefore, activation of HIF-1 α and iNOS under liver stress conditions can protect against acute metabolic collapse. However, prolonged and chronic activation of the pathway is deleterious. Under chronic inflammatory conditions, such as NASH (Figure 1), this could lead to fibrosis and insulin resistance. This positive-feedback loop of HIF-1 α activation leading to NO production to further stabilize HIF-1 α levels (even under normoxia) may be continuously and strongly activated by cholesterol [20]. Indeed, a similar phenomenon of a positive-feedback loop between HIF-1 α stabilization and the activation of iNOS expression was recently reported to operate during the inflammatory activation of macrophages [115]. In conclusion, the activation of HIFs likely occurs as an adaptive response to I/R-induced injury and acute metabolic stress. However, the consequences of prolonged activation of HIF and iNOS result in structural changes in the liver and damage that are relevant to NASH (Figure 1).

5. Clinical Relevance of Cholesterol and Cholesterol Level-Lowering Drugs in Liver Diseases

Understanding the risk factors and pathophysiology of NAFLD in nonobese and obese individuals is important. The hepatic cholesterol content is high, and hepatic cholesterol flux is robust [116, 117]. In addition, liver cholesterol levels were shown to be elevated in NASH patients [83, 118].

Despite its metabolic role in NASH development, the main function of cholesterol in NASH development is inducing liver damage via lipotoxicity (causing damage of hepatocytes and nonparenchymal liver cells). In that context, the effect of cholesterol accumulation in the liver would be most apparent in nonobese NAFLD patients, acting as a mechanism for the progression from simple steatosis to NASH and fibrosis in the absence of metabolic impairment. In addition, preventing hepatic absorption of dietary cholesterol by a drug treatment may constitute a good therapeutic strategy.

The NAFLD-promoting effect of cholesterol in obese individuals might be important from a metabolic point of view. Little clinical information is available regarding the specific effect of cholesterol on metabolism in NASH patients. Compared with normal liver, the fatty liver metabolism is altered in obese patients with NASH, as determined in the Kuopio Obesity Surgery Study [119]. The study involved 92 obese participants and confirmed that cholesteryl ester fatty acid composition was altered in NASH patients. Obese NASH patients with metabolic impairment would benefit from a treatment to improve the clinical lipoprotein profile.

The effect of ezetimibe (a drug that reduced cholesterol absorption and plasma cholesterol levels to treat NASH) was evaluated in a recent meta-analysis [120]. A significant

reduction of liver enzyme activity in the serum, steatosis, and hepatocyte ballooning was observed. However, ezetimibe treatment did not ameliorate hepatic inflammation and fibrosis in patients with NAFLD and NASH [120]. Based on accumulated data, ezetimibe was suggested to affect only hepatocytes ballooning in NASH [121], but it is not recommended by the American and the European association of study of the liver.

Clinical trials indicate some positive effects of statins as cholesterol-lowering drugs for NASH treatment, as summarized by Pastori et al. [122]. One of the side effects of long-term statin treatment is elevated ALT levels in the blood; however, severe hepatic damage is rarely described. The relative safety of statin treatment was evidenced in 13 randomized, placebo-controlled trials in which statins were used for the treatment of hyperlipidemia and for secondary prevention of the cardiovascular disease. The observations supported the notion of safety of moderate doses of statins [122]. In patients exhibiting elevated liver enzyme levels and steatosis from the beginning of the trials, statin treatment does not exacerbate liver-related adverse effects [122]. Further, the frequency of such effects was low and did not differ from that among statin-untreated NAFLD patients. Moreover, a sustained 3-year treatment substantially ameliorated liver disease and improved blood liver enzyme levels in patients. Regarding the official recommendation of statin use for treating NAFLD and NASH, preliminary studies have shown that statins might improve the hepatic histology in patients [122]. Additional randomized controlled trials are required to assess the effect of statin administration on NAFLD activity score and liver fibrosis.

In another review [123], the authors suggested that statins are a safe NAFLD/NASH treatment and that their use is underappreciated. Three major prospective, randomized, controlled survival trials indicated the beneficial effect of statin use in NAFLD/NASH. These clinical trials demonstrated reduced cardiovascular disease (CVD) morbidity and mortality among statin-treated NAFLD/NASH patients compared to statin-treated patients without NASH. Statins reduced the number of CVD events in NAFLD/NASH CVD patients as compared to patients who were not receiving statin treatment [123]. Liver biopsy analyses revealed that NASH was resolved after a year of statin monotherapy, and liver enzymes, serum uric acid, and glucose returned to normal levels, and that statins exerted a protective effect against steatosis, steatohepatitis, and fibrosis [123]. Therefore, it is apparent that statin treatment is relatively safe, exerts a protective effect in human subjects with NAFLD/NASH, and might reduce cardiovascular disease-related morbidity and mortality. Altogether, these observations indicate that lowering endogenous cholesterol levels can significantly improve the symptoms and risk factors in obese NASH patients.

The clinical relevance of cholesterol in liver pathology may also be correlated with dietary patterns of NAFLD/NASH patients. Indeed, the diet of these patients appears to be rich in high saturated fat, cholesterol, and sweeteners [124]. In subjects with NAFLD, the consumption of high levels of fructose per day was associated with more extensive fibrosis [125]. In a study of 427 adults enrolled in the NASH

Clinical Research, food questionnaires showed that fructose consumption classified into none, minimum to moderate (<7 servings/week), and daily (> or =7 servings/week) was associated with lower liver steatosis but higher fibrosis, increased hepatic inflammation, and hepatocyte ballooning [125]. This raises the possibility that fructose may promote the progression of simple steatosis to steatohepatitis [126]. Fructose might exert a proinflammatory effect because of its negative impact on the gut barrier and endotoxin leakage to the portal vein. It was recently demonstrated that fructose- and cholesterol-rich diets work synergistically to induce liver inflammation by affecting the gut barrier [127].

The cholesterol dose that results in liver toxicity in humans has not been established. However, it seems that both low-fat as well as low-carbohydrate diets are equally effective in the treatment of fatty liver disease and are implicated in some beneficial effects, for example, reducing ALT levels in the serum [126]. Regardless of the weight loss, therefore, restriction and modulation of dietary carbohydrates and reduction of the proinflammatory fat consumption (e.g., restriction of the total and saturated fat and cholesterol) may be beneficial to NASH patients, in addition to improving such metabolic parameters as insulin resistance and liver steatosis.

6. Conclusions

Current data regarding the effect of cholesterol loading in hepatocytes and nonparenchymal cells in the liver indicate that dietary cholesterol is a major nutrient that induces liver damage and lipotoxicity, both in obese and in nonobese individuals. Cholesterol might activate several redox, oxidative stress, and inflammatory signaling pathways to induce NAFLD progression. Its capacity to activate HIF-1 α and iNOS is relevant to cholesterol-induced chronic liver diseases that are related to impaired lipid metabolism. Development of personal drug and dietary treatment strategies to ameliorate cholesterol lipotoxicity and to prevent sustained HIF-1 α activation in NASH and NAFLD patients should be considered.

Abbreviations

DETA-NO:	Diethylenetriamine-NONOate
eNOS:	Endothelial nitric oxide synthase
FC:	Free cholesterol
FFA:	Free fatty acids
HCC:	Hepatocellular carcinoma
HCD:	High-cholesterol diet
HFD:	High-fat diet
HIF-1 α :	Hypoxia-inducible factor 1 α
HIG2:	Hypoxia-inducible protein 2
HRE:	Hypoxia-response element
HSC:	Hepatic stellate cell
I/R:	Ischemia/reperfusion
iNOS:	Inducible nitric oxide synthase
LD:	Lipid droplet
LOX:	Lysyl oxidase
LPS:	Lipopolysaccharide

MDSC:	Myeloid-derived suppressor cell
NAFLD:	Nonalcoholic fatty liver disease
NASH:	Nonalcoholic steatohepatitis
NF- κ B:	Nuclear factor- κ B
NO:	Nitric oxide
NPC1L1:	Niemann–Pick C1-like 1
OSAS:	Obstructive sleep apnea syndrome
ROS:	Reactive oxygen species
TGF- β :	Transforming growth factor β
TLR:	Toll-like receptor
TNF- α :	Tumor necrosis factor α
VHL:	von Hippel–Lindau
WT:	Wild-type.

Conflicts of Interest

The author declares that there is no conflict of interest regarding the publication of this article.

Acknowledgments

The author would like to acknowledge the help of Dr. Irena Peri in English language editing. This work was supported by the Israel Science Foundation (Grant no. 371/12).

References

- [1] L. Rui, “Energy metabolism in the liver,” *Comprehensive Physiology*, vol. 4, no. 1, pp. 177–197, 2014.
- [2] H. Fujii and N. Kawada, “Inflammation and fibrogenesis in steatohepatitis,” *Journal of Gastroenterology*, vol. 47, no. 3, pp. 215–225, 2012.
- [3] A. Lade, L. A. Noon, and S. L. Friedman, “Contributions of metabolic dysregulation and inflammation to nonalcoholic steatohepatitis, hepatic fibrosis, and cancer,” *Current Opinion in Oncology*, vol. 26, no. 1, pp. 100–107, 2014.
- [4] S. Anavi, Z. Madar, and O. Tirosh, “Non-alcoholic fatty liver disease, to struggle with the strangle: oxygen availability in fatty livers,” *Redox Biology*, vol. 13, pp. 386–392, 2017.
- [5] F. Marra and G. Svegliati-Baroni, “Lipotoxicity and the gut-liver axis in NASH pathogenesis,” *Journal of Hepatology*, vol. 68, no. 2, pp. 280–295, 2018.
- [6] S. Spahis, E. Delvin, J. M. Borys, and E. Levy, “Oxidative stress as a critical factor in nonalcoholic fatty liver disease pathogenesis,” *Antioxidants & Redox Signaling*, vol. 26, no. 10, pp. 519–541, 2017.
- [7] T. Tsuchida and S. L. Friedman, “Mechanisms of hepatic stellate cell activation,” *Nature Reviews Gastroenterology & Hepatology*, vol. 14, no. 7, pp. 397–411, 2017.
- [8] K. M. Flegal, D. Kruszon-Moran, M. D. Carroll, C. D. Fryar, and C. L. Ogden, “Trends in obesity among adults in the United States, 2005 to 2014,” *JAMA*, vol. 315, no. 21, pp. 2284–2291, 2016.
- [9] M. A. Konerman, J. C. Jones, and S. A. Harrison, “Pharmacotherapy for NASH: current and emerging,” *Journal of Hepatology*, vol. 68, no. 2, pp. 362–375, 2018.
- [10] G. Musso, M. Cassader, and R. Gambino, “Non-alcoholic steatohepatitis: emerging molecular targets and therapeutic strategies,” *Nature Reviews Drug Discovery*, vol. 15, no. 4, pp. 249–274, 2016.
- [11] T. Hardy, Q. M. Anstee, and C. P. Day, “Nonalcoholic fatty liver disease: new treatments,” *Current Opinion in Gastroenterology*, vol. 31, no. 3, pp. 175–183, 2015.
- [12] M. N. Kabbany, P. K. Conjeevaram Selvakumar, K. Watt et al., “Prevalence of nonalcoholic steatohepatitis-associated cirrhosis in the United States: an analysis of National Health and Nutrition Examination Survey data,” *The American Journal of Gastroenterology*, vol. 112, no. 4, pp. 581–587, 2017.
- [13] A. Lonardo, S. Ballestri, G. Guaraldi et al., “Fatty liver is associated with an increased risk of diabetes and cardiovascular disease - evidence from three different disease models: NAFLD, HCV and HIV,” *World Journal of Gastroenterology*, vol. 22, no. 44, pp. 9674–9693, 2016.
- [14] K. C. Sung, S. Ryu, J. Y. Lee et al., “Fatty liver, insulin resistance, and obesity: relationships with increase in coronary artery calcium over time,” *Clinical Cardiology*, vol. 39, no. 6, pp. 321–328, 2016.
- [15] S. Ballestri, S. Zona, G. Targher et al., “Nonalcoholic fatty liver disease is associated with an almost twofold increased risk of incident type 2 diabetes and metabolic syndrome. Evidence from a systematic review and meta-analysis,” *Journal of Gastroenterology and Hepatology*, vol. 31, no. 5, pp. 936–944, 2016.
- [16] D. Kim and W. R. Kim, “Nonobese fatty liver disease,” *Clinical Gastroenterology and Hepatology*, vol. 15, no. 4, pp. 474–485, 2017.
- [17] R. Kumar and S. Mohan, “Non-alcoholic fatty liver disease in lean subjects: characteristics and implications,” *Journal of Clinical and Translational Hepatology*, vol. 5, no. 3, pp. 216–223, 2017.
- [18] N. Hirsch, A. Konstantinov, S. Anavi et al., “Prolonged feeding with green tea polyphenols exacerbates cholesterol-induced fatty liver disease in mice,” *Molecular Nutrition & Food Research*, vol. 60, no. 12, pp. 2542–2553, 2016.
- [19] S. Anavi, M. Eisenberg-Bord, M. Hahn-Obercyger, O. Genin, M. Pines, and O. Tirosh, “The role of iNOS in cholesterol-induced liver fibrosis,” *Laboratory Investigation*, vol. 95, no. 8, pp. 914–924, 2015.
- [20] S. Anavi, M. Hahn-Obercyger, Z. Madar, and O. Tirosh, “Mechanism for HIF-1 activation by cholesterol under normoxia: a redox signaling pathway for liver damage,” *Free Radical Biology and Medicine*, vol. 71, pp. 61–69, 2014.
- [21] M. H. Yousef, A. A. Juboori, A. A. Albarrak, J. A. Ibdah, and V. Tahan, “Fatty liver without a large ‘belly’: magnified review of non-alcoholic fatty liver disease in non-obese patients,” *World Journal of Gastrointestinal Pathophysiology*, vol. 8, no. 3, pp. 100–107, 2017.
- [22] A. C. Dela Cruz, E. Bugianesi, J. George et al., “379 characteristics and long-term prognosis of lean patients with nonalcoholic fatty liver disease,” *Gastroenterology*, vol. 146, no. 5, article S-909, 2014.
- [23] L. N. Tu, M. R. Showalter, T. Cajka et al., “Metabolomic characteristics of cholesterol-induced non-obese nonalcoholic fatty liver disease in mice,” *Scientific Reports*, vol. 7, no. 1, article 6120, 2017.
- [24] S. Sookoian and C. J. Pirola, “Systematic review with meta-analysis: risk factors for non-alcoholic fatty liver disease suggest a shared altered metabolic and cardiovascular profile between lean and obese patients,” *Alimentary Pharmacology & Therapeutics*, vol. 46, no. 2, pp. 85–95, 2017.

- [25] S. Sookoian and C. J. Pirola, "Systematic review with meta-analysis: the significance of histological disease severity in lean patients with nonalcoholic fatty liver disease," *Alimentary Pharmacology & Therapeutics*, vol. 47, no. 1, pp. 16–25, 2018.
- [26] N. Alkhouiri, L. J. Dixon, and A. E. Feldstein, "Lipotoxicity in nonalcoholic fatty liver disease: not all lipids are created equal," *Expert Review of Gastroenterology & Hepatology*, vol. 3, no. 4, pp. 445–451, 2009.
- [27] J. Ludwig, T. R. Viggiano, D. B. McGill, and B. J. Oh, "Nonalcoholic steatohepatitis: Mayo Clinic experiences with a hitherto unnamed disease," *Mayo Clinic Proceedings*, vol. 55, no. 7, pp. 434–438, 1980.
- [28] C. P. Day and O. F. W. James, "Steatohepatitis: a tale of two 'hits'?", *Gastroenterology*, vol. 114, no. 4, pp. 842–845, 1998.
- [29] M. Mari, F. Caballero, A. Colell et al., "Mitochondrial free cholesterol loading sensitizes to TNF- and Fas-mediated steatohepatitis," *Cell Metabolism*, vol. 4, no. 3, pp. 185–198, 2006.
- [30] N. Matsuzawa, T. Takamura, S. Kurita et al., "Lipid-induced oxidative stress causes steatohepatitis in mice fed an atherogenic diet," *Hepatology*, vol. 46, no. 5, pp. 1392–1403, 2007.
- [31] K. Yamaguchi, L. Yang, S. McCall et al., "Inhibiting triglyceride synthesis improves hepatic steatosis but exacerbates liver damage and fibrosis in obese mice with nonalcoholic steatohepatitis," *Hepatology*, vol. 45, no. 6, pp. 1366–1374, 2007.
- [32] M. S. Han, S. Y. Park, K. Shinzawa et al., "Lysophosphatidylcholine as a death effector in the lipooptosis of hepatocytes," *Journal of Lipid Research*, vol. 49, no. 1, pp. 84–97, 2008.
- [33] H. Tilg and A. R. Moschen, "Evolution of inflammation in nonalcoholic fatty liver disease: the multiple parallel hits hypothesis," *Hepatology*, vol. 52, no. 5, pp. 1836–1846, 2010.
- [34] T. Matsuzaka, A. Atsumi, R. Matsumori et al., "Elovl6 promotes nonalcoholic steatohepatitis," *Hepatology*, vol. 56, no. 6, pp. 2199–2208, 2012.
- [35] S. Raichur, S. T. Wang, P. W. Chan et al., "CerS2 haploinsufficiency inhibits β -oxidation and confers susceptibility to diet-induced steatohepatitis and insulin resistance," *Cell Metabolism*, vol. 20, no. 4, pp. 687–695, 2014.
- [36] M. Pagadala, T. Kasumov, A. J. McCullough, N. N. Zein, and J. P. Kirwan, "Role of ceramides in nonalcoholic fatty liver disease," *Trends in Endocrinology & Metabolism*, vol. 23, no. 8, pp. 365–371, 2012.
- [37] G. N. Ioannou, S. Subramanian, A. Chait et al., "Cholesterol crystallization within hepatocyte lipid droplets and its role in murine NASH," *Journal of Lipid Research*, vol. 58, no. 6, pp. 1067–1079, 2017.
- [38] G. L. Semenza, "Hypoxia-inducible factor 1: control of oxygen homeostasis in health and disease," *Pediatric Research*, vol. 49, no. 5, pp. 614–617, 2001.
- [39] L. Schito and G. L. Semenza, "Hypoxia-inducible factors: master regulators of cancer progression," *Trends in Cancer*, vol. 2, no. 12, pp. 758–770, 2016.
- [40] M. Y. Koh, T. R. Spivak-Kroizman, and G. Powis, "HIF-1 regulation: not so easy come, easy go," *Trends in Biochemical Sciences*, vol. 33, no. 11, pp. 526–534, 2008.
- [41] E. M. Dioum, R. Chen, M. S. Alexander et al., "Regulation of hypoxia-inducible factor 2 α signaling by the stress-responsive deacetylase sirtuin 1," *Science*, vol. 324, no. 5932, pp. 1289–1293, 2009.
- [42] J. Zhao, F. Du, G. Shen, F. Zheng, and B. Xu, "The role of hypoxia-inducible factor-2 in digestive system cancers," *Cell Death & Disease*, vol. 6, no. 1, article e1600, 2015.
- [43] G. Musso, C. Olivetti, M. Cassader, and R. Gambino, "Obstructive sleep apnea-hypopnea syndrome and nonalcoholic fatty liver disease: emerging evidence and mechanisms," *Seminars in Liver Disease*, vol. 32, no. 1, pp. 49–64, 2012.
- [44] T. Y. Lau, J. Xiao, E. C. Liong et al., "Hepatic response to chronic hypoxia in experimental rat model through HIF-1 α , activator protein-1 and NF-kappa B," *Histology and Histopathology*, vol. 28, no. 4, pp. 463–471, 2013.
- [45] P. Loria, A. Lonardo, S. Lombardini et al., "Gallstone disease in non-alcoholic fatty liver: prevalence and associated factors," *Journal of Gastroenterology and Hepatology*, vol. 20, no. 8, pp. 1176–1184, 2005.
- [46] Y. Asai, T. Yamada, S. Tsukita et al., "Activation of the hypoxia inducible factor 1 α subunit pathway in steatotic liver contributes to formation of cholesterol gallstones," *Gastroenterology*, vol. 152, no. 6, pp. 1521–1535.e8, 2017.
- [47] R. M. Carr and R. S. Ahima, "Pathophysiology of lipid droplet proteins in liver diseases," *Experimental Cell Research*, vol. 340, no. 2, pp. 187–192, 2016.
- [48] F. Mattijssen, A. Georgiadi, T. Andasari et al., "Hypoxia-inducible lipid droplet-associated (HILPDA) is a novel peroxisome proliferator-activated receptor (PPAR) target involved in hepatic triglyceride secretion," *Journal of Biological Chemistry*, vol. 289, no. 28, pp. 19279–19293, 2014.
- [49] T. Gimm, M. Wiese, B. Teschemacher et al., "Hypoxia-inducible protein 2 is a novel lipid droplet protein and a specific target gene of hypoxia-inducible factor-1," *The FASEB Journal*, vol. 24, no. 11, pp. 4443–4458, 2010.
- [50] I. Mylonis, H. Sembongi, C. Befani, P. Liakos, S. Simiosoglou, and G. Simos, "Hypoxia causes triglyceride accumulation by HIF-1-mediated stimulation of lipin 1 expression," *Journal of Cell Science*, vol. 125, no. 14, pp. 3485–3493, 2012.
- [51] M. Aharoni-Simon, S. Anavi, U. Beifuss, Z. Madar, and O. Tirosh, "Nitric oxide, can it be only good? Increasing the antioxidant properties of nitric oxide in hepatocytes by YC-1 compound," *Nitric Oxide*, vol. 27, no. 4, pp. 248–256, 2012.
- [52] C. Zhang, M. Bian, X. Chen et al., "Oroxlylin A prevents angiogenesis of LSECs in liver fibrosis via inhibition of YAP/HIF-1 α signaling," *Journal of Cellular Biochemistry*, vol. 119, no. 2, pp. 2258–2268, 2018.
- [53] O. A. Mesarwi, M. K. Shin, S. Bevans-Fonti, C. Schlesinger, J. Shaw, and V. Y. Polotsky, "Hepatocyte hypoxia inducible factor-1 mediates the development of liver fibrosis in a mouse model of nonalcoholic fatty liver disease," *PLoS One*, vol. 11, no. 12, article e0168572, 2016.
- [54] E. Ceni, T. Mello, S. Polvani et al., "The orphan nuclear receptor COUP-TFII coordinates hypoxia-independent proangiogenic responses in hepatic stellate cells," *Journal of Hepatology*, vol. 66, no. 4, pp. 754–764, 2017.
- [55] J. Moczydlowska, W. Miltyk, A. Hermanowicz, D. M. Lebensztejn, J. A. Palka, and W. Debek, "HIF-1 α as a key factor in bile duct ligation-induced liver fibrosis in rats," *Journal of Investigative Surgery*, vol. 30, no. 1, pp. 41–46, 2017.
- [56] C. Bocca, E. Novo, A. Miglietta, and M. Parola, "Angiogenesis and fibrogenesis in chronic liver diseases," *Cellular and Molecular Gastroenterology and Hepatology*, vol. 1, no. 5, pp. 477–488, 2015.

- [57] V. Wang, D. A. Davis, and R. Yarchoan, "Identification of functional hypoxia inducible factor response elements in the human lysyl oxidase gene promoter," *Biochemical and Biophysical Research Communications*, vol. 490, no. 2, pp. 480–485, 2017.
- [58] S. B. Liu, N. Ikenaga, Z. W. Peng et al., "Lysyl oxidase activity contributes to collagen stabilization during liver fibrosis progression and limits spontaneous fibrosis reversal in mice," *The FASEB Journal*, vol. 30, no. 4, pp. 1599–1609, 2016.
- [59] C. Ju, S. P. Colgan, and H. K. Eltzschig, "Hypoxia-inducible factors as molecular targets for liver diseases," *Journal of Molecular Medicine*, vol. 94, no. 6, pp. 613–627, 2016.
- [60] B. L. Copple, S. Kaska, and C. Wentling, "Hypoxia-inducible factor activation in myeloid cells contributes to the development of liver fibrosis in cholestatic mice," *The Journal of Pharmacology and Experimental Therapeutics*, vol. 341, no. 2, pp. 307–316, 2012.
- [61] J. Wang, Y. Ma, H. Jiang et al., "Overexpression of von Hippel–Lindau protein synergizes with doxorubicin to suppress hepatocellular carcinoma in mice," *Journal of Hepatology*, vol. 55, no. 2, pp. 359–368, 2011.
- [62] D. K.-C. Chiu, A. P.-W. Tse, I. M.-J. Xu et al., "Hypoxia inducible factor HIF-1 promotes myeloid-derived suppressor cells accumulation through ENTPD2/CD39L1 in hepatocellular carcinoma," *Nature Communications*, vol. 8, no. 1, p. 517, 2017.
- [63] O. Warburg, "On the origin of cancer cells," *Science*, vol. 123, no. 3191, pp. 309–314, 1956.
- [64] B. Li, L. He, D. Zuo et al., "Mutual regulation of MiR-199a-5p and HIF-1 α modulates the Warburg effect in hepatocellular carcinoma," *Journal of Cancer*, vol. 8, no. 6, pp. 940–949, 2017.
- [65] T. Hamaguchi, N. Iizuka, R. Tsunedomi et al., "Glycolysis module activated by hypoxia-inducible factor 1 α is related to the aggressive phenotype of hepatocellular carcinoma," *International Journal of Oncology*, vol. 33, no. 4, pp. 725–731, 2008.
- [66] M. Mandl and R. Depping, "ARNT is a potential direct HIF-1 target gene in human Hep3B hepatocellular carcinoma cells," *Cancer Cell International*, vol. 17, no. 1, p. 77, 2017.
- [67] D. Y. Lu, H. C. Liou, C. H. Tang, and W. M. Fu, "Hypoxia-induced iNOS expression in microglia is regulated by the PI3-kinase/Akt/mTOR signaling pathway and activation of hypoxia inducible factor-1 α ," *Biochemical Pharmacology*, vol. 72, no. 8, pp. 992–1000, 2006.
- [68] S. Anavi, M. Hahn-Obercyger, R. Margalit, Z. Madar, and O. Tirosh, "A novel antihypoglycemic role of inducible nitric oxide synthase in liver inflammatory response induced by dietary cholesterol and endotoxemia," *Antioxidants & Redox Signaling*, vol. 19, no. 16, pp. 1889–1901, 2013.
- [69] S. K. Mantena, A. L. King, K. K. Andringa, H. B. Eccleston, and S. M. Bailey, "Mitochondrial dysfunction and oxidative stress in the pathogenesis of alcohol- and obesity-induced fatty liver diseases," *Free Radical Biology and Medicine*, vol. 44, no. 7, pp. 1259–1272, 2008.
- [70] J. Mateo, M. Garcia-Lecea, S. Cadenas, C. Hernandez, and S. Moncada, "Regulation of hypoxia-inducible factor-1 α by nitric oxide through mitochondria-dependent and -independent pathways," *Biochemical Journal*, vol. 376, no. 2, pp. 537–544, 2003.
- [71] N. Olson and A. van der Vliet, "Interactions between nitric oxide and hypoxia-inducible factor signaling pathways in inflammatory disease," *Nitric Oxide*, vol. 25, no. 2, pp. 125–137, 2011.
- [72] J. Liu and M. Waalkes, "Nitric oxide and chemically induced hepatotoxicity: beneficial effects of the liver-selective nitric oxide donor, V-PYRRO/NO," *Toxicology*, vol. 208, no. 2, pp. 289–297, 2005.
- [73] R. M. Rai, F. Y. J. Lee, A. Rosen et al., "Impaired liver regeneration in inducible nitric oxide synthase-deficient mice," *Proceedings of the National Academy of Sciences of the United States of America*, vol. 95, no. 23, pp. 13829–13834, 1998.
- [74] Y. Mei and S. Thevananther, "Endothelial nitric oxide synthase is a key mediator of hepatocyte proliferation in response to partial hepatectomy in mice," *Hepatology*, vol. 54, no. 5, pp. 1777–1789, 2011.
- [75] Y. Yu, M. Tamai, and Y. I. Tagawa, "Nitric oxide is critical for avoiding hepatic lipid overloading via IL-6 induction during liver regeneration after partial hepatectomy in mice," *Experimental Animals*, vol. 66, no. 4, pp. 293–302, 2017.
- [76] O. Tirosh, E. Ilan, N. Budick-Harmelin, G. Ramadori, and Z. Madar, "Downregulation of eNOS in a nutritional model of fatty liver," *e-SPEN, the European e-Journal of Clinical Nutrition and Metabolism*, vol. 4, no. 2, pp. e101–e104, 2009.
- [77] Y. Nozaki, K. Fujita, K. Wada et al., "Deficiency of iNOS-derived NO accelerates lipid accumulation-independent liver fibrosis in non-alcoholic steatohepatitis mouse model," *BMC Gastroenterology*, vol. 15, no. 1, p. 42, 2015.
- [78] L. Zhu, R. D. Baker, and S. S. Baker, "Gut microbiome and nonalcoholic fatty liver diseases," *Pediatric Research*, vol. 77, no. 1-2, pp. 245–251, 2014.
- [79] O. Tirosh, A. Artan, M. Aharoni-Simon, G. Ramadori, and Z. Madar, "Impaired liver glucose production in a murine model of steatosis and endotoxemia: protection by inducible nitric oxide synthase," *Antioxidants & Redox Signaling*, vol. 13, no. 1, pp. 13–26, 2010.
- [80] M. S. Bosner, L. G. Lange, W. F. Stenson, and R. E. Ostlund Jr., "Percent cholesterol absorption in normal women and men quantified with dual stable isotopic tracers and negative ion mass spectrometry," *Journal of Lipid Research*, vol. 40, no. 2, pp. 302–308, 1999.
- [81] L. Jia, J. L. Betters, and L. Yu, "Niemann-pick C1-like 1 (NPC1L1) protein in intestinal and hepatic cholesterol transport," *Annual Review of Physiology*, vol. 73, no. 1, pp. 239–259, 2011.
- [82] S. Kidambi and S. B. Patel, "Cholesterol and non-cholesterol sterol transporters: ABCG5, ABCG8 and NPC1L1: a review," *Xenobiotica*, vol. 38, no. 7-8, pp. 1119–1139, 2008.
- [83] G. N. Ioannou, "The role of cholesterol in the pathogenesis of NASH," *Trends in Endocrinology & Metabolism*, vol. 27, no. 2, pp. 84–95, 2016.
- [84] F. Caballero, A. Fernandez, A. M. De Lacy, J. C. Fernandez-Checa, J. Caballeria, and C. Garcia-Ruiz, "Enhanced free cholesterol, SREBP-2 and StAR expression in human NASH," *Journal of Hepatology*, vol. 50, no. 4, pp. 789–796, 2009.
- [85] J. M. Schattenberg and P. R. Galle, "Animal models of non-alcoholic steatohepatitis: of mice and man," *Digestive Diseases*, vol. 28, no. 1, pp. 247–254, 2010.
- [86] S. Subramanian, L. Goodspeed, S. Wang et al., "Dietary cholesterol exacerbates hepatic steatosis and inflammation in obese LDL receptor-deficient mice," *Journal of Lipid Research*, vol. 52, no. 9, pp. 1626–1635, 2011.

- [87] H. Basciano, A. Miller, C. Baker, M. Naples, and K. Adeli, "LXR α activation perturbs hepatic insulin signaling and stimulates production of apolipoprotein B-containing lipoproteins," *American Journal of Physiology-Gastrointestinal and Liver Physiology*, vol. 297, no. 2, pp. G323–G332, 2009.
- [88] I. Tabas, "Apoptosis and plaque destabilization in atherosclerosis: the role of macrophage apoptosis induced by cholesterol," *Cell Death & Differentiation*, vol. 11, Supplement 1, pp. S12–S16, 2004.
- [89] D. M. Van Rooyen, C. Z. Larter, W. G. Haigh et al., "Hepatic free cholesterol accumulates in obese, diabetic mice and causes nonalcoholic steatohepatitis," *Gastroenterology*, vol. 141, no. 4, pp. 1393–1403.e5, 2011.
- [90] K. Wouters, P. J. van Gorp, V. Bieghs et al., "Dietary cholesterol, rather than liver steatosis, leads to hepatic inflammation in hyperlipidemic mouse models of nonalcoholic steatohepatitis," *Hepatology*, vol. 48, no. 2, pp. 474–486, 2008.
- [91] M. N. B. Kristiansen, S. S. Veidal, K. T. G. Rigbolt et al., "Obese diet-induced mouse models of nonalcoholic steatohepatitis-tracking disease by liver biopsy," *World Journal of Hepatology*, vol. 8, no. 16, pp. 673–684, 2016.
- [92] D. M. Van Rooyen and G. C. Farrell, "SREBP-2: a link between insulin resistance, hepatic cholesterol, and inflammation in NASH," *Journal of Gastroenterology and Hepatology*, vol. 26, no. 5, pp. 789–792, 2011.
- [93] L. P. Bechmann, P. Kocabayoglu, J. P. Sowa et al., "Free fatty acids repress small heterodimer partner (SHP) activation and adiponectin counteracts bile acid-induced liver injury in superobese patients with nonalcoholic steatohepatitis," *Hepatology*, vol. 57, no. 4, pp. 1394–1406, 2013.
- [94] I. Voloshin, M. Hahn-Obercyger, S. Anavi, and O. Tirosh, "L-arginine conjugates of bile acids-a possible treatment for non-alcoholic fatty liver disease," *Lipids in Health and Disease*, vol. 13, no. 1, p. 69, 2014.
- [95] M. Hahn-Obercyger, L. Graeve, and Z. Madar, "A high-cholesterol diet increases the association between caveolae and insulin receptors in rat liver," *Journal of Lipid Research*, vol. 50, no. 1, pp. 98–107, 2009.
- [96] C.-C. C. Key, M. Liu, C. L. Kurtz et al., "Hepatocyte ABCA1 deletion impairs liver insulin signaling and lipogenesis," *Cell Reports*, vol. 19, no. 10, pp. 2116–2129, 2017.
- [97] K. A. Lytle, C. P. Wong, and D. B. Jump, "Docosahexaenoic acid blocks progression of western diet-induced nonalcoholic steatohepatitis in obese *Ldlr*^{-/-} mice," *PLoS One*, vol. 12, no. 4, article e0173376, 2017.
- [98] C. Garcia-Ruiz, V. Ribas, A. Baulies, and J. C. Fernandez-Checa, "Mitochondrial cholesterol and the paradox in cell death," in *Pharmacology of Mitochondria*, H. Singh and S. S. Sheu, Eds., vol. 240 of Handbook of Experimental Pharmacology, pp. 189–210, Springer, Cham, 2017.
- [99] S. Anavi, N. B. Harmelin, Z. Madar, and O. Tirosh, "Oxidative stress impairs HIF1 α activation: a novel mechanism for increased vulnerability of steatotic hepatocytes to hypoxic stress," *Free Radical Biology and Medicine*, vol. 52, no. 9, pp. 1531–1542, 2012.
- [100] A. Baulies, J. Montero, N. Matias et al., "The 2-oxoglutarate carrier promotes liver cancer by sustaining mitochondrial GSH despite cholesterol loading," *Redox Biology*, vol. 14, pp. 164–177, 2018.
- [101] F. Bellanti, R. Villani, R. Tamborra et al., "Synergistic interaction of fatty acids and oxysterols impairs mitochondrial function and limits liver adaptation during nafld progression," *Redox Biology*, vol. 15, pp. 86–96, 2018.
- [102] F. Bellanti, D. Mitarotonda, R. Tamborra et al., "Oxysterols induce mitochondrial impairment and hepatocellular toxicity in non-alcoholic fatty liver disease," *Free Radical Biology & Medicine*, vol. 75, Supplement 1, pp. S16–S17, 2014.
- [103] P. Malhotra, C. Aloman, A. Ankireddy et al., "Overactivation of intestinal sterol response element-binding protein 2 promotes diet-induced nonalcoholic steatohepatitis," *American Journal of Physiology-Gastrointestinal and Liver Physiology*, vol. 313, no. 5, pp. G376–G385, 2017.
- [104] G. N. Ioannou, W. G. Haigh, D. Thorning, and C. Savard, "Hepatic cholesterol crystals and crown-like structures distinguish NASH from simple steatosis," *Journal of Lipid Research*, vol. 54, no. 5, pp. 1326–1334, 2013.
- [105] G. Baffy, "Kupffer cells in non-alcoholic fatty liver disease: the emerging view," *Journal of Hepatology*, vol. 51, no. 1, pp. 212–223, 2009.
- [106] V. Bieghs, T. Hendriks, P. J. van Gorp et al., "The cholesterol derivative 27-hydroxycholesterol reduces steatohepatitis in mice," *Gastroenterology*, vol. 144, no. 1, pp. 167–178.e1, 2013.
- [107] K. Tomita, T. Teratani, T. Suzuki et al., "Free cholesterol accumulation in hepatic stellate cells: mechanism of liver fibrosis aggravation in nonalcoholic steatohepatitis in mice," *Hepatology*, vol. 59, no. 1, pp. 154–169, 2014.
- [108] T. Teratani, K. Tomita, T. Suzuki et al., "A high-cholesterol diet exacerbates liver fibrosis in mice via accumulation of free cholesterol in hepatic stellate cells," *Gastroenterology*, vol. 142, no. 1, pp. 152–164.e10, 2012.
- [109] K. Tomita, T. Teratani, T. Suzuki et al., "Acyl-CoA:cholesterol acyltransferase 1 mediates liver fibrosis by regulating free cholesterol accumulation in hepatic stellate cells," *Journal of Hepatology*, vol. 61, no. 1, pp. 98–106, 2014.
- [110] W. Huang, D. Mehta, S. Sif et al., "Dietary fat/cholesterol-sensitive PKC β -RB signaling: potential role in NASH/HCC axis," *Oncotarget*, vol. 8, no. 43, pp. 73757–73765, 2017.
- [111] H. Tanaka, Y. Nishikawa, T. Fukushima et al., "Lipopolysaccharide inhibits hepatic gluconeogenesis in rats: the role of immune cells," *Journal of Diabetes Investigation*, vol. 9, no. 3, pp. 494–504, 2018.
- [112] J. Wallington, J. Ning, and M. A. Titheradge, "The control of hepatic glycogen metabolism in an in vitro model of sepsis," *Molecular and Cellular Biochemistry*, vol. 308, no. 1–2, pp. 183–192, 2008.
- [113] T. Nomura, N. Keira, Y. Urakabe et al., "Chronic pericardial constriction induced severe ischemic hepatitis manifesting as hypoglycemic attack," *Circulation Journal*, vol. 73, no. 1, pp. 183–186, 2009.
- [114] H. Jain, S. Beriwal, and S. Singh, "Alcohol induced ketoacidosis, severe hypoglycemia and irreversible encephalopathy," *Medical Science Monitor*, vol. 8, no. 11, pp. CS77–CS79, 2002.
- [115] J. Braverman and S. A. Stanley, "Nitric oxide modulates macrophage responses to *Mycobacterium tuberculosis* infection through activation of HIF-1 α and repression of NF- κ B," *The Journal of Immunology*, vol. 199, no. 5, pp. 1805–1816, 2017.
- [116] C. Xie, S. D. Turley, and J. M. Dietschy, "Centripetal cholesterol flow from the extrahepatic organs through the liver is normal in mice with mutated Niemann-Pick type C protein (NPC1)," *Journal of Lipid Research*, vol. 41, no. 8, pp. 1278–1289, 2000.

- [117] C. D. Jolley, L. A. Woollett, S. D. Turley, and J. M. Dietschy, "Centripetal cholesterol flux to the liver is dictated by events in the peripheral organs and not by the plasma high density lipoprotein or apolipoprotein A-I concentration," *Journal of Lipid Research*, vol. 39, no. 11, pp. 2143–2149, 1998.
- [118] H. K. Min, A. Kapoor, M. Fuchs et al., "Increased hepatic synthesis and dysregulation of cholesterol metabolism is associated with the severity of nonalcoholic fatty liver disease," *Cell Metabolism*, vol. 15, no. 5, pp. 665–674, 2012.
- [119] P. Walle, M. Takkunen, V. Männistö et al., "Fatty acid metabolism is altered in non-alcoholic steatohepatitis independent of obesity," *Metabolism*, vol. 65, no. 5, pp. 655–666, 2016.
- [120] Y. Nakade, K. Murotani, T. Inoue et al., "Ezetimibe for the treatment of non-alcoholic fatty liver disease: a meta-analysis," *Hepatology Research*, vol. 47, no. 13, pp. 1417–1428, 2017.
- [121] A. Eshraghian, "Current and emerging pharmacological therapy for non-alcoholic fatty liver disease," *World Journal of Gastroenterology*, vol. 23, no. 42, pp. 7495–7504, 2017.
- [122] D. Pastori, L. Polimeni, F. Baratta, A. Pani, M. Del Ben, and F. Angelico, "The efficacy and safety of statins for the treatment of non-alcoholic fatty liver disease," *Digestive and Liver Disease*, vol. 47, no. 1, pp. 4–11, 2015.
- [123] V. G. Athyros, C. Boutari, K. Stavropoulos et al., "Statins: an under-appreciated asset for the prevention and the treatment of NAFLD or NASH and the related cardiovascular risk," *Current Vascular Pharmacology*, vol. 16, no. 3, pp. 246–253, 2018.
- [124] D. Papandreou and E. Andreou, "Role of diet on non-alcoholic fatty liver disease: an updated narrative review," *World Journal of Hepatology*, vol. 7, no. 3, pp. 575–582, 2015.
- [125] M. F. Abdelmalek, A. Suzuki, C. Guy et al., "Increased fructose consumption is associated with fibrosis severity in patients with nonalcoholic fatty liver disease," *Hepatology*, vol. 51, no. 6, pp. 1961–1971, 2010.
- [126] S. M. Ferolla, L. C. Silva, L. Ferrari Mde et al., "Dietary approach in the treatment of nonalcoholic fatty liver disease," *World Journal of Hepatology*, vol. 7, no. 24, pp. 2522–2534, 2015.
- [127] A. Brandt, C. Jin, K. Nolte, C. Sellmann, A. Engstler, and I. Bergheim, "Short-term intake of a fructose-, fat- and cholesterol-rich diet causes hepatic steatosis in mice: effect of antibiotic treatment," *Nutrients*, vol. 9, no. 9, p. 1013, 2017.